

Journal of Polymer Science

Part A-1: Polymer Chemistry

Contents

| | |
|---|-----|
| KATSUKIYO ITO: Collision between Polymeric Radicals for Termination Rate Constants | 577 |
| B. M. BAYSAL, H. N. ERTEN, and U. S. RAMELOW: Solid-State Polymerization of Acrylamide and Some Acrylates Initiated by Ultraviolet Radiation | 581 |
| RONALD D. LAW: Application of Gel-Permeation Chromatography to Studies of the Functionality Distribution of Carboxy- and Hydroxy-Polybutadienes | 589 |
| J. BOOR, JR.: Ziegler Polymerization of Olefins. IX. Donor Effects in Metal Alkyl-Free and Ziegler-Type Stereospecific Catalysts | 617 |
| TADASHI OKUYAMA and TAKAYUKI FUENO: Structure and Reactivity of α,β -Unsaturated Ethers. XIII. Cationic Copolymerization and Acid-Catalyzed Hydrolysis of 1,2-Dialkoxyethylenes | 629 |
| KUNIO MORI and YOSHIRO NAKAMURA: Modification of Poly(vinyl Chloride). XIII. Crosslinking of Poly(vinyl Chloride) with Dithiols and Properties of the Crosslinked Products | 639 |
| JOHN C. LAI, THANE ROUNSFELL, and CHARLES U. PITTMAN, JR.: Free-Radical Homopolymerization and Copolymerization of Vinylferrocene | 651 |
| DWAIN M. WHITE: Polymerization by Oxidative Coupling. II. Co-Redistribution of Poly(2,6-diphenyl-1,4-phenylene Ether) with Phenols | 663 |
| A. F. HALASA, H. ADAMS, and C. J. HUNTER: Elastomers from the Copolymerization of Conjugated Dienes and Styrenes Containing Chlorine | 677 |
| JENO SZITA, L. H. BRANNIGAN, and C. S. MARVEL: Ladder Pyrrolone Structures with Anthraquinone Recurring Units | 691 |
| C. G. OVERBERGER, R. A. VENESKI, and JAN ŠEBENDA: Use of Phosphite Amides in the Synthesis of Polyamides | 701 |
| R. W. WARREN, D. S. GATES, and G. L. DRISCOLL: NMR Identification of C_{11} to C_{40} Branched Hydrocarbons Derived from the Decomposition of Polyisobutylene | 717 |
| S. KOHJIYA, Y. IMANISHI, and T. HIGASHIMURA: Propagation Rate Constant in Cationic Polymerization of Cyclic Dienes. I. Polymerization of Cyclopentadiene with Titanium Tetrachloride-Trichloroacetic Acid | 747 |

(continued inside)

Board of Editors: H. Mark • C. G. Overberger • T. G. Fox

Advisory Editors:

R. M. Fuoss • J. J. Hermans • H. W. Melville • G. Smets

Editor: C. G. Overberger

Associate Editor: E. M. Pearce

Advisory Board:

| | | | |
|-------------------|-------------------|------------------|------------------|
| T. Alfrey, Jr. | N. D. Field | R. W. Lenz | C. C. Price |
| W. J. Bailey | F. C. Foster | Eloisa Mano | B. Rånby |
| John Boor, Jr. | H. N. Friedlander | C. S. Marvel | J. H. Saunders |
| F. A. Bovey | K. C. Frisch | F. R. Mayo | C. Schuerch |
| J. W. Breitenbach | N. G. Gaylord | R. B. Mesrobian | W. H. Sharkey |
| W. J. Burlant | W. E. Gibbs | Donald Metz | V. T. Stannett |
| G. B. Butler | A. R. Gilbert | H. Morawetz | J. K. Stille |
| S. Bywater | M. Goodman | M. Morton | M. Szwarc |
| W. L. Carrick | J. E. Guillet | James Mulvaney | A. V. Tobolsky |
| H. W. Coover, Jr. | George Hulse | S. Murahashi | E. J. Vandenberg |
| W. H. Daly | Otto Kauder | G. Natta | Herbert Vogel |
| F. Danusso | J. P. Kennedy | K. F. O'Driscoll | L. A. Wall |
| F. R. Eirich | W. Kern | S. Okamura | O. Wichterle |
| E. M. Fettes | J. Lal | P. Pino | F. H. Winslow |

Contents (continued)

| | |
|---|-----|
| JERRY HIGGINS, JOE F. JONES, and ALLAN THORNBURGH: Polyaromatic Pyrazines: Synthesis and Thermogravimetric Analysis | 763 |
| YU. I. ERMAKOV, V. A. ZAKHAROV, and E. G. KUSHNAREVA: Dependence of Reactivity of Propagation Centers of Oxide Catalysts for Ethylene Polymerization on Catalyst Composition and Activation Conditions | 771 |
| M. RÄTZSCH, W. SCHNEIDER, and D. MUSCHE: Reactivity of Ethylene in the Radically Initiated Copolymerization of Ethylene with Vinylacetate | 785 |
| M. KOLÍNSKÝ, D. DOSKOČILOVÁ, B. SCHEIDER, J. ŠTOKR, E. DRAHORÁDOVÁ, and V. KUŠKA: Structure of Chlorinated Poly(vinyl Chloride). I. Determination of the Mechanism of Chlorination from Infrared and NMR Spectra | 791 |

(continued on inside back cover)

The Journal of Polymer Science is published in four sections as follows: Part A-1, Polymer Chemistry, monthly; Part A-2, Polymer Physics, monthly; Part B, Polymer Letters, monthly; Part C, Polymer Symposia, irregular.

Published monthly by Interscience Publishers, a Division of John Wiley & Sons, Inc., covering one volume annually. Publication Office at 20th and Northampton Sts., Easton, Pa. 18042. Executive, Editorial, and Circulation Offices at 605 Third Avenue, New York, N. Y. 10016. Second-class postage paid at Easton, Pa. Subscription price, \$325.00 per volume (including Parts A-2, B, and C). Foreign postage \$15.00 per volume (including Parts A-2, B, and C).

Copyright © 1971 by John Wiley & Sons, Inc. All rights reserved. No part of this publication may be reproduced by any means, nor transmitted, nor translated into a machine language without the written permission of the publisher.

Collision between Polymeric Radicals for Termination Rate Constants

KATSUKIYO ITO, *Government Industrial Research Institute of
Nagoya, Kita-ku, Nagoya, Japan*

Synopsis

The motion of each polymeric radical during a collision between the polymeric radicals with the same radius is treated as completely random motion. The result obtained is: $k_t = 0.250k_s$ (where k_t is the chain-termination rate constant and k_s is the reaction rate constant between radical chain ends). On taking the motion of the primary radical during a collision between a primary radical and a large polymeric radical to be completely random, the result obtained is: $k_{ti} = 0.250k_{si}$ (where k_{ti} is the primary radical termination rate constant and k_{si} is the reaction rate constant between primary radical and radical chain end). On substituting k_s for k_{si} in the second equation, the rate constant obtained becomes the chain termination rate constant between the very small polymeric radical and the very large polymeric radical, and identical to the former equation. This identity indicates that the effect of the difference of the size of the polymeric radicals on the collision process relating to the chain termination rate constant should not be large.

Introduction

In previous papers, the collision process between polymeric radicals has been treated by collision theory^{1,2} and a modified Smoluchowski's theory.³ In these treatments, motion during the collision is considered to be linear motion. However, actually, this motion is not linear, but random.

In Moroni and Schulz's treatment,⁴ this motion is not completely random, but approximately random, because the direction of motion is partially decided.

In this paper, this motion is treated as completely random motion. This treatment is mathematically very simple.

Collision between Polymeric Radicals with the Same Radius

In the initial state for a collision process between two polymeric radicals with the same radius R , one of them exists in contact with another (Fig. 1A). One of them (a) is fixed, and the other is diffusing (b). The diffusion constant D is the sum of the diffusion constants of the above two polymeric radicals. At time t thereafter, the center of the diffusing poly-

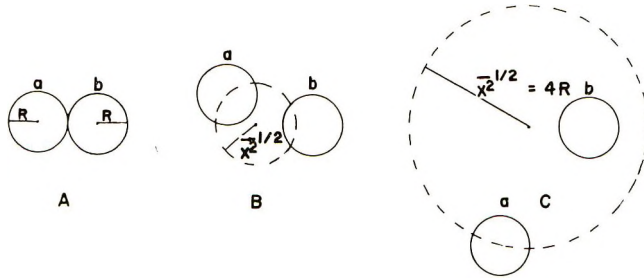


Fig. 1. Collision process between polymeric radicals with the same radius: (A) initial state; (B) intermediate state; (C) final state (a denotes the diffusing polymeric radical, b the fixed polymeric radical).

meric radical is placed at a root-mean-square average distance $(\bar{x}^2)^{1/2}$ from the initial site (Fig. 1B). This relation is given by

$$t = \bar{x}^2/6D \quad (1)$$

In the time range 0 to T , where T is the time for the final state of contact being possible (Fig. 1C), overlap and contact between polymeric radicals are possible. A root-mean-square average distance $(\bar{x}^2)^{1/2} = 4R$ indicates the final state. Thus, T becomes

$$T = (4R)^2/6D = 8R^2/3D \quad (2)$$

In the above treatment, it must be assumed that the rotational motion of the polymeric radicals is not hindered.^{3,4}

The volume V of the sphere with radius $(\bar{x}^2)^{1/2} = 4R$ is given by:

$$V = (4/3)\pi(4R)^3$$

The collision state is referred to the overlap and contact between polymeric radicals, and given by the volume of the fixed polymeric radical:

$$V = (4/3)\pi R^3$$

Thus, the collision time is given by

$$T[(4/3)\pi R^3]/[(4/3)\pi(4R)^3] = (1/64)T = R^2/24D \quad (3)$$

The reaction probability p_t for the collision between the polymeric radicals relating to the reaction rate constant k_s between radical chain ends is

$$\begin{aligned} p_t &= k_s(R^2/24D)(3 \times 10^{23}/4\pi N_L R^3) \\ &= k_s \times 10^{23}/32\pi N_L R D \end{aligned} \quad (4)$$

where N_L is Avogadro's number.^{3,4}

On applying the original Smoluchowski theory,⁵ the chain termination rate constant is given by

$$k_t = 4\pi N_L v_{12} D p_t \times 10^{-3} \text{ l./mole-sec} \quad (5)$$

where r_{12} is the distance to which two polymeric radicals approach for bimolecular reaction. By using eqs. (4) and (5) at $r_{12} = 2R$, k_t is calculated to be:

$$k_t = 0.250 k_3 \text{ l./mole-sec.} \quad (6)$$

Collision between Large Polymeric Radical and Small Polymeric Radical or Primary Radical

In order to analyze the effect of a difference in size between the polymeric radicals on the collision process relating to the chain termination rate constant, the collision process between a very large polymeric radical and a very small polymeric radical is considered. This collision process is typically illustrated for bimolecular reaction between large polymeric radical and primary radical. Thus, in this section, a collision between a primary radical and large polymeric radical is treated.

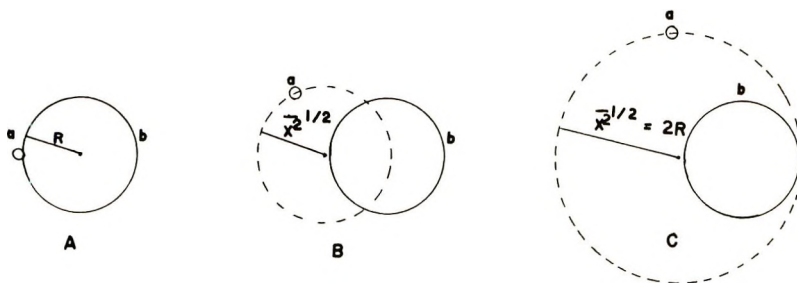


Fig. 2. Collision process between primary radical and large polymeric radical: (A) initial state; (B) intermediate state; (C) final state (a denotes the primary radical, b the large polymeric radical).

The very large polymeric radical (b) is considered to be fixed and the primary radical (a) is diffusing. At time t after the initial state for contact between the primary radical and the polymeric radical (Fig. 2A), the primary radical is placed at a root-mean-square average distance:

$$\bar{x}^{2/2} = (6D_i t)^{1/2} \quad (7)$$

where D_i is the diffusion constant of the primary radical (Fig. 2B). The root-mean-square average distance $\bar{x}^{2/2} = 2R$ indicates the final state (Fig. 2C). Thus, the time for the final state of possible contact is given by

$$T_i = 2R^2/3D_i \quad (8)$$

The collision time becomes:

$$T_i [(4/3)\pi R^3] / [(4/3)\pi (2R)^3] = R^2/12D_i \quad (9)$$

The reaction probability p_{ti} between the primary radical and the polymeric radical relating to the reaction rate constant k_{si} between the primary radical and the radical chain end is given by:

$$\begin{aligned} p_{ti} &= k_{si}(R^2/12D_i)(3 \times 10^3/4\pi N_L R^3) \\ &= 10^3 k_{si}/16\pi N_L R D_i \end{aligned} \quad (10)$$

For this probability, the primary radical termination rate constant is calculated to be:

$$\begin{aligned} k_t &= 4\pi N_L R D_i p_{ti} \times 10^{-3} \quad (\text{at } r_{12} = R) \\ &= 0.250 k_{si} \text{ l./mole-sec.} \end{aligned} \quad (11)$$

On taking k_s for k_{si} in eq. (11), this rate constant becomes the chain termination rate constant between the very large polymeric radical and the very small polymeric radical, and identical to eq. (6). This identity indicates that the effect of the difference of the size of the polymeric radicals on the collision process relating to the chain termination rate constant should not be large.

Discussion

On taking the motion during the collision to be linear, we obtain:³

$$k_t = 0.778 k_s \text{ l./mole-sec.} \quad (12)$$

Taking the motion to be partially random, we obtain:⁴

$$k_t = k_s \text{ l./mole-sec.} \quad (13)$$

Taking the motion to be completely random, we obtain:

$$k_t = 0.250 k_s \text{ l./mole-sec.} \quad (6)$$

As stated in the introduction, because the motion is completely random, the chain termination rate constant given by eq. (6) seems to be correct. The primary radical termination rate constant given by eq. (11) seems to be also correct.

References

1. K. Ito, *J. Polym. Sci. A-1*, **7**, 827 (1969).
2. K. Ito, *J. Polym. Sci. A-1*, **7**, 2247 (1969).
3. K. Ito, *J. Polym. Sci. A-1*, **8**, 1823 (1970).
4. A. F. Moroni and G. V. Schultz, *Makromol. Chem.*, **118**, 313 (1968).
5. M. V. Smoluchowski, *Z. Physik. Chem.*, **29**, 129 (1917).

Received June 5, 1970

Revised August 10, 1970

Solid-State Polymerization of Acrylamide and Some Acrylates Initiated by Ultraviolet Radiation

B. M. BAYSAI, H. N. ERTEN, and Ü. S. RAMELOW, *Department of Chemistry, Middle East Technical University, Ankara, Turkey*

Synopsis

The solid-state polymerization of acrylamide, potassium acrylate, and calcium acrylate by ultraviolet radiation have been investigated. For these polycrystalline monomers both in-source and post-irradiation reactions were studied by using various sources of different intensities at constant temperatures. It is concluded that the polymerization reactions take place primarily on the surfaces of crystals. The high molecular weight material obtained at low conversions show a rapid decrease in intrinsic viscosities, probably due to degradation. Both the rate and degree of polymerization were decreased by the presence of oxygen. The various behaviors observed for these three monomers under ultraviolet radiation were regarded as another indication of the importance of crystal structures upon the solid-state polymerization reactions.

INTRODUCTION

In the past decade, the solid-state polymerization of acrylamide,¹⁻⁴ acrylates, and methacrylates⁵⁻⁷ initiated by γ -radiation have been studied extensively, and detailed kinetic studies have been published on both in-source and post irradiation reactions. It was shown that the resulting polymer is amorphous,^{8,9} the polymer nucleated as a second phase early in the reaction,⁸⁻¹¹ and that defects were favored as nucleation sites.¹²

Various aspects of ultraviolet-initiated solid-state polymerization of acrylic and methacrylic acids, including the radical mechanism of initiation and termination and the effects of small applied stresses as a function of temperature and of trace impurities on the polymerization, have been reported.^{13,14}

This paper brings together the results of our recent studies on ultraviolet-initiated solid-state polymerization of acrylamide, potassium acrylate, and calcium acrylate. For these crystalline monomers both the in-source and post-irradiation reactions were studied by using various sources with different intensities. Polymerization reactions were carried out at constant temperatures in air as well as under vacuum by using polycrystalline samples. It was observed that the polymerization reactions take place primarily on the surfaces of crystals.

EXPERIMENTAL

Preparation of Materials

The acrylamide used was an American Cyanamide product. It was recrystallized several times from chloroform and dried under vacuum before use. The melting point was 84°C.

Potassium acrylate was a product of K and K Laboratory Inc., dissolved in methanol and precipitated with ethyl ether. The salt was filtered, washed with ether and acetone, dried, and stored under vacuum.⁵

Calcium acrylate was a product of K and K Laboratory Inc., dissolved in hot methanol, filtered, and crystallized by cooling for a long time, filtered, and dried under vacuum.⁶

Hexamethylcyclotrisiloxane was also a product of K and K Laboratory Inc. It was dissolved in 2-butanone, crystallized in cold water, and dried under vacuum.

Unpowdered polycrystalline monomeric samples, about 50–100 mesh size, were used throughout the experiments.

Irradiation Sources

Several sources of ultraviolet radiation were used with different intensities in about the 250–300 m μ range: Source 1 was a strong Hanau Quartzlamphen, Model S500/PI-324 tube at 250–315 m μ ; source 2, was a weak Hanovia Chromatolite lamp at 2537 Å; source 3 was a moderate UV-Phillips, MLU-M.5 mercury vapor quartz lamp.

Procedure

Irradiation of samples was carried out in air or under vacuum (10^{-4} mm) in Pyrex tubes. The temperature of the samples was held constant during irradiation. The geometry was fixed for a certain set of experiments for all runs. Post-polymerization reactions were carried out in appropriate thermostated water baths.

The tubes were opened immediately after irradiation for the in-source experiment, and for the post-irradiation experiments the tubes were stored in thermostated baths for the required time.

After opening the tubes, the irradiated contents were immediately dissolved in water and polymer precipitated in methanol.

Viscosities of aqueous solutions of polymer were measured in an Ubbelohde viscometer. The molecular weights of polyacrylamides were calculated from intrinsic viscosity by the relationships¹⁵ (1) and (2) for in-source polymers and for post-irradiation polymers, respectively.

$$[\eta] = 4.65 \times 10^{-4} \bar{M}_n^{0.64} \quad (1)$$

$$[\eta] = 4.07 \times 10^{-6} \bar{M}_n^{1.07} \quad (2)$$

The intrinsic viscosities of poly(potassium acrylates) were determined after converting these samples into poly(acrylic acid). For this purpose the

polymeric samples were dissolved in water, precipitated by 12*N* HCl, filtered, and dried under vacuum. The molecular weights were calculated by the relationship¹⁶ (3) in dioxane:

$$[\eta] = 7.6 \times 10^{-4} M^{0.50} \quad (3)$$

RESULTS

The conversion-time curves for the solid-state polymerization of acrylamide initiated by ultraviolet radiation are given in Figure 1. The data presented in this figure related to the samples which were open to atmosphere at two different temperatures. The conversion curves at 45°C were for polymers which were obtained under a strong source (source 1), whereas the curves at 28°C were for polymers obtained under a weak source (source 2). The thickness of the samples is specified in the legend to the figure. It can be seen that higher yields were obtained with thin samples.

The data on conversion versus time for the solid-state polymerization of acrylamide under the strong ultraviolet source (source 1) at 45°C in evacuated Pyrex tubes are given in Figure 2. Each tube contained about 2 g of polycrystalline monomer with an approximate thickness of 3 mm. It can be seen that conversions up to 55% could be obtained with an initial rate of polymerization of about 1%/hr. The molecular weights of the polyacrylamide obtained are also given in Figure 2.

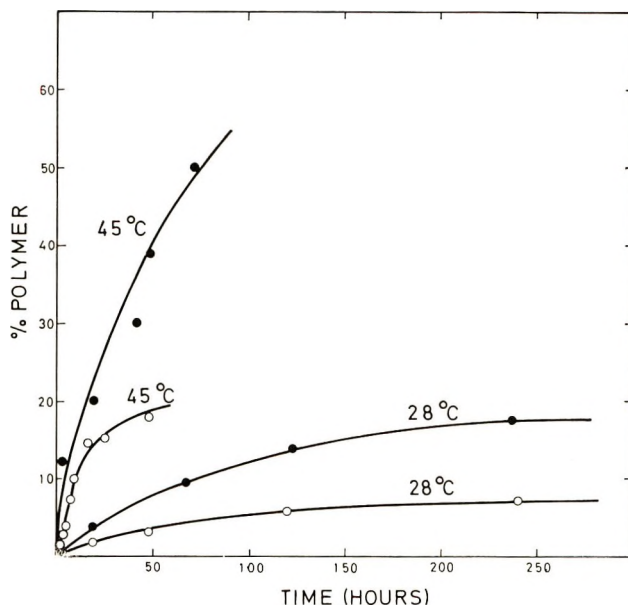


Fig. 1. Polymerization of acrylamide by ultraviolet radiation in air. For runs at 45°C under source 1 (○) sample weight 0.8 g; (●) sample weight 0.3 g. For runs at 28°C under source 2; (○) Sample weight 0.8 g (thickness about 1 mm); (●) sample weight 2.0 g, (thickness about 2 mm).

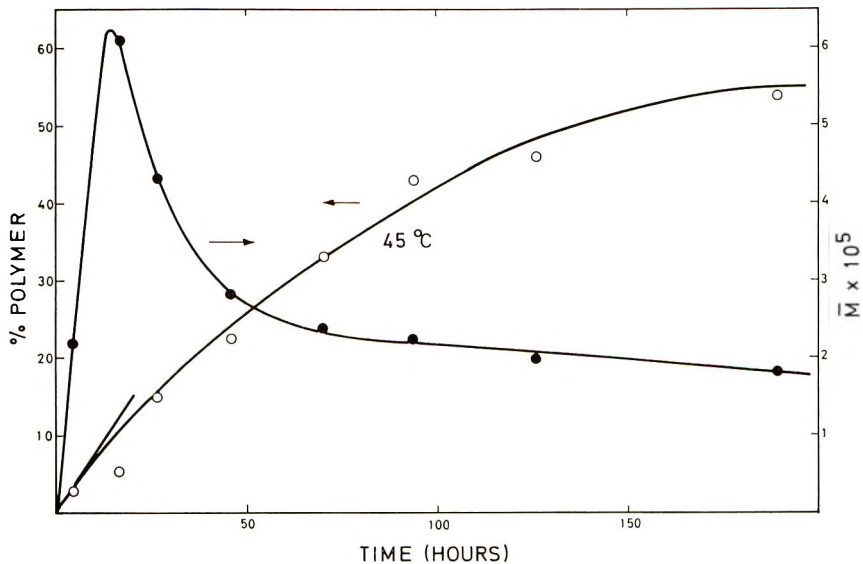


Fig. 2. Plots of (○) conversion and (●) \bar{M} , for polymerization of acrylamide by ultraviolet radiation *in vacuo* under source 1 at 45 °C. Sample weight 2.1 g (thickness about 3 mm).

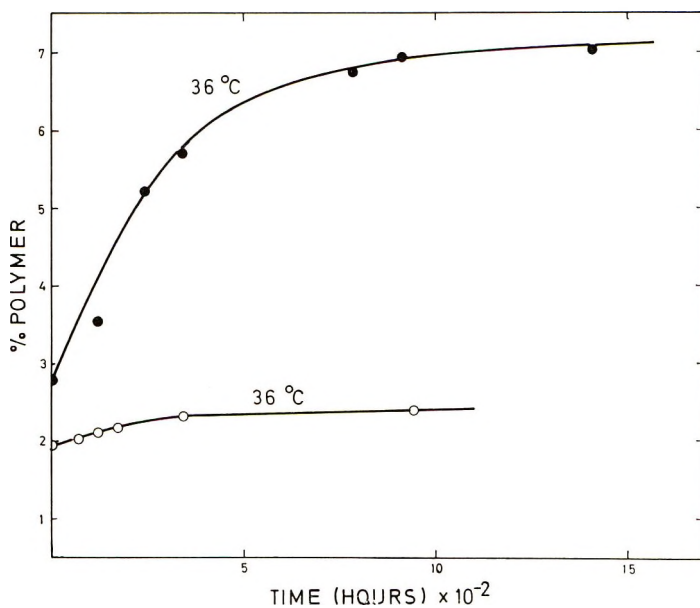


Fig. 3. Post-polymerization of acrylamide by ultraviolet radiation at 36 °C: (●) 2.1 g samples irradiated 4.5 hr at 45 °C under source 1; (○) 1.3 g samples irradiated 19 hr at 28 °C under source 2.

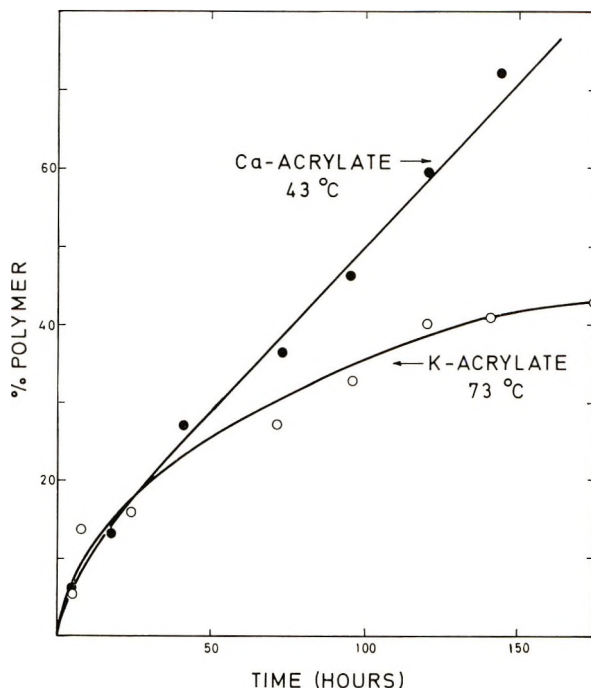


Fig. 4. Polymerization of potassium acrylate and calcium acrylate by ultraviolet radiation under source 3. (Samples weight, about 2 g with a thickness of about 3 mm.)

Results on the post-polymerization of acrylamide at 36°C are given in Figure 3. The lower curve refers to samples open to the atmosphere while the upper curve refers to samples in vacuo. The molecular weights of polyacrylamides post-irradiated in vacuo show a regular increase from 1.48×10^5 to 2.04×10^5 . Corresponding data are not available for the samples open to the atmosphere.

The conversion-time curves for the solid-state polymerization of potassium acrylate and calcium acrylate by ultraviolet radiation (source 3) at 73 and 43°C, respectively are given in Figure 4. Molecular weight data are available only for poly(potassium acrylate) and indicate a decrease from 4.7×10^5 to 2.2×10^5 as the conversion increases from 15.8 to 43.6-%.

The evacuated Pyrex or quartz tubes containing hexamethylcyclotrisiloxane were irradiated at 55°C under source 3 for a period of 16 hr. The material was dissolved in 2-butanone and poured into methanol; no polymer was obtained.

DISCUSSION

A free-radical reaction mechanism proposed for the solid-state polymerization of acrylamide and related monomers is supported by various observations including detailed analysis of the ESR spectrum.^{4,12} The

polymerization of crystalline monomers under ultraviolet radiation provides additional evidence for the free-radical initiation.

Higher yields are obtained with thin polycrystalline acrylamide samples, as seen in Figure 1, indicating that the polymerization reaction takes place essentially on the surface of crystals. This would be expected, since high scattering and absorption would permit little of the radiation to penetrate below the surface of the sample.

The γ -radiation-initiated solid-state polymerization of acrylamide was not influenced by the presence of oxygen,³ although oxygen is normally an efficient inhibitor of free-radical reactions. It was shown that oxygen can not penetrate into the lattice of acrylamide.¹⁷ We have observed that both the rate and degree of polymerization are decreased by the presence of oxygen.

The molecular weights for polyacrylamide samples obtained with ultraviolet initiation under vacuum can reach 6×10^5 at the beginning of the reaction. It will be seen from the Figure 2 that molecular weight decreases at high conversions. In the solid-state polymerization of acrylamide initiated by γ -radiation the effect of radiation on the polymer formed was studied in detail.¹⁵ By comparing the intrinsic viscosities and number-average molecular weights of branched and linear polymer chains of fractionated polymeric samples it was shown that extensive branching occurs during polymerization. However, the rapid decrease in molecular weight observed in Figure 2 is probably due to chain scission under these experimental conditions.

The effect of oxygen on polymerization rates may not be seen directly from the comparison of the data given in Figures 1 and 2, since the runs *in vacuo* were carried out in Pyrex tubes. However, with about 16 hr of irradiation (Figs. 1 and 2) *in vacuo* and in air, molecular weights of 6.10×10^5 and 1.73×10^4 , respectively, for the polymeric materials were obtained.

Post-polymerization is also more rapid when the ultraviolet irradiation is carried out in vacuum. The results shown in Figure 3 indicate a post-polymerization of about 5%, whereas very high conversions were observed in post-polymerizations after γ -irradiation.³ This difference might relate to the restriction of the ultraviolet-justified reaction to the surface of the sample.

It will be seen from the data presented in Figure 4 that conversion in ultraviolet-initiated solid-state polymerizations of potassium acrylate and calcium acrylate follows a different course. A limiting value of conversion was obtained for acrylamide (Figs. 1 and 2) and potassium acrylate, whereas the polymerization rate is almost constant after a 15% conversion in calcium acrylate. This is another indication of the importance of crystal structures in solid-state polymerization reactions.

This work was supported by the Turkish Scientific and Technical Research Council.

References

1. H. Morawetz and T. A. Fadner, *Makromol. Chem.*, **34**, 162 (1959).
2. T. Fadner, I. Rubin, and H. Morawetz, *J. Polym. Sci.*, **37**, 549 (1959).
3. B. Baysal, G. Adler, D. Ballantine, and P. Colombo, *J. Polym. Sci.*, **44**, 117 (1960).
4. G. Adler, D. Ballantine, and B. Baysal, *J. Polym. Sci.*, **48**, 195 (1960).
5. H. Morawetz and I. D. Rubin, *J. Polym. Sci.*, **57**, 669 (1962).
6. J. B. Lando and H. Morawetz, in *Macromolecular Chemistry, Paris 1963* (*J. Polym. Sci. C*, **4**), M. Magat, Ed., Interscience, New York, 1964, p. 789.
7. H. C. Heller, S. Schick, H. C. Yao, and T. Cole, *Mol. Cryst.*, **9**, 401 (1969).
8. G. Adler, *J. Chem. Phys.*, **31**, 348 (1959).
9. G. Adler and W. Reams, *J. Chem. Phys.*, 1698 (1960).
10. C. Sella and J. J. Trilatt, *C.R. Acad. Sci. (Paris)*, **253**, 1511 (1961).
11. C. Sella and R. Bensasson, *J. Polym. Sci.*, **56**, 277 (1962).
12. G. Adler and B. Baysal, *Mol. Cryst.*, **9**, 361 (1969).
13. C. H. Bamford, G. C. Eastmond, and C. Ward, *Proc. Roy. Soc. (London)*, **A271**, 357 (1963).
14. G. C. Eastmond, *Mol. Cryst.*, **9**, 383 (1969).
15. B. Baysal, G. Adler, D. Ballantine, and A. Glines, *J. Polym. Sci. B*, **1**, 257 (1963).
16. S. Newman, W. R. Krigbaum, C. Langier, and P. J. Flory, *J. Polym. Sci.*, **14**, 451 (1954).
17. G. Adler, in *Macromolecular Chemistry, Prague 1965* (*J. Polym. Sci. C*, **16**), O. Wichterle and B. Sedláček, Eds., Interscience, New York, 1967, p. 1211.

Received June 24, 1970

Revised September 3, 1970

Application of Gel-Permeation Chromatography to Studies of the Functionality Distribution of Carboxy- and Hydroxy-Polybutadienes

RONALD D. LAW, *Thiokol Chemical Corporation, Wasatch Division, Brigham City, Utah 84302*

Synopsis

Separations of carboxy-polybutadienes and hydroxy-polybutadienes according to functionality have been effected using stepwise elution from silica gel. Recoveries in the 95-100% range have been achieved. Subjection of the fractions obtained from the silica gel separation to analysis via gel-permeation chromatography and infrared or near-infrared spectroscopy yields not only functionality distribution data, but also provides the relationship between molecular weight distribution and functional type. Analytical techniques and interpretation of data are discussed.

INTRODUCTION

The primary objective of this work has been determination of the functionality distribution of polybutadiene liquid polymers used in the binder portion of solid propellants, especially carboxyl- and hydroxyl-terminated materials. The functionality distribution of a polymer is defined as the relative proportion of nonfunctional, monofunctional, difunctional, trifunctional, etc, present in the polymer and is a fundamental polymer property. Obviously, the relative proportions of each functional type within a polymer will exert a major influence on the mechanical behavior of any propellant compounded using that polymer. Functionality is defined as the ratio of number-average molecular weight (\bar{M}_n) to equivalent weight, and is a measure of the number of chemically reactive sites per molecule. A secondary objective of this work has been determination of the molecular weight distribution (MWD) within each functionality type, since this is also presumed to exert an influence on propellant mechanical properties.

The separation of polymers according to functionality has been a long-standing goal of the polymer chemist. Recently, a liquid-solid chromatographic technique has been developed, utilizing stepwise elution from activated silica gel,^{1,2} which holds considerable promise for effecting separations of this type. Application of this method to unsaturated polymers has generally been unsatisfactory, however, due to poor recovery from the column, apparently caused by polymerization on the column. Work in this laboratory has circumvented this problem by using partially deacti-

vated silica gel, and recycling the unfractionated portion through additional columns of increasing activity to obtain the desired resolution. Once the separation according to functionality has been achieved, gel-permeation chromatography (GPC) offers the potential of measuring the molecular weight distribution within each functionality type.

DISCUSSION

Data have been presented² showing that saturated carboxyl- and hydroxyl-terminated prepolymers can be separated according to functionality by gravity-fed column chromatography on 100–200 mesh activated silica gel by employing stepwise desorption. Stepwise desorption is accomplished by starting with a nonpolar solvent which washes the nonfunctional material through the column, followed by stepwise addition of a more polar solvent to the eluting stream, which selectively desorbs the more polar materials of high functionality. Each polymer requires different solvent systems and different solvent programming. This method has been successfully adapted to unsaturated systems. This has been accomplished by partially deactivating the silica gel by adding a small amount of ethanol to the slurry used in packing the chromatographic column. Because the column is less active, the first material which comes through has not been efficiently fractionated and must be put through another column of higher activity, prepared using less ethanol. The optimum column activity is different for each polymer and must be determined empirically.

Since both the number-average molecular weight (\bar{M}_n) and the molecular weight distribution (MWD) are of interest, GPC has been used extensively in testing the fractions. This technique has the advantage of requiring only about 5–10 mg of sample and provides MWD, from which \bar{M}_n can be calculated.

An additional refinement consists of the analysis of a large number of fractions to minimize mixing between functionality types. This has been accomplished by using semimicro infrared and near-infrared techniques for the measurement of equivalent weight.

It should be noted that the key to this separation apparently lies in the stepwise change in solvent, as opposed to a gradual continuous change. The well-known elution-gradient technique⁴ which employs a gradual change in solvent composition in conjunction with a thermal gradient, is known to effect fractionation on the basis of molecular weight presumably due to solubility factors. By contrast, the data in Tables V–XII indicate that fractionation by a stepwise change in solvent composition, in the presence of suitably active adsorption sites, is more responsive to equivalent weight. The originators of this type of technique² suggest that this effect is explainable simply by the difference in the number of polar groups per molecule which can be adsorbed on the surface of the silica gel as one progresses from nonfunctional, which would not adsorb at all, through monofunctional to difunctional and above, the stepwise change in solvent pre-

sumably effecting a cleaner desorption. We have also assumed that this is the primary mechanism of separation, but there is one notable exception when dealing with unsaturated systems. The final one or two fractions in a run almost always exhibit a rise in equivalent weight compared to the trend of preceding fractions. These last fractions are also extremely high in *cis* unsaturation compared to the bulk of the polymer, strongly suggesting that steric factors have come into play for this last bit of material to come off the column.

Fractionation systems have been developed for four hydroxy-terminated polybutadienes (HTPB), two carboxy-terminated polybutadienes (CTPB), and for three randomly polymerized polybutadiene-acrylic acid-acrylonitrile polymers (PBAN).

In practice, the separation according to functionality is not completely clean, with such factors as column activity, nature of neighboring chemical groups, and the type of unsaturation (*cis*, *trans*, vinyl) all contributing to the behavior of the polymer on the column. This is particularly true for unsaturated polymers where a less active column must be employed to obtain complete recovery. This renders the decision as to where the fractions are to be grouped for final analysis somewhat arbitrary, and in practice a "cut try" approach has been used. Experience has shown that material under a peak on the elution profile is usually homogeneous, and this is normally the basis for grouping the fractions. The fractions for analysis are first subjected to infrared analysis for carboxyl equivalent weight or near-infrared analysis for hydroxyl equivalent weight. Calibration curves are prepared from a solution of whole polymer whose exact equivalent weight has been determined by chemical analysis. The fractions are then subjected to GPC for determination of molecular weight distribution and number-average molecular weight (\bar{M}_n). Commercially certified polystyrene, polyglycol, and alkane standards are used in GPC calibration, but absolute molecular weight determinations are possible only if the elution characteristics of these standards are demonstrated to be identical to those of the polymer being tested. If not identical, the difference must be determined and a correction applied to the raw GPC data. To do this, fractions of narrow molecular weight distribution of the polymers tested have been isolated by using preparative-scale GPC. The apparatus and technique used have been described elsewhere.³ The true number-average molecular weight of selected fractions have been determined independently via vapor pressure osmometry (VPO). The weight-average molecular weight (\bar{M}_w) of these fractions cannot be determined directly, due to their low molecular weight, but \bar{M}_w may be estimated from the ratio of \bar{M}_w/\bar{M}_n as calculated from raw GPC data and then corrected from the observed dispersion of known standards.³ The molecular weight corresponding to the GPC elution peak is then calculated as the root mean square of \bar{M}_n and \bar{M}_w . A plot of GPC elution volume versus peak molecular weight, in connection with similar data from known standards, yields a series of suitable calibration curves, as shown in Figure 1.

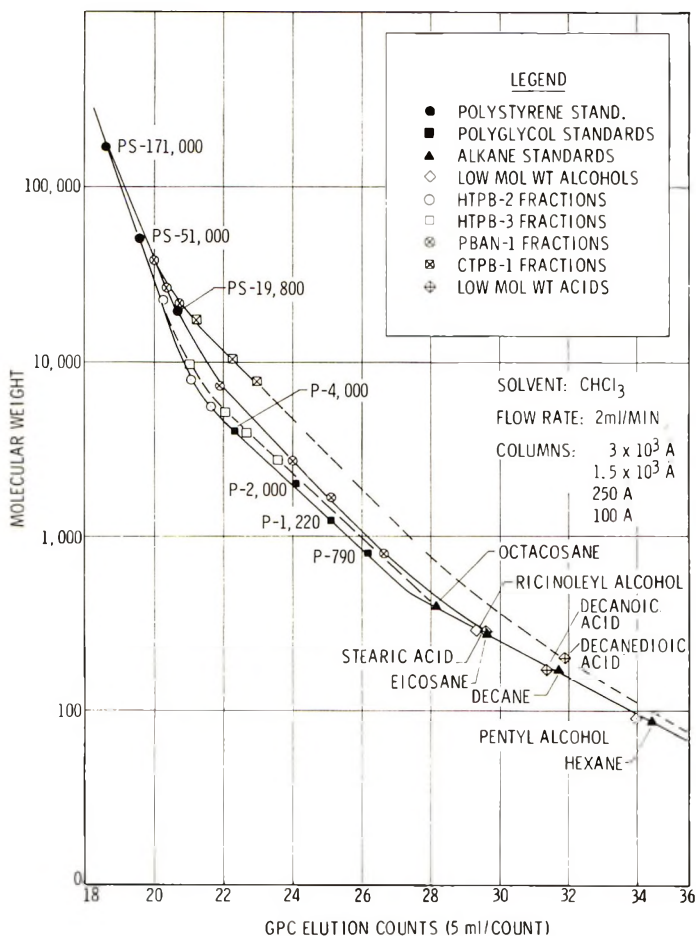


Fig. 1. Calibration curves.

As a check on the accuracy of \bar{M}_n values calculated from corrected GPC data, a comparison of \bar{M}_n for the whole polymer via VPO and GPC is given

TABLE I
Comparison of \bar{M}_n via GPC and VPO

| Material | \bar{M}_n | | Equiv weight | Average functionality | |
|----------|-------------|--------|--------------|-----------------------|---------------|
| | By GPC | By VPO | | From GPC data | From VPO data |
| PBAN-1 | 2989 | 2947 | 1524 | 1.96 | 1.93 |
| PBAN-2 | 2933 | 2840 | 1548 | 1.90 | 1.84 |
| HTPB-4 | 2250 | 2225 | 993 | 2.27 | 2.24 |
| HTPB-1 | 2531 | 2282 | 1346 | 1.88 | 1.70 |
| HTPB-3 | 3636 | 3564 | 1370 | 2.66 | 2.60 |
| HTPB-2 | 5906 | 5193 | 2924 | 2.02 | 1.78 |
| CTPB-1 | 4149 | 4159 | 1942 | 2.14 | 2.14 |
| CTPB-2 | 3440 | 3470 | 2123 | 1.62 | 1.63 |

in Table I. Although the VPO results are consistently slightly lower than GPC results, the agreement is considered excellent for this type of work. Since GPC is considerably less time-consuming and less tedious, it is the preferred method in this laboratory, provided that a good calibration curve based on VPO data has been previously established.

EXPERIMENTAL

Vapor-Pressure Osmometry

VPO data were obtained in chloroform by using a Mechrolab model 301A instrument. Pure octacosane (Aldrich Chemical) was used as primary standard. Both standard and samples were run at four different concentration levels and the results were extrapolated to infinite dilution by using the method of Muenker and Hudson.¹

Gel-Permeation Chromatography

GPC data were obtained at ambient temperature by using a Waters Model 100 instrument with chloroform as solvent. Four 4 ft \times 3/8 in. columns were employed, packed with Styragel having nominal porosities of $3 \times 10^3 \text{ \AA}$, $1.5 \times 10^3 \text{ \AA}$, 250 \AA , and 100 \AA , and at a flow rate of 2 ml/min. Calibration standards are presented in Figure 1.

Hydroxyl Equivalent Weight

Hydroxyl equivalent weight of the whole polymer was determined as follows. A 3-g sample was refluxed with 5 ml of freshly prepared 20% acetic anhydride in pyridine for 1 hr on a steam bath. After cooling, 80 ml water and 20 ml benzene were added and the solution was back-titrated with 0.5 *N* standard KOH to a phenolphthalein end point. A reagent blank was carried through the entire procedure. The one-sigma standard deviation of this method is ± 0.0013 equivalent/100 g. Hydroxyl equivalent weight of polymer fractions was determined by near-infrared spectroscopy using a Beckman DK-2 recording spectrophotometer. The hydroxyl peak at 2760 $m\mu$ was measured in CCl_4 solution with solvent in the reference beam, with the use of 5 cm matched cells. Equivalent weights were calculated by comparison with a standard curve prepared from analysis of whole polymer solutions.

Carboxyl Equivalent Weight

Carboxyl equivalent weight of the whole polymer was determined as follows. A 2-g sample was dissolved in 100 ml toluene and the solution titrated with standard 0.1*N* alcoholic KOH to a thymolphthalein end point. A reagent blank was carried through the procedure. The one sigma standard deviation of this method is ± 0.0007 equivalent/100 g. Carboxyl equivalent weight of polymer fractions was determined by infrared spectroscopy by using a Beckman IR-IV spectrophotometer. The carboxyl band

TABLE II
Operating Conditions for Silica Gel Separations

| Polymer | Column activity, ml C ₂ H ₅ OH/150 g SiO ₂ | | | | SiO ₂ , g/g of Polymer | | | |
|-------------|---|-------|-------|-------|-----------------------------------|-------|-------|-------|
| | Run A | Run B | Run C | Run D | Run A | Run B | Run C | Run D |
| PBAN-1 | 40 | 26 | — | — | 150 | 455 | — | — |
| PBAN-2 | 40 | 25 | — | — | 150 | 428 | — | — |
| Aged PBAN-2 | 40 | 26 | 0 | — | 150 | 313 | 556 | — |
| CTPB-1 | 26 | 26 | 26 | 7.5 | 115 | 161 | 518 | 150 |
| CTPB-2 | 26 | 23 | 20 | — | 115 | 211 | 341 | — |
| HTPB-3 | 25 | 15 | 4 | — | 150 | 146 | 150 | — |
| HTPB-2 | 17 | 13 | 9 | 6.5 | 75 | 75 | 75 | 100 |
| HTPB-1 | 20 | 10 | — | — | 150 | 278 | — | — |
| HTPB-4 | 20 | 11 | — | — | 150 | 625 | — | — |

TABLE III-A
Solvent Programs for SiO₂ Separations, Run A

| Solvent | Volume solvent, ml | | | | | | | | | |
|--|--------------------|--------|----------------|--------|--------|--------|--------|--------|--------|--|
| | PBAN-1 | PBAN-2 | Aged PBAN-2 | CTPB-1 | CTPB-2 | HTPB-3 | HTPB-2 | HTPB-1 | HTPB-4 | |
| CCl ₄ | 700 | 700 | 700 | 200 | 1000 | 1000 | 1000 | 1000 | 1000 | |
| CCl ₄ -CHCl ₃ (90:10) | 100 | 100 | 100 | 50 | 50 | 100 | 100 | 100 | 100 | |
| CCl ₄ -CHCl ₃ (80:20) | 100 | 100 | 100 | 50 | 50 | 100 | 100 | 100 | 100 | |
| CCl ₄ -CHCl ₃ (60:40) | 100 | 100 | 100 | 50 | 50 | 300 | 300 | 100 | 100 | |
| CCl ₄ -CHCl ₃ (40:60) | 100 | 100 | 100 | 50 | 50 | 100 | 100 | 100 | 100 | |
| CCl ₄ -CHCl ₃ (20:80) | 100 | 100 | 100 | 50 | 50 | 300 | 300 | 100 | 100 | |
| CHCl ₃ | 1200 | 1200 | 1200 | 500 | 500 | 600 | 600 | 1000 | 1000 | |
| CHCl ₃ -C ₂ H ₅ OH (99:1) | 100 | 100 | 100 | — | — | 100 | 100 | 200 | 200 | |
| CHCl ₃ -C ₂ H ₅ OH (98:2) | 100 | 100 | 100 | — | — | 100 | 100 | 200 | 200 | |
| CHCl ₃ -C ₂ H ₅ OH (96.5:3.5) | 200 | 200 | 200 | — | — | 100 | 100 | 200 | 200 | |
| CHCl ₃ -C ₂ H ₅ OH (95:5) | 800 | 800 | 800 | 500 | 500 | 300 | 100 | 500 | 600 | |
| CHCl ₃ -C ₂ H ₅ OH (90:10) | 200 | 200 | 200 | 100 | 100 | 100 | 100 | 100 | 100 | |
| CHCl ₃ -C ₂ H ₅ OH (80:20) | 100 | 100 | 100 | 100 | — | 100 | — | 100 | 100 | |
| CHCl ₃ -C ₂ H ₅ OH (70:30) | 100 | 100 | 100 | — | 100 | 100 | 100 | 100 | 100 | |
| CHCl ₃ -C ₂ H ₅ OH (60:40) | 100 | 100 | 100 | — | — | 100 | — | 100 | 100 | |
| CHCl ₃ -C ₂ H ₅ OH (50:50) | 100 | 100 | 100 | 100 | 100 | 100 | 100 | 100 | 100 | |
| CHCl ₃ -C ₂ H ₅ OH (25:75) | 600 | 600 | 600 | — | 100 | 100 | 100 | 100 | 200 | |
| C ₂ H ₅ OH | — | — | — | 300 | 500 | 500 | 400 | 500 | 300 | |

TABLE III-B
Solvent Programs for SiO₂ Separations, Run B

| Solvent | Volume solvent, ml | | | | | | | | | |
|--|--------------------|--------|----------------|--------|--------|--------|--------|--------|--------|--|
| | PBAN-1 | PBAN-2 | Aged PBAN-2 | CTPB-1 | CTPB-2 | HTPB-3 | HTPB-2 | HTPB-1 | HTPB-4 | |
| CO ₂ | 500 | 500 | 600 | 200 | 500 | 1000 | 1000 | 1000 | 800 | |
| CO ₂ -CHCl ₃ (90:10) | 100 | 100 | 100 | 50 | 50 | 300 | 100 | 100 | 100 | |
| CO ₂ -CHCl ₃ (80:20) | 100 | 100 | 100 | 50 | 50 | 100 | 100 | 100 | 100 | |
| CO ₂ -CHCl ₃ (60:40) | 100 | 100 | 100 | 50 | 50 | 100 | 100 | 100 | 100 | |
| CO ₂ -CHCl ₃ (40:60) | 100 | 100 | 100 | 50 | 50 | 100 | 100 | 100 | 100 | |
| CO ₂ -CHCl ₃ (20:80) | 100 | 100 | 100 | 50 | 50 | 100 | 100 | 100 | 100 | |
| CHCl ₃ | 500 | 500 | 500 | 500 | 500 | 600 | 1000 | 800 | 500 | |
| CHCl ₃ -C ₂ H ₅ OH (99:1) | 100 | 100 | 100 | — | — | — | 100 | 100 | 100 | |
| CHCl ₃ -C ₂ H ₅ OH (98:2) | 100 | 100 | 100 | — | 100 | 100 | 100 | 100 | 100 | |
| CHCl ₃ -C ₂ H ₅ OH (96.5:3.5) | 100 | 100 | 100 | — | — | — | 100 | 100 | 100 | |
| CHCl ₃ -C ₂ H ₅ OH (95:5) | 500 | 500 | 500 | 500 | 500 | 100 | 100 | 100 | 500 | |
| CHCl ₃ -C ₂ H ₅ OH (90:10) | 100 | 100 | 100 | 100 | 100 | 100 | 50 | 100 | 100 | |
| CHCl ₃ -C ₂ H ₅ OH (80:20) | 100 | 100 | 100 | 100 | — | — | — | 100 | 100 | |
| CHCl ₃ -C ₂ H ₅ OH (70:30) | 100 | 100 | 100 | — | 100 | 100 | 50 | 100 | 100 | |
| CHCl ₃ -C ₂ H ₅ OH (60:40) | 100 | 100 | 100 | — | — | 100 | — | 100 | — | |
| CHCl ₃ -C ₂ H ₅ OH (50:50) | 100 | 100 | 100 | 100 | 100 | 100 | 50 | 100 | 100 | |
| CHCl ₃ -C ₂ H ₅ OH (25:75) | 300 | 400 | 500 | — | 100 | 100 | 50 | 100 | 100 | |
| C ₂ H ₅ OH | — | — | — | 300 | 500 | 400 | 500 | 200 | 300 | |

TABLE III-C
Solvent Programs for SiO₂ Separations, Runs C and D

| Solvent | Volume solvent, ml | | | | | | | |
|--|--------------------|-------|--------|-------|---------|-------|---------|-------|
| | Aged PEAN-2, | | CTPB-1 | | CTPB-2, | | HTPB-3, | |
| | run C | Run D | Run C | Run D | run C | run C | Run C | Run D |
| CCl ₄ | 500 | 300 | 500 | 500 | 500 | 1000 | 1000 | 1000 |
| CCl ₄ -CHCl ₃ (90:10) | 50 | 100 | 50 | 50 | 50 | 100 | 100 | 100 |
| CCl ₄ -CHCl ₃ (80:20) | 50 | 100 | 50 | 50 | 50 | 100 | 100 | 300 |
| CCl ₄ -CHCl ₃ (60:40) | 50 | 100 | 50 | 50 | — | 100 | 300 | 100 |
| CCl ₄ -CHCl ₃ | 50 | 50 | 50 | 50 | 50 | 100 | 100 | 300 |
| CCl ₄ -CHCl ₃ (20:80) | 50 | 50 | 50 | 50 | 50 | 100 | 300 | 100 |
| CHCl ₃ | 300 | 500 | 300 | 300 | 500 | 100 | 500 | 300 |
| CHCl ₃ -C ₂ H ₅ OH (99:1) | 100 | 100 | — | — | — | — | 50 | — |
| CHCl ₃ -C ₂ H ₅ OH (98:2) | 100 | 100 | 100 | 100 | 100 | 100 | 50 | 100 |
| CHCl ₃ -C ₂ H ₅ OH (96.5:3.5) | 100 | 100 | — | — | — | — | 50 | — |
| CHCl ₃ -C ₂ H ₅ OH (95:5) | 200 | 500 | 500 | 500 | 500 | 100 | 50 | 100 |
| CHCl ₃ -C ₂ H ₅ OH (90:10) | 50 | 100 | 100 | 100 | 100 | 100 | 50 | 100 |
| CHCl ₃ -C ₂ H ₅ OH (80:20) | 50 | 100 | 100 | 100 | — | — | — | — |
| CHCl ₃ -C ₂ H ₅ OH (70:30) | 50 | — | — | — | 100 | 100 | 50 | 100 |
| CHCl ₃ -C ₂ H ₅ OH (60:40) | — | — | — | — | — | — | — | — |
| CHCl ₃ -C ₂ H ₅ OH (50:50) | 100 | 100 | 100 | 100 | 100 | 100 | 50 | 100 |
| CHCl ₃ -C ₂ H ₅ OH (25:75) | 500 | 100 | 100 | 100 | 100 | 100 | 50 | 100 |
| C ₂ H ₅ OH | — | 200 | 600 | 600 | 500 | 400 | 500 | 600 |

TABLE IV
Analytical Data for PBAN-1 Separation, Runs 6 and 7

| Fraction | Polymer, % | \bar{M}_n | COOH equivalent weight | C≡N equivalent weight | COOH weight | C≡N functionality | Unsaturation, % | |
|----------|------------|-------------|------------------------------|-----------------------------|----------------|----------------------|-----------------|-------------|
| | | | | | | | Cis | Trans Vinyl |
| 1B | 10.7 | 1625 | 7136 | 1028 | 0.23 | 1.58 | 40 | 50 |
| 2B | 3.0 | 2159 | 2565 | 714 | 0.84 | 3.02 | 30 | 60 |
| 3B | 9.4 | 3465 | 1688 | 491 | 2.05 | 7.03 | 30 | 58 |
| 4B | 6.0 | 4380 | 1642 | 547 | 2.67 | 8.01 | 26 | 63 |
| 5B | 2.5 | 4203 | 1358 | 900 | 3.09 | 4.67 | 38 | 54 |
| 6B | 1.2 | 2712 | 560 | ∞ | 4.84 | 0.00 | 73 | 23 |
| 2A | 3.7 | 2524 | 2707 | 744 | 0.93 | 3.39 | 11 | 76 |
| 3A | 1.5 | 2288 | 1659 | 688 | 1.38 | 3.33 | 19 | 68 |
| 4A | 3.4 | 2999 | 2008 | 591 | 1.49 | 5.07 | 22 | 67 |
| 5A | 10.5 | 3549 | 1602 | 430 | 2.22 | 8.25 | 24 | 60 |
| 6A | 5.0 | 3185 | 1570 | 442 | 2.03 | 7.21 | 22 | 68 |
| 7A | 4.9 | 2985 | 1645 | 453 | 1.81 | 6.59 | 24 | 63 |
| 8A | 3.2 | 3843 | 1433 | 433 | 2.68 | 8.88 | 21 | 69 |
| 9A | 6.1 | 2928 | 1119 | 521 | 2.62 | 5.62 | 19 | 70 |
| 10A | 4.2 | 2523 | 661 | 615 | 3.82 | 4.10 | 19 | 69 |
| 11A | 5.2 | 3291 | 839 | 693 | 3.92 | 4.75 | 23 | 69 |
| 12A | 3.3 | 3430 | 1188 | 802 | 2.89 | 4.28 | 38 | 53 |
| 13A | 8.1 | 2246 | 1879 | 1887 | 1.20 | 1.19 | 89 | 9 |
| | 91.9* | | | | | | | |

* Unrecovered material known to include 5% soap (nonfunctional) plus 1-2% carboxy cyclohexenes (monofunctional).

in the 5.7–5.9 μ region was measured in CHCl_3 solution with solvent in the reference beam by use of 1.0 mm matched cells. Equivalent weights were calculated by reference to a standard curve prepared from analysis of whole polymer solutions.

Liquid-Solid Chromatography

A glass chromatography column, 24 in. \times 1 in., was slurry packed with activated 60–200 mesh silica gel (average particle size 123 μ), grade 950 from Grace Chemical. The slurry was prepared using 350 ml CHCl_3 for each 150 g of SiO_2 plus the amount of ethanol indicated in Table II. After packing, the column was purged with 300 ml of CCl_4 for each 150 g of SiO_2 . Polymer sample sizes were as indicated in Table II, and the solvent programs are given in Table III. Commercial reagent-grade solvents were used as received. The ethanol employed was denatured 3A alcohol containing 5% 2-propanol (J. T. Baker). Approximately 40 ml fractions were collected during the run, and were weighed after evaporation. An elution profile was obtained by plotting weight of polymer/50 ml versus total volume of eluant, and the material under elution peaks was placed together for determination of equivalent weight, \bar{M}_n , and MWD.

Calculation of Final Data

Since most of the fractions tested did not yield functionalities which were exact integers, the functionality distributions were calculated from the data in Tables IV thru XII by assuming that only two functional types are present in a given fraction, i.e., a measured functionality of 0.85 reflects a mixture of 15% nonfunctional and 85% monofunctional. Obviously this

TABLE V
Analytical Data for PBAN-2 Separation, Runs 1 and 2

| Fraction | Polymer, % | \bar{M}_n | COOH equivalent weight | C \equiv N equivalent weight | COOH func- tionality | C \equiv N func- tionality |
|----------|---------------|-------------|------------------------------|--------------------------------------|----------------------------|------------------------------------|
| 1B | 9.1 | 1681 | 6372 | 899 | 0.27 | 1.87 |
| 2B | 3.0 | 2232 | 3097 | 530 | 0.72 | 4.21 |
| 1A { 3B | 10.3 | 3112 | 2564 | 418 | 1.21 | 7.44 |
| 4B | 7.4 | 3709 | 1432 | 546 | 2.59 | 6.79 |
| 5B | 5.5 | 2728 | 663 | 1359 | 4.11 | 2.01 |
| 2A | 3.2 | 2315 | 1898 | 390 | 1.22 | 5.94 |
| 3A | 4.2 | 2799 | 2103 | 415 | 1.32 | 5.74 |
| 4A | 11.7 | 3364 | 1777 | 257 | 1.90 | 13.09 |
| 5A | 8.5 | 3408 | 1563 | 260 | 2.17 | 13.11 |
| 6A | 4.7 | 2728 | 1332 | 388 | 2.05 | 7.03 |
| 7A | 5.8 | 3304 | 1061 | 338 | 3.11 | 9.78 |
| 8A | 7.8 | 2685 | 708 | 374 | 3.79 | 7.18 |
| 9A | 10.4 | 4108 | 1472 | 325 | 2.79 | 12.64 |
| 10A | 7.6 | 1396 | 1265 | 2914 | 1.10 | 0.48 |
| | 99.2 | | | | | |

TABLE VI
Analytical Data for PBAN-2 Aged 90 Days at 200°F, Runs 1 and 2

| Fraction | Polymer, % | \bar{M}_n | COOH equivalent weight | C≡N equivalent weight | COOH func- tionality | C≡N func- tionality | |
|----------|---------------|-------------|------------------------------|-----------------------------|----------------------------|---------------------------|-------|
| 1B | 1C | 6.5 | 8034 | 6135 | 1196 | 1.31 | 6.83 |
| | 2C | 1.1 | 4074 | 5387 | 897 | 0.73 | 4.54 |
| | 3C | 6.1 | 1820 | 4367 | 1195 | 0.42 | 1.52 |
| | 4C | 10.8 | 3662 | 1321 | 710 | 2.77 | 5.16 |
| | 2B | 3.5 | 2052 | 3401 | 902 | 0.60 | 2.27 |
| 1A | 3B | 7.0 | 3443 | 2793 | 411 | 1.23 | 8.38 |
| | 4B | 3.0 | 4192 | 1678 | 491 | 2.50 | 8.54 |
| | 5B | 5.3 | 5545 | 1370 | 528 | 4.05 | 10.50 |
| | 6B | 4.2 | 4964 | 1119 | 493 | 4.44 | 10.07 |
| | 2A | 5.2 | 2321 | 1887 | 554 | 1.23 | 4.19 |
| 3A | 4.3 | 2845 | 2198 | 519 | 1.29 | 5.48 | |
| 4A | 12.1 | 2695 | 1631 | 250 | 1.65 | 10.78 | |
| 5A | 5.6 | 2616 | 1326 | 892 | 1.97 | 2.93 | |
| 6A | 2.6 | 3459 | 1057 | 400 | 3.27 | 8.65 | |
| 7A | 8.0 | 3153 | 582 | 367 | 5.42 | 8.59 | |
| 8A | 6.3 | 4527 | 1428 | 577 | 3.17 | 7.85 | |
| 9A | 7.2 | 3789 | 2825 | ∞ | 1.34 | 0.00 | |
| | 98.8 | | | | | | |

TABLE VII
Analytical Data for CTPB-1 Separation, Runs 12, 13, 14, and 18

| Fraction | Polymer, % | \bar{M}_n | COOH equivalent weight | COOH functionality | |
|----------|------------|-------------|------------------------------|-----------------------|------|
| 1D | 1D | 8.2 | 8474 | 6257 | 1.35 |
| | 2D | 4.1 | 8435 | 3333 | 2.53 |
| | 3D | 3.0 | 5480 | 2290 | 2.39 |
| | 4D | 2.4 | 8478 | 2836 | 2.99 |
| | 5D | 2.7 | 4424 | 1662 | 2.66 |
| 1B | 2C | 3.6 | 4395 | 3133 | 1.40 |
| | 3C | 5.2 | 4084 | 2785 | 1.47 |
| | 4C | 1.9 | 4158 | 3380 | 1.23 |
| | 5C | 0.8 | 3674 | 6759 | 0.54 |
| | 6C | 5.1 | 4150 | 2328 | 1.78 |
| 1A | 7C | 1.4 | 3896 | 1745 | 2.23 |
| | 2B | 5.5 | 3219 | 1732 | 1.86 |
| | 3B | 5.5 | 3183 | 1847 | 1.99 |
| | 4B | 2.1 | 3481 | 2460 | 1.42 |
| | 5B | 0.6 | 1771 | 1210 | 1.46 |
| 2A | 20.3 | 3204 | 1349 | 2.38 | |
| 3A | 22.6 | 2216 | 837 | 2.65 | |
| 4A | 1.6 | 3598 | 1258 | 2.86 | |
| | 96.6 | | | | |

TABLE VIII
Analytical Data for CTPB-2 Separation, Runs 1, 2, and 3

| Fraction | Polymer, % | \bar{M}_n | COOH equivalent weight | COOH functionality | |
|----------|------------|-------------|------------------------------|-----------------------|------|
| 1B | 1C | 15.5 | 5991 | 3534 | 1.70 |
| | 2C | 4.7 | 4619 | 2092 | 2.21 |
| | 3C | 2.4 | 4152 | 1550 | 2.68 |
| | 4C | 5.8 | 3879 | 1742 | 2.23 |
| | 5C | 5.7 | 4504 | 1585 | 2.84 |
| 1A | 2B | 3.1 | 4045 | 2353 | 1.72 |
| | 3B | 6.9 | 3667 | 2049 | 1.79 |
| | 4B | 3.9 | 3367 | 1689 | 1.99 |
| | 5B | 4.3 | 3199 | 1538 | 2.08 |
| | 2A | 7.7 | 1681 | 2439 | 0.69 |
| | 3A | 6.5 | 1568 | 1724 | 0.91 |
| | 4A | 11.1 | 2197 | 1342 | 1.64 |
| | 5A | 14.9 | 2422 | 1460 | 1.66 |
| | | 92.5 | | | |

TABLE IX
Analytical Data for HTPB-3, Runs 9, 10, and 11

| Fraction | Polymer, % | \bar{M}_n | OH equivalent weight | OH functionality | |
|----------|------------|-------------|----------------------------|---------------------|------|
| 1B | 1C | 1.7 | 7466 | 6070 | 1.23 |
| | 2C | 1.0 | 4411 | 12253 | 0.36 |
| | 3C | 11.4 | 6585 | 3228 | 2.04 |
| | 4C | 3.2 | 6537 | 3423 | 1.91 |
| | 5C | 2.0 | 4186 | 3460 | 1.21 |
| 1A | 2B | 4.4 | 6137 | 3023 | 2.03 |
| | 3B | 4.8 | 4424 | 2190 | 2.02 |
| | 4B | 5.1 | 4413 | 1532 | 2.88 |
| | 5B | 4.9 | 4834 | 1726 | 2.80 |
| | 6B | 3.8 | 5173 | 2155 | 2.40 |
| | 7B | 2.5 | 4611 | 1830 | 2.52 |
| | 8B | 2.0 | 3068 | 2324 | 1.32 |
| | 2A | 11.3 | 3490 | 1466 | 2.38 |
| | 3A | 17.3 | 3275 | 1110 | 2.95 |
| | 4A | 8.5 | 2153 | 727 | 2.96 |
| 5A | 8.1 | 1562 | 615 | 2.54 | |
| 6A | 3.1 | 1007 | 425 | 2.37 | |
| 7A | 3.0 | 2561 | 813 | 3.15 | |
| | 98.1 | | | | |

assumption is valid only if the separation has been good, sufficiently small fractions are taken, and the distribution of equivalent weights within a fraction is reasonably narrow. These conditions are judged to be met in the present case, but it should be recognized that the final functionality distribution data presented are subject to errors which are somewhat diffi-

TABLE X
Analytical Data for HTPB-2, Runs 5, 6, 7, and 8

| Fraction | Weight, % | \bar{M}_n | OII equivalent weight | OH functionality | |
|----------|-----------|-------------|-----------------------|------------------|------|
| 1C | 1E | 4.3 | ∞ | 0.00 | |
| | 2E | 9.6 | 11628 | 0.69 | |
| | 3E | 4.1 | 5930 | 3745 | 1.58 |
| | 2D | 2.5 | 7179 | 9253 | 0.78 |
| | 3D | 15.3 | 7533 | 4136 | 1.82 |
| | 4D | 6.9 | 7067 | 2930 | 2.41 |
| | 2C | 7.8 | 5969 | 3650 | 1.64 |
| | 3C | 5.7 | 5802 | 3398 | 1.71 |
| | 4C | 2.0 | 3859 | 2618 | 1.47 |
| | 5C | 2.7 | 3269 | 1603 | 2.04 |
| 2A | 1B | 4.6 | 5685 | 1484 | 3.83 |
| | 2B | 2.8 | 4857 | 1354 | 3.59 |
| | 3B | 2.7 | 4502 | 2118 | 2.13 |
| | 3A | 4.2 | 4694 | 2045 | 2.30 |
| | 4A | 6.1 | 3965 | 1750 | 2.27 |
| | 5A | 4.2 | 3400 | 1300 | 2.62 |
| | 6A | 3.3 | 2263 | 1060 | 2.13 |
| | 7A | 3.5 | 3446 | 1997 | 1.73 |
| | 92.2 | | | | |

TABLE XI
Analytical Data for HTPB-1 Separation, Runs 1 and 2

| Fraction | Polymer, % | \bar{M}_n | OH equivalent weight | OH functionality |
|----------|------------|-------------|----------------------|------------------|
| 1B | 6.4 | 2192 | ∞ | 0.00 |
| 2B | 5.4 | 5536 | 5111 | 1.08 |
| 3B | 5.9 | 4894 | 5055 | 0.97 |
| 4B | 5.1 | 2488 | 2848 | 0.87 |
| 5B | 3.9 | 1676 | 2384 | 0.70 |
| 2A | 5.0 | 2364 | 2175 | 1.09 |
| 3A | 19.7 | 2838 | 1347 | 2.11 |
| 4A | 33.2 | 2068 | 973 | 2.13 |
| 5A | 5.7 | 1441 | 693 | 2.08 |
| 6A | 6.9 | 1346 | 916 | 1.47 |
| | 97.2 | | | |

cult to evaluate at present. The data are presented to the nearest whole per cent for convenience sake, but in most cases are probably accurate only to the nearest 2-3%. Greater confidence may be placed in the nonfunctional and monofunctional data, since they are easier to separate. Final functionality distribution data are given in Figures 4-12. Also presented are molecular weight distributions for each functional type. These MWD curves were synthetically constructed from individual fraction GPC scans by assuming that each fraction contributes to each overall functionality

TABLE XII
Analytical Data for HTPB-4 Separation, Runs 2 and 3

| Fraction | Polymer, % | \bar{M}_n | OH equivalent weight | OH functionality | |
|----------|------------|-------------|----------------------|------------------|------|
| 1A | 1B | 3.2 | 1864 | ∞ | 0.00 |
| | 2B | 4.8 | 2622 | 2142 | 1.22 |
| | 3B | 3.7 | 2252 | 1780 | 1.27 |
| | 4B | 3.3 | 2226 | 1514 | 1.47 |
| | 2A | 5.9 | 2017 | 1919 | 1.05 |
| | 3A | 52.6 | 2254 | 964 | 2.34 |
| | 4A | 12.0 | 1962 | 729 | 2.69 |
| | 5A | 6.0 | 2495 | 565 | 4.42 |
| | 6A | 7.5 | 2305 | 888 | 2.60 |
| | 99.0 | | | | |

TABLE XIII
Functionality Distribution Versus Molecular Weight, PBAN-1^a

| Molecular weight | Weight, % | Functionality distribution, % | | | | | Penta |
|------------------|-----------|-------------------------------|------|------|------|-------|-------|
| | | Non | Mono | Di | Tri | Tetra | |
| 100,000 | 0.6 | 0 | 13 | 42 | 29 | 14 | 2 |
| 50,000 | 1.9 | 0 | 10 | 43 | 30 | 15 | 2 |
| 30,000 | 3.8 | 0 | 11 | 42 | 29 | 16 | 2 |
| 20,000 | 7.9 | 2 | 13 | 41 | 28 | 14 | 1 |
| 10,000 | 16.7 | 5 | 16 | 41 | 25 | 12 | 1 |
| 5,000 | 21.5 | 10 | 20 | 40 | 20 | 9 | 1 |
| 3,000 | 18.2 | 16 | 22 | 37 | 17 | 7 | 1 |
| 2,000 | 14.3 | 22 | 24 | 33 | 14 | 6 | 1 |
| 1,000 | 7.7 | 29 | 26 | 26 | 12 | 6 | 1 |
| 500 | 3.3 | 31 | 27 | 22 | 12 | 8 | 1 |
| 300 | 2.2 | 21 | 28 | 25 | 11 | 14 | 2 |
| X | — | 13 | 20 | 36 | 19 | 9 | 1 |
| \bar{M}_n | — | 1470 | 1980 | 2890 | 3220 | 2570 | 2420 |

^a Recovery = 98%.

type in proportion to the amount of that functionality type present in the fraction. An example of this calculation is given in Table XXII. Construction of the curves in Figures 4–12 also permits calculation of the functionality distribution at selected molecular weights within the molecular weight distribution range. These data are given in Tables XIII thru XXI.

RESULTS

Typical elution profiles from the stepwise liquid chromatography runs for PBAN-1 and HTPB-1 are presented in Figures 2 and 3. For the sake of brevity, the elution profiles from all the polymer runs have not been included, nor have the GPC scans for the many fractions which were collected; analytical data and results are given in Tables IV thru XII.

TABLE XIV
Functionality Distribution Versus Molecular Weight, PBAN-2^a

| Molecular weight | Weight, % | Functionality distribution, % | | | | | |
|------------------|-----------|-------------------------------|------|------|------|-------|-------|
| | | Non | Mono | Di | Tri | Tetra | Penta |
| 100,000 | 0.2 | 0 | 13 | 43 | 27 | 17 | 0 |
| 50,000 | 1.4 | 3 | 18 | 35 | 27 | 16 | 1 |
| 30,000 | 3.1 | 2 | 17 | 35 | 28 | 16 | 2 |
| 20,000 | 7.1 | 2 | 16 | 36 | 30 | 14 | 2 |
| 10,000 | 16.5 | 2 | 19 | 37 | 28 | 13 | 1 |
| 5,000 | 22.1 | 4 | 24 | 35 | 24 | 12 | 1 |
| 3,000 | 18.5 | 8 | 28 | 33 | 20 | 11 | 1 |
| 2,000 | 14.3 | 12 | 31 | 29 | 17 | 10 | 1 |
| 1,000 | 8.2 | 17 | 34 | 25 | 13 | 10 | 1 |
| 500 | 4.0 | 18 | 34 | 23 | 13 | 12 | 1 |
| 300 | 2.8 | 12 | 42 | 22 | 10 | 12 | 1 |
| X | — | 7 | 25 | 32 | 21 | 12 | 1 |
| \bar{M}_n | — | 1730 | 2360 | 3260 | 3650 | 2760 | 2730 |

^a Recovery = 98%.

Final functionality distribution and molecular weight distribution results are presented graphically in Figures 4–12, to which the reader is particularly directed. Quantitative correlation of these functionality distribution patterns with final cured formulation properties has not yet been established. It is extremely informative, however, to note the differences in functionality distribution and molecular weight distribution for polymers having similar

TABLE XV
Functionality Distribution Versus Molecular Weight, PBAN-1 Aged 90 Days at 200°F (0.35% Fe)^a

| Molecular weight | Weight, % | Functionality distribution, % | | | | | | |
|------------------|-----------|-------------------------------|------|------|------|-------|-------|------|
| | | Non | Mono | Di | Tri | Tetra | Penta | Hexa |
| 200,000 | 4.3 | 8 | 27 | 21 | 22 | 12 | 7 | 1 |
| 100,000 | 4.3 | 7 | 27 | 20 | 22 | 14 | 8 | 2 |
| 50,000 | 5.3 | 7 | 28 | 21 | 21 | 14 | 8 | 2 |
| 30,000 | 6.7 | 7 | 28 | 22 | 21 | 13 | 8 | 2 |
| 20,000 | 8.9 | 6 | 28 | 23 | 20 | 12 | 8 | 2 |
| 10,000 | 13.6 | 6 | 29 | 25 | 17 | 11 | 8 | 2 |
| 5,000 | 16.9 | 7 | 32 | 29 | 15 | 8 | 7 | 2 |
| 3,000 | 15.2 | 9 | 34 | 29 | 13 | 7 | 6 | 2 |
| 2,000 | 12.5 | 11 | 35 | 29 | 12 | 5 | 6 | 2 |
| 1,000 | 7.3 | 17 | 35 | 25 | 11 | 4 | 5 | 2 |
| 500 | 3.0 | 22 | 30 | 22 | 12 | 5 | 7 | 2 |
| 300 | 1.9 | 21 | 29 | 22 | 14 | 4 | 7 | 2 |
| X | — | 9 | 31 | 26 | 16 | 9 | 7 | 2 |
| \bar{M}_n | — | 2010 | 3640 | 3410 | 3730 | 5120 | 3670 | 3150 |

^a Recovery = 99%.

TABLE XVI
Functionality Distribution Versus Molecular Weight, CTPB-1^a

| Molecular weight | Weight, % | Functionality distribution, % | | | |
|------------------|-----------|-------------------------------|------|------|------|
| | | Non | Mono | Di | Tri |
| 200,000 | 0.5 | 0 | 30 | 40 | 27 |
| 100,000 | 1.6 | 0 | 36 | 43 | 18 |
| 50,000 | 4.2 | 0 | 34 | 45 | 18 |
| 30,000 | 7.0 | 1 | 33 | 45 | 18 |
| 20,000 | 10.6 | 1 | 29 | 46 | 22 |
| 10,000 | 15.2 | 1 | 20 | 52 | 25 |
| 7,000 | 18.9 | 1 | 12 | 54 | 29 |
| 5,000 | 18.9 | 1 | 9 | 53 | 34 |
| 3,000 | 11.1 | 1 | 8 | 50 | 38 |
| 2,000 | 6.7 | 1 | 7 | 48 | 41 |
| 1,000 | 3.1 | 1 | 9 | 47 | 40 |
| 500 | 1.4 | 1 | 14 | 44 | 39 |
| 300 | 0.6 | 1 | 15 | 49 | 32 |
| X | — | 1 | 15 | 51 | 30 |
| \bar{M}_n | 4149 | 3870 | 4380 | 3890 | 3670 |

^a Recovery = 97%.

average functionalities. The insight gained from this type of data is analogous to the difference between average molecular weight and molecular weight distribution, and should permit a much more meaningful evaluation of a polymer's potentialities for a given application. Attention is also directed to the variation in molecular weight distribution for each functionality type. In some polymers (CTPB-1, HTPB-1, and HTPB-4) the average molecular

TABLE XVII
Functionality Distribution Versus Molecular Weight, CTPB-2^a

| Molecular weight | Weight, % | Functionality distribution, % | | | |
|------------------|-----------|-------------------------------|------|------|------|
| | | Non | Mono | Di | Tri |
| 200,000 | 0.6 | 0 | 0 | 60 | 33 |
| 100,000 | 0.7 | 0 | 0 | 62 | 31 |
| 50,000 | 0.6 | 0 | 12 | 64 | 17 |
| 30,000 | 1.0 | 0 | 15 | 63 | 15 |
| 20,000 | 1.6 | 0 | 18 | 60 | 15 |
| 10,000 | 15.3 | 1 | 18 | 59 | 15 |
| 7,000 | 31.6 | 1 | 18 | 61 | 13 |
| 5,000 | 22.7 | 2 | 25 | 57 | 9 |
| 3,000 | 12.6 | 4 | 34 | 49 | 6 |
| 2,000 | 7.5 | 6 | 38 | 45 | 4 |
| 1,000 | 3.7 | 7 | 40 | 42 | 4 |
| 500 | 1.6 | 6 | 38 | 45 | 4 |
| 300 | 0.5 | 10 | 47 | 33 | 3 |
| X | — | 3 | 27 | 54 | 9 |
| \bar{M}_n | 3440 | 1660 | 2780 | 3780 | 4310 |

^a Recovery = 93%.

TABLE XVIII
Functionality Distribution Versus Molecular Weight, HTPB-3, LOT 90871^a

| Molecular weight | Weight, % | Functionality distribution, % | | | | |
|------------------|-----------|-------------------------------|------|------|------|-------|
| | | Non | Mono | Di | Tri | Tetra |
| 100,000 | 2.2 | 0 | 10 | 43 | 45 | 1 |
| 30,000 | 7.9 | 1 | 11 | 50 | 36 | 1 |
| 10,000 | 16.7 | 1 | 9 | 55 | 32 | 1 |
| 6,000 | 23.5 | 2 | 7 | 53 | 36 | 1 |
| 4,000 | 24.2 | 1 | 3 | 42 | 51 | 1 |
| 2,500 | 14.5 | 0 | 1 | 25 | 70 | 1 |
| 1,500 | 6.7 | 0 | 1 | 22 | 73 | 2 |
| 1,000 | 2.8 | 0 | 3 | 33 | 60 | 2 |
| 600 | 1.1 | 0 | 4 | 44 | 48 | 1 |
| 400 | 0.3 | 2 | 7 | 52 | 36 | 2 |
| 300 | 0.2 | 0 | 14 | 61 | 23 | 0 |
| X | — | 1 | 5 | 42 | 49 | 1 |
| \bar{M}_n | — | 4160 | 4900 | 4290 | 3226 | 2561 |

^a Recovery = 98%.

weight for all functionalities is nearly constant. In some cases \bar{M}_n increases with increasing functionality (CTPB-2) and in other cases it decreases (HTPB-3). In one case (PBAN-1), the \bar{M}_n starts low, rises to a maximum, and then decreases as functionality increases. For HTPB-2 the non- and monofunctional components are higher in \bar{M}_n than are the higher functionalities, which in turn are essentially constant in \bar{M}_n . Not surprisingly, therefore, functionality distribution for most polymers is not constant over the molecular weight range within the polymer, but can vary considerably from point to point across the molecular weight range. Data showing this relationship between functionality distribution and MWD are presented in Tables XIII–XXI. In one unusual case (HTPB-1) the mono-

TABLE XIX
Functionality Distribution Versus Molecular Weight, HTPB-2 LOT 46M-8^a

| Molecular weight | Weight, % | Functionality distribution, % | | | | |
|------------------|-----------|-------------------------------|------|------|------|-------|
| | | Non | Mono | Di | Tri | Tetra |
| 100,000 | 1.2 | 13 | 22 | 49 | 7 | 1 |
| 30,000 | 10.1 | 19 | 26 | 40 | 6 | 2 |
| 10,000 | 25.4 | 12 | 22 | 49 | 6 | 3 |
| 6,000 | 40.3 | 6 | 21 | 47 | 11 | 7 |
| 4,000 | 17.5 | 4 | 13 | 48 | 20 | 7 |
| 2,500 | 4.1 | 2 | 7 | 53 | 28 | 2 |
| 1,500 | 0.9 | 2 | 8 | 55 | 24 | 3 |
| 1,000 | 0.4 | 2 | 7 | 67 | 14 | 2 |
| 600 | 0.2 | 3 | 13 | 60 | 15 | 1 |
| X | — | 8 | 19 | 48 | 12 | 5 |
| \bar{M}_n | — | 8060 | 6420 | 5490 | 5350 | 5370 |

^a Recovery = 92%.

TABLE XX
Functionality Distribution Versus Molecular Weight, HTPB-1^a

| Molecular weight | Weight, % | Functionality distribution, % | | | |
|------------------|-----------|-------------------------------|------|------|------|
| | | Non | Mono | Di | Tri |
| 50,000 | 0.1 | 29 | 71 | 0 | 0 |
| 30,000 | 0.5 | 18 | 43 | 35 | 4 |
| 20,000 | 1.5 | 17 | 57 | 23 | 3 |
| 10,000 | 11.4 | 18 | 70 | 11 | 1 |
| 5,000 | 15.8 | 9 | 34 | 51 | 6 |
| 3,000 | 31.0 | 5 | 16 | 70 | 9 |
| 2,000 | 28.9 | 6 | 16 | 69 | 9 |
| 1,000 | 6.3 | 9 | 19 | 65 | 7 |
| 500 | 1.0 | 23 | 41 | 35 | 1 |
| 300 | 0.7 | 26 | 57 | 16 | 0 |
| X | — | 8 | 26 | 56 | 7 |
| \bar{M}_n | — | 2330 | 2830 | 2320 | 2410 |

^a Recovery = 97%.

and nonfunctional components are bimodal in MWD whereas the di- and trifunctional components are nearly normal in distribution. In another case (PBAN-1), the peak molecular weight increases steadily as functionality increases but \bar{M}_n for tetra- and pentafunctional material decreases due to a low molecular weight tail, and changes in functionality distribution and MWD due to accelerated aging are readily apparent.

CONCLUSIONS

The determination of functionality distribution by stepwise elution from silica gel has been successfully adapted to the analysis of unsaturated carboxy- and hydroxy-terminated polybutadienes.

TABLE XXI
Functionality Distribution Versus Molecular Weight, HTPB-4^a

| Molecular weight | Weight, % | Functionality distribution, % | | | | | |
|------------------|-----------|-------------------------------|------|------|------|-------|-------|
| | | Non | Mono | Di | Tri | Tetra | Penta |
| 50,000 | 0.2 | 0 | 13 | 21 | 15 | 34 | 17 |
| 30,000 | 0.4 | 0 | 16 | 21 | 21 | 28 | 14 |
| 20,000 | 0.9 | 0 | 8 | 25 | 28 | 26 | 13 |
| 10,000 | 3.2 | 5 | 6 | 36 | 30 | 15 | 8 |
| 5,000 | 9.6 | 3 | 15 | 42 | 30 | 7 | 4 |
| 3,000 | 29.6 | 3 | 16 | 46 | 30 | 3 | 1 |
| 2,000 | 43.5 | 3 | 13 | 49 | 33 | 2 | 1 |
| 1,000 | 10.6 | 3 | 16 | 41 | 32 | 5 | 2 |
| 500 | 0.9 | 19 | 8 | 30 | 27 | 11 | 6 |
| X | — | 3 | 14 | 45 | 31 | 4 | 2 |
| \bar{M}_n | — | 2050 | 2120 | 2150 | 2120 | 2400 | 2400 |

^a Recovery = 99%.

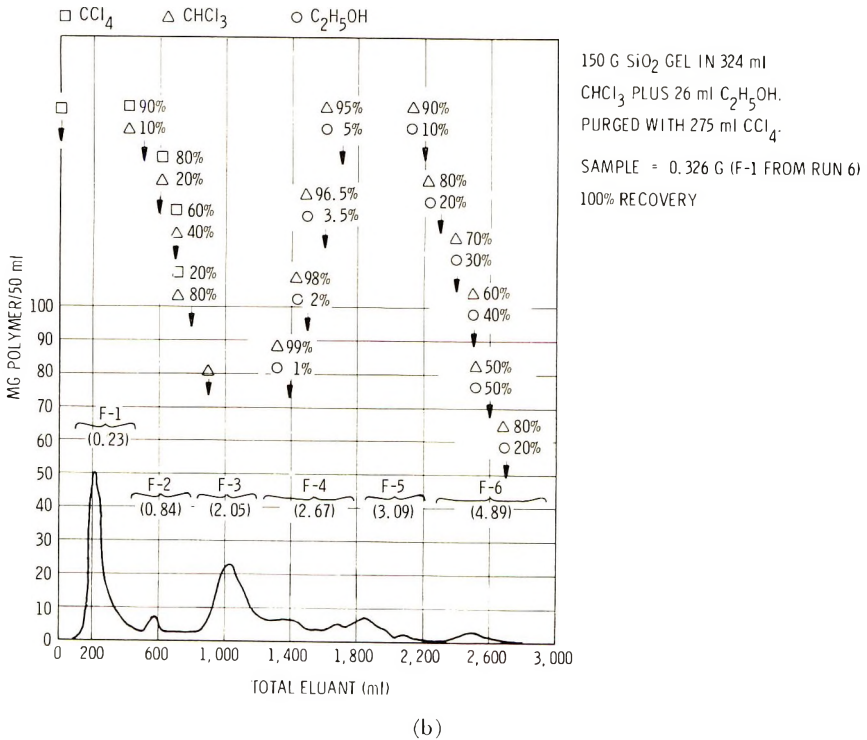
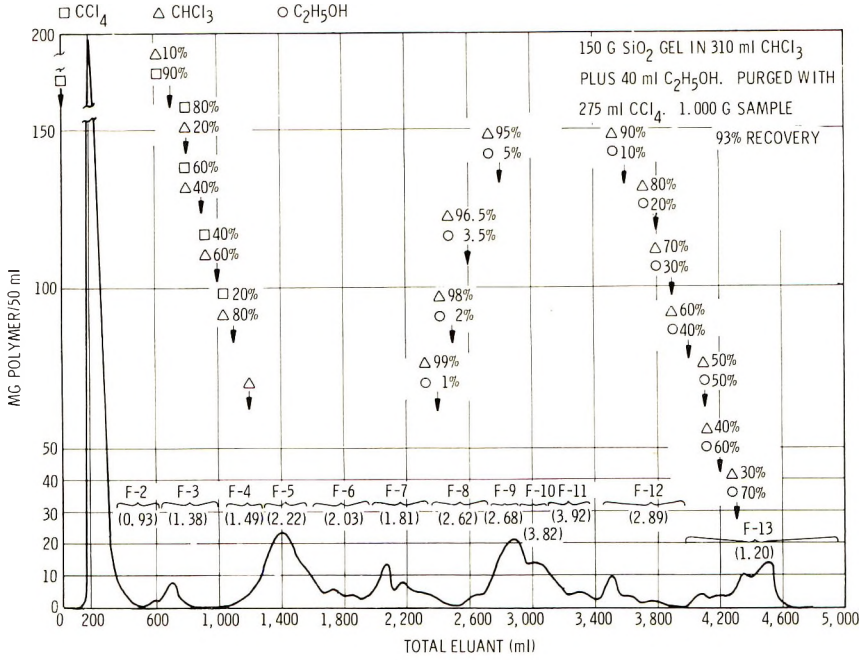


Fig. 2. Elution profiles: (A) PBAN-1 polymer, run 6; (B) PBAN-1 polymer, run 7.

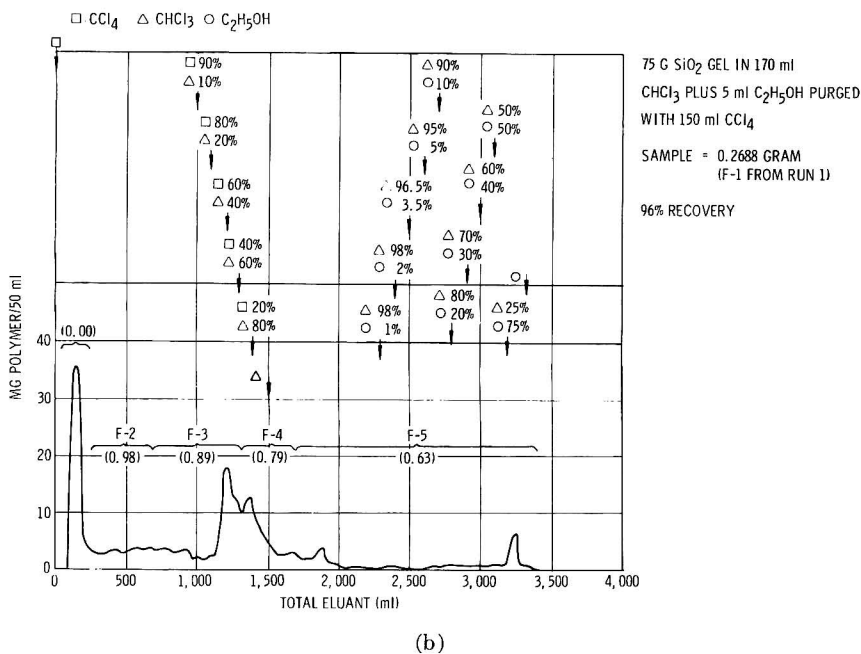
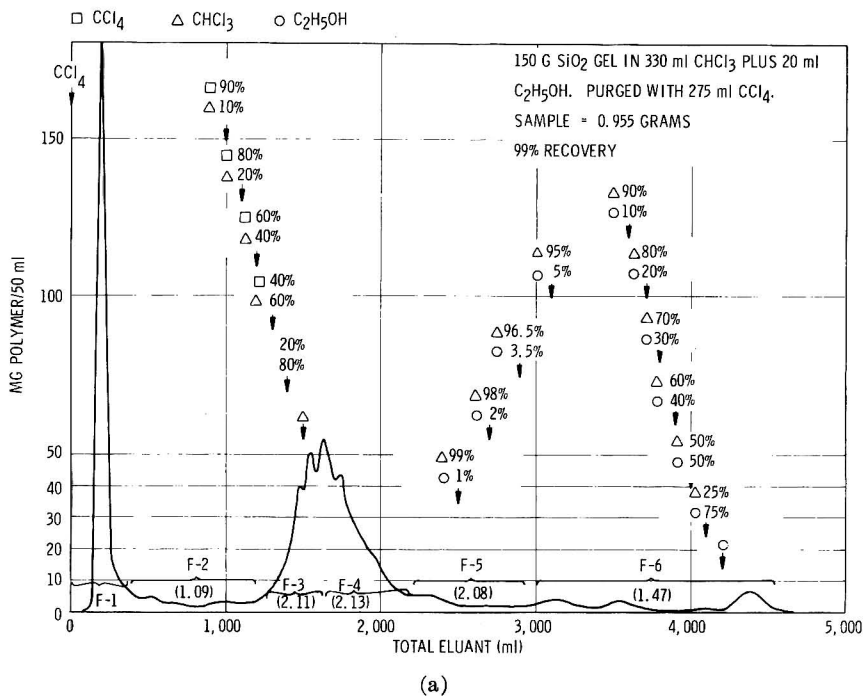


Fig. 3. Elution profiles: (A) HTPB-1, run 1; HTPB-1, run 2.

| FUNCTIONALITY | % | \bar{M}_n |
|---------------|----|-------------|
| 0 | 13 | 1,470 |
| 1 | 20 | 1,980 |
| 2 | 36 | 2,890 |
| 3 | 19 | 3,220 |
| 4 | 9 | 2,570 |
| 5 | 1 | 2,420 |

NOTE: ALL MOLECULAR WEIGHTS BY GPC
PER CORRECTED CALIBRATION

$$\text{AVERAGE FUNCTIONALITY} = \frac{2,989}{1,524} = 1.96\%$$

RECOVERY = 98%

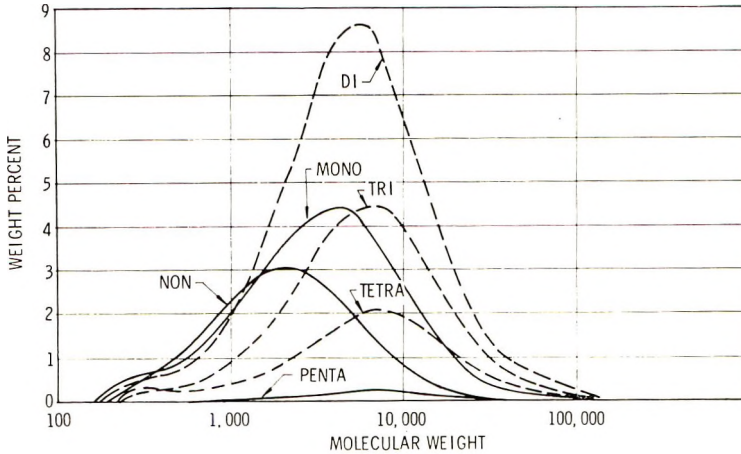


Fig. 4. PBAN-1 polymer, lot 9404-0112.

Application of gel-permeation chromatography in connection with the liquid-solid chromatography has permitted the determination of molecular weight distribution within each functional type, and has permitted calculation of the interrelationship between functionality distribution and molecular weight distribution.

TABLE XXII-A
Example of Synthetic Construction of MWD Curve
Difunctional Material in HTPB-1

| Fraction | Functionality | Wt-% of polymer | Proportion of difunctional material in fraction | Difunctional material in polymer, % | Total difunctional in fraction, % |
|----------|---------------|--------------------|---|---|---|
| 2B | 1.08 | 5.4 | 0.08 | 0.42 | 0.8 |
| 2A | 1.09 | 5.0 | 0.09 | 0.45 | 0.8 |
| 3A | 2.11 | 19.7 | 0.89 | 17.53 | 31.4 |
| 4A | 2.13 | 33.2 | 0.87 | 28.88 | 51.8 |
| 5A | 2.08 | 5.7 | 0.92 | 5.24 | 9.4 |
| 6A | 1.47 | 6.9 | 0.47 | 3.24 | 5.8 |
| | | | | 55.76 | 100.0 |

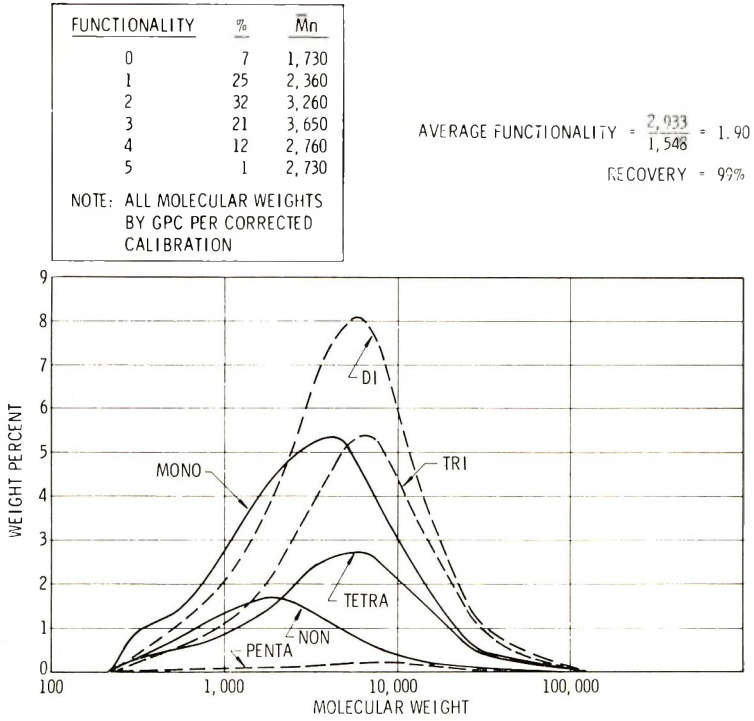


Fig. 5. PBAN-2 polymer.

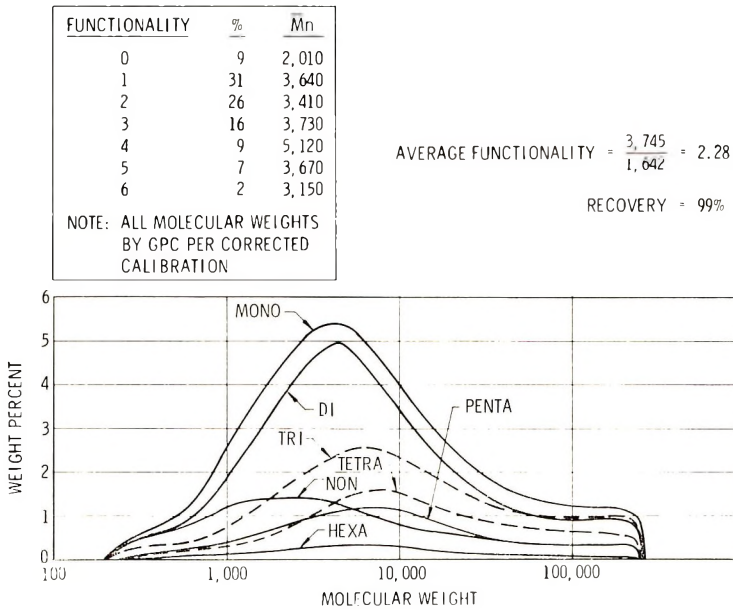


Fig. 6. PBAN-2 aged 90 days at 200°F in mild steel (0.35% Fe).

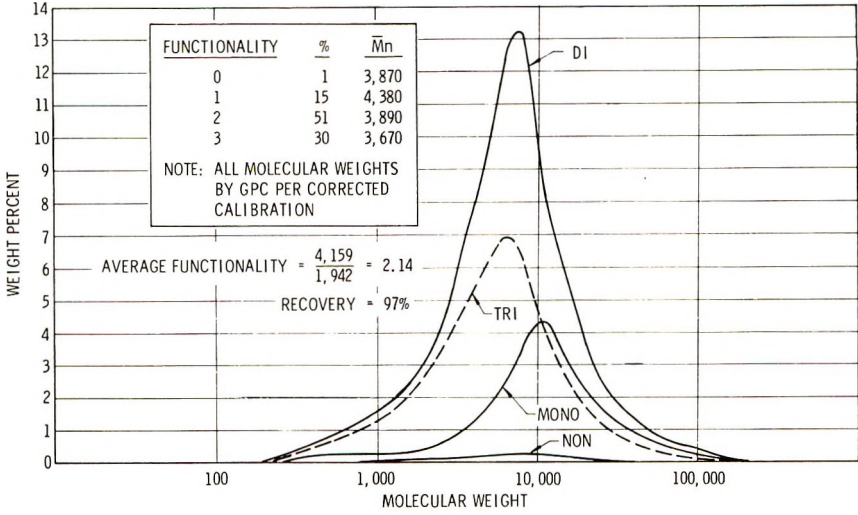


Fig. 7. CTPB-1, lot 9407-0111.

The interrelationship between functionality distribution and molecular weight distribution is undoubtedly a fundamental property of a given polymer, and may eventually prove to be more descriptive and more meaningful for prediction of end use properties than any polymer parameter heretofore measured.

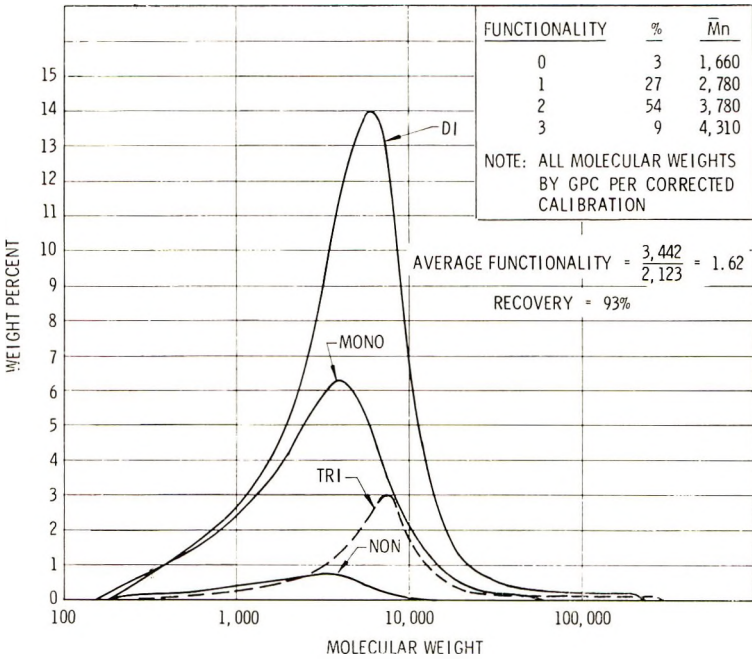


Fig. 8. CTPB-2.

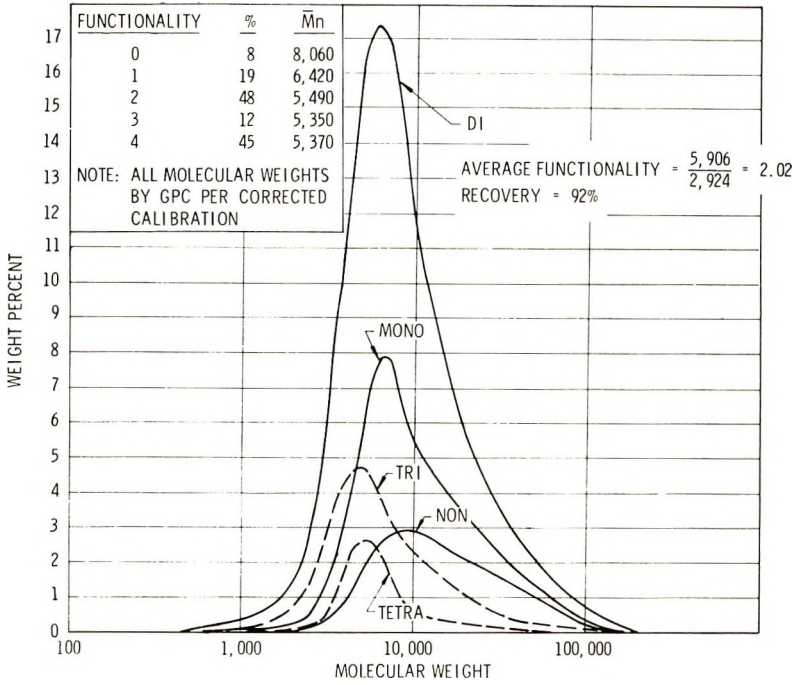


Fig. 9. HTPB-2, lot 46M-8.

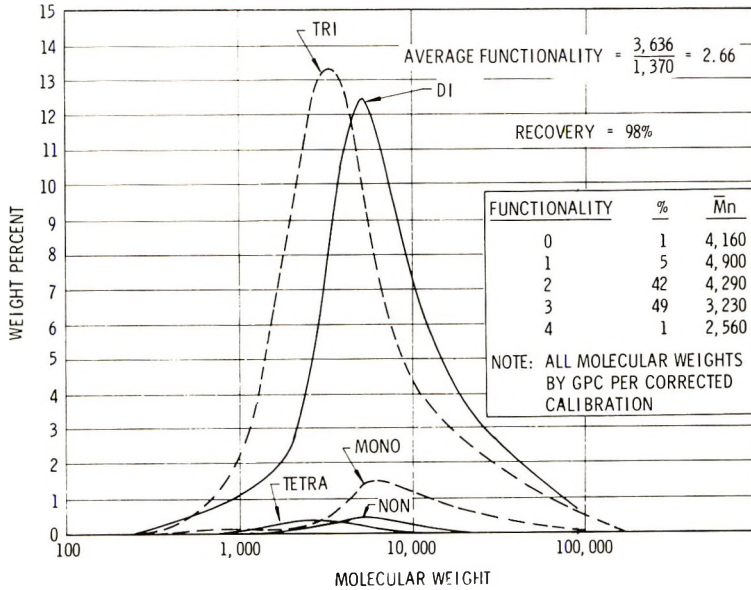


Fig. 10. HTPB-3, lot 908071.

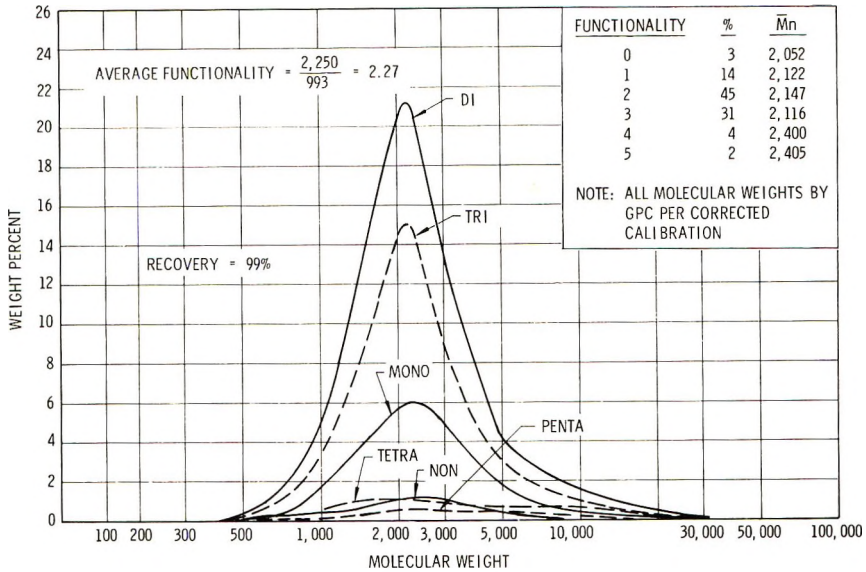


Fig. 11. HTPB-4.

The type of information generated by this work is of particular value to the formulating chemist in selecting a candidate polymer for a new program. Ultimately, when the relationships between functionality distribution and propellant properties are quantitatively established, it should theoretically be possible to optimize propellant properties by controlling or modifying the functionality distribution of the polymer.

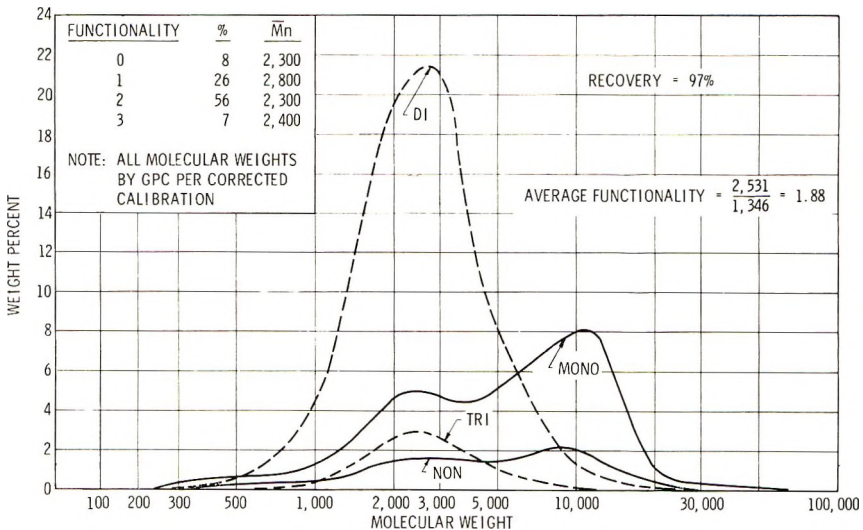


Fig. 12. HTPB-1.

TABLE XXII-B
Per cent of Difunctional Material^a

| Molecular weight | Difunctional material, % | | | | | | Σ | $\Sigma, \%$ |
|------------------|--------------------------|-------------|-------------|-------------|-------------|-------------|----------|--------------|
| | Fraction 2A | Fraction 2B | Fraction 3A | Fraction 4A | Fraction 5A | Fraction 6A | | |
| 50,000 | — | — | — | — | — | — | 0.0 | 0.0 |
| 30,000 | 0.01 | 0.01 | 0.13 | 0.16 | 0.03 | — | 0.34 | 0.3 |
| 20,000 | 0.06 | 0.02 | 0.22 | 0.26 | 0.08 | — | 0.64 | 0.6 |
| 10,000 | 0.55 | 0.07 | 0.72 | 0.57 | 0.14 | 0.12 | 2.17 | 2.2 |
| 5,000 | 0.11 | 0.21 | 9.01 | 3.84 | 0.62 | 0.61 | 14.39 | 14.4 |
| 3,000 | 0.02 | 0.17 | 15.76 | 18.96 | 2.07 | 1.67 | 38.65 | 38.7 |
| 2,000 | 0.03 | 0.24 | 5.21 | 24.76 | 3.29 | 2.06 | 35.59 | 35.6 |
| 1,000 | 0.01 | 0.08 | 0.31 | 3.26 | 2.88 | 0.79 | 7.33 | 7.3 |
| 500 | — | — | — | — | 0.29 | 0.35 | 0.64 | 0.6 |
| 300 | — | — | — | — | — | 0.21 | 0.21 | 0.2 |
| | | | | | | | | 100.0 |

^a A plot of molecular weight versus $\Sigma \%$ gives the molecular weight distribution of the difunctional material in HTPB-1, as seen in Figure 12.

Since the stepwise silica gel-chromatographic separation as applied in these studies is time-consuming and somewhat tedious, refinements should be sought to optimize the separation, especially by application of high-pressure, high-speed liquid chromatography.

References

1. A. H. Muenker and B. E. Hudson, "Functionality Determination of Binder Prepolymers," AFRPL-TR-68-327, Oct. 1, 1966–Sept. 30, 1968, ESSO Research and Engineering Report GR-8-FBP-68.
2. A. H. Muenker "Determination of Prepolymer Functionality and its Relationship to Binder Properties," AFRPL-TR-69-214, Feb. 3, 1969–Aug. 31, 1969.
3. R. D. Law, *J. Polym. Sci. A-1*, **7**, 2097 (1969).
4. C. A. Baker and R. J. R. Williams, *J. Chem. Soc.*, **1956**, 2352.

Received August 7, 1970

Revised October 8, 1970

Ziegler Polymerization of Olefins. IX. Donor Effects in Metal Alkyl-Free and Ziegler-Type Stereospecific Catalysts

J. BOOR, JR.,

Shell Development Company, Emeryville, California 94608

Synopsis

Electron donors, especially trialkylamines and azulene, have been examined in aluminum alkyl-, CH_3TiCl_3 - and hydrogen-activated TiCl_3 catalysts for the polymerization of propylene to isotactic polymer. A comparison and an evaluation were made with findings which were established earlier with zinc alkyl-based TiCl_3 catalysts. We find that the donor, when it is present in low concentrations in all of the above catalysts, can inactivate preferentially the less stereoregulating sites. In this way the isotactic content and the molecular weight of the polymer are increased, but only at the expense of a lower catalyst activity. The addition of hydrogen to the TiCl_3 -donor catalyst at -78°C produced a threefold effect: (1) the activity of the catalyst was increased about 5 to 15 times and higher, (2) the polypropylene formed with this more active catalyst was more isotactic (ca. 10–15%), and (3) the polymer had a lower molecular weight. It is proposed that the increase in catalyst activity was due to the generation of Ti-H bonds to which propylene molecules then added, the Ti-H bonds thus being transformed into active Ti-C centers.

INTRODUCTION

The application of electron donors to elucidate the nature of the active centers in metal alkyl-free and in Ziegler-type catalysts has been described in previous papers.¹⁻⁸ A number of recent reviews⁹⁻¹³ discuss the influence of electron donors in Ziegler-type catalysts and in metal alkyl-free catalysts which do not contain an added base-material alkyl such as AlEt_3 . In the earlier investigations, the Ziegler catalyst (ZnEt_2 plus TiCl_3) and the metal alkyl-free catalyst, (TiCl_3 plus amine) were mostly used. We have now examined similarly several aluminum alkyl-based and CH_3TiCl_3 -based Ziegler-type catalysts under variable polymerization conditions. Also, we have examined further the metal alkyl-free catalyst, especially the influence of hydrogen on its activity and on the isotacticity of the polypropylene which is formed with it.

This paper describes our experimental work and attempts further to elucidate the nature of the active centers in these types of stereoregulating catalysts.

The experimental findings and their interpretation will be presented ac-

ording to the nature of the effect of the electron donor on the activity of Ziegler and metal alkyl-free catalysts.

The experiments in which the added donor caused a lowering of the catalyst activity, will be described and interpreted first, while the enhancement of catalyst activity due to the donor will be discussed in a subsequent section.

MATERIAL AND EXPERIMENTAL METHODS

The polymerization and characterization methods as well as materials which have been previously described in detail¹⁻⁵ have also been used in this investigation. All operations were carried out under nitrogen, and the dry TiCl_3 salts were handled in a dry box containing about 1 ppm or less oxygen or water.

Most of the polymerizations were done in 8-ounce bottles as reaction vessels.²

Isotactic contents of thin polymer films (ca. 0.001 in.) were determined by infrared spectroscopy as described previously.² Crystallinities of about 65 and 30% corresponded to infrared indices ($A_{10.02\mu}/A_{10.28\mu}$) of 0.90 and 0.65, respectively.

The nomenclature used for various titanium trichloride salts^{2,4} follows that generally accepted in the literature (Table I).

TABLE I
Titanium Trichloride Salts

| Nomenclature | Source | Preparation |
|----------------------------|--|--|
| TiCl_3AA^a | Stauffer Chemical Company, Richmond, California | $\text{TiCl}_4 + \text{Al}$, activation |
| TiCl_3A^a | " " | $\text{TiCl}_4 + \text{Al}$, no activation |
| TiCl_3HA | " " | $\text{TiCl}_4 + \text{H}_2$, activation |
| TiCl_3H | " " | $\text{TiCl}_4 + \text{H}_2$, no activation |
| $\beta\text{-TiCl}_3^a$ | See reference 2 | $\text{TiCl}_4 + 3 \text{AlEt}_3$, 25°C |
| $\gamma\text{-TiCl}_3^a$ | " " | Heat $\beta\text{-TiCl}_3$, 160°C |

^a These salts actually contain ionic aluminum. These have often been designated $3\text{TiCl}_3 \cdot \text{AlCl}_3$. This author introduced¹⁻⁷ the nomenclature $\text{Al}_x\text{Ti}_y\text{Cl}_z$ ($x \approx 1$, $y \approx 3$, $z \approx 12$) for these salts to stress that they contain aluminum and that x , y , and z are not constant. For sake of conformity the generally accepted nomenclature is used in this paper.

LOWERING OF CATALYST ACTIVITY

Experimental Results

Azulene and dimethylfulvene were added as third components to aluminum alkyl-based Ziegler catalysts when the latter were used to polymerize propylene at 60, 80, and 115°C. Their effects on catalyst activity (conversion of propylene), on the isotactic crystallinity of the formed polymer (as infrared $A_{10.02\mu}/A_{10.28\mu}$ ratios) and polymer molecular weight (as intrinsic viscosities) were observed.

The effect of azulene on a highly isotactic specific catalyst ($\text{AlEt}_2\text{Cl} +$

TABLE II
Azulene in Highly Specific Catalysts ($\text{AlEt}_2\text{Cl} + \gamma\text{-TiCl}_3$ at 60°C)^a

| Expt no. ^b | Azulene, mmole | Azulene | Conversion, wt-% | $A_{10.02\mu}$ ^b |
|-----------------------|----------------|------------------------|------------------|-----------------------------|
| | | $\gamma\text{-TiCl}_3$ | | $A_{10.28\mu}$ |
| 1 | 0 | 0 | 89 | 0.90 |
| 2 | 0.1 | 0.15 | 83 | 0.90 |
| 3 | 0.5 | 0.77 | 79 | 0.91 |
| 4 | 1.5 | 2.3 | 74 | 0.91 |

^a Experimental conditions: 8-oz bottles as reaction vessels, 100 ml heptane, 3.0 mmole AlEt_2Cl , 0.65 mmole $\gamma\text{-TiCl}_3$, 30 g propylene (see Boor² for further details); rotated in thermostated baths for 50 min at 60°C .

^b Indices which are related to polymer isotacticity. A value of 0.90 corresponds to a crystallinity of about 65%. See Boor² for methods used to determine these values.

$\gamma\text{-TiCl}_3$) is described in Table II. In this situation azulene lowered catalyst activity but there was no substantial change in the isotacticity of the polymer formed with the azulene-containing catalyst.

Tables III–V show the effect of azulene on catalysts which produce only partially isotactic crystalline polypropylene, e.g., $\text{AlEt}_2\text{Cl} + \beta\text{-TiCl}_3$, $\text{AlEt}_3 + \text{VCl}_3$, $\text{AlEt}_3 + \beta\text{-TiCl}_3$, $\text{AlEt}_3 + \gamma\text{-TiCl}_3$ and $\text{AlEt}_2\text{F} + \gamma\text{-TiCl}_3$ (Table III); $\text{AlEt}_2\text{Cl}/\text{ZnEt}_2 + \gamma\text{-TiCl}_3$ (Table IV); $\text{AlEt}_2\text{Cl} + \gamma\text{-TiCl}_3$ (115°C) (Table V).

In all cases azulene lowered the catalyst activity and simultaneously increased both the isotacticity and molecular weight of the polymer which formed with the azulene-modified catalyst.

Discussion

The effect of azulene in low concentrations in the aluminum alkyl-based catalysts resembled its effect in the ZnEt_2 -based catalysts when both were

TABLE III
Azulene in Partially Specific Catalysts Based on AlEt_2Cl , AlEt_2F , AlEt_3 , VCl_3 or $\beta\text{-TiCl}_3$ and $\gamma\text{-TiCl}_3$ ^a

| Expt. no. | Metal alkyl | Transition Metal compound | Azulene, mmole | Conversion, wt-% | $A_{10.02\mu}$ |
|-----------|--------------------------|---------------------------|----------------|------------------|-----------------|
| | | | | | $A_{10.28\mu}$ |
| 1 | AlEt_2Cl | $\beta\text{-TiCl}_3$ | 0 | 41 | 0.84 (IV = 2.3) |
| 2 | " | " | 0.5 | 22 | 0.90 (IV = 3.9) |
| 3 | AlEt_2F | $\gamma\text{-TiCl}_3$ | 0 | 96 | 0.66 |
| 4 | " | " | 4.0 | 58 | 0.87 |
| 5 | AlEt_3 | VCl_3 | 0 | 83 | 0.60 |
| 6 | " | " | 4.0 | 95 | 0.70 |
| 7 | AlEt_3 | $\beta\text{-TiCl}_3$ | 0 | 92 | .69 |
| 8 | " | " | 4.0 | 21 | .84 |
| 9 | AlEt_3 | $\gamma\text{-TiCl}_3$ | 0 | 95 | .74 |
| 10 | " | " | 4.0 | 74 | .86 |

^a Experimental conditions: 8-oz bottles as reaction vessels, 100 ml heptane, 3.0 mmole AlR_3 or AlR_2X , 0.65 mmole transition metal salt (except 1.3 mmole VCl_3), 30 g propylene; Rotated in thermostated baths for 50 minutes at 60°C .

TABLE IV
Azulene in Partially Specific Catalysts
(AlEt₂Cl + ZnEt₂ + γ -TiCl₃ at 80°C)^a

| Expt. no. | ZnEt ₂ mmole | Azulene, mmole | Con- version, wt-% | $A_{10.02\mu}$ | | I.V., dl/g |
|-----------------|-------------------------|----------------|--------------------------|----------------|----------------|---------------|
| | | | | $A_{10.28\mu}$ | $A_{10.28\mu}$ | |
| 1 | 0 | 0 | 80 | 0.90 | | 2.0 |
| 2 | 0.5 | 0 | 58 | 0.85 | | 0.60 |
| 3 | 0.5 | 0.5 | 33 | 0.98 | | 0.89 |
| 4 | 1.0 | 0 | 52 | 0.78 | | 0.57 |
| 5 | 1.0 | 0.5 | 32 | 0.98 | | 1.08 |
| 6 | 2.0 | 0 | 48 | 0.66 | | 0.69 |
| 7 | 2.0 | 0.5 | 29 | 0.96 | | 1.30 |
| Dimethylfulvene | | | | | | |
| 8 | 1.5 | 0 | 47 | 0.61 | | 0.71 |
| 9 | 1.5 | 0.85 | 4 | 0.96 | | 1.80 |

^a Experimental conditions: 8-oz bottles as reaction vessels, 100 ml heptane, 3.0 mmole AlEt₂Cl, 0.65 mmole γ -TiCl₃, 20 g propylene (see Boor² for further details); rotated in a thermostated bath for 30 min at 80°C.

TABLE V
Azulene in Partially Specific Catalysts (Polymerization at 115°C)

| Expt. no. ^a | Azulene, mmole | Polymer, g | $A_{10.02\mu}$ | | I.V., dl/g |
|------------------------|-------------------|------------|----------------|----------------|------------|
| | | | $A_{10.28\mu}$ | $A_{10.28\mu}$ | |
| 1 | 0 | 20.7 | 0.68 | | 1.1 |
| 2 | 0.05 | 6.1 | 0.90 | | 1.4 |
| 3 | 0.25 | 8.1 | 0.90 | | 1.5 |
| 4 | 0.50 | 5.2 | 0.92 | | 1.9 |
| 5 | 1.00 | 5.6 | 0.94 | | 2.1 |
| 6 | 0.25 ^b | 6.0 | 0.93 | | — |

^a Experimental conditions: Magne Dash autoclave as reaction vessel, 150 ml heptane, 2.25 mmole AlEt₂Cl, 0.25 mmole γ -TiCl₃, 140 psig propylene pressure.

^b Cyclohexane was used as solvent in this experiment; the formed polymer remained in solution under these conditions.

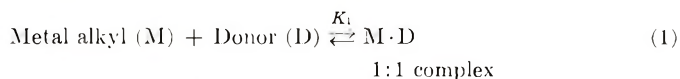
used to polymerize propylene⁵ as already stated above. In both situations a lowering of catalyst activity was simultaneously accompanied by an increase in polymer isotacticity and molecular weight.

These findings were interpreted to mean that azulene complexed and inactivated preferentially first the more exposed and less isotactic-specific sites. Since these sites also produced polymer which had a lower molecular weight than polymer formed at the more specific sites, the molecular weight of the polymer also increased.

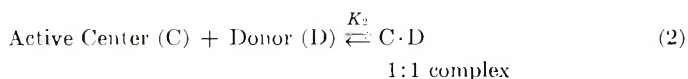
Consistent with this view are the data of Table II which show that only a small improvement in polymer isotacticity takes place when azulene was added to a catalyst (AlEt₂Cl + γ -TiCl₃ at 60°C) which was already produced a very highly isotactic polypropylene. Here the lowering of catalyst activity which occurred resulted from complexing and inactivation of some of the isotactic-specific sites.

Particularly significant are the experimental findings of Table V; here a high polymerization temperature (115°C) was used to induce the same $\text{AlEt}_2\text{Cl}-\gamma\text{-TiCl}_3$ catalyst to produce a partially crystalline polypropylene. In contrast to an infrared ratio of 0.90–0.91 (65–70% crystallinity) obtained for polypropylene prepared at 60°C with this catalyst (Table II), at 115°C the infrared ratio was only 0.68 (35% crystallinity). By addition of 0.05 mmole azulene per 0.25 mmole $\gamma\text{-TiCl}_3$ and per 2.25 mmole AlEt_2Cl , this catalyst at 115°C (Table V) produced a polymer whose crystallinity was about 65% (infrared ratio = 0.90). Interestingly, experiment 6 of Table V shows that a 65–70% crystalline polymer can be formed even if during polymerization it remains in solution.

Langer has recently reported that the incorporation of azulene into the $\text{AlEt}_3\text{-TiCl}_3$ catalyst led to a polymer with a higher tensile strength.¹⁴ For example, the tensile strength increased from 2850 psi to 4200–4400 psi on addition of 0.5–1.0 mmole azulene per 2 mmole AlEt_3 . Langer attributed the improvement to the presence of an equimolar complex of the donor and the metal alkyl, and suggested that an excess of the donor be added in order to ensure its presence in a substantial amount in the premix:



We disagree. In our view, as stated in this and in previous papers, the uncomplexed donor interacts preferentially with less isotactic-specific sites directly via the reaction (2):



Langer did not elaborate how the $\text{M}\cdot\text{D}$ complex [eq. (1)] modified the catalyst.

We suggest that if the complex-forming tendency according to eq. (1) is very large, then the site-forming ability of the metal alkyl may be greatly diminished. Also, very little donor would remain to effect site removal via eq. (2).

The general conclusions drawn from this present work are in reasonable agreement with conclusions derived by Schindler⁸ from his investigations of ethylene polymerization with the $\text{AlEt}_2\text{Cl-TiCl}_4$ catalyst. In the latter catalyst, preferential complexing was recognized also for tetravalent sites which were strongly adsorbed on the TiCl_3 surface. Schindler used donors such as Et_3N to differentiate these centers.

ENHANCEMENT OF CATALYST ACTIVITY

Experimental Results

The activating effect of different donors was examined under a variety of experimental conditions for the polymerization of propylene (Tables VI–X and Figs. 1–3).

The activity of a number of titanium trichloride-based metal alkyl-free

TABLE VI
Influence of Hydrogen on Metal Alkyl-Free Catalysts
Based on γ -TiCl₃, TiCl₃AA, TiCl₃HA, and TiCl₃A^a

| Expt. no. | TiCl ₃ ^b | Weight, g | H ₂ present | Time, hr | Polymer, g |
|-----------|--------------------------------|-----------|---------------------------|----------|------------|
| 1 | TiCl ₃ AA | 2.0 | Yes | 4 | 20 |
| 2 | " | " | No | " | 2 |
| 3 | γ -TiCl ₃ | 2.0 | Yes | 20 | 3.3 |
| 4 | " | " | No | " | 0.8 |
| 5 | TiCl ₃ HA | 4.0 | Yes | 110 | 0.70 |
| 6 | " | " | No | " | 0.01 |
| 7 | TiCl ₃ A | 3.0 | Yes | 336 | 0.1 |
| 8 | " | " | No | " | 0 |

^a Polymerization conditions: into 8-oz bottles were added 100 ml heptane, the TiCl₃ and 10 mmole *n*-Bu₃N. The bottle and contents were cooled to -78°C , and 30 g propylene was condensed into the bottle. Then hydrogen was bubbled into the mixture (still at -78°C) for 10 min and the bottle was capped under an atmosphere of hydrogen. The bottles were rotated in a thermostated bath at $+25^{\circ}\text{C}$.

^b Mixtures of *n*-Bu₃N and TiCl₃, TiCl₃H, or VCl₃ were not similarly activated by molecular hydrogen.

catalysts was increased significantly when hydrogen was introduced into the catalyst (Tables VI and VII).^{*} Hydrogen was added by bubbling it into the catalyst-monomer-solvent mixture at -78°C for about 10 min. The reaction bottle was then sealed under an atmosphere of hydrogen. Various titanium trichlorides were used with *n*-Bu₃N as the donor component, e.g., TiCl₃AA, γ -TiCl₃, TiCl₃HA, and TiCl₃A. The best results were achieved with TiCl₃AA; about 20 g polypropylene was obtained in 4 hr from 2 g TiCl₃AA, 10 mmole *n*-Bu₃N, and 30 g propylene in 100 ml heptane at 25°C .

Figure 1 shows that a maximum activity was achieved for the H₂-*n*-Bu₃N-TiCl₃AA catalyst when the *n*-Bu₃N/TiCl₃AA ratio (mmole/g) was about 1. In absence of hydrogen the same catalyst attained a maximum activity at only a slightly higher *n*-Bu₃N/TiCl₃AA ratio (Fig. 2). In both cases about 0.3 mmole *n*-Bu₃N had to be added per gram TiCl₃ before the catalyst became measurably active.

Hydrogen did not increase the activity of the CH₃TiCl₃-TiCl₃-*n*-Bu₃N catalyst when either γ -TiCl₃ or TiCl₃AA was used (Table VIII). In Table IX the influence of *n*-Bu₃N in this catalyst is shown when hydrogen was absent.

Table X compares various donors in their ability to active both the TiCl₃AA and γ -TiCl₃ salt to polymerize propylene. In absence of donor only low molecular weight oils were formed.

Apparently *n*-Bu₃N did not function as an effective transfer agent in the TiCl₃AA-based catalyst (Fig. 3). In a 144-hr polymerization at 25°C , the polymer intrinsic viscosities increased from about 3 dl/g (1 hr, 0.3 wt-% conversion) to about 18 dl/g (144 hr, 52% conversion).

^{*} This catalyst was briefly reported in an earlier investigation.⁶

TABLE VII
Influence of Molecular Hydrogen on Isotacticity and Molecular Weight of Polypropylene^a

| Expt. no. | Heptane, ml | TiCl ₃ AA, g | Donor | | | | | Polymerization conditions | | | | | <i>A</i> _{10.02μ} | |
|-----------|------------------|-------------------------|----------------------------------|--------|----------|----------|-----------------------|---------------------------|------------|----------------------------|--|--|----------------------------|--|
| | | | Type | Vol ml | Time, hr | temp, °C | wt C ₃ , g | H ₂ | Polymer, g | <i>A</i> _{10.38μ} | | | | |
| 1 | 100 | 2.07 | Et ₃ N | 1.4 | 4 | 35 | 30 | No | 0.1 | 0.83 | | | | |
| 2 | " | 2.05 | " | " | " | " | " | Yes | 1.6 | 0.93 | | | | |
| 3 | " | 2.05 | <i>n</i> -Bu ₃ N | 2.4 | " | " | " | No | 0.5 | 0.73 | | | | |
| 4 | " | 2.06 | " | " | " | " | " | Yes | 5.5 | 0.88 | | | | |
| 5 | " | 2.10 | Amyl ₃ N | 2.9 | " | " | " | No | 0.2 | 0.73 | | | | |
| 6 | " | 2.06 | " | " | " | " | " | Yes | 7.8 | 0.87 | | | | |
| 7 | " | 2.04 | <i>n</i> -Bu ₃ N | 0 | 20 | 25 | 32 | No | Oil | 0.75 | | | | |
| 8 | " | 2.01 | " | 2.4 | 144 | " | 29 | No | 6.6 | 0.91 | | | | |
| 9 | " | 2.00 | " | " | 20 | " | 32 | Yes | 15.2 | 0.92 | | | | |
| 10 | 100 ^b | 4.00 | Et ₃ NBH ₄ | 1.25 g | 240 | " | 30 | No | 17.2 | 0.92 | | | | |
| 11 | " | 2.00 | " | " | 20 | " | 32 | Yes | 8.2 | 0.92 | | | | |

^a Polymerization conditions: the solvent, catalyst, and propylene contained in 8-oz bottles were rotated in a thermostated bath under conditions indicated for each experiment.

^b Toluene was used as solvent.

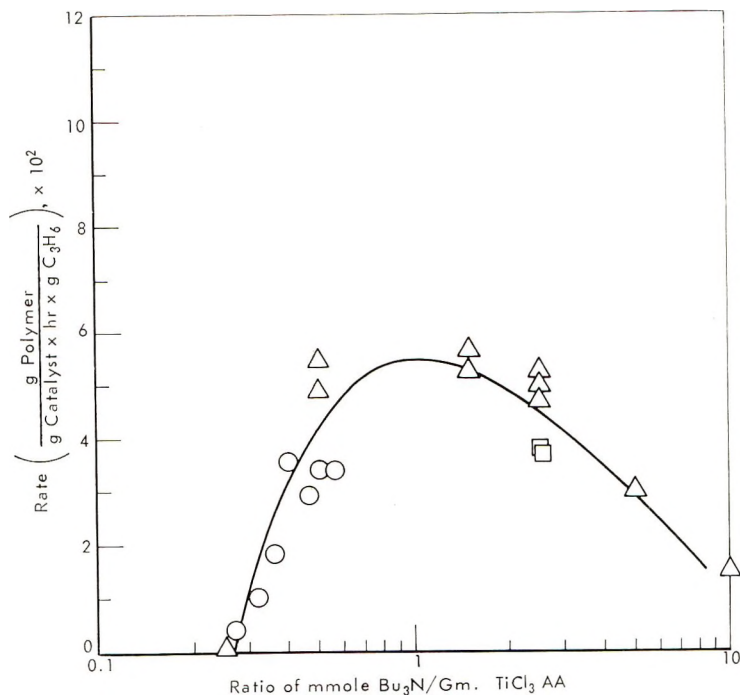


Fig. 1. Dependence of polymerization rate on $n\text{-Bu}_3\text{N}/\text{TiCl}_3\text{AA}$ ratio when either $n\text{-Bu}_3\text{N}$ or TiCl_3AA is kept separately constant: (O) $n\text{-Bu}_3\text{N}$ constant (0.8 mmole), TiCl_3AA varied; (Δ , \square) TiCl_3AA kept constant (2.0 g), concentration of $n\text{-Bu}_3\text{N}$ varied. H_2 present in all experiments.

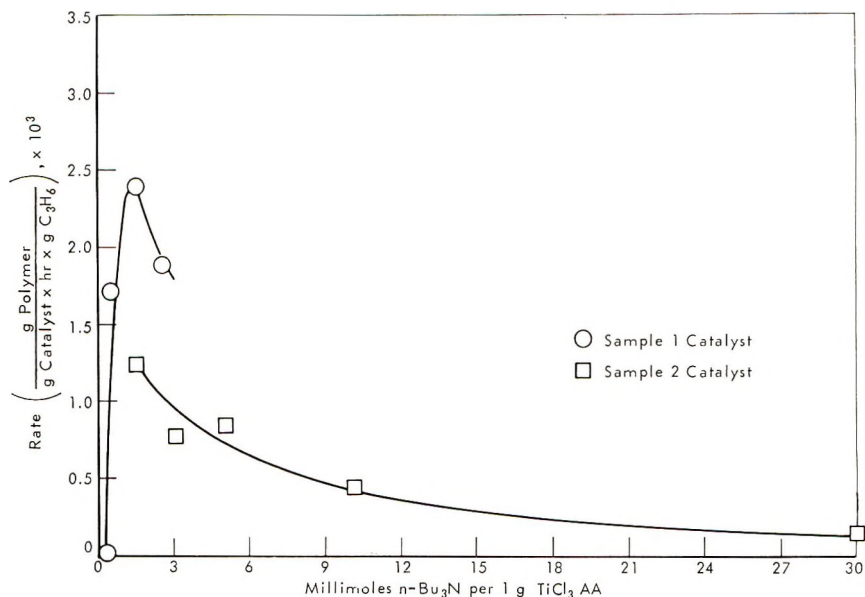


Fig. 2. Dependence of polymerization rate on millimoles $n\text{-Bu}_3\text{N}$ per 2.0 g TiCl_3AA . Conditions: 25°C , 84 hr. Discontinuity in curve arises because the two samples of TiCl_3AA used had different activities.

TABLE VIII
Hydrogen as the Third Component in the
CH₃TiCl₃-TiCl₃-*n*-Bu₃N System^a

| Expt. no. | TiCl ₃ (0.2 g) | <i>n</i> -Bu ₃ N, mmole | CH ₃ TiCl ₃ , mmole | H ₂ present | Polymer g |
|-----------|---------------------------|------------------------------------|---|------------------------|-----------|
| 1 | TiCl ₃ AA | 3.0 | 2.6 | No | 7.7 |
| 2 | " | " | " | Yes | 7.5 |
| 3 | " | " | 0 | Yes | 0.1 |
| 4 | γ-TiCl ₃ | " | 2.6 | No | 5.2 |
| 5 | " | " | " | Yes | 3.6 |

^a Polymerization conditions: 8-oz bottles containing 100 ml heptane; the catalyst and 30 g propylene were rotated at 25°C for 2.5 hr.

TABLE IX
Activation of CH₃TiCl₃ by *n*-Bu₃N (Propylene)^a

| Expt. no. | TiCl ₃ (0.2 g) | <i>n</i> -Bu ₃ N, mmole | CH ₃ TiCl ₃ , mmole ^b | Polymer, g |
|-----------|-----------------------------------|------------------------------------|--|------------|
| 1 | TiCl ₃ AA ^c | 0 | 2.6 | 0.7 |
| 2 | " | 0 | 1.3 | 0.1 |
| 3 | " | 3.0 | 2.6 | 7.7 |
| 4 | " | 3.0 | 1.3 | 10.5 |
| 5 | γ-TiCl ₃ ^d | 0 | 2.6 | 0.1 |
| 6 | " | 3.0 | 2.6 | 5.2 |
| 7 | " | 3.0 | 2.6 | 7.0 |
| 8 | " | 3.0 | 1.3 | 7.2 |

^a Conditions: 100 ml heptane in 8-oz bottles, 30 g propylene, 2.5 hr at 25°C with rotation in bath.

^b Prepared according to a slightly modified procedure described in Ref. 17.

^c Purchased from Stauffer Chemical Company, Richmond, California. It is reported to be made by reduction of TiCl₄ with subsequent activation. Its actual composition is approximately Al_{0.9}Ti₃Cl₁₂.

^d Prepared by reduction of TiCl₄ with AlEt₃ (see Boor² for further details); this also has an approximate composition of Al_{0.9}TiCl₁₂.

TABLE X
Relative Ability of Donors to Activate TiCl₃AA and γ-TiCl₃^a

| Good activators ^b | Weak activators ^c |
|--|--|
| R ₃ N (R ≥ Et) | (C ₆ H ₅) ₃ PH |
| R ₃ P (R ≥ Pr) | 2,6-Dimethylpyridine |
| [C ₆ H ₅] ₃ P | Azulene |
| Et ₃ NBH ₄ | α-R-pyridine (R = Me, Et) |
| (C ₁₀) ₃ N plus <i>n</i> -BuI (1:1) | α-Me-quinoline |
| | Pyridine (very poor) |

^a These donors were examined with both the TiCl₃AA and the γ-TiCl₃ compositions for the polymerization of propylene (100 ml heptane, 30 g propylene, 2.0 g TiCl₃, 10 mmole donor for 144 hr at 25°C in 8-oz bottles).

^b 1-10 g polymer was formed, the exact amount varying with the donor.

^c 0.03-0.3 g polymer was formed, the exact amount varying with the donor.

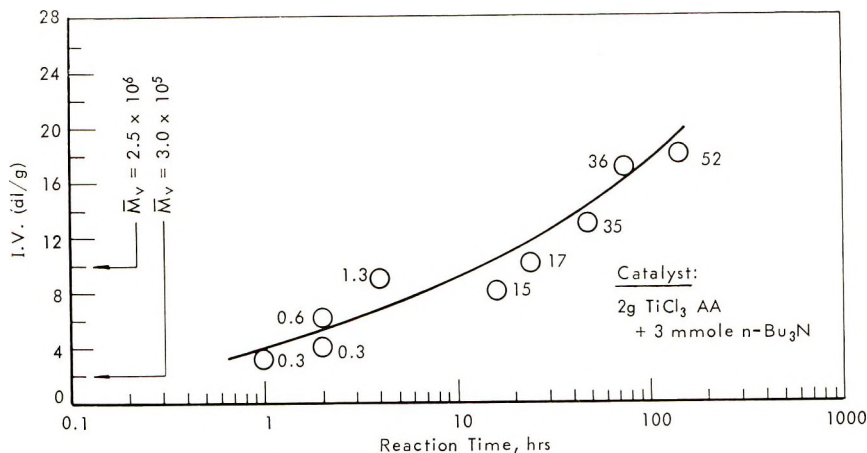


Fig. 3. Dependence of molecular weight (from intrinsic viscosity, IV) on time of polymerization. Numbers at points represent per cent conversion.

Discussion

Previous papers have reported that TiCl_3 alone produced only low molecular weight oils when propylene was polymerized.⁴ The addition of certain electron donors resulted in the activation of the TiCl_3 to produce high molecular isotactic-crystalline polypropylene⁴ (see Table X).

The chemisorbed amine⁵ was proposed to induce existing latent sites to become active rather than actually to cause their formation.^{4,9} These active centers are presumed to have been formed earlier during the synthesis and post-treatment of the TiCl_3 salt. The low activity of the TiCl_3 -donor catalyst has been demonstrated to be due to the presence of a low concentration of active centers.⁷

Concurrently with the activation process described here and in earlier papers,³⁻⁷ the donor can also remove preferentially the more exposed and less stereospecific sites. Thus, the observed activity in both the conventional Ziegler-type catalysts and the TiCl_3 donor-type catalysts (where no metal alkyl was added) reflects the net result of both processes.

Evidence has been presented indicating that the activation by trialkyl amines in the ZnEt_2 - TiCl_3 and in the TiCl_3 metal alkyl-free catalysts is associated with chemisorption of the donor on the chlorine surface of TiCl_3 .⁵ However, the detailed mechanistic path by which this takes place was not established. Speculative mechanistic paths have been already discussed.⁹ The general phenomena of activation by electron donors have been reviewed by a number of authors.⁹⁻¹³

The further activation of these TiCl_3 -donor-catalyst mixtures at -78°C by molecular hydrogen is shown in Tables VI and VII. Earlier this hydrogen effect was briefly reported^{6,9} but was not elaborated upon in detail.

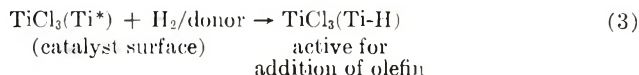
The hydrogen effect is unique. Not only does the TiCl_3 -donor catalyst become more active, but also the polymer which was formed in the presence

of hydrogen had a higher isotactic crystallinity and a lower molecular weight.

Depending on experimental conditions, the activities of the TiCl_3 donor catalyst were increased up to 70 times (experiments 5 and 6, Table VI), although in most cases the increase was about 5- to 10-fold (experiments 1 and 2, Table VI). The isotactic crystallinity of the corresponding polypropylene was increased by about 10–20% (Table VII). In all cases the molecular weights of the polymers prepared with hydrogen present in the catalyst had substantially lower molecular weights (e.g., intrinsic viscosities of about 2 dl/g versus about 7 dl/g). The use of hydrogen as a transfer agent has been well substantiated^{9–13,15} since Vandenberg's original discovery,¹⁶ and therefore the latter finding was expected. From Figure 3 we see that *n*- Bu_3N did not function as a good transfer agent in the TiCl_3 -donor catalyst.

In absence of a donor, the TiCl_3 - H_2 components produced only low molecular weight oils, as did TiCl_3 alone. By addition of trialkyl amines (e.g., R_3N with $\text{R} = \text{Et}$, *n*- Bu , and amyl) or the quaternary salt, $\text{Et}_4\text{N}\text{BH}_4$, hydrogen became activating (Table VIII). The activating effect of hydrogen was observed when TiCl_2/AA , TiCl_3/A , TiCl_3/HA , or $\gamma\text{-TiCl}_3$ but not TiCl_2 , TiCl_3/H , or VCl_4 were used (Table VI). The full scope of the hydrogen effect, in so far as other donors, transition metal salts and experimental conditions are considered, is not obvious from the present data.

An appealing explanation for the activating effect of hydrogen is that new sites are generated [eqs. (3) and (4)].



In these reactions Ti^* represents an active titanium on the surface of TiCl_3 . According to this speculation, molecular hydrogen, like the metal alkyl in a conventional Ziegler catalyst, generates active centers by a chemical reaction. We cannot, however, specify the nature of Ti^* above or on the reaction above.

A number of years ago Mattlack and Breslow¹⁵ reported the formation of active catalysts for the polymerization of ethylene by ball-milling transition metals in presence of hydrogen. A M-H active center was also proposed.

We consider as evidence for the proposal that new sites were generated by hydrogen our observation that the more active catalyst was also more stereoregulating. For example, a comparison of experiments 3 and 4 in Table VII shows that the isotactic index increased from 0.73 to 0.88 in presence of hydrogen, an increase of about 15% crystallinity. According to our view the larger number of active centers generated by hydrogen are more isotactic than are the smaller number of sites which were initially present.

That hydrogen did not increase the activity of the $\text{CH}_3\text{TiCl}_3\text{-TiCl}_3\text{-}n\text{-Bu}_3\text{N}$ catalyst is not surprising (Table VIII). Relative to CH_3TiCl_3 , hydrogen is a poorer site former. For example, we found the $\text{CH}_3\text{TiCl}_3\text{-TiCl}_3\text{-}n\text{-Bu}_3\text{N}$ catalyst to be about 15 times as active as the $\text{H}_2\text{-TiCl}_3\text{-}n\text{-Bu}_3\text{N}$ catalyst, (compare experiment 2 of Table VI and experiment 1 of Table VIII). Thus, the increase in activity in the former catalyst due to hydrogen would be expected to be small.

That catalyst activity maximized at about the same amine/ TiCl_3 ratio in both the $\text{TiCl}_3\text{AA-}n\text{-Bu}_3\text{N}$ and the $\text{TiCl}_3\text{AA-}n\text{-Bu}_3\text{N-H}_2$ systems suggests that the mechanism by which it activates these catalysts is similar.

The author is grateful to Mr. L. R. Roberts of this laboratory and to Drs. P. Cossee and S. Mostert of the Koninklijke/Shell Laboratorium, Amsterdam, Netherlands for reading and criticizing this paper. Also, the excellent technical assistance of Mr. D. W. Penhale is acknowledged. Discussions with Dr. E. A. Youngman during the experimental work are also appreciated.

References

1. J. Boor, Jr., *J. Polym. Sci.*, **45**, 62S (1962).
2. J. Boor, Jr., in *First Biannual American Chemical Society Polymer Symposium (J. Polym. Sci. C, 1)*, H. W. Starkweather, Ed., Interscience, New York, 1965, p. 237.
3. J. Boor, Jr., in *First Biannual American Chemical Society Polymer Symposium (J. Polym. Sci. C, 1)*, H. W. Starkweather, Ed., Interscience, New York, 1963, p. 257.
4. J. Boor, Jr., and E. A. Youngman, *J. Polym. Sci. B*, **2**, 265 (1965).
5. J. Boor, Jr., *J. Polym. Sci. A*, **3**, 995 (1965); *J. Polym. Sci. B*, **3**, 7 (1965).
6. J. Boor, Jr., paper presented at American Chemical Society Meeting, 1965; *Polym. Preprint*, **6**, No. 2, 890 (1965).
7. E. A. Youngman and J. Boor, Jr., *J. Polym. Sci. B*, **3**, 577 (1965).
8. A. Schindler, *Makromol. Chem.*, **105**, 204 (1967).
9. J. Boor, Jr., in *Macromolecular Reviews*, Vol. 2, by A. Peterlin, M. Goodman, S. Okamura, B. H. Zimm and H. F. Mark, Eds., Interscience, New York, 1967.
10. L. Reich and A. Schindler, *Polymerization by Organometallic Compounds*, Interscience, New York, 1966.
11. D. C. Feay, in *Organic Chemistry of Synthetic High Polymers* R. W. Lenz, Ed., Interscience, New York, 1967, Chap. 15.
12. D. O. Jordan, in *Stereochemistry of Macromolecules*, A. D. Ketley, Ed., Dekker, New York, 1967, Chap. 1.
13. D. Hoeg, in *Stereochemistry of Macromolecules*, A. D. Ketley, Ed., Dekker, New York, 1967, Chap. 2.
14. A. W. Langer (to Esso Research and Engineering Company), U. S. Pat. 3,278,511 (October 11, 1966).
15. A. S. Mattlack and D. S. Breslow, *J. Polym. Sci. A*, **3**, 2853 (1965); earlier patent publication of authors is found in this reference.
16. E. J. Vandenberg, U.S. Pat. 3,051,690 (Hercules Chem. Co., August 28, 1962).
17. G. L. Karapinka and W. Carrick, U. S. Pat. 3,072,692 (Union Carbide Corp., January 8, 1963).

Received August 20, 1970

Revised October 15, 1970

Structure and Reactivity of α,β -Unsaturated Ethers.

XIII. Cationic Copolymerization and Acid-Catalyzed Hydrolysis of 1,2-Dialkoxyethylenes

TADASHI OKUYAMA and TAKAYUKI FUENO,
*Faculty of Engineering Science, Osaka University,
Toyonaka, Osaka 560, Japan*

Synopsis

The cationic copolymerizations of geometrical isomers of 1,2-dimethoxy- and 1,2-diethoxyethylenes with vinyl isobutyl ether as a reference monomer have been carried out in methylene chloride at -70° using boron trifluoride etherate as catalyst. The kinetics of the acid-catalyzed hydrolysis of these ethers has also been investigated in 80% aqueous dioxane, in order to compare the results with the polymerizabilities. It has been found that the *cis* ethers are ca. four times as reactive as their *trans* isomers in both reactions. On the other hand, it has been proved that a β -alkoxy substitution reduces the hydrolysis reactivity of vinyl alkyl ethers by a factor of ca. 10^{-3} while it even enhances the cationic polymerizability. These contrasting results are interpretable from the nature of the transition states which are different for the two reactions.

INTRODUCTION

α,β -Unsaturated ethers are a class of compounds that are very reactive toward electrophilic reagents. Extensive investigations have recently been undertaken on the kinetics of cationic polymerization and acid-catalyzed hydrolysis of the ethers, including vinyl,¹⁻⁶ alkenyl,^{1,7-14} styryl,¹⁵⁻¹⁸ and β -chlorovinyl ethers.¹⁹ However, it appears that the effects of polar substituents at the β -position on the reactivity of vinyl ethers still remain to be inquired. It is known only that β -chloro substitution of vinyl ethyl ether greatly reduces the reactivity in cationic polymerization.¹⁹

All the *cis* ethers studied so far were more reactive than the corresponding *trans* isomers. In most cases, it is consistent with the observation that the *cis* isomers are less stable than the *trans* in the ground state.²⁰ However, *cis*- β -chlorovinyl ethyl ether, which is a more reactive isomer, has proved to be more stable than its *trans* isomer.²⁰ 1,2-Dialkoxyethylenes are another type of ether that are more stable in the *cis* form.²⁰ Thus, it seems of interest to investigate which isomer of a dialkoxyethylene is more reactive in relation to its ground-state stability.

The present paper describes the investigations on the effects of β -alkoxy substitution and geometrical isomerism upon the reactivities of

vinyl alkyl ethers both in cationic polymerization and in acid-catalyzed hydrolysis. It has been found that an alkoxy group significantly enhances the reactivity of vinyl ether in the former reaction whereas it greatly reduces the reactivity in the latter. The *cis* isomers have proved to be more reactive in both reactions. All these results appear to be interpretable from the transition-state stabilities of the relevant elementary steps and reinforce the validity of the transition state model which has previously been proposed for the cationic polymerization of α,β -unsaturated ethers.²¹

EXPERIMENTAL

Materials

1,2-Dimethoxyethylene (DME) and 1,2-diethoxyethylene (DEE) were prepared from glyoxal and alcohols by the method of Baganz et al.^{22,23} Isomeric compositions were about unity, and the isomers of DME were fractionated through a spinning-band column. Boiling points were: *cis*-DME (isomeric purity 98%), 96.5°C (lit.²³ bp, 97°C); *trans*-DME (isomeric purity 97%), 93°C (lit.²³ bp, 93°C); DEE, 132–133°C (lit.²³ bp, *cis*, 134.7°C; *trans*, 132.4°C).

Dioxane, methylene chloride, vinyl isobutyl ether (VIBE), and boron trifluoride etherate ($\text{BF}_3 \cdot \text{OEt}_2$) were purified as described previously.^{1,9} Other materials used as internal standards were commercially obtained and distilled.

Polymerization Procedure

Polymerizations were carried out in methylene chloride at ca. -70°C (methanol–Dry Ice bath) by use of $\text{BF}_3 \cdot \text{OEt}_2$ as catalyst. The concentrations of total monomer feed and an internal standard were 7 and 3 vol-%, respectively. Details of the procedures were the same as have been described previously.⁹ The methods of calculation of the monomer reactivity ratios and the relative reactivities were also the same as used before.^{9,17}

Kinetics of the Hydrolysis

Hydrolyses were carried out in 80% aqueous dioxane containing ca. 0.2M hydrochloric acid at a specified temperature between 25 and 45°C. The initial concentrations of the reactant ethers were typically ca. 0.15M. The courses of the hydrolysis reactions were followed by the gas-chromatographic determination of the ethers remaining in the reaction mixtures. Details of the procedures for the rate measurements were the same as those described previously.¹

Determinations of Ether Concentrations

The ether concentrations in a reaction mixture were determined by use of a Shimadzu gas chromatograph Model 4APT with hydrogen as

TABLE I
Internal Standards and Operating Conditions of a Gas Chromatograph
for the Ether Determinations

| Reaction | Ether | Internal standard | Column | | |
|----------------|-------|-----------------------|----------------------|-----------|----------|
| | | | Packing ^a | Length, m | Temp, °C |
| Hydrolysis | DME | Benzene | PEG-DOP (3:1) | 3 | 90 |
| | DEE | <i>n</i> -Butyl ether | AGL | 4.5 | 95 |
| Polymerization | DME | <i>n</i> -Heptane | DOP-AGL (2:1) | 4.5 | 85 |
| | DEE | Toluene | PEG | 2.25 | 90 |

^a PEG = poly(ethylene glycol) 6000, DOP = dioctyl phthalate, AGL = Apiezon grease L.

carrier gas. Column packings and operating conditions are given in Table I, together with the internal standards used. It was found by calibration that the half-height width method fully sufficed for linearly correlating the obtained peak area to the ether concentration.

RESULTS

Cationic Polymerization

In a preliminary experiment, an isomeric mixture of DME was polymerized in methylene chloride at ca. -70°C by use of $\text{BF}_3 \cdot \text{OEt}_2$ as catalyst. There was observed no sign that either isomer undergoes geometrical isomerization concurrently with polymerization, in agreement with the the previous results found for the cases of various α,β -unsaturated ethers.^{9,10,18,19}

Mixtures of *cis*- and *trans*-DME of varying isomeric ratios were mutually copolymerized. The results are given in Table II. From these data

TABLE II
cis-trans Copolymerization of DME^a

| Polymer- ization time, hr | Monomer feed ^b | | Residual monomer ^c | | | |
|------------------------------------|---------------------------|---------|-------------------------------|-------|-------|--------|
| | M_c^0 | M_t^0 | M_c | M_t | m | b |
| 3 | 0.400 | 0.600 | 0.263 | 0.552 | 0.116 | -0.374 |
| 2 | 0.264 | 0.736 | 0.207 | 0.705 | 0.058 | -0.149 |
| 4 | 0.520 | 0.480 | 0.333 | 0.424 | 0.253 | -0.634 |
| 4 | 0.520 | 0.480 | 0.305 | 0.410 | 0.258 | -0.591 |
| 2 | 0.520 | 0.480 | 0.415 | 0.454 | 0.239 | -0.752 |
| 3 | 0.733 | 0.267 | 0.508 | 0.248 | 0.478 | -2.153 |
| 5 | 0.733 | 0.267 | 0.415 | 0.233 | 0.511 | -1.936 |

^a $[\text{BF}_3 \cdot \text{OEt}_2] = 0.038M$.

^b Initial molar compositions of the monomer mixture.

^c Molar fractions of the residual monomers with respect to the monomer feed.

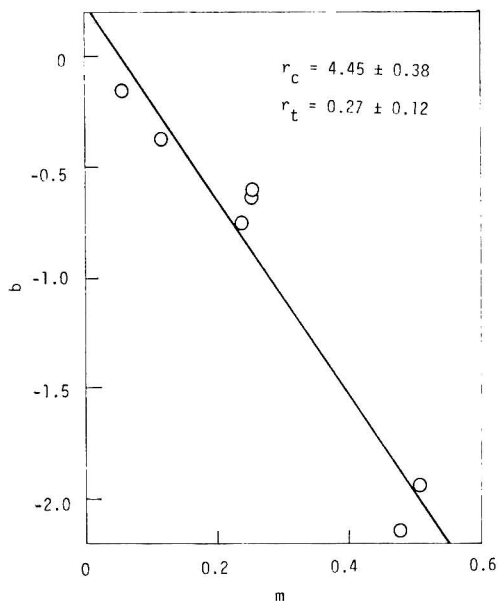


Fig. 1. Linear relationship, $b = -r_c m + r_t$, for the copolymerization between *cis*- and *trans*-DME.

monomer reactivity ratios, r_c and r_t , were calculated by the aid of the integral form of the Mayo-Lewis copolymerization equation. The r_c - r_t relations obtained from the equation were essentially linear, $r_t = m r_c + b$. The constants r_c and r_t were evaluated by the least-squares treatment of

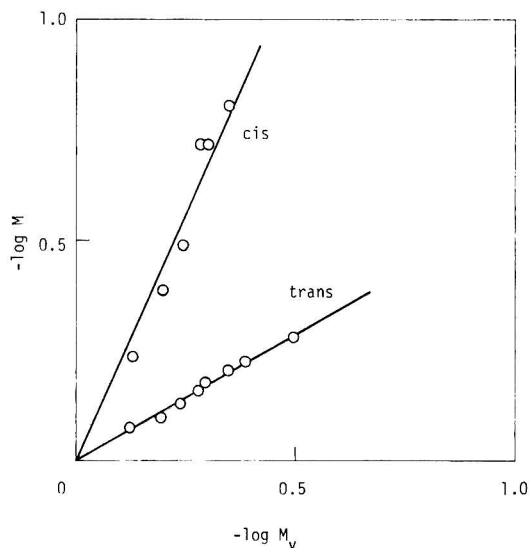


Fig. 2. Log-log plots of residual monomer fractions for the copolymerizations of VIBE(M_v) with *cis*- and *trans*-DME (M). $[\text{BF}_3 \cdot \text{OEt}_2] = 8.7$ mmole/l. $[\text{VIBE}]_0$:- $[\text{cis-DME}]_0$: $[\text{trans-DME}]_0 = 0.322$: 0.386 : 0.292 .

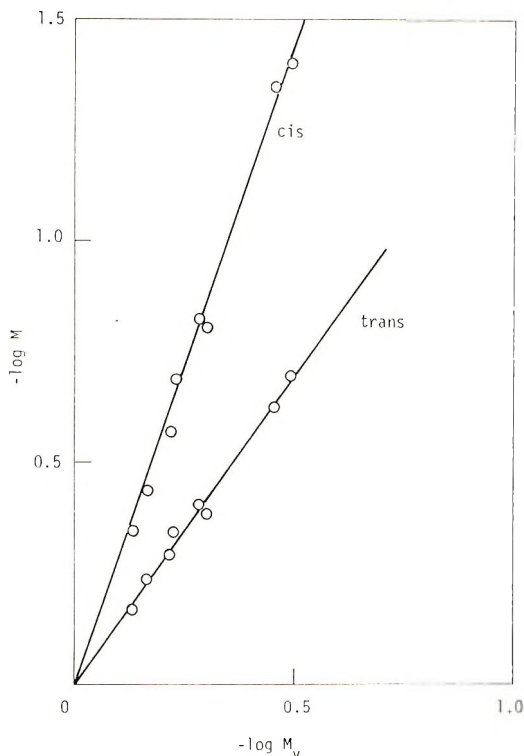


Fig. 3. Log-log plots of residual monomer fractions for the copolymerizations of VIBE(M_v) with *cis*- and *trans*-DEE (M). $[\text{BF}_3 \cdot \text{OEt}_2] = 8.7$ mmole/l. $[\text{VIBE}]_0 : [\text{cis-DEE}]_0 : [\text{trans-DEE}]_0 = 0.327 : 0.504 : 0.169$.

the observed quantities m and b .³ An m - b plot is shown in Figure 1, yielding $r_c = 4.45 \pm 0.38$ and $r_t = 0.27 \pm 0.12$. *cis*-DME is about four times as reactive as *trans*-DME $[(r_c/r_t)^{1/2} = 4.06]$.

Next, the ternary mixture of VIBE and *cis*- and *trans*-DME was copolymerized in order to compare their reactivities. The relative reac-

TABLE III
Relative Polymerizabilities of Dialkoxyethylenes and Vinyl Alkyl Ethers

| Ether | Relative polymerizability ^a | |
|-------------------|--|--------|
| VEE ^b | 1.09 | (1.00) |
| <i>cis</i> -DEE | 2.88 | 2.28 |
| <i>trans</i> -DEE | 1.38 | 1.06 |
| VME ^c | 0.55 | 0.41 |
| <i>cis</i> -DME | 2.23 | 1.71 |
| <i>trans</i> -DME | 0.57 | 0.44 |
| VIBE | (1.00) | 0.92 |

^a Figures in parentheses show the reference reactivity.

^b Vinyl ethyl ether.^{2,5}

^c Vinyl methyl ether.⁵

tivities were conveniently evaluated from the log-log plots of residual monomer fractions as described previously.¹⁷ Such plots for the present system are shown in Figure 2. Relative reactivities were evaluated from the slopes of the plots and are given in Table III. It may be worth noting that *cis*-DME is more reactive than VIBE. Reactivity of *cis*-DME relative to *trans*-DME is calculated to be 3.91, in fair agreement with the value 4.06 obtained from the more precise treatments of the *cis-trans* copolymerization.

The copolymerization of VIBE and *cis*- and *trans*-DEE was carried out in the same manner as described above. The log-log plots are shown in Figure 3. Relative reactivities are given in Table III. Both *cis*- and *trans*-DEE were found to be more reactive than VIBE. *cis*-DEE is *ca.* twice as reactive as its *trans* isomer.

Acid-Catalyzed Hydrolysis

The hydrolysis of α,β -unsaturated ethers is of the first order with respect to both ether and acid. The kinetic measurements were carried out with the mixtures of isomeric ethers as before.^{1,16} The first-order decay of the isomeric ethers was followed separately and, as is seen in Figure 4, was found to hold uniformly down to over 70% conversions of the ethers.

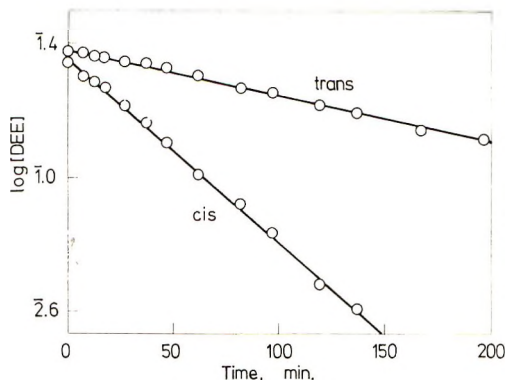
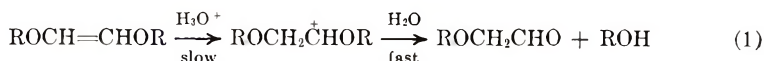


Fig. 4. First-order plots for the hydrolysis of *cis*- and *trans*-DEE at 35°C. $[HCl] = 0.189$ mole/l.

This fact indicates that neither isomer suffers geometrical isomerization during the course of hydrolysis and that the rate constants obtained with isomeric mixtures are significant. Furthermore, it indicates that the reaction under question may proceed through the rate-determining protonation of the ether.^{1,3,16}



The second-order rate constants, $k_2 = k_1/[HCl]$, obtained in the temperature range 25–45°C are shown in Table IV. In the ordinary temperature

region, the *cis* isomers are about four times as reactive as the corresponding *trans* isomers, despite their greater stability as compared with the latter isomers.²⁰ The reactivities of these ethers are as low as one-thousandth those of vinyl alkyl ethers.

TABLE IV
Kinetic Data for the Acid-Catalyzed Hydrolysis
of Dialkoxyethylenes and Vinyl Alkyl Ethers

| Ether | $10^4 k_2$, l/mol-sec | | | ΔH^\ddagger , kcal/mole | ΔS^\ddagger , eu | Relative rate |
|-------------------|------------------------|-------------------|------|------------------------------------|-----------------------------|----------------------|
| | 25°C | 35°C | 45°C | | | |
| VEE ^a | 751 | | | 17.5 | -4.9 | (1.0) |
| <i>cis</i> -DEE | 3.23 | 11.0 ₅ | 36.0 | 20.7 | -5.4 | 4.3×10^{-3} |
| <i>trans</i> -DEE | 0.82 ₀ | 2.87 | 9.82 | 22.8 | -0.9 | 1.1×10^{-3} |
| VME ^b | | | | | | ~ 0.5 |
| <i>cis</i> -DME | 1.53 | 5.38 | 18.3 | 22.7 | 0.2 | 2.0×10^{-3} |
| <i>trans</i> -DME | 0.38 | 1.22 | 4.53 | 22.6 | -2.9 | 0.5×10^{-3} |

^a Data of Kreevoy and Williams.²

^b Data of Ledwith and Woods.²¹

The heats and the entropies of activation, ΔH^\ddagger and ΔS^\ddagger , were evaluated from the k_2 values listed in Table IV and are given in the same table. The magnitudes of the ΔS^\ddagger values are small, mostly negative in sign, in agreement with the results obtained for the case of usual enol ethers.¹

DISCUSSION

Effects of Geometrical Isomerism

The *cis* isomer of either DME or DEE was several times more reactive than the corresponding *trans* isomer both in the cationic polymerization and in the acid-catalyzed hydrolysis, in spite of the greater stability²⁰ of the former isomer. This situation is similar to that observed in the case of β -chlorovinyl ethyl ether.¹⁹ It was previously concluded that the greater reactivity of the *cis* isomers of alkenyl ethers may be due to their lower stabilities in the ground state.^{1,9,10} The results for 1,2-dialkoxyethylenes and β -chlorovinyl ether are completely incompatible with the previous conclusion for alkenyl ethers.

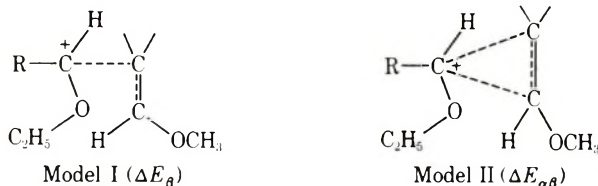
In the cases of a class of olefins carrying polar groups at the both ends of double bond, their polar nature must be substantially different between their geometrical isomers. The *cis* isomers, which bear two polar groups on the same side, are much more polar than the corresponding *trans* isomers, which are symmetrically substituted with two polar groups. Thus, the former isomer might be more amenable to the polar attack of reagents than the latter. This would be a possible interpretation of the difference in the *cis-trans* reactivities of this class of ethers.

Effects of β -Alkoxy Substitution

In the acid-catalyzed hydrolysis, DME and DEE are less reactive than the corresponding vinyl alkyl ethers by a factor of about 10^{-3} . The reactivities of this order are similar to those of styryl ethyl ether¹⁶ and β -chlorovinyl ethyl ether.²⁵ These low reactivities have been considered to be ascribable mainly to the breakdown of an important stabilization effect of a conjugative β -substituent on forming a carbonium-ion-like transition state.¹⁶

On the other hand, cationic polymerizabilities of vinyl alkyl ethers are apparently enhanced by the β -alkoxy group. This observation is similar to that found in the case of propenyl alkyl ethers, where β -methyl substitution reduces the reactivity of vinyl alkyl ethers in hydrolysis while it enhances their cationic polymerizability.^{1,9,10,21} The present results are more conspicuous in this respect.

In order to examine how the β -methoxy group should enhance the polymerizability of vinyl alkyl ethers, extended Hückel molecular orbital calculations have been carried out on vinyl methyl ether (VME) and *cis*- and *trans*-DME completely in the same manner as described previously.²¹ For the sake of simplicity, conformation of the methoxy group has been taken as *s-trans* in all the cases examined. The delocalization energies, ΔE_{β} and $\Delta E_{\alpha\beta}$, for the transition state models, I and II, have been com-



puted according to eqs. (6) and (7) of the previous paper,²¹ respectively. The results of calculations are summarized in Table V. The ΔE_{β} values for model I predict the lower reactivity of DME as compared with VME. Thus, the reactivity indices at the β -carbon of vinyl ether derivatives are in agreement with their hydrolysis reactivities but not with their polymerizabilities.

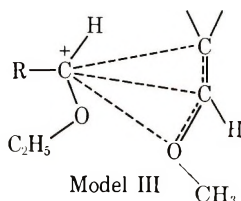
On the other hand, the energies $\Delta E_{\alpha\beta}$ for model II correctly predict the polymerizability of DME relative to VME. Thus, a cyclic transition

TABLE V
Results of Extended Hückel MO Calculations

| Ether | Total energy, eV | ΔE_{β} , γ^2 /eV | $\Delta E_{\alpha\beta}$, γ^2 /eV |
|-------------------|------------------|-------------------------------------|---|
| VME | -463.847 | 0.3377 | 1.1385 |
| <i>cis</i> -DME | -716.648 | 0.3297 | 1.2695 |
| <i>trans</i> -DME | -716.568 | 0.3299 | 1.2698 |

state as depicted by model II seems to be likely for the cationic polymerization of vinyl ethers, in agreement with our previous conclusion drawn from both experimental and theoretical reasonings.^{6,18,21} Results of our recent investigations concerning the substituent effects on the cationic polymerization of benzo uran provide further experimental support to this conclusion.²⁶

On the basis of theoretical calculations which are seemingly analogous to our own, Higashimura et al.²⁷ claim that in the cationic polymerization of vinyl ether derivatives, a polymer-end cation should interact also with an alkoxy oxygen atom as well as α - and β -carbons (model III). However, their calculations of delocalization energies have been based on too



rough a procedure, which makes the results somewhat dubious and hence cannot be considered to provide a foundation reliable enough to permit discrimination between these transition states II and III. Probably, all that we can state for sure at this moment is that the reaction must involve simultaneous attack of the chain end on both the α - and β -carbons of the olefinic bond.

Finally, the present treatments predict almost equal reactivities for the geometrical isomers of DME. As has been discussed in the preceding section, the observed higher reactivity of the *cis* isomer would be due to its polar nature, which was not embodied at all in the above calculations.

The authors are grateful to Mr. Tadao Yoneda, undergraduate trainee, 1967, for able technical assistance.

References

1. T. Okuyama, T. Fueno, H. Nakatsuji, and J. Furukawa, *J. Amer. Chem. Soc.*, **89**, 5826 (1967).
2. M. M. Kreevoy and J. M. Williams, Jr., *J. Amer. Chem. Soc.*, **90**, 6809 (1968); and references cited in ref. 1.
3. T. Fueno, I. Matsumura, T. Okuyama, and J. Furukawa, *Bull. Chem. Soc. Japan*, **41**, 818 (1968).
4. T. Higashimura, J. Masamoto, and S. Okamura, *Kobunshi Kagaku*, **26**, 702 (1968).
5. H. Yuki, K. Hatada, and M. Takeshita, *J. Polym. Sci. A-1*, **7**, 667 (1969).
6. T. Fueno, T. Okuyama, I. Matsumura, and J. Furukawa, *J. Polym. Sci. A-1*, **7**, 1447 (1969).
7. P. Salomaa and P. Nissi, *Acta Chem. Scand.*, **21**, 1386 (1967).
8. A. Mizote, S. Kusudo, T. Higashimura, and S. Okamura, *J. Polym. Sci. A-1*, **5**, 1727 (1967).
9. T. Okuyama, T. Fueno, and J. Furukawa, *J. Polym. Sci. A-1*, **6**, 993 (1968).

10. T. Okuyama, T. Fueno, J. Furikawa, and K. Uyeo, *J. Polym. Sci. A-1*, **6**, 1001 (1968).
11. T. Higashimura, S. Kusudo, Y. Ohsumi, and S. Okamura, *J. Polym. Sci. A-1*, **6**, 2523 (1968).
12. T. Higashimura, S. Kusudo, and S. Okamura, *Kobunshi Kagaku*, **25**, 694 (1968).
13. T. Okuyama, T. Fueno, and J. Furukawa, *J. Polym. Sci. A-1*, **7**, 3045 (1969).
14. T. Higashimura, Y. Ohsumi, S. Okamura, R. Chujo, and T. Kuroda, *Makromol. Chem.*, **126**, 99 (1969).
15. A. Mizote, T. Higashimura, and S. Okamura, *J. Macromol. Sci. (Chem.)*, **A2**, 717 (1968).
16. T. Okuyama, T. Fueno, and J. Furukawa, *Bull. Chem. Soc. Japan*, **43**, 3256 (1970).
17. T. Okuyama, N. Asami, and T. Fueno, *Bull. Chem. Soc. Japan*, **43**, 3549 (1970).
18. T. Okuyama, N. Asami, and T. Fueno, *Bull. Chem. Soc. Japan*, **43**, 3553 (1970); Part XII of this series.
19. T. Okuyama, T. Fueno, and J. Furukawa, *J. Polym. Sci. A-1*, **7**, 2433 (1969).
20. T. Okuyama, T. Fueno, and J. Furukawa, *Tetrahedron*, **25**, 5409 (1969).
21. T. Fueno, T. Okuyama, and J. Furukawa, *J. Polym. Sci. A-1*, **7**, 3219 (1969).
22. H. Baganz and L. Domaschke, *Chem. Ber.*, **91**, 2405 (1958).
23. H. Baganz, K. Praefcke, and J. Rost, *Chem. Ber.*, **96**, 2657 (1963).
24. A. Ledwith and H. J. Woods, *J. Chem. Soc. B*, **1966**, 753.
25. T. Okuyama, unpublished results.
26. T. Okuyama, K. Kunugiza, and T. Fueno, to be published.
27. T. Higashimura, T. Masuda, S. Okamura, and T. Yonezawa, *J. Polym. Sci. A-1*, **7**, 3129 (1969).

Received June 9, 1970

Modification of Poly(vinyl Chloride). XIII. Crosslinking of Poly(vinyl Chloride) with Dithiols and Properties of the Crosslinked Products

KUNIO MORI and YOSHIRO NAKAMURA, *Department of Applied Chemistry, Iwate University, Morioka, Japan*

Synopsis

PVC was crosslinked by immersing PVC-dithiol blends in ethylenediamine at 30°C. Properties of the products depended on the chain length and chemical structure of the crosslinkage and on the molecular weight of the polymer chain between crosslinks M_c . Crosslinking by the agent of soft structure and long molecular chain resulted in high tensile strength at break and impact strength and low brittle temperature. The use of the crosslinking agent of short molecular chain gave high yield strength, Young's modulus, and heat distortion temperature. The relation of M_c and the chemical structure of the crosslinks to the properties of the crosslinked rigid polymer was discussed in regard to the crosslinking effect and plasticizing effect.

INTRODUCTION

A number of studies have been carried out on the modification of poly(vinyl chloride) (PVC) by crosslinking reactions.¹⁻³ The aim of these investigations was to improve the polymer in regard to its dimensional stability, resistance to solvent, creep ratio, heat distortion, and softening temperatures, but the products were inferior to the original PVC in shock resistance and brittle temperature.

Little is known on the relation of the structure of the crosslink to the stress-strain and thermal properties of rigid polymers. In one of our earlier studies,⁴ crosslinked PVC of improved toughness was obtained by the use of elastomer such as liquid thiokol which contains soft segment, and the results suggested that the properties of the crosslinked polymer were dependent mainly upon the following factors: (1) average molecular weight M_c of the polymer chain between crosslinks; (2) chain length L_c , molecular weight, and structure of the crosslink; and (3) structure of the polymer chain.

The present studies were undertaken to confirm these relations. The properties of the crosslinked PVC are discussed in regard to crosslinking effect and plasticizing effect.

EXPERIMENTAL

Materials

PVC was obtained commercially and used without purification; degrees of polymerization (\bar{P}) were 800, 1450, and 2700. Dithiols, except for 1,10-decylidithiol which was obtained commercially, were prepared from the corresponding dichlorides by the thiuronium salt method; their properties are shown in Table I. Poly(ethylene glycols) used in the syntheses were of average molecular weight of 200, 300, 400, 600, and 1000. Ethylenediamine (EDA) was substituted for liquid ammonia, which had been used in our earlier study,⁴ since EDA is easier to handle and accelerates the cross-linking reaction.

TABLE I
Properties of Thiol Compounds

| Dithiol | Molecular weight | SH, % | | Bp, °C mm Hg |
|--|------------------|-------|-------|-----------------|
| | | Found | Calcd | |
| HSCH ₂ (CH ₂ OCH ₂) _n CH ₂ SH | | | | |
| <i>n</i> = 1 (EG-140) | 134 | 47.7 | 47.8 | 84/4 |
| <i>n</i> = 5 (EG-300) | 314 | 21.3 | 21.0 | 130/0.1 |
| <i>n</i> = 9 (EG-500) | 490 | 13.9 | 13.5 | — |
| <i>n</i> = 11 (EG-600) | 630 | 10.4 | 10.5 | — |
| <i>n</i> = 21 (EG-1000) | 1020 | 6.2 | 6.45 | — |
| HSC ₁₀ H ₂₀ SH | 206 | 32.0 | 32.1 | — |
| HSCH ₂ C ₆ H ₄ CH ₂ SH | 176 | 38.5 | 38.8 | 94/0.07 |
| HSCH ₂ C ₆ H ₄ CH ₂ C ₆ H ₄ CH ₂ SH | 260 | 25.4 | 25.4 | — |
| Dimercaptodichloro-paraffin, C ₁₆ H ₃₀ (SH) ₂ Cl ₂ | 360 | 20.1 | 20.1 | — |

Methods of Blending and Crosslinking

PVC and dithiols were blended in a two-roller mill with heating at 150–160°C for 5–10 min without additives. Blending was easily done when more than 2 parts of dithiol were used with 100 parts of PVC. The blended sheets, colorless, about 0.25 mm thick, and soluble in tetrahydrofuran (THF), were immersed in EDA and maintained at 30°C for 90–120 minutes. The whitened sheets were taken out, washed with methanol, and then heated at 100°C for 30 min under reduced pressure (<0.01 mm Hg) to remove residual EDA. The crosslinked PVC thus obtained was colorless, transparent, insoluble in THF, and had a constant swelling ratio.

Methods of Analysis

Chlorine, nitrogen, and thiol groups were determined by Schöniger, Kjeldahl, and iodine methods, respectively. Swelling ratio and THF-insoluble fraction were determined as in our previous paper.⁴ M_c was evaluated from the values of V_2 in the Flory-Rehner equation⁵ as in a previous paper.⁶ Tensile strength, Young's modulus, and elongation at break

were determined with a recording Autograph P-100 at a drawing rate of 5 mm/min at 20°C. Breaking energy was similarly determined at a drawing rate of 500 mm/min and calculated by the equation:

$$\text{Breaking energy (kg-cm/cm}^2\text{)} = 0.01 AL$$

where A is the area enclosed by the stress-strain curve and L is the length of the specimen. The breaking energy can be considered a criterion for the impact strength or shock resistance.⁷ Heat distortion temperature was measured with a Toyoseiki tensile heat distortion apparatus (ASTM D1637-59T) under a specified stress of 15 kg/cm² at the heating rate of 2°C/min. Brittle temperature was determined by measuring the temperature at which a specimen was cracked with scissors in cold methanol.⁸

RESULTS

Crosslinking Conditions

Properties of the products obtained at various immersion temperatures are shown in Table II. At temperatures higher than 50°C, the products were colored, and a small amount of nitrogen was detected; these results suggest the presence of a conjugated double bond and EDA-type crosslink in the products.

TABLE II
Effect of Temperature on the Crosslinking Reaction^a

| Immersion temperature, °C | EDA permeated, wt-% | Crosslinked PVC | | | |
|---------------------------|---------------------|-----------------|------------------------------|----------------|---------|
| | | Color | THF-insoluble fraction, wt-% | Swelling ratio | N, wt-% |
| 10 | 0 | Colorless | 0 | | (0.012) |
| 20 | 4 | " | 30.0 | 6.10 | (0.003) |
| 25 | 11.6 | " | 76.0 | 4.50 | (0.016) |
| 30 | 16.7 | " | 100.0 | 2.90 | (0.011) |
| 40 | 25.6 | " | " | 2.86 | (0.010) |
| 50 | 32.6 | Pale yellow | " | 3.08 | (0.067) |
| 60 | 36.8 | Orange | " | 2.98 | 0.76 |
| 70 | 39.1 | Reddish purple | " | 3.00 | 2.39 |

^a All samples were obtained by immersing PVC blends containing 7 g of EG-600 per 100 g of PVC ($\bar{P} = 1450$) for 60 min in EDA.

Effects of immersion time are shown in Figures 1-3. The degrees of crosslinking depended on the weight of EDA permeated in the blends.

Immersion of the PVC-dithiol blends in EDA at 30°C for 90-120 min seems to give the best results. It was difficult to obtain completely cross-linked PVC of M_c below 4000, as the weight of EDA permeated in the network structure was limited with the increase of crosslinking density.

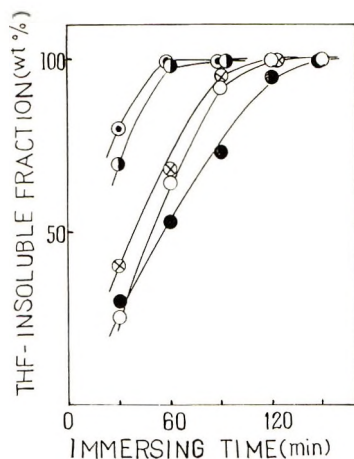


Fig. 1. Effect of THF-insoluble fraction and immersing time on the crosslinking reaction at 30°C: (○) EG-300(3.5, 10); (●) EG-600(7.0, 10); (⊙) EG-300(7.0, 20); (⊗) bis(benzylmercapto)methane (5.2, 20); (●) xylylenedithiol(3.9, 20). Figures in parentheses indicate weight parts per 100 g of PVC and mole parts per 1450 of vinyl chloride units, respectively.

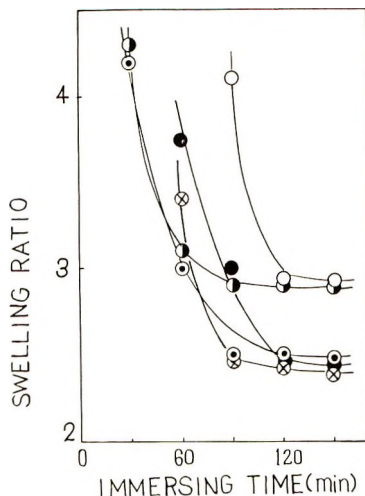


Fig. 2. Effect of the swelling ratio and immersion time on the crosslinking reaction at 30°C: (○) EG-300(3.5, 10); (●) EG-600(7.0, 10); (⊙) EG-300(7.0, 20); (⊗) bis(benzylmercapto)methane(5.2, 20); Xylyleneditriol(3.9, 20). Figures in parentheses indicate weight parts per 100 g of PVC and mole parts per 1450 of vinyl chloride units, respectively.

Properties of PVC Crosslinked with Di(thioethyl) Polyglycols

Properties of the products obtained by crosslinking PVC ($\bar{P} = 1450$) with di(thioethyl) polyglycols are shown in Figures 4-10. Samples were obtained by immersing PVC blends at 30°C until the THF swelling ratio of crosslinked PVC reached an equilibrium value (60-120 min). Cross-

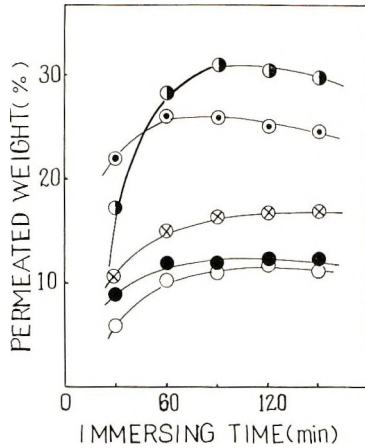


Fig. 3. Effect of permeated weight of EDA and immersion time on the crosslinking reaction at 30°C: (○) EG-300(3.5, 10); (●) EG-600(7.0, 10); (⊙) EG-300(7.0, 20); (⊗) bis(benzylmercapto) methane (5.2, 20); (●) xylylenedithiol (3.9, 20). Figures in parentheses indicate weight parts per 100 g of PVC and mole parts per 1450 of vinyl chloride units, respectively.

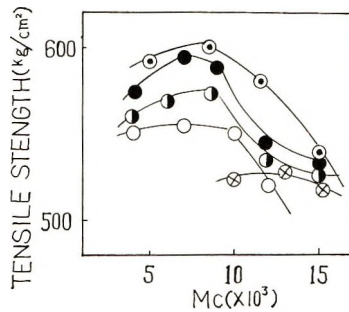


Fig. 4. Effect of M_c and L_c on the tensile strength: (○) EG-140; (●) EG-300; (●) EG-500; (⊙) EG-600; (⊗) EG-1000.

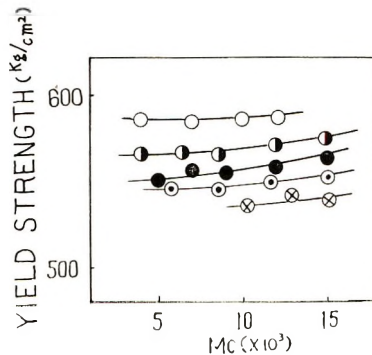


Fig. 5. Effect of M_c and L_c on the yield strength: (○) EG-140; (●) EG-300; (●) EG-500; (⊙) EG-600; (⊗) EG-1000.

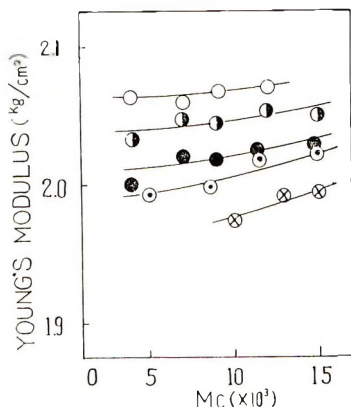


Fig. 6. Relation of M_c and L_c on the Young's modulus: (○) EG-140; (◐) EG-300; (●) EG-500; (◑) EG-600; (⊗) EG-1000.

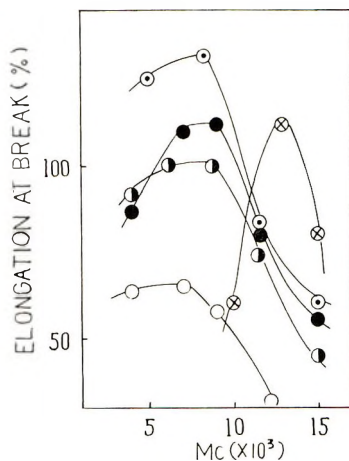


Fig. 7. Effect of M_c and L_c on the elongation at break: (○) EG-140; (◐) EG-300; (●) EG-500; (◑) EG-600; (⊗) EG-1000.

linker concentrations were 5, 7.5, 10, 15, and 20 mole parts per 1450 parts of vinyl chloride units, respectively.

As shown in Figure 4, values of tensile strength were highest at M_c of about 8000; higher values were observed with higher L_c except the case of EG-1000. It might be noted here that L_c increases in the order, EG-140, -300, -500, -600, and -1000 when the molecular chain of the crosslinking agent is completely straight. Commonly the yield strength and Young's modulus tend to increase with decreasing M_c or increasing crosslinking density, but the present results were almost contrary (Figs. 5 and 6). In the case of vulcanized rubber, the elongation at break decreases with decreasing M_c . In the present results, however, the value was lower with higher M_c and highest at M_c of 7000–8000; higher values were observed with higher L_c except in the case of EG-1000 (Fig. 7). As to the elongation

at break, EG-500 and EG-600 gave favorable results. Similar tendencies were observed in regard to the breaking energy (Fig. 8). Slightly lower heat distortion temperature and markedly lower brittle temperature were

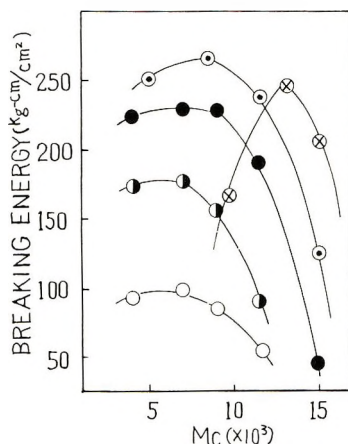


Fig. 8. Effect of M_c and L_c on the breaking energy: (○) EG-140; (●) EG-300; (●) EG-500; (○) EG-600; (⊗) EG-1000.

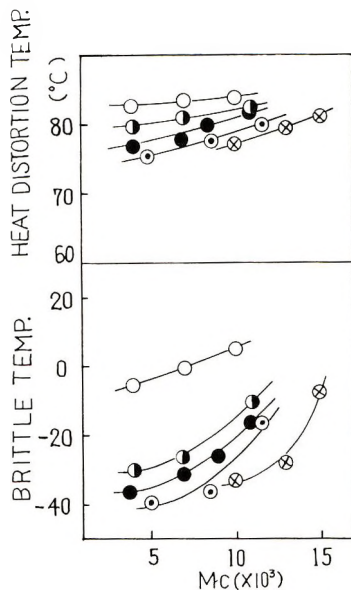


Fig. 9. Effect of M_c and L_c on the heat distortion temperature and brittle temperature: (○) EG-140; (●) EG-300; (●) EG-500; (○) EG-600; (⊗) EG-1000.

observed with lower M_c and with higher L_c (Fig. 9). High heat distortion temperature and fairly low brittle temperature were observed with the crosslinked PVC compared with the uncrosslinked (Fig. 10).

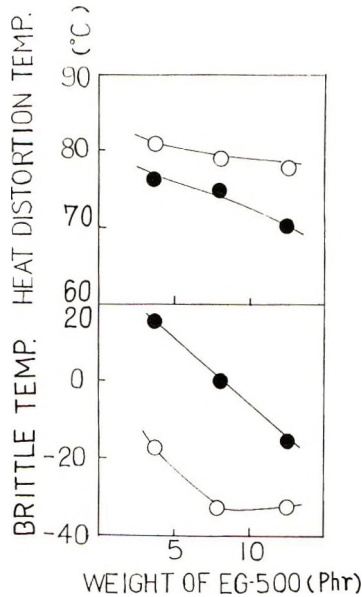


Fig. 10. Effect of (●) uncrosslinked and (○) crosslinked PVC-dithiol blends with EG-600 on the heat distortion temperature and brittle temperature.

The properties of the PVC crosslinked by the crosslinking agent containing a soft segment thus differed from those of other crosslinked amorphous polymers.

The properties of the crosslinked PVC differed with \bar{P} of the original PVC. As shown in Table III, higher tensile strength, Young's modulus and heat distortion temperature but lower brittle temperature were observed with higher \bar{P} . The elongation at break and breaking energy were highest with \bar{P} of 1450.

The properties also differed with the structure of the crosslinking agent (Table IV). When a crosslinking agents containing a soft segment and having a longer molecular chain were used, the products showed high values

TABLE III
Effect of the Degree of Polymerization of PVC^a

| Degree of polymerization | Yield strength, kg/cm ² | Tensile strength, kg/cm ² | Elongation at break, % | Breaking energy, kg-cm/cm ² | Heat distortion temperature, °C | Brittle temperature, °C |
|--------------------------|------------------------------------|--------------------------------------|------------------------|--|---------------------------------|-------------------------|
| 800 | 530 | 560 | 102 | 146 | 79 | -36 |
| 1450 | 535 | 600 | 126 | 230 | 80 | -34 |
| 2160 | 550 | 605 | 96 | 212 | 86 | -33 |

^a All samples were obtained by immersing PVC blends containing 8.8 mole parts of EG-600 per 1000 parts of vinyl chloride units for 90 min at 30°C in EDA, and modulated in M_c of 7500.

TABLE IV
Structure of Crosslinking Agents and Properties of Uncrosslinked PVC and Crosslinked PVC (PVCX)

| Crosslinking agents (CA) | CA, g/100 g of PVC | Crosslinking conditions | | Yield strength, kg/cm ² | | Tensile strength, kg/cm ² | | Elongation at break, % | | Breaking energy, kg-cm/cm ² | | Heat distortion temperature, °C | | Brittle Temperature, °C | |
|---|--------------------|-------------------------|-----------|------------------------------------|-----|--------------------------------------|-----|------------------------|-----|--|-----|---------------------------------|-----|-------------------------|-----|
| | | Temp, °C | Time, min | PVC-X | PVC | PVC-X | PVC | PVC-X | PVC | PVC-X | PVC | PVC-X | PVC | PVC-X | PVC |
| EG-140 | 2.8 | 30 | 120 | 595 | 600 | 580 | 575 | 68 | 45 | 100 | 84 | 85 | 82 | -5 | 15 |
| EG-600 | 8.8 | 30 | 60 | 535 | 500 | 600 | 500 | 135 | 46 | 262 | 90 | 83 | 70 | -35 | -7 |
| EG-1000 | 7.9 | 30 | 90 | 535 | 490 | 535 | 460 | 123 | 42 | 255 | 73 | 80 | 67 | -32 | -5 |
| HSC ₁₀ C ₂₀ SH | 4.5 | 30 | 90 | 540 | 550 | 540 | 525 | 88 | 39 | 146 | 80 | 70 | 62 | -20 | -3 |
| HSCH ₂ C ₆ H ₄ CH ₂ SH | 3.5 | 30 | 120 | 605 | 560 | 570 | 540 | 53 | 41 | 104 | 69 | 93 | 81 | -4 | 18 |
| HSCH ₂ C ₆ H ₄ CH ₂ - C ₆ H ₄ CH ₂ SH | 10.0 | 30 | 60 | 600 | 580 | 570 | 550 | 58 | 20 | 128 | 45 | 91 | 78 | -8 | 16 |
| Dimercapto- dichloroparaffin | 10.0 | 30 | 90 | 560 | 580 | 580 | 575 | 105 | 39 | 170 | 49 | 80 | 69 | -20 | -1 |

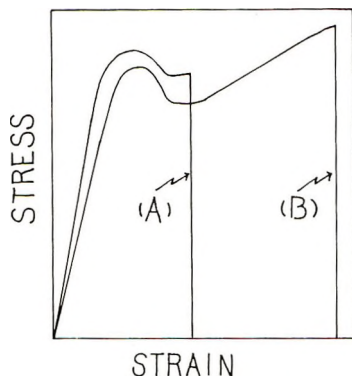


Fig. 11. Types of stress-strain curves.

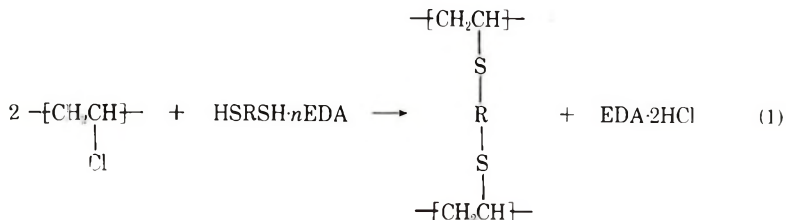
of elongation at break and impact strength and low brittle temperature. Similar results were observed when dithiodichloroparaffin of short chain length was used. However, this was not the case when crosslinking agents with inflexible, short chains were used.

The stress-strain curves of crosslinked PVC can be classified into two types, as shown in Figure 11. The following crosslinking agents gave the products having stress-strain curves, of the type shown in Figure 11A: EG-140, $\text{HSCH}_2\text{C}_6\text{H}_4\text{CH}_2\text{SH}$, and $\text{HSCH}_2\text{C}_6\text{H}_4\text{CH}_2\text{C}_4\text{H}_6\text{CH}_2\text{SH}$; with EG-500, EG-600 and dimercaptodichloroparaffin, curves of the type shown in Figure 11B were obtained.

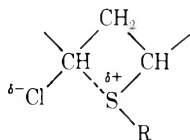
DISCUSSION

Crosslinking Reaction

When PVC-dithiol blends were immersed in EDA, the condensation of PVC with dithiol takes place [eq. (1)].



As reported in a previous paper,⁹ the novel reaction of PVC and dithio was found to be selectively accelerated by primary diamine or liquid ammonia, which lead to formation of an activated complex with dithiol and react as acid acceptors in this reaction. The aliphatic sulfide structure formed may activate the chlorine atoms of neighboring vinylchloride units such as the formation of sulfonium salt:



The activated chlorine atom may react with thiol selectively, and zipper-like substitution readily takes place. Therefore, it is reasonable to assume that the distribution of the crosslinkage is not in a random but a bundle state.

Plasticized Crosslinking Effects

The effect of crosslinking on the stress-strain properties of a rigid polymer such as PVC is considered to be very little, as the segment of the polymer has no mobility at temperatures below T_g . However, crosslinking by a segment which is mobile at room temperature yielded crosslinked PVC of interesting properties, which may be explained in regard to the crosslinking and plasticizing effect as follows.

Crosslinking, causes a decrease in the mobility of the molecular segment and the free volume of the polymer: the shrinkage of the polymer results in the development of internal stress which leads to the growth of submicroscopic cracks. Because of this crosslinking effect, the crosslinked polymers become hard and brittle. When a rigid polymer is fixed (here, PVC), this effect can be related to M_c and its distribution. With low M_c a marked crosslinking effect was observed on the tensile strength, elongation at break, and impact strength, but there was little effect on Young's modulus, yield strength, and thermal properties. This may be because the free volume change due to crosslinking is small as the crosslinks in the bundle state.

When the crosslinking segment is soft and flexible, this portion mobilizes the polymer chain as plasticizer. Such a plasticizing effect depends on the L_c , molecular weight, and flexibility of the crosslink. A long L_c may produce relaxation of the internal stress of network, and flexible and high molecular weight crosslinks are favorable to the mobility of the polymer chain. Consequently, the plasticizing effect of the soft crosslinkage is beneficial to the tensile strength, elongation at break, impact strength, and brittle temperature. The crosslinked polymer is slightly inferior to the original PVC in yield strength, Young's modulus, and heat distortion temperature, however. The plasticizing effect of a crosslink of short L_c , low molecular weight, and hard molecular structure, is little, and the crosslinking effect is predominant. This seems to be also the case with crosslinks of longer L_c , such as EG-1000, probably due to the orientation of the crosslinkages. These effects are clearly observed with the stress-strain curves. In the stress-strain curves of the type shown in Figure 11A, the crosslinking effect is predominant, but in those of Figure 11B, the plasticizing effect predominates.

In conclusion, the plasticized crosslinking of PVC emphasized in this paper should be widely applicable to the improvement of the rigid polymers.

References

1. H. Kozima, *Japan Plastics*, **19**, 1 (1968).
2. K. Mori and Y. Nakamura, *Kobunshi Kagaku*, **25**, 775 (1968); *ibid.*, **26**, 491 (1969).
3. K. Mori and Y. Nakamura, *J. Polym. Sci. B*, **8**, 7 (1970).
4. Y. Nakamura and K. Mori, *J. Polym. Sci. A-1*, **6**, 3269 (1968).
5. P. J. Flory, *J. Chem. Phys.*, **18**, 108 (1950).
6. K. Sofue et al., *Kogyo Kagaku Zasshi*, **61**, 1328 (1958).
7. R. M. Evans, *SPE J.*, **16**, 76 (1960).
8. H. Amagi, *Kobunshi*, **17**, 562 (1968).
9. K. Mori and Y. Nakamura, *Kogyo Kagaku Zasshi*, **72**, 1652 (1968).

Received May 4, 1970

Revised September 3, 1970

Free-Radical Homopolymerization and Copolymerization of Vinylferrocene

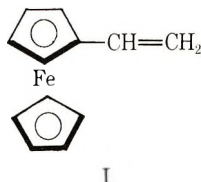
JOHN C. LAI,* THANE ROUNSFELL,† and CHARLES U. PITTMAN, JR.,‡ *Department of Chemistry, University of Alabama, University, Alabama 35486*

Synopsis

The benzene solution homopolymerization of vinylferrocene, initiated by azobisisobutyronitrile, gave a series of benzene-soluble homopolymers. Thus, free-radical copolymerization studies were performed with styrene, methyl acrylate, methyl methacrylate, acrylonitrile, vinyl acetate, and isoprene in benzene. With the exception of vinyl acetate and isoprene, which did not give copolymers with vinylferrocene under these conditions, smooth production of copolymers occurred. The relative reactivity ratios, r_1 and r_2 , were obtained for vinylferrocene-styrene copolymerizations by using the curve-fitting method for the differential form of the copolymer equation, by the Fineman-Ross technique, and by computer fitting of the integrated form of the copolymer equations applied to higher conversion copolymerizations. In styrene (M_2) copolymerizations, the curve-fitting and Fineman-Ross methods both gave $r_1 = 0.08$, $r_2 = 2.50$, while the integration method gave $r_1 = 0.097$, $r_2 = 2.91$. Application of the integration method to methyl acrylate and methyl methacrylate (M_2) gave values of $r_1 = 0.82$, $r_2 = 0.63$; $r_1 = 0.52$, $r_2 = 1.22$, respectively. The curve-fitting method gave $r_1 = 0.15$, $r_2 = 0.16$ for acrylonitrile (M_2) copolymerizations. From styrene copolymerizations, vinylferrocene exhibited values of $Q = 0.145$ and $e = 0.47$.

INTRODUCTION

A number of polymers, which contain the ferrocene group, have been prepared in recent years, and have now been reviewed.¹⁻⁴ While many condensation polymers and unusual structures have been studied, the number of studies of free-radical addition polymers containing ferrocene have been few in number. Vinylferrocene(I) has been homopolymerized by cationic and free-radical routes. Arimoto and Haven^{5,6} homopoly-



* Petroleum Research Fund Predoctoral Fellow 1969-1970.

† Undergraduate Research Fellow 1969-1970.

‡ To whom inquiries should be addressed.

merized vinylferrocene using azobisisobutyronitrile (AIBN) initiation, but they did not extensively characterize the polymers. Cassidy et al.⁷ bulk polymerized vinylferrocene, using AIBN initiation, and obtained polyvinylferrocene with a \bar{M}_n of 48,600. Low molecular weight ($4000 > \bar{M}_n$) polyvinylferrocene was produced by cationic polymerization with $\text{BF}_3 \cdot \text{OEt}_2$, TiCl_4 , AlCl_3 , SnCl_4 , and Et_2AlCl .⁸ In that study, the cationic copolymerization with styrene incorporated styrene into the copolymer only when the styrene content in the monomer feed exceeded 90%. With $\text{BF}_3 \cdot \text{OEt}_2$ -catalyzed initiation in toluene, vinyl isobutyl ether (M_2) copolymerized with vinylferrocene (M_1) giving $r_1 = 0.01 \pm 0.1$ and $r_2 = 9.7 \pm 1.0$. Vinylferrocene has recently been copolymerized with butadiene in toluene solutions by one of us using cobaltic and manganic acetylacetonates as initiators.⁹ Radical-initiated copolymerizations with methyl acrylate, methyl methacrylate, acrylonitrile, vinyl acetate, or isoprene have not been reported.

The most extensive study of vinylferrocene homopolymerization and copolymerization previously published is the study by Baldwin and Johnson.¹⁰ The rate of AIBN-initiated solution polymerization of vinylferrocene ($k = R_p/[\text{M}][\text{I}]^{1/2} = 1.1\text{--}1.8 \times 10^{-4}$) was similar to that of styrene. This study also suggested that ferrocene was very similar to styrene in its effect on the rates of polymerization of methyl methacrylate (MMA) and ethylacrylate. While the data were not precise enough for the determination of relative reactivity ratios, rough estimates were made indicating that r_1 and r_2 ($M_1 = \text{MMA}$ and $M_2 = \text{VF}$) were both less than one and in the same range as that for MMA-styrene copolymerizations where $r_1 = 0.46$ and $r_2 = 0.52$.¹¹ Since polymers containing the ferrocene group might have interesting redox or electron-exchange properties,^{7,12,13} possibilities as charge-transfer complexed polymers,¹³⁻¹⁵ potential as semi-conducting polymers,^{13,16} or ultraviolet- and γ -radiation-absorbing materials,¹⁷⁻¹⁹ we undertook this investigation of the copolymerizability of vinylferrocene with a series of commercially important organic monomers.*

EXPERIMENTAL

Materials

Vinylferrocene was prepared starting with commercial acetylferrocene (Arapahoe Chemical Company). This was reduced with NaBH_4 to hydroxyethylferrocene²¹ in ethanol solution. Hydroxyethylferrocene was dehydrated by using CuSO_4 catalysis in boiling toluene with hydroquinone inhibitor²² or by direct sublimation from an alumina-hydroxyethylferrocene powder mixture.²³ The vinylferrocene was sublimed before use, mp 46.5-47.5°C.⁵ Styrene was washed with 10% aqueous NaOH , with water, dried over anhydrous Na_2SO_4 and then distilled, with a center cut used for

* Initial reports of our work on the homopolymerization of vinylferrocene have appeared.²⁰

all polymerizations. Methyl acrylate, methyl methacrylate, acrylonitrile, vinylacetate, and isoprene were washed with 5% aqueous NaOH, water, dried over Na_2SO_4 and distilled under vacuum. Only center cuts were used. Benzene was distilled from P_2O_5 and AIBN was recrystallized from methanol (mp 102–103°C, decomposition).

Techniques

Monomers and AIBN were weighed, using an analytical balance, and dissolved into benzene. These solutions were placed in Fisher-Porter Aerosol compatibility tubes, equipped with a valve, and degassed at 10^{-3} mm by three alternate freeze-thaw cycles. After degassing, the tubes were placed in constant temperature baths controlled to $\pm 0.01^\circ\text{C}$. All copolymerizations were run at 70°C . After completion of the polymerizations, the benzene solutions were added dropwise to rapidly stirring petroleum ether or methanol to precipitate the polymer. The polymer was filtered and reprecipitated in this manner two more times to insure its purity. The polymers were then dried under vacuum and weighed. Infrared spectra were taken on a Perkin-Elmer Model 237 instrument, and the glass transition temperatures were approximated by using the differential scanning calorimetry technique on a Perkin-Elmer DSC Model 1B calorimeter. Number-average molecular weights were determined by using a Mel-Labs vapor pressure osmometer (VPO), and molecular weight distributions were measured on a Waters Model 200 gel-permeation chromatograph. The molecular weight distributions were then calculated by using the VPO-determined values of \bar{M}_n at the number-average chain length \bar{A}_n on the gel-permeation chromatogram. A Q factor of 88 was used for vinylferrocene as in previous work.²⁰ Viscosities were measured in benzene by using Cannon-Fenske viscometers.

Determination of Relative Reactivity Ratios

The relative reactivity ratios were determined by using both the differential form of the copolymer composition equation,^{24a} eq. (1), and

$$\frac{d[M_1]}{d[M_2]} = \left(\frac{[M_1]}{[M_2]} \right) \frac{r_1[M_1] + [M_2]}{r_2[M_2] + [M_1]} \quad (1)$$

the integrated form of this equation²⁵ [eq. (2)].

$$r_2 = \frac{\log([M_2^0]/[M_2]) - (1/P) \log\{(1 - P)([M_1]/[M_2])/(1 - P)([M_1^0]/[M_2^0])\}}{\log([M_1^0]/[M_1]) + \log\{(1 - P)([M_1]/[M_2])/(1 - P)([M_1^0]/[M_2^0])\}} \quad (2)$$

where

$$P = (1 - r_1)/(1 - r_2)$$

The differential form [eq. (1)] was applied to vinylferrocene-styrene (and acrylonitrile) copolymerizations by performing a series of polymerizations to low conversions, the $[M_1^0]/[M_2^0]$ ratio being varied for the monomer pair in each run. At low conversion $d[M_1]/d[M_2]$ becomes m_1/m_2 (the monomer mole ratio found in the copolymer). In each case vinylferrocene is defined as M_1 . A plot was made of m_1 versus $[M_1^0]$ (mole fraction of M_1 in the starting solution), and the values of r_1 and r_2 were obtained by fitting the curve generated by the best r_1, r_2 pair to the experimental curve. Alternatively, the Fineman-Ross²⁶ method was applied to this data. Substituting F for $[M_1]/[M_2]$ and f for m_1/m_2 in eq. (1) and rearranging results in eq. (3), which can be rearranged, in turn, to eq. (4).

$$F/f(f-1) = r_1 F^2/f - r_2 \quad (3)$$

$$(f-1)/F = -r_2 f/F^2 + r_1 \quad (4)$$

A plot of $(F/f)(f-1)$ as the ordinate and F^2/f as the abscissa gives a straight line whose slope is r_1 and whose intercept is $-r_2$ by eq. (3). In equation (4), a plot of $(f-1)/F$ versus f/F^2 gives a slope of $-r_2$ and an intercept of r_1 . The advantage of having both forms of the equation is that in some cases one gives a better straight line than the other.

The most convenient method for determining reactivity ratios was by use of the integrated equation, eq. (2). This permitted polymerizations to higher conversions which is important with an expensive monomer such as vinylferrocene. In this technique, a series of polymerizations, to different per cent conversions, were performed at two different initial monomer concentration ratios, $[M_1^0]/[M_2^0]$. For each initial ratio, a plot of the copolymer composition (in weight per cent of M_1) versus the weight per cent conversion was constructed. One point from each of the two curves was selected, and this set of points was fed into a computer program developed by Montgomery and Fry²⁷ and adapted by us to an IBM-360-Model 50 computer by using Fortran IV. Each such data point gives r_2 as a function of P . For any set of two points there is a unique value of P that gives identical values of r_2 . The program accepts initial monomer concentrations and both polymer composition and conversion data for two points and varies P so as to rapidly converge r_2 for this data. These r_2 and P values are then used to calculate r_1 . For each copolymer, we used 16 sets of data points (one taken from each of the two curves) for each determination of r_1 and r_2 . This gives a range of r_1 and r_2 values which are then used to reconstruct new polymer composition versus conversion curves by using a second computer program.²⁷ The best values of r_1 and r_2 are those which give calculated composition versus conversion curves which most closely fit the experimental curves.

Any two data points from a single experimental composition-conversion curve could be used to get r_1 and r_2 , but this requires input experimental data accurate to an order of $\pm 0.01\%$. Our experimental data are not nearly that good. By using two appropriately different initial monomer

compositions, one point from each of the resulting composition versus conversion curves can be used with a much lower experimental accuracy necessary to obtain acceptable r_1 , r_2 values. By using 16 such sets of points we are able to cover a range in which the true r_1 and r_2 values surely lie. The best r_1 and r_2 values for our data are then chosen by picking the specific r_1 and r_2 values in this range which regenerated composition-conversion curves most closely duplicating the experimental curves.

RESULTS

Homopolymerization

The results of homopolymerizations in benzene solution are summarized in Table I. While good yields of poly(vinylferrocene) could be obtained,

TABLE I
Homopolymerization of Vinylferrocene in Benzene Solution

| No. | \bar{M}_n | \bar{M}_w | n | AIBN, wt-% | Temp, °C | Reaction time, hr | Yield, % |
|-----|-------------|-------------|------|---------------|-------------|-------------------------|-------------------|
| 1 | 11,400 | 19,000 | 6.80 | 0.985 | 70 | 96 | 69.5 |
| 2 | 10,900 | 18,100 | 6.56 | 1.006 | 80 | 96 | 62.0 |
| 3 | 11,400 | 18,900 | 6.54 | 1.152 | 70 | 94.5 | 73.0 |
| 4 | 6,800 | 10,500 | 4.08 | 1.000 | 90 | 96 | 29.1 |
| 5 | 7,320 | 11,100 | 4.22 | 0.996 | 100 | 96 | 23.8 |
| 6 | 5,560 | 9,200 | 3.85 | 0.995 | 120 | 96 | 33.3 |
| 7 | 9,730 | 16,600 | 6.02 | 1.090 | 60 | 143 | 39.3 |
| 8 | 10,700 | 15,400 | 4.81 | 0.600 | 80 | 96 | 28.2 ^a |

^a 80% benzene-soluble and 20% benzene-insoluble.

the molecular weights were not very high. Since the range of molecular weight in these samples was not large, no meaningful correlation of $[\eta]$ with \bar{M}_n or \bar{M}_w could be obtained.

By using differential scanning calorimetry, the glass transition temperature T_g for all the polyvinylferrocene samples were found at approximately 190°C. Since the chromatograms exhibited broad curves, this value is approximate. However, compared with polystyrene's T_g of 88°C, it is clear the ferrocene nucleus sharply increases the cohesive energy in these polymers relative to a benzene ring. Polyvinylferrocene gave ultraviolet bands at 440, 323 (sh), 260, and 232 $m\mu$ with extinction coefficients of 109, 4960, 6600, and 6460, respectively.

Copolymerization

The low conversion copolymerizations of vinylferrocene with styrene and acrylonitrile are summarized in Table II and III; these data were treated by curve fitting (see Fig. 1) and by the Fineman-Ross method (see Fig. 2). Copolymerizations of vinylferrocene with styrene, methyl

TABLE II
Copolymerization of Vinylferrocene and Styrene at 70°C to Low Conversion

| Vinylferrocene in Feed, mole-% | Reaction time, hr | Conversion, % | Fe in copolymer, % | Vinylferrocene in copolymer, mole-% |
|--------------------------------------|----------------------|------------------|-----------------------|---|
| 10.03 | 1.0 | 2.63 | 2.17 | 4.22 |
| 25.40 | 3.5 | 9.27 | 4.87 | 10.02 |
| 40.08 | 3.6 | 4.35 | 7.65 | 16.75 |
| 50.12 | 5.0 | 6.30 | 9.45 | 21.57 |
| 62.25 | 9.2 | 6.61 | 12.02 | 36.75 |
| 79.94 | 20.0 | 5.26 | 16.45 | 44.97 |
| 89.97 | 20.0 | 7.36 | 19.34 | 57.61 |

* The weight ratio of vinylferrocene to AIBN was always between 150 to 1000 in these studies.

acrylate, and methyl methacrylate to higher conversions are summarized in Table IV. Smooth copolymerizations took place, and the copolymers obtained gave homogeneous, single polymer gel-permeation chromatograms. The relative reactivity ratios in these copolymerizations are tabulated in Table V along with calculated Q and e values for vinylferrocene. Determinations of r_1 and r_2 by using integrated eq. (2) were performed by using 16 pairs of data points for each monomer pair. Example data for the styrene copolymerization is summarized in Table VI.

Several attempts to copolymerize vinylferrocene with vinyl acetate and isoprene were unsuccessful. Vinylferrocene, vinyl acetate, and AIBN in a mole ratio of 0.48/1/0.0124, respectively, were added to benzene (10.92 g

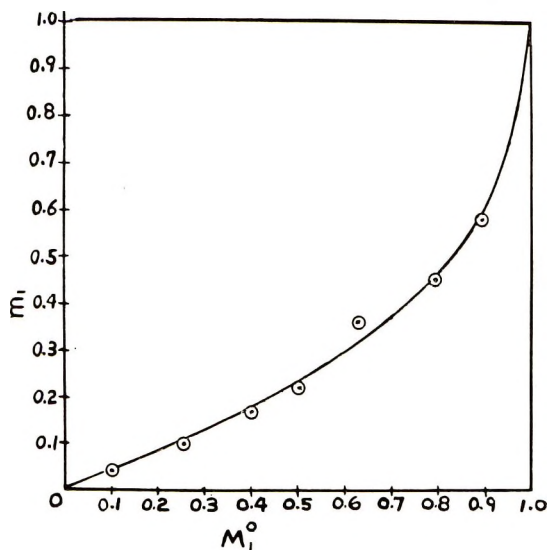


Fig. 1. Copolymerization of vinylferrocene (M_1) with styrene to low conversions: (○) experimental points; (—) theoretical curve generated for $r_1 = 0.08$, $r_2 = 2.50$.

TABLE III
 Copolymerization of Vinylferrocene and Acrylonitrile at 70°C to Low Conversion^a

| Vinylferrocene in feed, mole-% | Reaction time hr | Conversion, % | Fe in copolymer, % | Vinylferrocene in copolymer, mole-% |
|--------------------------------------|---------------------|------------------|-----------------------|---|
| 9.92 | 0.25 | 1.83 | 16.45 | 29.3 |
| 25.25 | 0.40 | 3.85 | 18.88 | 38.8 |
| 39.98 | 0.50 | 2.99 | 19.72 | 45.2 |
| 47.97 | 0.75 | 6.70 | 20.99 | 49.1 |
| 64.49 | 1.00 | 1.91 | 22.05 | 56.0 |
| 77.46 | 12.0 | 6.87 | 22.49 | 59.6 |
| 89.79 | 13.2 | 7.40 | 23.13 | 64.0 |

^a Each initiated by 0.1 mole-% AIBN.

TABLE IV
 Copolymerizations of Vinylferrocene (M_1) at 70°C in Benzene Initiated by AIBN^a

| No. | M_2 | Weight fraction in feed, vinylferro- cene/ M_2 | Reaction time, hr | Con- version, % | % Fe in Co- polymer | Weight Fraction M_1/M_2 in Copolymer |
|----------------|--------------------------|--|-------------------------|-----------------------|---------------------------|---|
| 1 | Styrene | 0.404/0.596 | 3.5 | 9.23 | 4.87 | 0.185/0.815 |
| 2 | " | " | 9.0 | 18.71 | 5.06 | 0.192/0.808 |
| 3 | " | " | 15.0 | 22.49 | 5.10 | 0.194/0.806 |
| 4 | " | " | 23.0 | 24.91 | 5.12 | 0.195/0.805 |
| 5 | " | 0.780/0.220 | 15.0 | 2.61 | 12.82 | 0.487/0.513 |
| 6 | " | " | 24.0 | 8.76 | 12.97 | 0.492/0.508 |
| 7 | " | " | 36.0 | 10.66 | 13.02 | 0.495/0.505 |
| 8 | " | " | 38.8 | 21.93 | 13.18 | 0.500/0.500 |
| 1 | Methyl acrylate | 0.477/0.523 | 6.0 | 17.4 | 14.10 | 0.535/0.465 |
| 2 | " | " | 18.5 | 51.0 | 13.83 | 0.525/0.475 |
| 3 | " | " | 24.0 | 66.0 | 13.63 | 0.517/0.483 |
| 4 | " | " | 36.0 | 78.8 | 13.20 | 0.501/0.499 |
| 5 | " | 0.387/0.613 | 3.0 | 6.5 | 12.16 | 0.461/0.539 |
| 6 | " | " | 16.6 | 44.0 | 11.71 | 0.444/0.556 |
| 7 | " | " | 8.0 | 12.0 | 12.10 | 0.459/0.541 |
| 1 | Methyl meth- acrylate | 0.440/0.560 | 38.0 | 75.2 | 10.73 | 0.407/0.593 |
| 2 | " | " | 24.0 | 36.2 | 10.11 | 0.384/0.616 |
| 3 | " | " | 10.0 | 8.9 | 9.66 | 0.367/0.633 |
| 4 | " | " | 20.0 | 34.0 | 10.09 | 0.382/0.618 |
| 5 | " | 0.361/0.639 | 5.0 | 14.4 | 7.89 | 0.300/0.700 |
| 6 | " | " | 16.0 | 43.4 | 8.34 | 0.317/0.683 |
| 7 ^b | " | " | 20.0 | 51.2 | 8.44 | 0.321/0.679 |

^a With 0.1 mole-% AIBN unless otherwise noted.

^b With 0.2 mole-% AIBN.

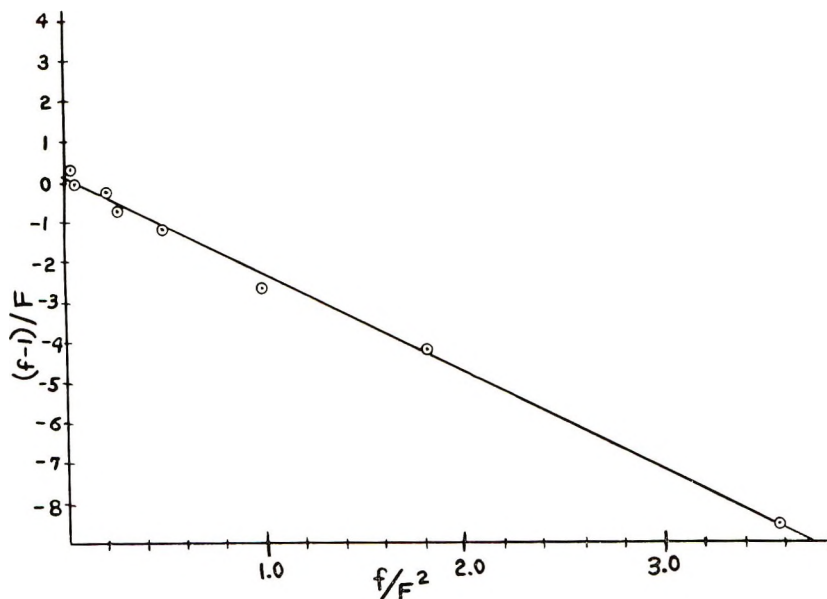


Fig. 2. Fineman-Ross plot for vinylferrocene-styrene copolymerizations.

vinylferrocene to 100 ml of solution) and polymerizations at 70°C were carried out for reaction times ranging from 47 to 144 hr. On work-up, unreacted vinylferrocene was recovered. Other unsuccessful attempts were made when the mole ratio was changed to 0.206/1/0.075. A series of unsuccessful attempts to copolymerize vinylferrocene with isoprene were

TABLE V
Relative Reactivity Ratios in Vinylferrocene Copolymerizations
at 70°C Initiated by AIBN in Benzene

| M_2^a | r_1 | r_2 | $r_1 r_2$ | Q | e |
|---------------------------------------|---------------|-------------|-----------|--------------------|-------------------|
| Styrene ^b | 0.08 ± 0.04 | 2.50 ± 0.20 | 0.20 | 0.145 ^c | 0.47 ^c |
| Styrene ^d | 0.08 ± 0.02 | 2.50 ± 0.50 | 0.20 | | |
| Styrene ^e | 0.097 ± 0.043 | 2.91 ± 0.07 | 0.28 | | |
| Methyl acrylate ^e | 0.82 ± 0.05 | 0.63 ± 0.03 | 0.52 | 1.16 ^f | 1.39 ^f |
| Methyl meth- acrylate ^e | 0.52 ± 0.27 | 1.22 ± 0.37 | 0.64 | 0.79 ^g | 1.07 ^g |
| Acrylonitrile ^e | 0.15 ± 0.05 | 0.16 ± 0.05 | 0.024 | 0.05 ^h | 0.73 ^h |

^a Vinylferrocene is M_1 in all cases.

^b From curve-fitting technique by use of differential form of the copolymer equation.

^c Based on $Q_2 = 1.0$ and $e_2 = -0.8$ for styrene.²⁸

^d By use of the Fineman-Ross treatment.

^e Using the integrated form of the copolymer equation on copolymerizations to higher conversions.

^f Based on $Q_2 = 0.46$ and $e_2 = 0.58$ for methyl acrylate.²⁸

^g Based on $Q_2 = 0.74$ and $e_2 = 0.40$ for methyl methacrylate.^{24b, 29}

^h Based on $Q_2 = 0.44$ and $e_2 = 1.2$ for acrylonitrile.^{24b}

TABLE VI
Individual Vinylferrocene-Styrene Relative Reactivity Ratios Generated from Various Combinations of Data Points from Copolymerizations at Two Different Monomer Feed Ratios by the Integrated Form of Copolymer Equation^a

| Combination number ^a | r_1 | r_2 |
|---------------------------------|--------|--------|
| 1-5 | 0.1290 | 2.9171 |
| 1-6 | 0.1079 | 2.8940 |
| 1-7 | 0.1058 | 2.8917 |
| 1-8 | 0.0542 | 2.8354 |
| 2-5 | 0.1299 | 2.9233 |
| 2-6 | 0.1085 | 2.8985 |
| 2-7 | 0.1063 | 2.8960 |
| 2-8 | 0.0547 | 2.8356 |
| 3-5 | 0.1348 | 2.9567 |
| 3-6 | 0.1127 | 2.9302 |
| 3-7 | 0.1104 | 2.9274 |
| 3-8 | 0.0569 | 2.8632 |
| 4-5 | 0.1395 | 2.9888 |
| 4-6 | 0.1167 | 2.9607 |
| 4-7 | 0.1143 | 2.9577 |
| 4-8 | 0.0595 | 2.8902 |

^a Initial mole ratios of vinylferrocene to styrene were 0.725/1 for runs 1-4 and 0.139/1 for runs 5-8.

^b From Table III.

made at 70°C in mole ratios of 0.32/1, respectively (weight ratio 1/1 with 0.01 AIBN).

The values of Q and e for vinylferrocene (M_1) were determined from the experimental values of r_1 and r_2 , summarized in Table V, and from literature values of Q_2 and e_2 for the comonomer (see footnotes, Table V). The standard equations (5)-(7)^{24c} were used in these calculations.

$$r_1 = (Q_1/Q_2) \exp\{-e_1(e_1 - e_2)\} \quad (5)$$

$$r_2 = (Q_1/Q_2) \exp\{-e_2(e_2 - e_1)\} \quad (6)$$

$$r_1 r_2 = \exp\{-(e_1 - e_2)^2\} \quad (7)$$

A Q - e map was constructed to include all four copolymerizations.^{24d} Q_1 was plotted versus e_1 for both extremes of uncertainty of both r_1 and r_2 . The intersecting area is the region for the correct Q and e . This was done for all four copolymerizations in hopes of finding a region where Q and e would be a best fit for all copolymerizations. It was clear that no such region exists in these copolymerizations and the normal Q - e predictions do not appear to be possible with vinylferrocene.

This behavior is not unexpected for vinylferrocene. When compared to a phenyl ring, the ferrocene nucleus exhibits an extraordinary ability to stabilize adjacent positive charge.³⁰⁻³³ For example, σ^+ of p -ferrocene (determined from p -ferrocenylphenylethyl chloride solvolyses) is -0.71 and σ^+

of the α -ferrocenyl substituent is -1.4^{32} . Even in the meta position, ferrocene exhibits σ_1 of -0.88^{34} (-0.05).³⁵

Under the conditions of weaker electron demand exhibited when *p*-ferrocenylbenzoic acid dissociates, ferrocene shows a Hammett σ_p of 0.18 which is roughly equivalent to that of a methyl group.³⁴ On the other hand, available evidence indicates the ferrocenyl group destabilizes radical anions³⁶ and radical^{37,38} centers in comparison with the effect exerted by a phenyl ring. Thus, one could not expect vinylferrocene to fit neatly into the $Q-e$ scheme.

Certain trends can be noted by observing the values of r_1 and r_2 reported in Table V. A growing polymer chain, ending in either styryl or a ferrocenyl radical, prefers to add to styrene as opposed to vinylferrocene. This is expected since the ferrocene nucleus does not stabilize radical centers as much as a phenyl ring. [The Q_1 value for vinylferrocene (M_1) of 0.145 in styrene copolymerizations emphasizes this low reactivity.] As the reactivity of M_2 decreases on going from styrene to methyl acrylate, r_1 increases. Now the terminal ferrocenyl radical on a propagating chain has a choice between two rather unreactive (compared to styrene) monomers: methyl acrylate or vinylferrocene. Thus, no great selectivity is exhibited, and r_1 becomes 0.82.

Methyl acrylate is an electron-withdrawing monomer compared to styrene. The transition state for a ferrocenyl radical adding to methyl acrylate could be stabilized by a polar resonance contribution which contributes more strongly than when a styryl radical adds to methyl acrylate. This follows from ferrocene's remarkable ability to supply electron density as the demand increases. However, this tendency is not so strong as to cause alternation or to cause $r_1 r_2$ to approach zero. A ferrocenyl radical can add to methyl methacrylate, relative to vinylferrocene, more readily than it can add to methyl acrylate. This follows from the r_1 value of 0.52 (versus 0.82 for methyl acrylate). This is expected because methyl methacrylate can be attacked by many radicals more rapidly than methyl acrylate can; because the methyl group stabilizes the transition state of radical attack more than the starting materials. For instance, a styryl radical adds to methyl methacrylate and methyl acrylate at 60°C with propagation constants of 339 and 235, respectively.³⁹ The respective constants for the addition of the radical of vinyl acetate are 250,000 and 37,000.³⁹ Thus, methyl methacrylate should be attacked by ferrocenyl radicals more rapidly than methyl acrylate. The increase in r_2 going from methyl acrylate (0.63) to methyl methacrylate (1.22) in vinylferrocene copolymerizations also reflects methyl methacrylate's greater reactivity.

The vinylferrocene-acrylonitrile copolymerization shows a marked tendency to alternate. The small values of r_1 and r_2 (0.15 and 0.16, respectively) lead to an $r_1 r_2$ product of 0.024 which is close to zero. This is evidence for a significant polar contribution to the transition state when a ferrocenyl radical adds to acrylonitrile or when the radical of acrylonitrile adds to vinylferrocene. This is in accord with the great ability of ferrocene to supply electron density towards electron deficient centers. The vinyl

group in acrylonitrile is more strongly positively polarized than is the vinyl group in methyl acrylate. With this increased positive character, the polar contribution to the transition state increases in importance until a strong tendency to alternate is reached with acrylonitrile as M_2 . Further studies with maleic anhydride as M_2 are now under way.⁴⁰

Vinylferrocene should now be considered a promising monomer for copolymerization with a wide variety of organic monomers. It should become a useful specialty additive to copolymer and terpolymer systems currently in use.

This work was supported by Petroleum Research Fund, Grant No. 4479 AC 1-3, by Research Corporation funds to purchase a gel-permeation chromatograph, and by the Paint Research Institute's Fellowship Program. In addition, support from a Sigma Xi grant and by the College Work Study Program are gratefully acknowledged.

References

1. C. U. Pittman, Jr., *J. Paint Technol.*, **39**, No. 513, 585 (1967).
2. H. Valot, *Double Liaison* (France), **130**, 775 (1966).
3. M. Dub, "Compounds of the Transition Metals," Vol. 1, Springer-Verlag, Berlin (1966).
4. E. W. Neuse, in *Advances in Macromolecular Chemistry*, W. M. Pasika, Ed., Academic Press, New York, 1968.
5. F. S. Arimoto and A. C. Haven, Jr., *J. Amer. Chem. Soc.*, **77**, 6295 (1955).
6. A. C. Haven, Jr., U. S. Pat. 2,821,512 (Jan. 28, 1958).
7. Y. H. Chen, M. Fernandez-Refojo, and H. G. Cassidy, *J. Polym. Sci.*, **40**, 433 (1959).
8. C. Aso, T. Kunitake, and T. Nakashima, *Makromol. Chem.*, **124**, 232 (1969).
9. C. U. Pittman, Jr., *J. Polym. Sci. B*, **6**, 19 (1968).
10. M. G. Baldwin and K. E. Johnson, *J. Polym. Sci. A-1*, **5**, 2091 (1967).
11. F. R. Mayo and C. Walling, *Chem. Rev.*, **46**, 191 (1950).
12. R. L. Brandon, J. H. Osiecki, and A. Ottenberg, *J. Org. Chem.*, **31**, 1214 (1966).
13. C. U. Pittman, Jr., J. C. Lai, and D. P. Vanderpool, *Macromolecules*, **3**, 105 (1970).
14. E. Adams, M. Rosenblum, S. S. Sullivan, and T. N. Margulis, *J. Amer. Chem. Soc.*, **89**, 4540 (1967).
15. R. L. Collins and R. Pettit, *J. Inorg. Nucl. Chem.*, **29**, 503 (1967).
16. Ya. M. Paushkin et al., *J. Polym. Sci. A-1*, **5**, 1203 (1967).
17. J. H. Richards, *J. Paint Technol.*, **39**, No. 513, 569 (1967).
18. R. C. McIlhenny and S. A. Honigstein, Report No. AF MLTR-65-294, July 1965, AD 476623.
19. R. G. Schmitt and R. C. Hirt, Air Force WADE Technical Reports, 59-354; 60-704; 61-298 (available from the Defense Documentation Center, Alexandria, Va.).
20. J. C. Lai, T. Rounsfell, and C. U. Pittman, Jr., paper presented at the 160th National Meeting of the American Chemical Society, Chicago, Ill., Sept. 13-18, 1970, *Abstracts*; also preprint papers of Division of Polymer Chemistry and *Macromolecules*, **3**, No. 6, 746 (1970).
21. C. R. Hauser and J. K. Lindsay, *J. Org. Chem.*, **22**, 906 (1957).
22. I. Pascal and W. J. Borecki, U. S. Pat. 3,132,165 (1964).
23. M. D. Rausch and A. Siegal, *J. Organometal. Chem.*, **11**, 317 (1968).
24. T. Alfrey, Jr., J. J. Bohrer, and H. Mark, *Copolymerization* (High Polymers, Vol. VIII), Interscience, New York, 1952, (a) pp. 5-43; (b) p. 91; (c) p. 80; (d) pp. 96-104.
25. F. R. Mayo and F. M. Lewis, *J. Amer. Chem. Soc.*, **66**, 1954 (1944).

26. M. Fineman and S. D. Ross, *J. Polym. Sci.*, **5**, 259 (1950).
27. D. R. Montgomery and C. E. Fry, in *The Computer in Polymer Science (J. Polym. Sci. C, 25)*, J. B. Kinsinger, Ed., Interscience, New York, 1968, p. 59. We are indebted to Dr. Montgomery for sending us a copy of these programs.
28. C. C. Price, *J. Polym. Sci.*, **3**, 772 (1948).
29. K. Chikanishi and T. Tsuruta, *Makromol. Chem.*, **81**, 211 (1965).
30. E. M. Arnett and R. D. Bushick, *J. Org. Chem.*, **27**, 111 (1962).
31. C. U. Pittman, Jr., *Tetrahedron Letters*, **37**, 3619 (1967).
32. T. G. Traylor and J. C. Ware, *J. Amer. Chem. Soc.*, **89**, 2304 (1967).
33. M. Cais, *Organometal. Chem. Rev.*, **1**, 435 (1966).
34. A. N. Nesmeyanov, E. G. Perevalova, S. P. Gubin, K. I. Grandberg, and A. G. Kozlovsky, *Tetrahedron Letters*, **22**, 238 (1966).
35. S. P. Gubin and A. A. Lubovich, *J. Organomet. Chem.*, **22**, 183 (1970).
36. C. Elschenborvich and M. Cais, *J. Organomet. Chem.*, **18**, 135 (1969).
37. A. A. Berlin, *Khim. Prom.*, **1962**, 881.
38. E. G. Perevalova and Yu. A. Ustynayak, *Izvest. Akad. Nauk, USSR*, **1963**, 1776.
39. M. S. Matheson, E. E. Auer, E. B. Bevilacqua, and E. J. Hart, *J. Amer. Chem. Soc.*, **71**, 497, 2610 (1949).
40. R. Voges and C. U. Pittman, Jr., research in progress.

Received July 21, 1970

Revised September 9, 1970

Polymerization by Oxidative Coupling. II. Co-Redistribution of Poly(2,6-diphenyl-1,4-phenylene Ether) with Phenols

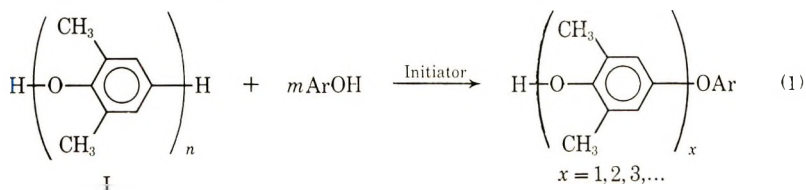
DWAINE M. WHITE, *General Electric Research & Development Center, Schenectady, New York 12301*

Synopsis

Poly(2,6-diphenyl-1,4-phenylene ether) reacts with phenols in the presence of an initiator to form a mixture of low molecular weight hydroxyarylene ethers. Although the reaction is similar to the equilibration of poly(2,6-dimethyl-1,4-phenylene ether) with phenols, higher reaction temperatures and larger initiator concentrations are required. Compounds as 3,3',5,5'-tetraphenyl-4,4'-diphenoquinone, *tert*-butyl perbenzoate, and benzoyl peroxide are active initiators. The structure of the polymer affects the extent to which the polymer equilibrates.

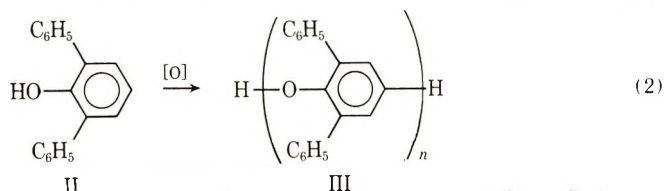
INTRODUCTION

Many phenols co-redistribute with poly(2,6-dimethyl-1,4-phenylene ether) I, to form a mixture of low molecular weight hydroxyarylene ethers

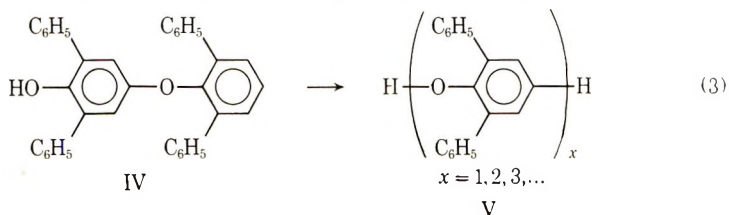


[reaction (1)].¹ The series of equilibration reactions which occurs in the co-redistribution is related to the redistribution mechanism for the oxidative coupling of 2,6-dimethylphenol to form polymer I.²

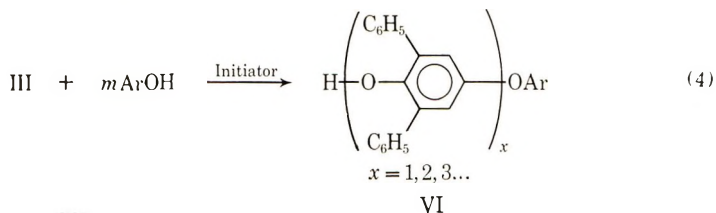
Poly(2,6-diphenyl-1,4-phenylene ether) (III) has been prepared by the oxidative coupling polymerization of 2,6-diphenylphenol, (II) [reaction (2)]^{3,4} and, by analogy to the synthesis of I, proceeds by a redistribution mechanism. Support for the redistribution mechanism has been presented



by Bolon,⁴ who showed that the dimer (IV) could redistribute to form a mixture of oligomers [reaction (3)] and could be oxidized to form (III).⁴ Evidence for a co-redistribution of III with phenols [reaction (4)] would aid



in the determination of structural details of polymer III (e.g., the nature of the head endgroups), would further elucidate the mechanism of the polymerization reaction and could provide a synthetic route to 4-aryloxy-2,6-diarylphenols. This report describes the reaction of III with four phenols, the reaction conditions and materials required for extensive reaction, and the isolation of one of the co-redistribution products.



EXPERIMENTAL

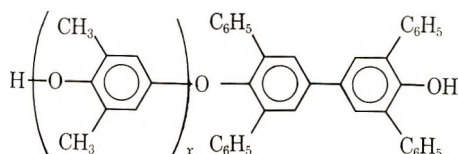
Small-Scale Equilibration Reactions

Poly(2,6-diphenyl-1,4-phenylene ether)⁵ (III, 0.500 g; intrinsic viscosity in chloroform at 30°C, 0.32 dl/g), 2,6-diphenylphenol⁶ (II, 0.500 g; 2.30 mmole) and 3,3',5,5'-tetraphenyl-4,4'-diphenoquinone^{6,7} (VII, 0.050 g; 0.103 mmole) in 25 ml chlorobenzene were heated at reflux for 2 hr. The solution was cooled to 25°C and added dropwise to vigorously stirred methanol (250 ml). After standing for several hours, the polymer was collected on a preweighed fritted (fine) filter funnel, washed with methanol, dried at 50°C/10 mm Hg overnight, and weighed. Recovered polymer yields were used as a measure of extent of reaction and are presented in the tables. A 5-ml aliquot of the filtrate was concentrated on a rotary evaporator, and the phenolic components were converted into trimethylsilyl ether derivatives by adding 2 drops of bis(trimethylsilyl)acetamide⁸ and analyzed by gas chromatography on a 2-ft silicone rubber column with a program from 100 to 300°C at 10°C/min. The unsilylated concentrated solution was analyzed by two-dimensional thin-layer chromatography on 8 × 8 ft silica gel plates with *trans*-1,2-dichloroethylene and benzene as developing solvents. Approximate R_f values for various values of x in V are listed in Table I for the two thin-layer solvents.

TABLE I

| x | R_f | |
|-----|---------|--------------------------------|
| | Benzene | <i>trans</i> -Dichloroethylene |
| 1 | 0.8 | 0.8 |
| 2 | 0.8 | 0.6 |
| 3 | 0.8 | 0.5 |
| 4 | 0.83 | 0.45 |
| 5 | 0.85 | 0.4 |
| 6 | 0.87 | 0.35 |
| <6 | 0.9 | 0.3 |

A second series of weaker spots on the thin layer chromatograms is attributed to compounds with the general structure:



which were derived from the equilibration of X with the polymer. R_f values for this series are given in Table II.

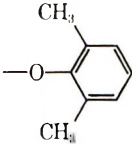
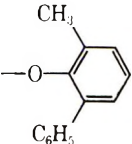
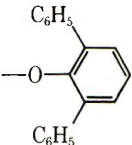
The spots were detected by spraying with a solution of 10% phosphomolybdic acid in 90% ethanol.

The equilibration procedure described above was used to determine effects of reaction variables. In these cases, the only change in the procedure was the specific variable (or variables) described in the text. For studies on various polymers, the polymers were materials described previously.⁵ For reactions with various phenols, the phenols were purified by recrystallization or distillation (in the case of 2-methyl-6-phenylphenol). Gas chromatograph retention times with the program described above for the volatile products with structure VI ($x = 1$; trimethylsilyl ether derivative) from equilibration of III with various phenols are listed in Table III. Side products which were trapped from gas chromatographs and were identical to authentic samples had the following retention times: X, 38 min; 4-benzoyloxy-2,6-diphenylphenol, 21 min; 4,4"-dihydroxy-3,3',5,5'-tetramethylbiphenyl, 17 min; 4,4'-dihydroxy-3,3'-dimethyl-5,5'-diphenylbiphenyl, 23 min. An increase in the maximum temperature of the gas chromatograph program to 350°C permitted elution of the trimethylsilyl-ether of V ($x = 3$) at 36 min.

TABLE II

| x | Benzene | <i>trans</i> -Dichloroethylene |
|----------------|---------|--------------------------------|
| 0 (compound X) | 0.6 | 0.4 |
| 1 | 0.55 | 0.3 |
| >1 | 0.5 | 0.2 |

TABLE III

| —OAr | Retention time, min |
|---|---------------------|
| —OC ₆ H ₅ | 19 |
|  | 20 |
|  | 21 |
|  | 25 |

To determine the approximate molecular weight at which equilibrated polymer was insoluble in methanol, a low molecular weight sample of III prepared with a CuCl-tetramethylethylenediamine catalyst³ was stirred with methanol (250 ml/g polymer). The methanol-insoluble fraction corresponded to 20% of the total weight. The intrinsic viscosity was 0.05 dl/g (CHCl₃, 30°C) and the number-average molecular weight (Mechrolab osmometer) was 1500 (or $\overline{DP}_n \sim 6$).

4-Phenoxy-2,6-diphenylphenyl Acetate VIII

Poly(2,6-diphenyl-1,4-phenylene ether)⁵ (III, 2.44 g, 10 mmole monomeric units; intrinsic viscosity in chloroform at 30°C, 0.1 dl/g), phenol (1.88 g, 20 mmole) and 3,3',5,5'-tetraphenyl-4,4'-diphenoquinone (VII, 0.244 g, 0.5 mmole) in 50 ml chlorobenzene were heated at reflux 1 hr. Acetic anhydride (10 ml) and 5 ml pyridine were added, and the solution was heated at reflux 1 hr. The solvent was removed at reduced pressure with a rotary evaporator and the white solid residue was triturated two times with boiling *n*-hexane (100 ml) leaving a residue (ca. 1.5 g). The *n*-hexane extracts were cooled to 0°C and the crystals that formed were isolated by filtration. The crystalline product was identified as compound IX by NMR, infrared spectra, and mixed melting point with the diacetate of an authentic sample of X.⁹ The yields were 0.20 g (mp 206–210°C) from the first crop and 0.05 g (mp 203–204°C) from the second crop. The NMR spectrum (in deuteriochloroform, TMS reference) showed singlet peaks at 1.78 and 7.65 ppm and a poorly resolved grouping at 7.45 and 7.48 ppm in the relative intensity ratio 6:4:20. Characteristic bands in the infrared (KBr pellet)

occurred at 1750 (carbonyl), 870 (isolated aryl hydrogen), and 745 and 695 cm^{-1} (phenyl).

The solvent was evaporated from the filtrates which left oily residues weighing 2.6 g and 0.55 g. The oil was chromatographed on a preparative scale gas chromatograph (2 ft silicone column, heated from 100°C to 300°C at 10°C/min), and the fraction eluted at 20 min was collected. The liquid sample solidified on standing. Recrystallization from *n*-pentane at -10°C gave VIII, 0.45 g, mp 102–103°C. The NMR spectrum (in deuteriochloroform, TMS reference) of IX showed peaks at 1.77, 7.05, 7.18, 7.27, and 7.38 and 7.40 ppm in the relative intensity ratio 3:3:2:2:10. Characteristic bands in the infrared (thin film of pure liquid) occurred at 1760 (carbonyl), 1215, and 1185 (C—O—C), 900 (isolated aryl hydrogen), and 750 and 695 cm^{-1} (phenyl).

ANAL. Calcd for $\text{C}_{26}\text{H}_{20}\text{O}_3$: C, 82.1%; H, 5.3%; Found: C, 82.0%; H, 5.3%.

Acetylation of the Terminal Phenolic Hydroxyl Group in III

A solution of poly(2,6-diphenyl-1,4-phenylene ether) (4.0 g, intrinsic viscosity 0.32 dl/g in chloroform at 30°C) in 48 ml pyridine and 48 ml toluene was heated to reflux under a nitrogen atmosphere. Acetic anhydride (3.0 ml) was added, the reaction temperature was maintained at reflux for 3 hr, then allowed to cool and left at 25°C for 3 days. The solution was filtered and the polymer was precipitated by adding the solution dropwise to 600 ml methanol. The polymer was washed twice in acetone and dried overnight at 45°C/12 mm. The product weighed 3.96 g, $[\eta]$ 0.30 dl/g. The sharp infrared absorption at 3550 cm^{-1} for the starting material in carbon disulfide (2.5% solution in a 1.0 cm cell, absorbance 0.137) disappeared completely in the acetylated product.

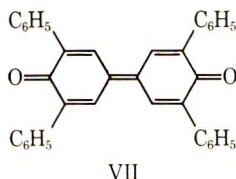
Equilibration of Acetylated III

The acetylated polymer was heated with 2,6-diphenylphenol and 3,3',-5,5'-tetraphenyl-4,4'-diphenquinone in chlorobenzene by the small-scale equilibration procedure described above. No low oligomers (e.g., IV) were detected by chromatography, and a 100% yield of polymer resulted. The polymer which had not been acetylated was equilibrated in an identical manner and was recovered in a 35% yield.

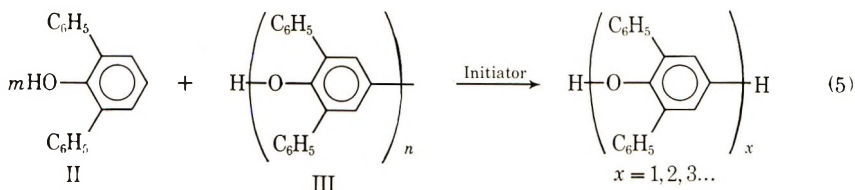
RESULTS

Reaction Products

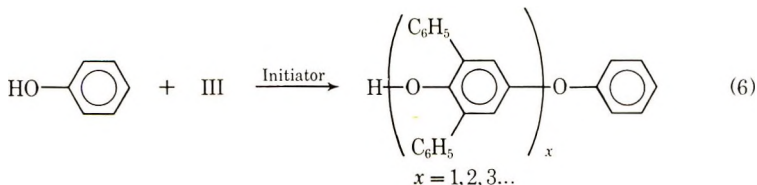
A chlorobenzene solution of 2,6-diphenylphenol (II) and an equal weight of polymer III in the presence of a catalytic quantity of the initiator, 3,3',-5,5'-tetraphenyl-4,4'-diphenquinone (VII) was heated at 132°C for 2 hr. A mixture of oligomers ranging from monomer II to methanol-insoluble polymer (VI, $x > \text{ca. } 5$) was produced. The lower molecular weight components (monomer through tetramer) were resolved with two-dimensional thin layer



chromatography. The dimer from the equilibration reaction had R_f values which were identical to the values for an authentic sample of IV. Furthermore, the redistribution products from reaction (3) and the initial oxidation products from reaction (2) displayed chromatographic behavior which was identical to that of the products of the monomer-polymer equilibration. The monomer, dimer, and trimer could also be detected by gas chromatography. The retention times were identical to the oligomers from reactions (2) and (3). The similarity that was found between dimer equilibration and monomer-polymer equilibration supports reaction (5) as an overall description of the monomer-polymer reaction. This was supported further by the similarity of product concentrations for the two reactions when II and III were present in equal weights in the monomer-polymer equilibration:

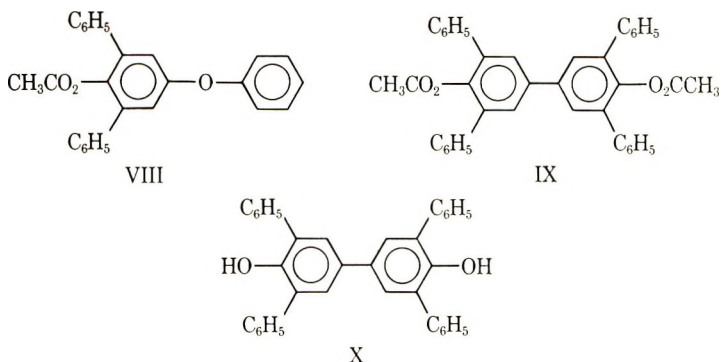


Phenol was equilibrated with polymer III [reaction (6)] and the components of the mixture converted to their acetate derivatives.



From the product mixture, the lowest boiling principal product was isolated and identified as 4-phenoxy-2,6-diphenylphenyl acetate (VII). The yield based on the formation of one molecule of VIII per repeating unit of polymer was 12%. A small amount of IX was also isolated.

* For reactions (3) and (5) under nitrogen with only a trace of initiator, the number-average degree of polymerization \overline{DP}_n of the equilibrated mixture is essentially the same as that of the starting mixture. Thus, when $n = m$ in reaction (5), $\overline{DP}_n = 2$ as in the case with the dimer [reaction (3)].



Compound IX arose primarily from the initiator, VII, after reduction to X during the initiation process. For this equilibration reaction, a low molecular weight polymer which had been found to undergo extensive equilibration when heated with II was used to provide a relatively high conversion to products. As a result, product yields in this case were greater than in another equilibration with phenol and a higher molecular weight polymer which is described in the next section.

Reaction Variables

To assess the effects of reaction conditions, solvents, polymer structure and type of initiator on the extent to which reaction (5) proceeded, the yields of recovered (methanol-insoluble) polymer were measured after equal weights of polymer III and 2,6-diphenylphenol were heated at reflux, usually in chlorobenzene. A 100% yield of recovered polymer indicated no equilibration, and lower yields indicated increasing extents of reaction. The extents of reaction were qualitatively proportional to the concentration of lower molecular weight products by gas and thin layer chromatographic analysis.

A comparison of the effectiveness of initiators for reaction (5) is presented in Table IV. Except for the benzoyl peroxide reaction which was in benzene at 80°C, the other reactions were in chlorobenzene at 132°C. Although the molar quantities of the initiators vary, their effectiveness toward

TABLE IV
Equilibration of II (500 mg) and III (500 mg)
With Various Initiators

| Initiator | Wt. of initiator, mg | Recovered polymer, % |
|--|-------------------------|-------------------------|
| VII | 50 | 35 |
| 3,3',5,5'-Tetramethyl- 4,4'-diphenylquinone | 50 | 98 |
| Dicumyl peroxide | 50 | 100 |
| Benzoyl peroxide | 100 | 67 |
| <i>tert</i> -Butyl hydroperoxide | 50 | 99 |
| <i>tert</i> -Butyl perbenzoate | 50 | 40 |

promoting equilibration can be assessed qualitatively. Three oxidizing agents were ineffective: 3,3',5,5'-tetramethyl-4,4'-diphenoquinone, *tert*-butyl hydroperoxide, and dicumyl peroxide. The remaining materials, 3,3',5,5'-tetraphenyldiphenoquinone, VII, *tert*-butyl perbenzoate, and benzoyl peroxide were initiators. Benzoyl peroxide was used at 80°C because of its relatively low decomposition temperature, yet was moderately effective. Compound VII appeared to be the most versatile initiator, since it could be used over a wide temperature range.

Initiator concentrations were varied for VII in chlorobenzene at 132°C and for benzoyl peroxide in benzene at 80°C. The effect on recovered polymer yield is listed in Table V. With VII, a quantity of ca. 50 mg/500

TABLE V
Equilibration of II (500 mg) and III (500 mg)
with Various Quantities of Initiators

| Initiator | Wt. of initiator, mg | Recovered polymer, % |
|------------------|-------------------------|-------------------------|
| VII | 5 | 73 |
| VII | 15 | 58 |
| VII | 50 | 35 |
| VII | 150 | 45 |
| Benzoyl peroxide | 20 | 91 |
| Benzoyl peroxide | 50 | 80 |
| Benzoyl peroxide | 100 | 67 |

mg polymer was most effective. Possibly, with the higher concentration of VII, the equilibration products were being oxidized to higher molecular weight insoluble products. With benzoyl peroxide quantities of 100 mg/500 mg polymer or more appeared to be required for extensive equilibration.

Polymer recovery from reaction (5) with VII as an initiator is listed in Table VI for four solvents at temperatures ranging from 80 to 180°C.

TABLE VI
Equilibration of II (500 mg) and III (500 mg) in
Various Solvents at Reflux Temperatures

| Solvent | Reaction temperature, °C | Recovered polymer, % |
|---------------------------|-----------------------------|-------------------------|
| Benzene | 80 | 71 |
| Toluene | 111 | 83 |
| Chlorobenzene | 132 | 35 |
| <i>o</i> -Dichlorobenzene | 180 | 14 |

Although there is a general trend toward more extensive equilibration with increased reaction temperature, the type of solvent appears to be of some importance since with toluene the least amount of equilibration occurred even though it was used at an intermediate temperature.

Three equilibration reactions were run in chlorobenzene at reflux for various time intervals (Table VII).

TABLE VII
Extent of Equilibration of II (500 mg) and III (500 mg) with Time

| Reaction time, hr | Recovered polymer, % |
|-------------------|----------------------|
| 0.5 | 53 |
| 2.0 | 35 |
| 18.0 | 22 |

Initially the reaction proceeded rapidly, but then became slower. This may have been due primarily to the loss of the initiator by reaction with 2,6-diphenylphenol:*



During the course of the reaction, a decrease in the color of VII was noted. Chromatographic analysis indicated the formation of 4,4'-dihydroxy-3,3',-5,5'-tetraphenylbiphenyl (X). The isolation of the diacetate of X was described above for the equilibration in which III was co-redistributed with phenol.

3,3',5,5'-Tetramethyldiphenoquinone was used as an initiator at lower temperatures to minimize side reactions. The reaction was very slow at 80°C. Yields of recovered polymer were: 99% after 0.5 hr, 98% after 2 hr, and 97% after 16 hr.

A variety of samples of polymer III with different molecular weights and from different catalyst systems were described previously.¹ Some of these samples were equilibrated with 2,6-diphenylphenol with initiation by VII in benzene at 80°C. Yields of recovered polymer are compared in Table VIII

TABLE VIII
Equilibration of Polymers Prepared from Various Catalysts with II in Chlorobenzene at 132°C

| $[\eta]$ dl/g | Amine in polymerization catalyst | Recovered polymer, % |
|---------------|---|----------------------|
| 0.05 | <i>N,N'</i> -Dimethyl-1,3-propanediamine | 37 |
| 0.06 | <i>N,N,N',N'</i> -Tetramethyl-1,6-hexanediamine | 42 |
| 0.07 | <i>N,N,N',N'</i> -Tetramethyl-1,3-butanediamine | 39 |
| 0.44 | " | 95 |
| 0.32 | <i>N,N,N',N'</i> -Tetramethylethylenediamine | 71 |
| 0.19 | Di- <i>n</i> -butylamine | 95 |
| 0.39 | " | 97 |
| 0.31 | <i>n</i> -Butylamine | 91 |

* The analogous oxidation of 2,6-xyleneol by 3,3',5,5'-tetramethyldiphenoquinone has been reported.^{10,11}

for polymers prepared with various amines in the catalyst and with the viscosity of the polymer before equilibration.

Polymers prepared with diamine catalysts showed a general progression of less equilibration with increasing intrinsic viscosity. When the catalyst contained either a primary or secondary monoamine, the polymers neither attained high molecular weights in the polymerization⁹ nor equilibrated appreciably. Thus, it is possible that the monoamines reacted with the phenolic end of the polymer to both terminate polymerization and deactivate the "redistribution-active" portion of the polymer.

To determine whether low molecular weight polymers did equilibrate more readily than high molecular weight polymers, six polymers which were isolated at different times from the same polymerization reaction were equilibrated with 2,6-diphenylphenol in *o*-dichlorobenzene at 180°C for 2 hr. The molecular weights of these samples ranged from $\bar{M}_n < 5000$ to ca. 80,000. Yields of recovered polymer are listed in Table IX.

TABLE IX
Effect of Molecular Weight on Extent of Equilibration

| $[\eta]$ dl/g | Recovered polymer, % |
|---------------|----------------------|
| 0.09 | 4 |
| 0.11 | 10 |
| 0.19 | 19 |
| 0.24 | 16 |
| 0.30 | 16, 17 |
| 0.41 | 28 |

The tendency toward less equilibration with higher molecular weight is similar to the behavior of poly(2,6-dimethylphenylene oxide), I, equilibrations, in which case both molecular weight (i.e., changes in endgroup concentration) and endgroup abnormalities affect the reactivity.¹

The reactivity of four phenols toward equilibration with III in chlorobenzene at 132°C with VII as an initiator was measured (Table X). 2,6-Diphenylphenol caused the most extensive equilibration. 2-Methyl-6-phenylphenol, with a structure closer to that of 2,6-diphenylphenol than the other phenols, was more reactive than the other two phenols. A somewhat similar reactivity series has been found for poly(2-methyl-6-phenylphenylene oxide). In this case, 2-methyl-6-phenylphenol equilibrated more extensively with the polymer than did phenol or 2,6-xylenol which do not contain an *o*-phenyl group.¹²

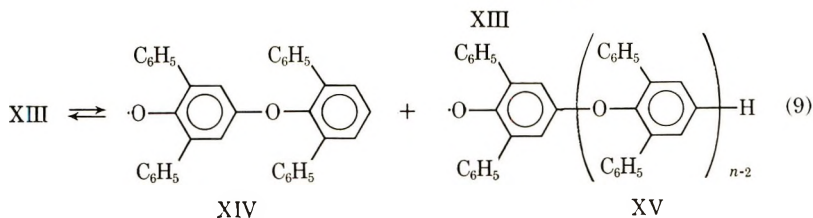
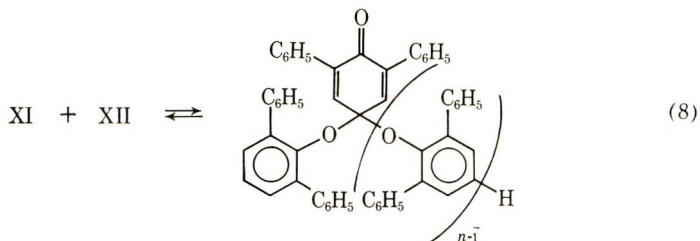
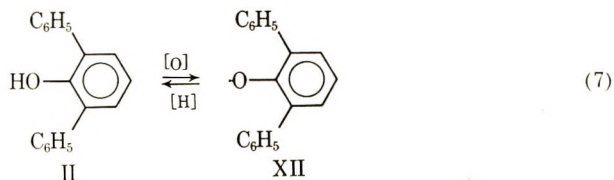
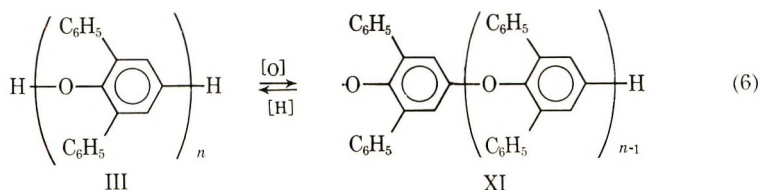
TABLE X
Equilibration of III with Various Phenols (1 mole phenol/monomer unit)

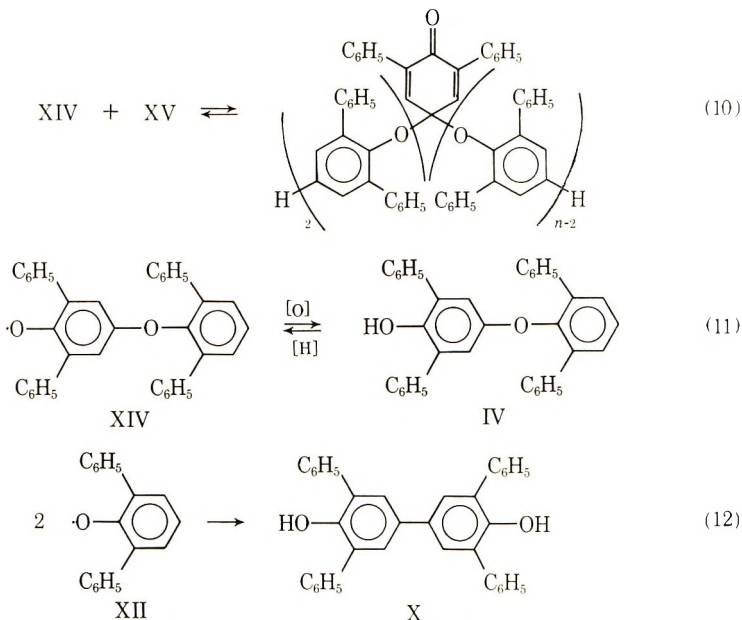
| Phenol | Recovered polymer, % |
|-------------------------|----------------------|
| Phenol | 93 |
| 2,6-Dimethylphenol | 94 |
| 2-Methyl-6-phenylphenol | 60 |
| 2,6-Diphenylphenol | 35 |

DISCUSSION

The reaction conditions which are required to equilibrate polymer III with phenols are more strenuous than for the equilibration of the corresponding polymer, I, from 2,6-dimethylphenol with phenols. Higher temperatures and higher concentrations of initiator are required. Furthermore, initiators with higher oxidation potentials are more effective (e.g., VII instead of the tetramethyl-substituted analog). The initiators also have to be able to oxidize the phenols at the higher temperatures without extensive side reactions.

There are many similarities between equilibration of phenols with III and with I. The extensiveness of both reactions depends on the molecular weight of the polymer and the method of polymerization. In both cases, one of the most effective initiators is the tetrasubstituted diphenoquinone which is obtained as a side product during the preparation of the polymer. The similarities of the two systems and the product analyses after equilibration indicate similar mechanisms for equilibration. Thus, for the case of reaction (5) with VII as initiator, the reactions (6)–(12) seem likely.





Reactions (6) and (7) represent initiation reactions. The oxidizing agent can be either VII or the semiquinone of VII. The reaction sequence is continued by carbon-oxygen coupling reactions and dissociation reactions which are illustrated by the reactions in equilibria (8), (9), and (10). Hydrogen abstraction reactions as (11) convert the radical species to the free phenol and either generate new aryloxy radicals or oxidize the reduced forms of VII. Termination is represented by the carbon-carbon coupling reaction (12).

Polymer III must have a free phenolic hydroxyl group at the end of the polymer chain to participate in the equilibration sequence described above; otherwise, co-redistribution should not occur. This requirement was demonstrated by an attempt to equilibrate polymer with the hydroxyl groups quantitatively acetylated. No low molecular weight co-redistribution products were detected, and the polymer was recovered quantitatively. Presumably then, the polymers which did not co-redistribute extensively with 2,6-diphenylphenol (Table VII) contain structural irregularities in the head ring. These inactive polymers are also inert toward further oxidation to high molecular weights in polymerization systems which normally produce high molecular weight polymers.

Further support for the presence of structural irregularities is presented by the reduced reactivity of higher molecular weight polymers toward equilibration. Two reasons why the differences in molecular weight alone do not account for variations in reactivity are described here. First, the lower molecular weight polymers should react at a more rapid rate than higher polymers since equal weights were used resulting in higher end group concentrations for solutions of low polymers. However, due to the high

reaction temperature (170°C), the reaction time was sufficient to approach a steady state condition even for the higher polymers. This was demonstrated by using longer reaction times and finding almost no further decrease in the yields of recovered polymer. Second, the possibility that complete equilibration of high molecular weight polymer would produce a larger concentration of higher molecular weight (and thereby methanol-insoluble) oligomers than would a low polymer is not the case since the molar concentration of II is so much greater than the molar concentration of either high or low polymer that the \overline{DP}_n of both reaction mixtures is almost identical.

The possibility that some of the polymer chains do not contain 4-hydroxy-2,6-diphenylphenoxy "head" endgroups and that there is a decrease in the percentage of chains bearing these end groups as polymerization proceeds can account for decreasing reactivity with increasing molecular weight. If the "head" end-groups can react during polymerization in an abnormal manner, i.e., to form stable products by reactions other than the normal oxidative coupling reactions for chain growth, or if intermediates such as the quinone-ketal moiety can rearrange or be intercepted by other species in the reaction medium, abnormal structural units can arise. Two types of abnormal reactions would be, for example, head-to-head coupling reactions [other than the normal quinone-ketal formation reaction such as reactions (8) or (10)] which would result in either unreactive polymers containing 2,6-diphenylphenoxy groups on each end of the chain instead of only on one end of the chain or in reactions in which another species such as the amine in the catalyst reacted with the "head" endgroup to form a new abnormal endgroup. The gradual incorporation of nitrogen into the polymer with increased polymerization time⁵ supports the possibility of reactions of polymer with the amine.

The author is indebted to Mr. H. J. Klopfer for assistance and Mr. E. M. Hadsell for preparative-scale chromatographic separations.

References

1. D. M. White, *J. Org. Chem.*, **34**, 297 (1969).
2. H. L. Finkbeiner and A. S. Hay, in *Newer Polymerization Reactions*, J. Heller, Ed., Interscience, New York, 1970.
3. A. S. Hay, *Macromolecules*, **2**, 107 (1969); U.S. Pat. 3,306,874; 3,306,875; 3,432,466.
4. D. A. Bolon, *J. Org. Chem.*, **34**, 2031 (1969).
5. D. M. White and H. J. Klopfer, *J. Polym. Sci., A-1*, **8**, 1427 (Part I).
6. J. Plesek, *Coll. Czech. Chem. Commun.*, **21**, 375 (1956).
7. A. S. Hay, U.S. Pat. 3,306,875.
8. J. F. Klebe, H. Finkbeiner, and D. M. White, *J. Amer. Chem. Soc.*, **88**, 3390 (1966).
9. A. S. Hay, U.S. Pat. 3,262,982.
10. A. S. Hay, *Tetrahedron Letters*, 4241 (1965).
11. R. G. R. Bacon and O. J. Stewart, *Chem. Commun.*, **1967**, 977.
12. D. M. White, unpublished results.

Received September 1, 1970

Elastomers from the Copolymerization of Conjugated Dienes and Styrenes Containing Chlorine

A. F. HALASA,* H. ADAMS, and C. J. HUNTER,
*Central Research Laboratories, The Firestone Tire & Rubber Company,
Akron, Ohio 44317*

Synopsis

Copolymers of 1,3-butadiene and *o*- and *p*-chlorostyrenes have been made by use of alkyllithium initiators. These copolymers have a uniform distribution of the chlorostyrene along the chain, suggesting that the reactivity ratio of 1,3-butadiene and chlorostyrene is close to unity.

INTRODUCTION

The chlorostyrene monomers have been available for many years, and synthetic rubbers have been made from them by copolymerizing butadiene and chlorostyrenes in emulsion systems. The present study was directed toward the preparation and elucidation of properties of copolymers of butadiene and chlorostyrene obtained with anionic polymerization systems. Special emphasis is given to alkyllithium-catalyzed polymerizations.

The polymerization rates of *o*- and *p*-chlorostyrene determined under free-radical conditions indicate that they polymerize faster than styrene.^{1,2} This points out the fact that ring chlorination enhances the rate of the polymerization by either electronic or hyperconjugational effects.^{3,4}

The literature contains many papers dealing with the copolymerization of butadiene and styrene in systems with various anionic catalysts. It is known that when butadiene and styrene copolymerize in an anionic system, the reactivity ratio of 1,3 butadiene (r_1) is 18 times the reactivity ratio of the styrene (r_2). Consequently, when the two monomers are loaded initially, butadiene polymerizes preferentially, leaving excess styrene which enters the polymer in increasing proportions as polymerization progresses. Ultimately, the styrene is blocked on the end of the polymer chain. This situation can be overcome by delaying addition of all of the butadiene or by adding suitable modifiers to change the reactivity ratios, bringing them closer together and producing more nearly "random" polymers.

The reactivity ratios for *o*-chlorostyrene and *p*-chlorostyrene toward styrene as well as 1,3-butadiene in the presence of cationic and free-radical initiators are known.⁵ Although no work was found in the literature on the

* To whom all inquiries should be directed.

stereospecific copolymerizations of halogenated styrenes with dienes by anionic initiator, some data were reported for polymerization with the Ziegler catalyst.⁵

Szwarc and co-workers,⁶ in studying the anionic homopolymerization and copolymerization of substituted styrenes in tetrahydrofuran, found that the absolute rate constant obeys the Hammett relations. However, no copolymerization data were found in the literature for the chlorostyrene-diolefin systems in either polar or nonpolar media.

The reaction of *n*-butyllithium and *o*-chlorostyrene as well as *p*-chlorostyrene in polar solvents has been reported in the literature.⁷ In these polar solvents the significant finding as expected was halogen-metal exchange. The resulting lithio derivatives were used as initiators for diene polymerization, using a large excess of catalyst.

The present study is concerned with copolymerization of ring-chlorinated styrene and diolefins by using organolithium initiator in hydrocarbon medium.

DISCUSSION

In view of the literature, one would not expect halogenated styrenes to polymerize on the addition of organolithium compounds. Rather, a simple metal-halogen reaction would be expected. If the monomers did polymerize, one would expect a portion of the chlorostyrene to form a block segment, as in the case with styrene in the copolymerization of 1,3-butadiene and styrene.

However, we found that both *o*-chlorostyrene and an *o-p*-chlorostyrene mixture (65% *ortho*, 35% *para*) copolymerized readily with butadiene when organolithium initiators in hydrocarbon solvents were used, to form high molecular weight polymers.

The butadiene portion of the resulting copolymer had the microstructure typically found in lithium-initiated polybutadiene.

It was also found that the copolymer had no chlorostyrene blocks as determined by the osmium tetroxide oxidation method and NMR analysis of the aromatic region. In Figure 1, the NMR spectra for polychlorostyrene homopolymer and an 80/20 butadiene-chlorostyrene copolymer are shown. The absorption of the aromatic protons of the copolymer appears at 7.50 ppm, while the same protons in polychlorostyrene show an upfield shift due to the *ortho* hydrogen resonance of neighboring chlorostyrene units in the polymer chain. Likewise, the position (2.5 ppm) of the α hydrogen of polychlorostyrene is shifted upfield from the position (3.0 ppm) of the same protons of the copolymer.

This copolymer has a constant composition as determined by chemical and physical methods of analysis over a wide range of conversion for any given set of polymerization conditions. However, the composition of the chlorostyrene (StCl)-butadiene (BD) copolymers did vary from one set of polymerization conditions to another. The temperature effect on the com-

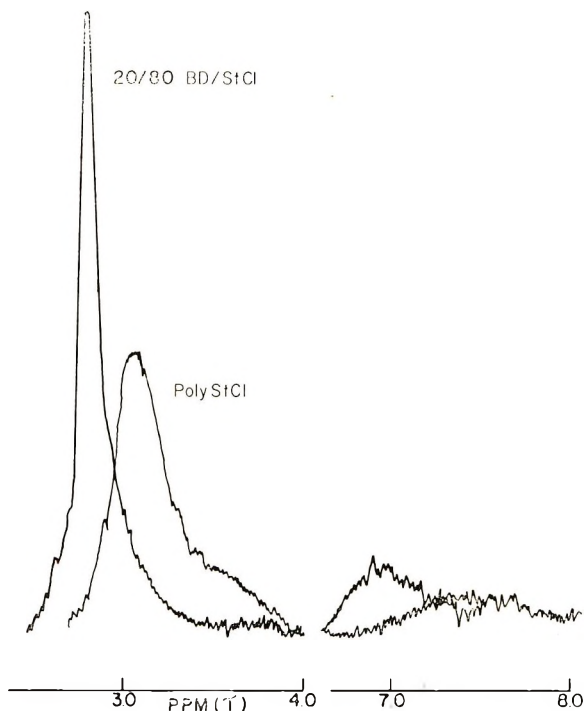


Fig. 1. NMR spectra of polychlorostyrene homopolymer and of copolymer of chlorostyrene and butadiene.

position and on the conversion of three 80/20 BD–StCl initial charge polymerizations can be seen in Figure 2. Also, the effect of the per cent chlorostyrene charged on the composition and per cent conversion is quite evident. All the copolymers had constant composition over a wide range of conversions. But in three runs made at different temperatures, we find by increasing the temperature the conversion and amount of chlorostyrene are decreased. However, the chlorostyrene is uniformly distributed throughout the copolymer. This points out that a termination reaction is occurring during the polymerization and that it is temperature-dependent.

The per cent chlorostyrene in the polymer prepared from the 80/20 BD–chlorostyrene initial charge at a constant initiator level is inversely proportional to temperature of polymerization. The polymer contained 24% chlorostyrene when formed at 30°C, 20% at 50°C, and 16% at 70°C, in all cases uniformly distributed in the polymer.

It is conceivable that if the polymerization could proceed to 100% conversion, the remaining monomer would block onto the chain since an excess quantity of the monomer (either BD or chlorostyrene) would be present.

On the right side of Figure 2, it can be seen that the amount of chlorostyrene is uniformly distributed throughout the polymer, but in some cases differs from the per cent charged. The four polymerizations were carried out at 50°C and a constant initiator level. With both the 10% and 20%

chlorostyrene charge, the same percentage is uniformly distributed throughout the polymer. However, in the case of a 30% charge, the polymer contains 35% chlorostyrene, which is a larger concentration than charged. In the final case of a 60% chlorostyrene charge, 50% is uniformly distributed throughout the polymer before the termination reaction predominates.

From Figure 2, it is quite evident that the reactivity ratio of the monomers are changing slightly and are dependent upon temperature of polymerization and composition charged. The reactivity ratio of the monomers

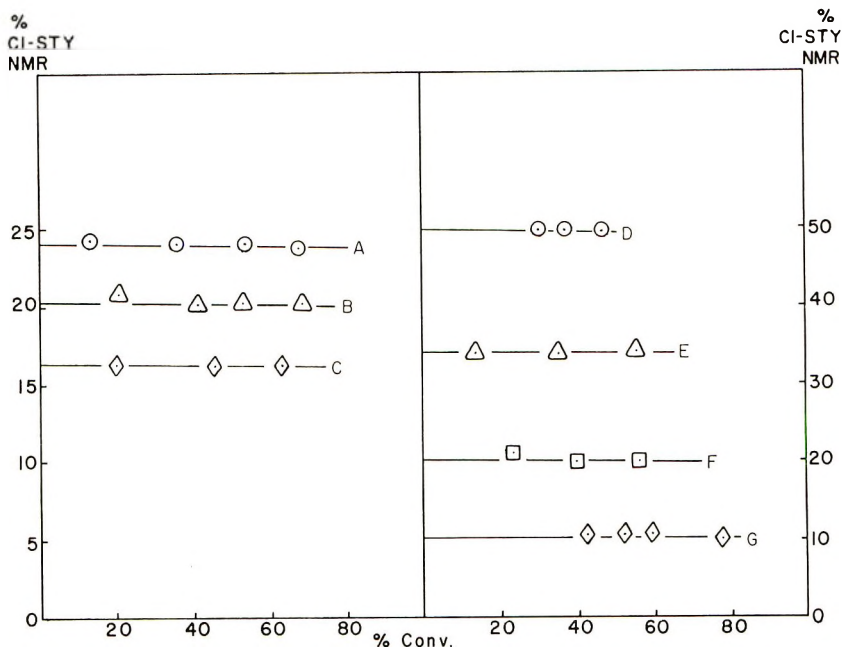


Fig. 2. Plots of conversion vs. per cent chlorostyrene incorporated in the copolymer prepared (left) at the same monomer ratio and different temperatures and (right) at different monomer ratios and the same temperature: (A) 80/20 BD-StCl, 30°C; (B) 80/20 BD-StCl, 50°C; (C) 80/20 BD-StCl, 70°C; (D) 90/10 BD-StCl, 50°C; (E) 70/30 BD-StCl, 50°C; (F) 80/20 BD-StCl, 50°C; (G) 40/60 BD-StCl, 50°C. [BuLi] for all polymerizations, 4 mmole/100 g monomer.

appear to be close to one for certain conditions. An attempt was made to determine the reactivity ratios, but the copolymerization of butadiene and chlorostyrene does not proceed by the usual copolymerization equations because of a competing termination reaction. The termination reaction is responsible for the variation in percent conversion under various conditions of temperature, initiator and chlorostyrene concentration.

In Figure 3, the molecular weight distribution of the copolymers as determined by gel-permeation chromatography also provides further evidence for the termination step. The molecular weight distribution becomes broader

and shifts to higher molecular weight with an increase in temperature or chlorostyrene concentration.

At high polymerization temperatures, there is a decrease in conversion. Evidently, the termination reaction has a higher activation energy and so predominates at higher temperatures. The termination step is dependent not only on temperature, but also on chlorostyrene concentration in the charge. With an increase in chlorostyrene, there is a decrease in conversion, an indication of the participation of chlorostyrene in the termination reaction.

Figure 4 shows the rate of polymerization in relation to temperature and chlorostyrene concentration. The data on the left of Figure 4 are for polymerization carried out at a constant temperature and initiator level while

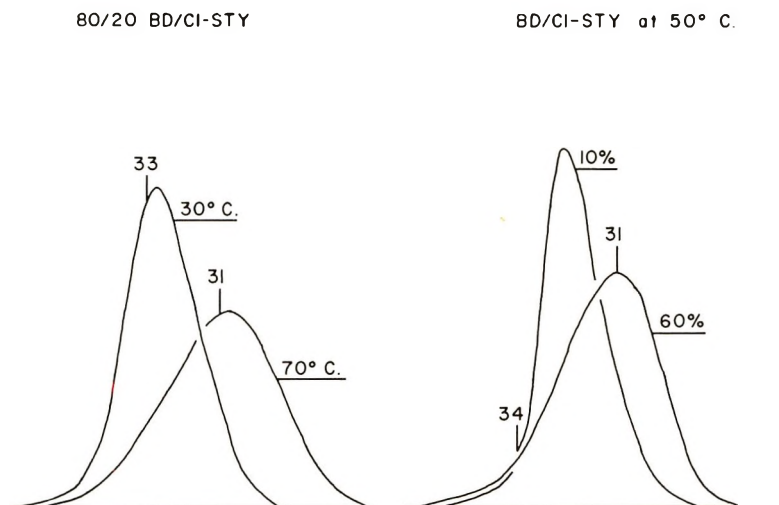


Fig. 3. Gel-permeation chromatography distribution of copolymer at different temperatures and different compositions.

the chlorostyrene content was varied in the initial charge. As the chlorostyrene level is increased, the apparent rate of polymerization decreases, while the rate of the termination reaction increases. The data on the right side of Figure 4 are for polymerization conducted at a constant chlorostyrene and initiator level. The temperature was varied. It can be seen that at lower temperature, the rate is slow and the polymerization proceeds to high conversion, while at high temperature, one observes an enhanced rate and the polymerization terminates at low conversions. The kinetics of this reaction cannot be accounted for by a simple kinetic equation due to the termination step in the reaction. In analyzing the kinetics of the copolymerization, the following conclusions were made from the experimental data presented.

The compositional analyses of the polymers indicate that the chlorostyrene content of the polymer varies very little from the charge ratio.

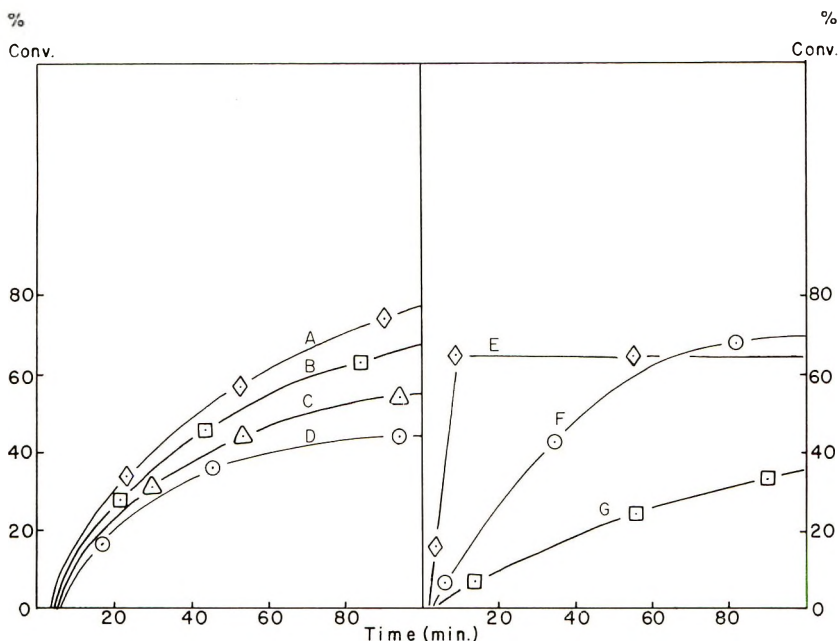


Fig. 4. Plots of conversion vs. time for copolymer prepared at (left) different monomer ratios and (right) same monomer ratios and different temperatures: (A) 90/10 BD-StCl, 50°C; (B) 80/20 BD-StCl, 50°C; (C) 70/30 BD-StCl, 50°C; (D) 40/60 BD-StCl, 50°C; (E) 80/20 BD-StCl, 70°C; (F) 80/20 BD-StCl, 50°C; (G) 80/20 BD-StCl, 30°C. [BuLi] for all polymerizations, 4 mmole/100 g monomer.

The reactivity ratios are very close to one. The polymerization equation contains a termination step.

An obvious reaction leading to termination would be between the alkyl lithium and chlorine of the chlorostyrene giving lithium chloride. However, it is possible that other reactions or adventitious impurities may be present that could lead to slow termination. Possible terminating mechanisms are: (1) metal halogen exchange reaction; (2) radical-ion formation; (3) metallation reaction; and (4) displacement reactions.

Any one of these reactions would lead to either termination or chain transfer processes.

Considering these experimental facts a polymerization equation can be written in the following simplified form:



assuming $r_1 = r_2 = 1.0$, where M represents the collective monomer of chlorostyrene and butadiene, PLi is the active polymer lithium, and k_i and k_p are the initiation and propagation rate constants, respectively. The concomitant reaction of the carbon-bound lithium, both butyllithium and poly-

mer lithium, with the chlorostyrene (StCl) may be represented in the generalized form:



It is not intended that these equations be specific as to the products of the reaction except that they represent a deactivation of the lithium as to its ability to add additional monomer. Consequently, these reactions may be considered as termination reactions and dead polymer (P) is produced. The reaction with the monomeric chlorostyrene or with chlorostyrene in the polymer is assumed to occur at the same rate. Therefore, the chlorostyrene concentration considered in these equations is decreased only by reacting with polymer lithium (k_T) or butyllithium (k'_T) and not by polymerization.

To simplify the mathematical equations, let $k_T = k'_T$. This assumption may be questionable but it certainly will be approached over the latter portion of the polymerization when the initiation reaction is minimized or most of the butyllithium has been converted over into polymer lithium. The rate of disappearance of active lithium is then given as follows:

$$d[\text{Li}]/dt = -k_T[\text{Li}][\text{StCl}] \quad (5)$$

where

$$[\text{Li}] = [\text{BuLi}] + [\text{PLi}]$$

and

$$[\text{StCl}] = [\text{StCl}]_0$$

with the solution

$$[\text{Li}] = [\text{BuLi}]_0 \exp\{-k_T[\text{StCl}]_0 t\} \quad (6)$$

The zero subscript refers to starting or original concentration. Thus, the total concentration of active lithium is decreased exponentially with time of reaction. Since $[\text{Li}]_0 \ll [\text{StCl}]_0$, $[\text{Li}]_0$ was neglected in the expression $[\text{StCl}]_0 \ll [\text{Li}]_0$.

Having obtained an expression for the active lithium as a function of the time of reaction, the polymerization rate equation can be represented as:

$$d[M]/dt = -k_p[M][\text{Li}] \quad (7)$$

Here, k_i was assumed equal to k_p and the same comments advanced previously for the termination reaction apply. A solution is

$$\ln(1 - c) = \frac{k_p}{k_T} \frac{[\text{BuLi}]_0}{[\text{StCl}]_0} [1 - \exp\{-k[\text{StCl}]_0 t\}] \quad (8)$$

where c is the fraction of conversion.

This equation is in line with the experimental results in that as the time approaches infinity the conversion becomes constant at less than 100%. That is, for

$$t \rightarrow \infty, \ln(1 - c)_{\max} = (k_p/k_T)/[\text{BuLi}]_0/[\text{StCl}]_0 \quad (9)$$

Thus, the maximum conversion can be increased by increasing the amount of butyllithium and decreased by increasing the chlorostyrene concentration.

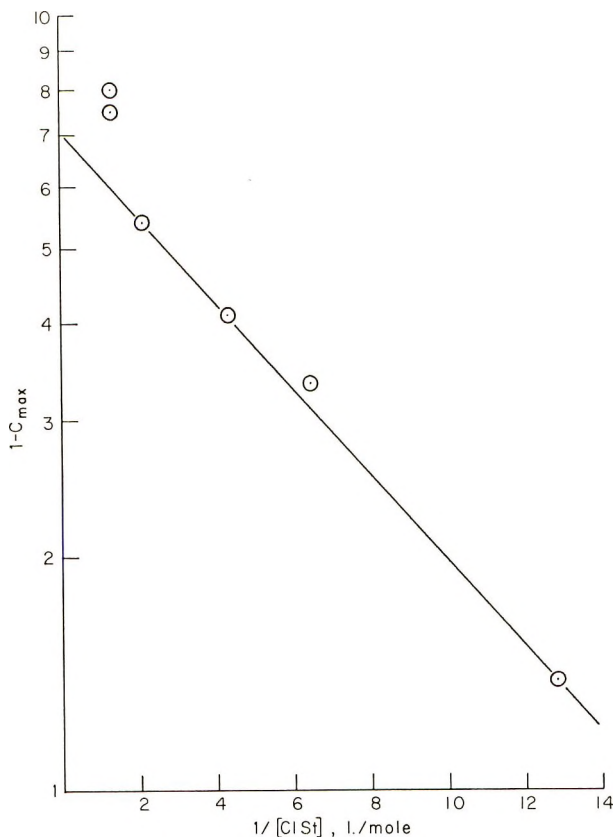


Fig. 5. Effect of concentration of chlorostyrene upon maximum conversion.

Fair agreement is obtained between the experimental values for the maximum conversion and the chlorostyrene concentration as shown in Figure 5. This semilogarithmic plot of $1 - c_{\max}$ against the reciprocal of the concentration of the chlorostyrene gives a straight line the slope of which can be used to calculate the k_p/k_T ratio

$$k_p/k_T = (2.303)_0 \times \text{slope}/[\text{BuLi}]_0 \quad (10)$$

in which the slope of 0.056 was calculated from Figure 5 at catalyst concentration of 1.37×10^{-2} mol/l. of *n*-butyllithium. Substitution in eq.

(10) gives the value for $k_p/k_T = 9.4$. This means that the rate of polymerization is approximately ten times the rate of termination.

Substitution of eq. (9) in eq. (8) gives a tractable equation

$$1 - [\ln(1 - c)/\ln(1 - c)_{\max}] = \exp\{-k_T[\text{StCl}]_0 t\} \quad (11)$$

For substitution of the rate data in eq. (11), the results are plotted in Figure 6. Straight lines were obtained with slopes that increase with increas-

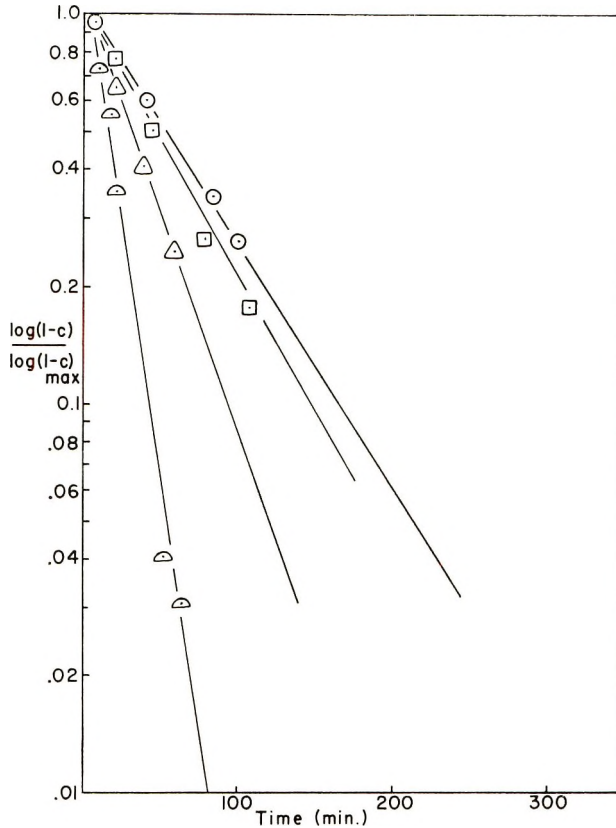


Fig. 6. Variation of conversion with time: (○) 10% StCl; (△) 20% StCl; (□) 30% StCl; (◊) 60% StCl.

ing amounts of chlorostyrene. The rate constant could be obtained from the slopes of these lines by means of eq. (12):

$$k_T = 2.303(\text{slope})/[\text{StCl}]_0 \quad (12)$$

Combination of the two slopes from Figures 5 and 6 makes it possible to obtain a value for the polymerization propagation constant (k_p).

Similarly, the data in Table I give us the values for k_T ; using the expression $k_p/k_T = 9.4$, one is able to obtain the values for $k_p = 1.04$ l./mole-min.

TABLE I
 Copolymerization Rates

| Ratio BD/StCl | [StCl], mole/l. | Slope | k_T l./mole-min |
|---------------|-----------------|---------|-------------------|
| 0/100 | 0.780 | — | — |
| 40/60 | 0.474 | 0.026 | 0.127 |
| 70/30 | 0.231 | 0.0110 | 0.110 |
| 80/20 | 0.156 | 0.00673 | 0.100 |
| 90/10 | 0.078 | 0.00605 | (0.180) |
| | | | Avg. 0.110 |

The energies of activation for the individual reactions can be obtained by applying three equations to the rate data obtained at different temperatures.

The fact that these equations predict fairly accurately the observations substantiates the general nature of the proposed mechanism. Of course, simplifying assumptions were made so that the details of the mechanism cannot be predicted but the major steps are outlined.

PHYSICAL PROPERTIES

The compounding data of the chlorostyrene-polybutadiene rubbers are listed in Tables II and III. From these tables, one can see that the test copolymer has significantly lower tensile strength than that of the BD/St copolymer control. It showed lower Young's modulus index and green strength, with (5-10%) lower wet traction than that of the control. Similarly, the test rubber showed lower rebound at 212°F.

The physical properties of this copolymer differ greatly from the emulsion-synthesized butadiene-chlorostyrene copolymer.⁸ The difference in

 TABLE II
 Tire Tread Stock Evaluation

| | BD-styrene (No. 556) | BD-chlorostyrene copolymer | | | |
|---|-------------------------|----------------------------|---------|---------|---------|
| | | No. 557 | No. 558 | No. 559 | No. 560 |
| Chlorostyrene content, % | (18% styrene) | 18.7 | 23.1 | 25.5 | 20.0 |
| 300% Modulus (30 min, 300°F), psi | 425 | 200 | 300 | 475 | 450 |
| Tensile strength, (30 min, 300°F), psi | 1850 | 475 | 750 | 1250 | 725 |
| Ultimate elongation (30 min, 300°F), % | 840 | 540 | 540 | 640 | 440 |
| Shore A Hardness (cured at 300°F, 35 min) | 61.0 | 58.0 | 62.0 | 62.0 | 54.0 |
| Wet traction rating (Stanley-London) | 50.1 | 47.7 | 48.1 | 48.6 | 43.5 |
| Young's bending modulus index (10,000 psi), °C | -46 | -54 | -50 | -55 | -63 |

TABLE III
Passenger Tire Body Stock Evaluation

| | BD-styrene | | BD-chlorostyrene copolymer | | | |
|---|------------|---------|----------------------------|---------|---------|--|
| | No. 551 | No. 552 | No. 553 | No. 554 | No. 555 | |
| Chlorostyrene content, % | 15.0 | 11.2 | 15.4 | 20.0 | 18.0 | |
| ML/4/212°F (18% styrene) | 73 | 78 | 73 | 91 | 120 | |
| Green strength | | | | | | |
| Peak, psi | 2.25 | 1.13 | 1.62 | 1.99 | 2.15 | |
| Break, psi | 1.90 | 1.90 | 0.5 | 1.95 | 1.00 | |
| Elongation, % | 933 | 408 | 680 | 325 | 600 | |
| 300% Modulus, psi (30 min, 300°F) | 725 | 700 | 800 | 825 | 925 | |
| Tensile strength, (30 min 300°F), psi | 1400 | 1425 | 1400 | 1525 | 1625 | |
| Elongation, (30 min, 300°F), % | 420 | 500 | 420 | 500 | 420 | |
| Steel Ball rebound, % | | | | | | |
| 73°F | 26 | 28 | 28 | 32 | 29 | |
| 212°F | 39 | 39 | 39 | 46 | 42 | |
| Shore A Hardness (35 min, 300°F) | | | | | | |
| 73°F | 50 | 52 | 50 | 54 | 52 | |
| 212°F | 49 | 50 | 49 | 53 | 52 | |
| Wet traction rating | | | | | | |
| (Stanley-London) | 46.9 | 42.7 | 44.8 | 43.7 | 44.4 | |
| Young's bending modulus index (10,000 psi), °C | -51 | -63 | -60 | -63 | -60 | |
| Stanley-London (30 min, 300°C) | 46.9 | 42.7 | 44.8 | 43.7 | 44.4 | |
| Internal friction | | | | | | |
| H_x | 5.18 | 5.28 | 4.92 | 4.84 | 5.01 | |
| H_f | 89.3 | 91.03 | 84.8 | 83.4 | 86.4 | |
| Young's modulus index | 278 | 464 | 371 | 371 | 428 | |
| | -51 | -63 | -60 | -63 | -60 | |

physical properties may be due to the sequence distribution of the chlorostyrene in the copolymer.

The processibility of the BD-StCl copolymers on milling and Banbury mixing was good in all cases.

EXPERIMENTAL

Reagents

o-Chlorostyrene (pure) and *o,p*-chlorostyrene mixture (65% *ortho*, and 35% *para*) were obtained from Dow Chemical Co. and were purified by vacuum distillation from calcium hydride.

Solvent

Hexane was purified by washing with sulfuric acid and distilled from sodium dispersion.

Polymer Preparation

The copolymer was prepared in beverage bottles in hexane solution containing the proper ratios of *o*-chlorostyrene or the *o,p*-chlorostyrene mixture and 1,3-butadiene, with *n*-butyllithium as the initiator.⁹ Several runs were made with pure *o*-chlorostyrene as compared to the *o,p*-chlorostyrene mixture and found to behave similarly.

Preparation of Copolymer Containing 20% *o*-Chlorostyrene and 80% 1,3-Butadiene

Into a 28-oz beverage bottle previously washed with distilled water, baked in a 140°C oven overnight, and cooled with a stream of nitrogen, was placed 260 g of a blend containing 75% hexane and 25% 1,3-butadiene. To this blend was added 17.5 g of freshly distilled *o*-chlorostyrene. The bottle was shaken well and catalyzed with 4.0 m moles of *n*-butyllithium. The bottle was then placed in a 50°C bath with tumbling action for 10 hr.

At the conclusion of the polymerization a solution of 2,2'-methylenebis-(4-methyl-6-*tert*-butyl phenol) antioxidant in isopropyl alcohol was added. The copolymer was recovered by coagulation in isopropyl alcohol and was separated and dried and used for compounding studies. The same procedure was used to prepare copolymers of 1,3-butadiene and *o,p*-chlorostyrene.

The authors wish to thank The Firestone Tire & Rubber Company for permission to publish this work. We also like to thank Dr. D. P. Tate of the Elastomer Division for his comments and suggestions.

References

1. S. N. Ushakov and P. A. Matuzov, *Zh. Obshch. Khim.*, **17**, 435 (1944).
2. L. C. Rubens, in *Styrene*, R. H. Boundy and R. F. Boyer, Eds., Reinhold, New York, 1952, pp. 220, 724.
3. A. V. Chernobia, *Vysokomol. Soedin. SA*, **10**, 1716 (1968).
4. J. W. Breitenbach, O. F. Olaj, and A. Schindler, *Kunststoff-Plastics*, **5**, 302 (1959).
5. G. Natta, F. Danusso, and D. Sianesi, *Makromol. Chem.*, **30**, 238 (1959).
6. M. Shina, D. N. Bhattacharyya, and M. Szwarc, *J. Amer. Chem. Soc.*, **85**, 1306 (1963).
7. G. Gerber and T. Joachim, *Angew. Makromol. Chem.*, **2**, 133 (1968).
8. C. S. Marvel, G. E. Inskeep, R. Deamin, A. E. Juve, C. H. Schroeder, and M. M. Goff, *Ind. Eng. Chem.*, **39**, 1486 (1947).
9. R. S. Stearn and L. E. Forman, *J. Polym. Sci.*, **41**, 381 (1959).

Received May 7, 1970

Revised August 10, 1970

Ladder Pyrrolone Structures with Anthraquinone Recurring Units

JENO SZITA, L. H. BRANNIGAN, and C. S. MARVEL, *Department of Chemistry, The University of Arizona, Tucson, Arizona 85721*

Synopsis

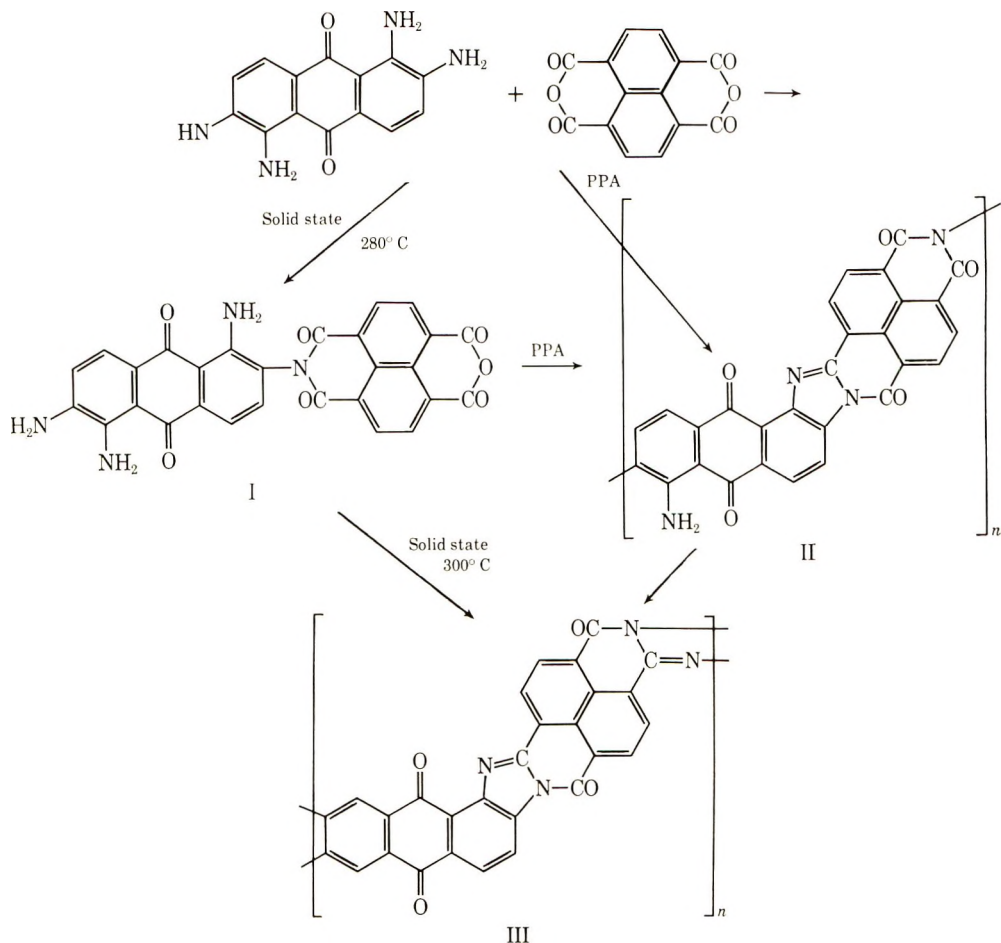
1,2,4,5-Tetraaminoanthraquinone and 1,4,5,8-naphthalene-tetracarboxylic acid dianhydride react in dimethylacetamide to give a tetrameric prepolymer with balanced endgroups of anhydride and diamine. When this prepolymer is carefully treated with polyphosphoric acid at elevated temperature it is converted to a soluble polypyrrolone type structure with an inherent viscosity of 2.3-2.7. Polymers of this molecular weight can be wet-spun into pliable fibers from methanesulfonic acid. The TGA curve in air shows little weight loss below 550°C. The polymer can also be solubilized by reduction with sodium dithionite in alkaline aqueous dimethyl sulfoxide.

Van Deusen et al.¹ have recently obtained extremely thermally stable and fabricable polymers by the condensation of 1,4,5,8-naphthalene-tetracarboxylic dianhydride with either 1,2,4,5-tetraaminobenzene or 3,3',4,4'-tetraaminodiphenyl. These polymers are soluble in concentrated sulfuric acid and have been wet-spun from this solvent to yield strong fibers. We thought that by using 1,2,5,6-tetraaminoanthraquinone as the tetraamine in this reaction, a polymer which could be solubilized in basic media by reduction would make an even more readily fabricable material.

Some model reactions were first carried out with the use of 1,8-naphthalic acid anhydride with 1,2-diaminoanthraquinone and 1,2,5,6-tetraaminoanthraquinone, and 1,4,5,8-naphthalenetetracarboxylic acid dianhydride with 1,2-diaminoanthraquinone. These reactions were carried out in acetic acid solution, in dimethylacetamide containing acetic acid, and in the melt. Usually a final heating of the first formed model compounds was required to form the pyrrolone structure. Polyphosphoric acid was not satisfactory as solvent for the reactions, as it appeared to cause some self-condensation of the aminoanthraquinone derivative. In the case of the reaction with 1,4,5,8-naphthalenetetracarboxylic dianhydride and 1,2-diaminoanthraquinone, it appeared that only one anhydride group reacted to the pyrrolone with one anhydride group remaining unreacted.

Polycondensation of the tetraacid anhydride and tetraamine was carried out in polyphosphoric acid to yield products which were only partially cyclized and completely soluble in sulfuric acid. On further heating to about 350°C products were obtained which by analysis and

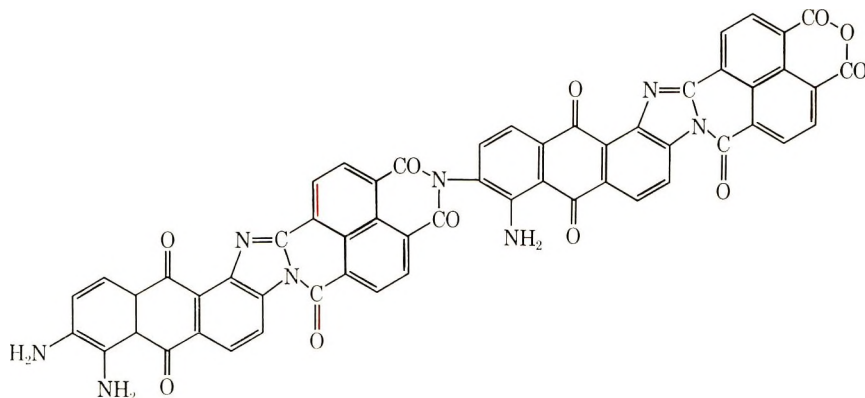
infrared data were shown to be completely cyclized. These condensations seemed to proceed in steps.



The exact structures were not determined as many isomers could be formed in these steps. The intermediate I was characterized by elemental analysis and an infrared spectrum which showed at 1775 cm^{-1} characteristics of anhydride carbonyl groups and at 1650 cm^{-1} characteristics of the imide group.

It was observed that when the two reagents were condensed in DMAc solution containing 10% of acetic acid a dark brown precipitate formed and could be isolated by filtration. This appeared to be a tetramer of structure IV.

The product had a low inherent viscosity (0.05) and showed strong absorption in the infrared at 1780 and 1745 cm^{-1} and a medium weak absorption at 1660 cm^{-1} . When heated in polyphosphoric acid at 160 – 170°C this prepolymer further condensed to a completely soluble (H_2SO_4) polymer with inherent viscosity of 1.34. This polymer gave analytical



IV

values and infrared data characteristic of the closed-ring structure III. Further heating of the polymer in the solid state gave a product which was only 42% soluble in sulfuric acid.

When the prepolymer was heated in polyphosphoric acid at 120°C for 1.5 hr and at 200°C for 1 hr, a polymer of $\eta_{inh} = 1.89$ was obtained. The optimum conditions for the polycondensation were found to be heating an 8% (weight) solution of the prepolymer in polyphosphoric acid at 120°C for 3 hr and at 200°C for 1 hour. Polymers obtained from the latter procedure had inherent viscosities of 2.4–2.7. The results of a variety of condensation experiments are shown in Table I. These higher molecular weight products were found to be nearly completely insoluble in sulfuric acid but at least 90% soluble in methanesulfonic acid and were shown by analysis and base degradation to be nearly completely of the closed structure III. It is obvious that the best results are obtained when the condensation is carried out in two steps. First, the prepolymer, which becomes an AB type monomer, is formed and purified. It is then balanced in reactive end groups to give high molecular weight products upon treatment with polyphosphoric acid.

The TGA curve (Fig. 1) in nitrogen atmosphere, for the polymer (run 7, Table I), showed slight weight loss at 100°C due to absorbed moisture and essentially no further loss below 600°C. Even the TGA curve taken in air shows no weight loss below about 550°C.

A sample of a polymer of inherent viscosity 2.7 (run 9, Table I), was reduced with sodium dithionite in DMSO–water–NaOH at 80–90°C. When the polymer was recovered from the resulting solution the inherent viscosity was lowered to 0.82. This indicates the presence of a small number of base-labile imide linkages in the polymer chain. Thus the regenerated polymer is the highly closed structure III. The TGA curve of this base-treated polymer is essentially the same as the TGA curve for the polymer before treatment with base (Fig. 1).

The fiber-forming properties of this polymer were also investigated. Solutions of the product of run 9 ($\eta_{inh} = 2.7$) in methanesulfonic acid were

TABLE I
 Polycondensation of Tetramer (IV) in Polyphosphoric Acid (PPA)

| Run no. | IV in PPA, wt-% | Temp, °C | Time, hr | Product solubility, % | | η_{inh} | | Elemental analysis ^a | | | | |
|---------|-----------------|-----------|----------|--------------------------------|----------------------------------|--------------------------------|----------------------------------|---------------------------------|------|-------|-------|--------|
| | | | | H ₂ SO ₄ | CH ₃ HSO ₃ | H ₂ SO ₄ | CH ₃ HSO ₃ | C, % | H, % | N, % | O, % | Res, % |
| 1 | 4 | 25-180 | 5 | 100 | — | 1.34 | — | 69.70 | 2.07 | 11.61 | 16.62 | — |
| 2 | 8 | 180 | 2 | 0 | 100 | — | 1.89 | — | — | — | — | — |
| | | to 120 | 1 | 0 | 100 | — | — | — | — | — | — | — |
| | | 120 | 1.5 | — | — | — | — | — | — | — | — | — |
| | | 120-190 | 1 | — | — | — | — | — | — | — | — | — |
| | | 190-200 | 1 | — | — | — | — | — | — | — | — | — |
| 3 | 4 | to 120 | 1 | 90 | — | 0.40 | — | — | — | — | — | — |
| | | 120 | 2 | — | — | — | — | — | — | — | — | — |
| | | 120-180 | 1 | — | — | — | — | — | — | — | — | — |
| | | 180 | 2 | — | — | — | — | — | — | — | — | — |
| 4 | 4 | to 125 | 2 | 24 | 100 | — | 0.78 | — | — | — | — | — |
| | | 125 | 4 | — | — | — | — | — | — | — | — | — |
| | | 125-175 | 1.5 | — | — | — | — | — | — | — | — | — |
| | | 175 | 4 | — | — | — | — | — | — | — | — | — |
| 5 | 2 | to 120 | 1.5 | 95 | — | 1.58 | — | 70.82 | 2.24 | 12.72 | — | 1.00 |
| | | 120 | 3 | — | — | — | — | 70.78 | 2.28 | 12.61 | — | 0.09 |
| | | 120-180 | 1 | — | — | — | — | — | — | — | — | — |
| | | 180 | 3 | — | — | — | — | — | — | — | — | — |
| 6 | 1.6 | Same as 5 | 3 | 100 | 100 | 2.21 | — | 71.81 ^b | 2.28 | 12.41 | — | 0.50 |
| | | Same as 5 | 3 | — | — | — | — | 71.61 | 2.26 | 12.36 | — | 0.50 |
| | | Same as 5 | 3 | — | — | — | — | 71.85 ^b | 2.05 | 11.99 | — | 0.80 |
| | | Same as 5 | 3 | — | — | — | — | 71.67 | 2.00 | 11.86 | — | 0.70 |
| 8 | 8 | Same as 2 | 0 | 0 | 90 | — | 2.4 | — | — | — | — | — |
| 9 | 8 | Same as 2 | 0 | 0 | 100 | — | 2.7 | — | — | — | — | — |
| 10 | 8 | Same as 2 | 0 | 0 | 100 | — | 1.52 | — | — | — | — | — |
| 11 | 8 | Same as 2 | 0 | 0 | 94 | — | 2.6 | — | — | — | — | — |

^a Calculated for C₃₃H₁₀O₄N₄ (closed structure III): C, 72.15%; H, 2.06%; N, 12.00%; O, 13.79%.

^b Corrected for residue.

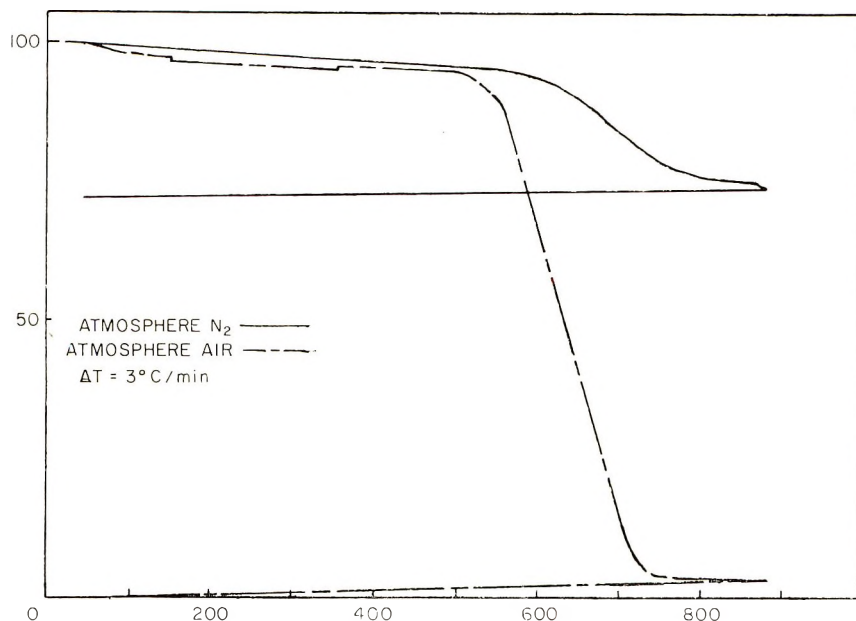


Fig. 1. TGA curve for run 7, Table I.

prepared. The very viscous solutions (5–7%) were extruded from a syringe into 70% methanesulfonic acid, and the precipitating fibers were hand-drawn from 18, 22, and 25 gauge needles. After washing and drying, the green fibers were quite strong and flexible. Good fibers were prepared in this same way from polymer samples with η_{inh} as low as 0.74. More brittle fibers were obtained by extruding the reductive solution into DMSO–H₂O, 0.1N HCl.

EXPERIMENTAL

Monomers

1,2-Diaminoanthraquinone (DAA) was purchased from Aldrich Chemical Co., and purified by recrystallization from nitrobenzene.

ANAL. Calcd for C₁₄H₁₀N₂O₂: C, 70.59%; H, 4.23%; N, 11.76%; O, 13.42%. Found: C, 70.03%; H, 3.88%; N, 12.05%; O, 14.17%.

1,2,5,6-Tetraaminoanthraquinone (TAA) was prepared from 2,6-diaminoanthraquinone as described² and recrystallized from acetophenone before use.

ANAL. Calcd for C₁₄H₁₂N₄O₂: C, 62.68%; H, 4.51%; N, 20.88%; O, 11.93%. Found: C, 62.83%; H, 4.51%; N, 19.49%; O, 12.41%; residue, 0.58%.

1,8-Naphthalic anhydride (NA) and 1,4,5,8-naphthalenetetracarboxylic dianhydride (NTDA) were purchased from Aldrich Chemical Co. NA was used as received and NTDA for model reactions was purified by reprecipita-

tion from DMSO solution in absolute alcohol. The NTDA used for polycondensation was received in highly purified form from Dr. Van Deusen, AFML (MANP) Wright-Patterson Air Force Base, Ohio.

Model Compounds

Condensation of 1,8-Naphthalic Anhydride (NA) and 1,2-Diaminoanthraquinone (DAA)

In Glacial Acetic Acid. To 25 ml of solvent were added 1.1913 g (0.005 mole) of DAA and 0.9909 g (0.005 mole) of NA; the mixture was heated under nitrogen atmosphere in the first 1.5 hr to 120°C and maintained for 5.5 hr. During the reaction a red-brown product precipitated. After cooling it was collected by filtration, washed several times with acetic acid and water, then extracted with water for 6 days. After drying in vacuum at 70–80°C the yield was 1.083 g (55%).

ANAL. Calcd for $C_{26}H_{14}N_2O_4$: C, 74.67%; H, 3.37%; N, 6.69%. Found: C, 74.72%; H, 2.98%; N, 7.10%.

About 600 mg of this product was heated in a glass tube under reduced pressure (0.5–1 mm Hg). In the first hour the temperature was raised to 280–300°C, in the second hour to 340°C and kept there for the next 2 hr. The heated product showed infrared bands in the range of 1800–1200 cm^{-1} : 1710(s), 1670(s), 1595–1585(s), 1545(m), 1460(m), 1415(m), 1355(s), 1330(s), 1290(s), 1250(m) cm^{-1} .

ANAL. Calcd for $C_{26}H_{12}N_2O_3$: C, 78.00%; H, 3.02%; N, 7.00%. Found: C, 77.03%; H, 2.95%; N, 7.04%.

In PPA. DAA (1.1913 g, 0.005 mole) and NA (0.9909 g, 0.005 mole) were heated in 25 g of PPA (82.5%) under nitrogen atmosphere to 130°C in 3 hr and kept for 4.5 hr. After cooling, the black solution was precipitated in 700 ml distilled water, the precipitate isolated, neutralized with ammonium carbonate, and washed and extracted with water for 4 days. A black granular solid was obtained in the yield of 1.18 g (60%).

ANAL. Calcd for $C_{26}H_{12}N_2O_3$: C, 78.00%; H, 3.02%; N, 7.00%; O, 11.98%. Found: C, 73.45%; H, 2.98%; N, 8.35%; O, 11.20%; residue, 3.02%.

Further Purification. The above product was ground (0.5 g in 50 ml of glacial acetic acid) and then boiled three times for 5–10 min. After filtration the product was washed with hot acetic acid and water and dried in a vacuum oven.

ANAL. Found: C, 74.84%; H, 2.99%; N, 8.97%; O, 11.34%; Res., 1.49%. Found after heating in the solid state as above described: C, 76.74%; H, 2.99%; N, 9.61%; O, 9.98%; residue, 1.40%.

Condensation of 1,8-Naphthalic anhydride with 1,2,5,6-Tetraaminoanthraquinone (TAA)

In the Melt. TAA (0.671 g, 0.0025 mole) was treated with an excess of NA (5 g, 0.025 mole). The temperature was raised to 240°C in 2 hr

and held there for another 2 hr, then slowly raised to 320°C in the last 1.5 hr. After purification by reprecipitation and extraction as described before, the weight of the product obtained (2.625 g) was too high. Therefore, the dark green powder was washed with hot DMSO several times and finally with hot toluene and benzene. Because the unsatisfactory elemental analysis (C, 71.94%; H, 2.86%; N, 9.48%; O, 13.26%; residue, 0.99%) and indication of anhydride in infrared spectrum the product was treated again with boiling acetic acid. The yield of the olive green product was 0.984 g (83%). The infrared spectrum had the following bands in the range of 1800–1200 cm^{-1} : 1710(s), 1670(s), 1595–1585(s), 1545(m), 1490(w), 1460(m), 1410(s), 1350(s), 1330(s), 1280(s), 1240(s) and a weak shoulder at 1640 cm^{-1} . This shoulder decreased after heating in the solid state under the same conditions as before.

ANAL. Calcd for $\text{C}_{38}\text{H}_{18}\text{N}_4\text{O}_6$: C, 74.74%; H, 2.98%; N, 9.18%. Calcd for $\text{C}_{38}\text{H}_{16}\text{N}_4\text{O}_4$: C, 77.02%; H, 2.72%; N, 9.40%. Found before final heating: C, 72.63%; H, 2.65%; N, 9.43%. Found after heating: C, 74.87%; H, 2.72%; N, 9.93%.

In the Melt. In a mortar 2.3825 g (0.01 mole) of DAA and 2.9727 g (0.015 mole) of NA were intimately mixed and placed in a round bottom flask. The system was evacuated and filled with nitrogen then heated under N_2 atmosphere to 300°C in 3.5 hr and kept for 1 hr. At about 200°C the mixture melted and began an intensive elimination of water. The dark solid mass thus obtained was ground in a mortar, dissolved in 10 ml of concentrated H_2SO_4 and precipitated in 400 ml of water then extracted for 6 days with water. The yield of dried dark green powder material thus obtained was 3.655 g (>100%). Infrared spectrum indicated anhydride groups. In order to remove the still present anhydride the product was treated with hot acetic acid as described above. The yield was then 81%.

ANAL. Calcd for $\text{C}_{46}\text{H}_{14}\text{N}_2\text{O}_4$: C, 74.64%; H, 3.37%; N, 6.69%. $\text{C}_{46}\text{H}_{12}\text{N}_2\text{O}_3$: C, 78.00%; H, 3.02%; N, 7.00%. Found: C, 76.84%; H, 2.85%; N, 7.26%.

Analysis shows ring closure was incomplete. This product was heated in the solid state under the same condition as before. The infrared spectrum of the heated product was identical with the spectrum of the polymer obtained in DMAc after heating.

*Condensation of 1,2-Diaminoanthraquinone with
1,4,5,8-Naphthalenetetracarboxylic Dianhydride*

In the Solid State. The mixture of 2.3825 g of DAA and 1.340 g of NTDA in 75 g of PPA was heated to 240°C for 1 hr and then 240–320°C for 4.5 hr. It was then treated as described for the condensation product of DAA and NA. Finally the product was extracted with water for 4 days. The yield was 2.433 g (75%). Elemental analysis indicated that the product was not pure. Therefore, about 0.5 g of the product was heated two times in about 50 ml of DMAc at 100–110°C for 10 min. After cooling, the solid part was collected by filtration and washed with DMAc and hot toluene and benzene. The purified product was dried in a vacuum

oven at 100–110°C then further heated in the solid state up to 340°C. The infrared spectrum had bands at 1710(s), 1665(s), 1585(s), 1545(m), 1490(m), 1460(m), 1410(s), 1370(m), 1350(s), 1310(s), 1280(s) and 1245(sh) cm^{-1} . The heated product showed weaker bands at 1490 and 1280 cm^{-1} .

ANAL. Calcd for $\text{C}_{42}\text{H}_{16}\text{N}_4\text{O}_6$: C, 75.00%; H, 2.40%; N, 8.34%. Found before heating: C, 74.14%; H, 2.39%; N, 8.02%; residue, 0.50%. Found after heating: C, 75.1%; H, 2.30%; N, 7.97%; residue, 0.51%.

Polymers

Condensation of TAA with 1,4,5,8-Naphthalenetetracarboxylic Dianhydride (NTDA) in PPA

A solution of 0.6707 g (0.0025 mole) of TAA and 0.6704 g (0.0025 mole) of NTDA in 27 g of PPA was heated to 240°C over a period of 3.5 hr. It was then heated to 200°C for about 1 hr when the mixture became too thick to stir. The highly viscous solvent was treated with 200 ml of distilled water; the precipitate was collected on a filter, neutralized with ammonium carbonate, then washed well and extracted with hot water for 4 days. A dark polymer weighing 0.852 g was obtained. It showed infrared bands at 1710(m), 1660 (with shoulder), 1580(m), 1340(m) and 1240(s) cm^{-1} . It was 90% soluble in concentrated sulfuric acid and had an inherent viscosity of 0.60.

ANAL. Calcd for $\text{C}_{28}\text{H}_{12}\text{N}_4\text{O}_3$: C, 69.43%; H, 2.50%; N, 11.55%. Found: C, 69.41%; H, 2.57%; N, 12.54%.

This compares to the open structure shown in formula II. When the solid polymer was heated to 300°C for 3 hr and then to 300°C for an additional 2 hr, it was mainly the ladder structure III as indicated by infrared bands at 1710(w), 1450(w), 1340(w), 1260–1200(sh) and 1710(sh) cm^{-1} and by the analysis.

ANAL. Calcd for $\text{C}_{28}\text{H}_{10}\text{N}_4\text{O}_4$: C, 72.15%; H, 2.06%; N, 12.00%. Found: C, 70.70%; H, 2.10%; N, 13.06%.

In Solid State. An intimate mixture of 0.6707 g of TAA and 0.6704 g of NTDA was heated under N_2 to 160°C in the first hour, then to 280°C in the next 4 hr and kept at this temperature for 1 hr. After cooling, the solid mass was ground and dissolved in 8 ml of concentrated H_2SO_4 then precipitated in 400 ml of water. The dark violet precipitate was extracted with water for 10 days. The yield was 0.627 g. A 400-mg portion of the product was dissolved in 10 g of PPA and heated under nitrogen atmosphere to 160°C and kept at 160–170°C for the next 3 hr until the reaction mixture became very viscous and ceased to flow. After precipitation in water the product was neutralized, washed and boiled four times in about 100–150 ml of water. The yield was 0.322 g. The final polymer ($\eta_{\text{inh}} = 1.04$) was further heated in the solid state as above described for the pre-

vious polymer. The infrared spectra showed bands in the range of 1800–1200 cm^{-1} : first polymer: 1775(s), 1750–1730(s), 1710(sh), 1650(s), 1595(s), 1570(m), 1515(s), 1435(s), 1365(s), 1315(s), 1285–1260(s), 1220(m) cm^{-1} . After heating in PPA: 1710(m), 1675–1645(m), 1580(m), 1460(m), 1410(m), 1345(s), 1260–1220(s) cm^{-1} . After heating in the solid state: 1710(w), 1450(w), 1340(w), 1260–1200(sh) cm^{-1} .

ANAL. Calcd for $\text{C}_{28}\text{H}_{14}\text{N}_4\text{O}_7$ (structure I): C, 64.87%; H, 2.72%; N, 10.51%. Calcd for $\text{C}_{28}\text{H}_{10}\text{N}_4\text{O}_5$ (structure II): C, 69.43%; H, 2.50%; N, 11.55%. Calcd for $\text{C}_{28}\text{H}_{10}\text{N}_4\text{O}_4$ (structure III): C, 72.15%; H, 2.06%; N, 12.00%. Found after first stage: C, 63.86%; H, 3.03%; N, 11.16%. Found after PPA treatment: C, 69.42%; H, 2.57%; N, 11.87%. Found after final heating: C, 70.08%; H, 1.99%; N, 12.30%.

In DMAc and CH_3COOH . The same amount of the monomers as before were heated under N_2 atmosphere in a mixture of 33 ml of DMAc and 3 ml of glacial acetic acid. In the first 1.5 hr the temperature was raised to 100°C, in the next 1 hr to 120°C and finally to 155–160°C for 4 hr. After standing overnight the black precipitate was collected by filtration, washed several times with small amounts of DMAc, then with water and finally boiled three times with water. After drying in a vacuum oven at 70–80°C, the yield was 1.402 g, $\eta_{\text{inh}} \cong 0.05$ (in concentrated H_2SO_4 at 30°C; $c = 0.5$ g/100 ml). This sample had the following infrared bands: 1780(s), 1750(m), 1710(s), 1660(m), 1615(w), 1580(s), 1540(s), 1500(w), 1440(m), 1410(s), 1370(m), 1345(s), 1310(m), 1270(s), 1230(s) cm^{-1} .

ANAL. Calcd for $\text{C}_{55}\text{H}_{26}\text{N}_8\text{O}_{11}$ (structure IV:) C, 68.55%; H, 2.16%; N, 16.37%. Found: C, 67.76%; H, 2.46%; N, 11.68%.

Heating this apparent tetramer in the solid state for 3 hr at 300°C and then 350°C for 2 hr longer made little change in either the infrared spectrum or the analysis.

General Procedure for Condensation of the Prepolymer IV in Polyphosphoric Acid (Table I)

The prepolymer was dissolved in a weighed amount of PPA contained in a three-necked round-bottomed flask equipped with mechanical stirrer and an inlet and outlet for dry nitrogen. The mixture was warmed in an oil bath to 80°C and stirred as rapidly as possible overnight to insure complete dissolution of the prepolymer. As in run 2, the mixture was then heated to 120°C in 1 hr and held at that temperature for 1.5 hr, then heated to 190–200°C in 1 hr and held at the latter temperature for 1 hr. After this final heating, the mixture became a rubbery mass. The mass was cooled to room temperature and broken up in water with a blender. The fine powder was mixed rapidly in the blender with water four more times, filtered and extracted in a Soxhlet overnight with water. The product was then extracted with ethanol for 4 hr and ether for 4 hr and dried under vacuum. The products of these procedures had analyses and inherent viscosities shown in Table I.

The infrared spectrum (KBr) of the product of Run 1 had bands at 1710(m), 1660(m), 1580(m), 1460(m), 1340(s), 1260(sh), 1220(s) cm^{-1} . The ultraviolet spectrum showed $\lambda_{\text{max}}^{\text{H}_2\text{SO}_4}$ at 435(sh), 473, 493, 503 $\text{m}\mu$.

Reduction and Solubilization

A 1-g portion of polymer (run 9, $\eta_{\text{inh}} = 2.7$) was covered with 5 ml DMSO in a 25 ml three-necked round-bottomed flask with mechanical stirrer and inlet and outlet for dry nitrogen. This mixture was stirred under nitrogen for 1 hr and 1 g of finely ground NaOH has added along with 1 g of sodium dithionite and 5 ml of water. The mixture was stirred under nitrogen at 80–90°C for 2 hr. The polymer became highly swollen and formed a partial solution. When the solution was exposed to air a rubbery film formed on the surface. Some brittle fibers were prepared by extruding the solution into 1:1 DMSO:H₂O, 0.1N HCl.

The polymer was reoxidized by pouring the solution into the extrusion solution. The black solid was collected by filtration, extracted with water in a Soxhlet overnight and with ethanol for 2 hr. After drying, the polymer had $\eta_{\text{inh}} = 0.82$ (0.52% in CH₃HSO₃) and gave a TGA curve nearly identical with that of Figure 1.

Wet Spinning from Methanesulfonic Acid Solutions

A spinning dope was prepared by heating a mixture of 1 g of polymer in 15 ml of methanesulfonic acid at 60–70°C overnight. The extremely viscous solution was poured into the barrel of a 10 ml syringe. An 18 gauge needle was attached and with as constant pressure as possible the solution was extruded into 70% methanesulfonic acid contained in a large shallow dish. The end of the precipitated fiber was grasped with a forceps and was drawn gently across the surface of the precipitation bath for about 6 in. while holding the pressure on the syringe steady. Fibers as long as 24 in. were drawn in this way. The fiber was then washed in water, 10% sodium carbonate, again in water and air dried. The fibers thus formed were strong and flexible. Finer filaments were also formed by using 22 and 25 gauge needles.

This work was supported by the Air Force Materials Laboratory, Air Force Systems Command, Wright-Patterson Air Force Base, Ohio.

We are indebted to Dr. G. F. L. Ehlers, Air Force Materials Laboratory, Wright-Patterson Air Force Base, for the thermogravimetric analyses.

References

1. R. L. Van Deusen, O. K. Goins, and A. J. Sicree, *J. Polym. Sci. A-1*, **6**, 1777 (1968).
2. W. C. Bracke and C. S. Marvel, *J. Polym. Sci.*, in press.

Received September 21, 1970

Use of Phosphite Amides in the Synthesis of Polyamides

C. G. OVERBERGER, R. A. VENESKI, and JAN ŠEBENDA,*
*Department of Chemistry and the Macromolecular Research Center,
The University of Michigan, Ann Arbor, Michigan 48104*

SYNOPSIS

The preparation of polyamides by the phosphite amide procedure was investigated. The yield of amidation was determined in the reaction of diethyl- or *o*-phenylenephosphite derivatives of piperidine, piperazine, or *trans*-2,5-dimethylpiperazine with either mono- or dicarboxylic acids. Higher yields were obtained by using diethyl phosphite derivatives; however, for both types of derivatives the yields were never greater than 90%. Only low molecular weight polymers could be obtained under optimum reaction conditions. In the polycondensation of (+)-*trans*-1,3-cyclohexanedicarboxylic acid or (+)-*trans*-1,2-cyclohexanedicarboxylic acid with phosphite derivatives of either piperazine or *trans*-2,5-dimethylpiperazine, the optical rotation of the polymers was lower than the rotation of the corresponding polyamides prepared by the interfacial condensation procedure with dicarboxylic acid chlorides. It was shown that an intermediate mixed anhydride was formed during the amidation reaction. This may account for the observed racemization.

INTRODUCTION

As part of a study to determine the conformational behavior of asymmetric polyamides,^{1,2} the preparation of a series of polymers containing cyclic dicarboxylic acids and piperazine units was undertaken. Since rigid, optically active cyclic diacids were used, it was necessary to employ a polymerization procedure which was expected to afford polymers of reasonably high molecular weight in nearly quantitative yields without racemization. Of the possible routes, those methods requiring the activation of the carbonyl group,^{3a} e.g., interfacial condensation using dicarbonyl chlorides, were undesirable because the electronegative substituent could facilitate nucleophilic displacement on the adjacent carbon atom causing racemization. On the other hand, no racemization would be expected if the coupling of an optically active dicarboxylic acid with an active derivative of the amine moiety.^{3b} Among these methods, the activation of the amine group through phosphite⁴⁻⁸ and phosphate^{8,9} derivatives has achieved considerable attention. It has been reported that under certain conditions the coupling reaction of protected amino acids with various phosphite amide

* Visiting Research Associate. Present address: Institute of Macromolecular Chemistry, Czechoslovak Academy of Science, Prague, Czechoslovakia.

derivatives proceeded in high yields⁷ without racemization.^{6,7} Therefore, the possibility of preparing rigid optically active polyamides by using this procedure was explored.

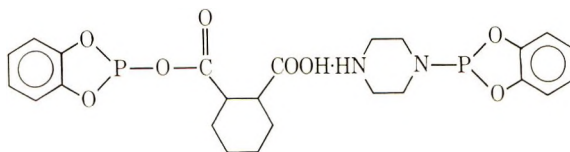
In using rigid and sterically hindered dicarboxylic acids, a different rate of reactivity was expected as compared to that for the flexible amino acids. In order to determine the best reaction condition for polymerization, factors such as time, temperature, rate of addition, concentration of reacting species, and solvent composition were investigated in the preparation of related model systems.

RESULTS AND DISCUSSION

The phosphite amides prepared for this study were: 1,4-bis (diethoxyphosphido)piperazine (I), 1,4-bis(diethoxyphosphido)-*trans*-2,5-dimethylpiperazine (II), 1,4-bis(1,2-*o*-phenylenedioxyphosphido)-piperazine (III), 1,4-bis(1,2-*o*-phenylenedioxyphosphido)-*trans*-2,5-dimethylpiperazine (IV), and 1-diethoxyphosphidopiperidine (V).

Mixed Anhydride Formation

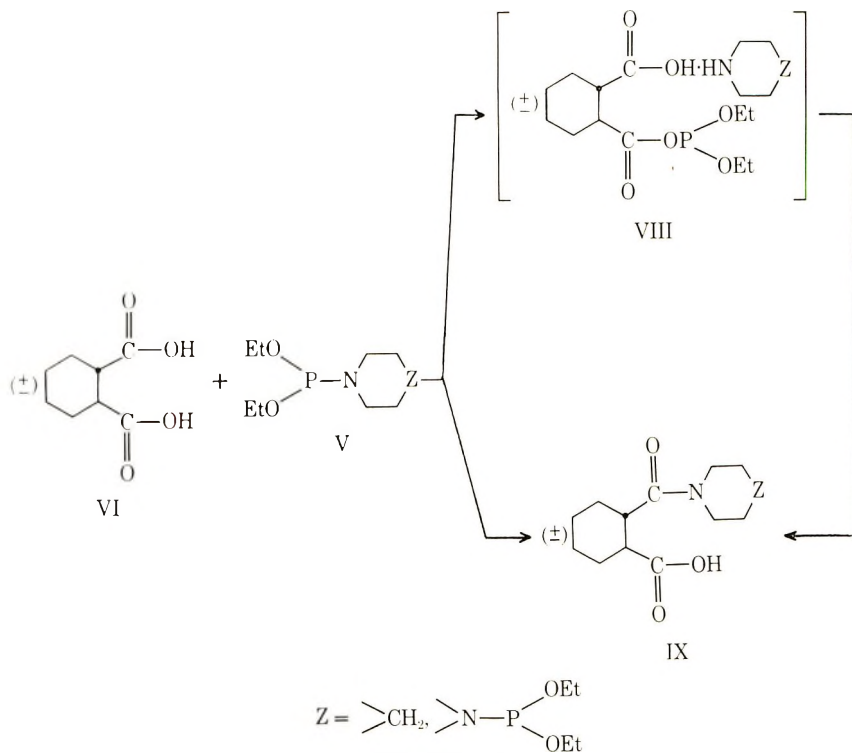
In the reaction of the phosphite amides with various mono or dicarboxylic acids, a substance insoluble in certain solvents was isolated from the reaction mixture. Appreciable amounts, up to 30% of the insoluble product were formed during the attempted polycondensation of *o*-phenylenephosphite amide (III) with (\pm)-*trans*-1,2-cyclohexanedicarboxylic acid (VI) in pyridine. From both the elemental analysis for phosphorus content and infrared determination, it was concluded that the insoluble product (salt VII) consisted of a mixed anhydride formed from *o*-phenylenephosphite III and diacid VI, and the monophosphite amide of piperazine.



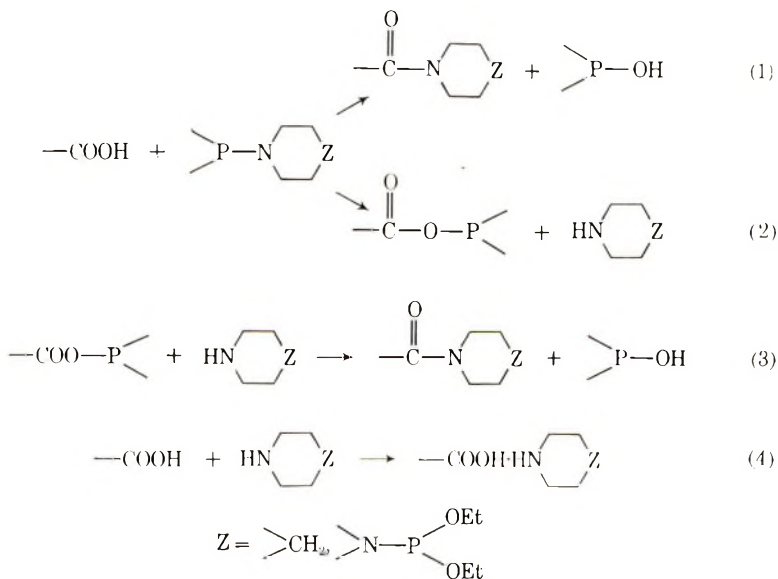
VII

Reacting piperidinophosphite (V) ($Z = >CH_2$) with the diacid VI (1:1 mixture) in diethyl ether, a high yield of the monopiperidine salt VIII was obtained. In toluene, dimethylformamide (DMF), or pyridine, high yields of the monoamide IX ($Z = >CH_2$) were obtained. These results suggested that the reaction proceeded by two paths; the final product depends upon the solubility and/or reactivity of the salt intermediate (VII or VIII).

The formation of the salts VII and VIII indicated that the amidation reaction (1) was not faster than the exchange reaction (2) which resulted in the mixed anhydride. The latter can react with the liberated cyclic amine



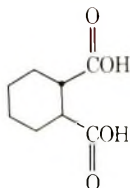
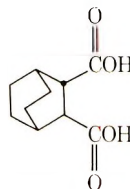
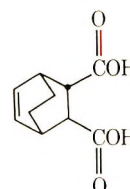
to form the amide [reaction (3)] or the free cyclic amine can react with the carboxylic group to form the salt [reaction (4)].



As soon as the salt becomes insoluble in the reaction medium, the concentration of both components decreases rapidly in the solution resulting in a decrease of the amidation reactions (1) and (3).

A quantitative yield of the monopiperidine salt was obtained from the reaction of piperidinophosphite (V) with (\pm)bicyclo[2.2.2]-octane-*trans*-2,3-dicarboxylic acid (X) (1:1 mixture) in toluene (Table I). On refluxing the reaction mixture, both the monoamide (IX) and the monopiperidine salt (VIII) could be obtained. It appeared as if reaction (1) did not significantly contribute to the condensation and that the major part of the amide bond was formed from the mixed anhydride by reaction (3). When the reaction of diacid X with the phosphite derivative V was carried out in DMF, no precipitation of the salt occurred, as was observed when the reaction was carried out in other solvents. After the usual work-up, a mixture of monopiperidine salt, monoamide, and some diamide could be isolated.

TABLE I
Reaction of 1-Diethoxyphosphidopiperidine (V) with Cyclic Dicarboxylic Acids

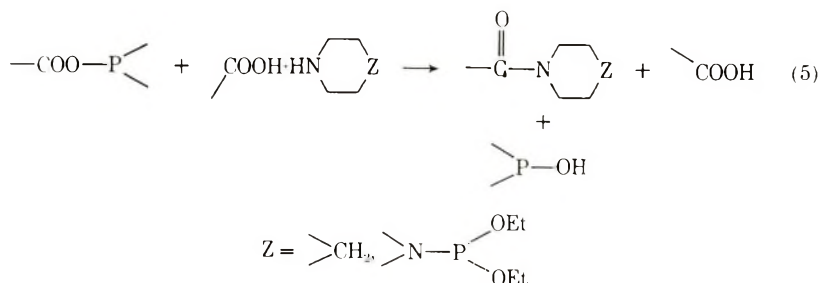
| Diacid | Solvent ^a | Ratio ^b | Temp, °C | Time, hr | Major product (s) ^c |
|---|----------------------|--------------------|----------|----------|--------------------------------|
|  | DIE | 1 | 25 | 2 | a + 10% b |
| | DMF | 1 | 25 | 1 | b, 85% |
| | P | 1 | 60 | 3 | b, 90% |
| (\pm)-VI (-)-VI | T | 2 | Reflux | 3 | c, 85% |
|  | T | 2 | Reflux | 2 | c, 88% |
| | T | 1 | 25 | 10 | a, 90% |
| | T | 1 | Reflux | 2 | a + b (54%) + c |
| | P | 2 | 60 | 5 | b + c (60%) + d |
| | P | 2 | 60 | 40 | c, 60% |
| | DMF | 1 | 30 | 6 | a + b |
| | DMF | 1 | 60 | 4 | 40% a + 40% b |
| (\pm)-X | | | | | |
|  | T | 1 | 25 | 10 | a, 95% |
| | T | 1 | 50 | 2 | a + b |
| | P | 1 | 60 | 4 | 50% b + a |
| | T | 2 | Reflux | 2 | c, 90% |
| | DIE | 1 | 25 | 2 | a, 97% |
| | DIE | 1 | 25 | 12 | a, 95% |
| | (\pm)-XI | | | | |

^a Solvents: T = toluene, P = pyridine, DIE = diethyl ether, DMF = dimethylformamide.

^b Ratio: 1-diethoxyphosphidopiperidine (V) to dicarboxylic acid.

^c Product(s): a = monopiperidine salt, b = monoamide, c = diamide, d = diacid.

An authentic sample of the monopiperidine salt of X was found to be very soluble in DMF. These results indicated that solubility, dissociation and reactivity [reaction (5)] of the intermediate salt were important for the amidation reaction.



Yield of Amidation

The corresponding diethyl and *o*-phenylenephosphite amides (I-IV) were prepared to compare the reactivity of the different types of phosphite

TABLE II
Reaction of Phosphite Amides with Cyclohexanecarboxylic
(CH) and Benzoic Acid (B)

| Phosphite amide ^a | Acid | Solvent ^b | Temp, °C | Time, hr | Yield, % |
|------------------------------|------|----------------------|----------|----------|-----------------|
| II | B | P | 100 | 20 | 88 |
| II | B | T | 60 | 20 | 19 |
| II | B | DMF | 60 | 20 | 8 |
| III | CH | DMF | 60 | 20 | 69 |
| III | CH | P | 60 | 2 | 45 |
| III | CH | P | 60 | 20 | 63 |
| III | CH | P | 60 | 2.5 | 73 ^c |
| III | B | P | 60 | 20 | 58 |
| III | B | P | 60 | 40 | 59 |
| III | B | DEP | 60 | 20 | 40 |
| III | B | DEP | 60 | 40 | 40 |
| III | B | DMF | 60 | 20 | 57 |
| III | B | DMF | 60 | 40 | 65 |
| III | B | T | 25 | 90 | 30 |
| III | B | T | 60 | 20 | 63 |
| III | B | T | 75 | 1.7 | 80 |
| IV | B | T | 100 | 22 | 32 |
| IV | B | T | 100 | 48 | 40 |
| IV | B | P | 100 | 20 | 43 |
| IV | B | P | 100 | 64 | 43 |

^a Amides: II = 1,4-bis(diethoxyphosphido)-*trans*-2,5-dimethylpiperazine; III = 1,4-bis(1,2-phenylenedioxyphosphido)piperazine; IV = 1,4-bis(1,2-phenylenedioxyphosphido)-*trans*-2,5-dimethylpiperazine.

^b Solvents: T = toluene, P = pyridine, DEP = diethylphosphite, DMF = dimethylformamide.

^c The acid was added during 1.5 hr.

amides derived from piperazine and *trans*-2,5-dimethylpiperazine. The *o*-phenylenephosphite amides, (III) and (IV), were promising because they were crystalline. They could be purified easily and weighed exactly in equimolar amounts with the dicarboxylic acids for the polycondensation reaction. However, the results which are summarized in Table II indicated that the yields of diacylated products obtained from *o*-phenylenephosphite derivatives (III) or (IV) were lower than the yields obtained from the diethylphosphite derivative (II). The observations were directly contrary to those reported in the literature, where it was stated that *o*-phenylenephosphite derivatives gave higher yields.¹⁰

Studying the influence of the solvent on the yield, it was observed that the yield varied for the different types of phosphite amides. The yield probably depends on the solubility and dissociation of the salt intermediate, and on the relative rates of reaction 1, 2, 3 and 5 in a particular solvent. Anderson et al.⁴ also found that amidation proceeded in higher yield in certain solvents.

To suppress salt formation during the preparation of the polymers, the reaction was studied in anhydrous pyridine. In the reaction of phosphite amides (I-IV) with monocarboxylic acids in pyridine, the yields obtained varied but were generally higher than those obtained in other solvents (Table II). Similar trends were obtained for the dicarboxylic acids (Table I).

No significant increase in the yield occurred when the reaction time was extended. An increase in the yield with an increase in temperature was attributed to the increased solubility, dissociation and reactivity of the intermediate salt with temperature (Tables I and II).

A pronounced effect of the rate of addition of the carboxylic acid to the phosphite amide solution on the yield was observed. Only 45% of the diamide was obtained when the acid was added all at once, whereas upon a slow addition of the acid the yield increased to 73% (Table II). In the latter case, the reaction proceeded at a low concentration of acid; therefore, the concentration of the free amine groups was higher than in the case when all the acid was added at the beginning of the reaction.

The reaction of *trans*-1,2-cyclohexanedicarboxylic acid (VI) with piperidinophosphite V gave a quantitative yield of the monoamide IX ($Z = >CH_2$) in a shorter time, as compared to that of the diacid VI with the phosphite V in DMF at 60°C, a precipitate appeared within 15 minutes of mixing which then redissolved. After the usual work-up, only the monoamide was collected in quantitative yield. When the reaction was repeated, the precipitate was isolated and identified as the *trans*-monopiperidine salt of VI. These results again indicated that reaction (2) predominates. The liberated piperidine reacted with the acid and formed a salt [reaction (4)]. However, for this acid, the mixed anhydride salt cyclized forming the dicarboxylic anhydride of VI which then reacted with piperidine to form the monoamide product. The reaction of the (\pm) anhydride of VI and piperidine in various solvents was studied and was found to be

very fast. The proposed formation of *trans*-1,2-cyclohexanedicarboxylic anhydride as an intermediate is realistic because attempts to prepare other reactive intermediates of diacid VI always resulted in the isolation of some *trans*-1,2-cyclohexanedicarboxylic anhydride.¹¹ Both the *trans*-1,3-cyclohexanedicarboxylic acid and bicyclic diacid (X) are unable to form the intermediate internal anhydride. This would suggest that the amidation proceeded predominantly by way of reaction (3) for these two acids. However, the formation of an anhydride between two diacid molecules cannot be ruled out entirely.

Polycondensation

Only low molecular weight polyamides were obtained in the polycondensation of various types of phosphite amides (I–IV) with the dicarboxylic acids. Even under optimum reaction conditions, the intrinsic viscosity of the polymers was never greater than 0.10 dl/g. The molecular weight of the polymers did not increase by extending the reaction time from 80 min to 82 hr. These results can be rationalized because the yields of the amidation reaction for the models did not exceed 90%. The yields were also unaffected by the length of time of the reaction (Table II).

The molecular weight of the polymers prepared by the use of *o*-phenyl-nephosphite amide was 50% lower than the molecular weight of the polymers prepared using diethylphosphite amides. Again, this corresponds to the lower yields of amidation found in the model studies (Table II). This is analogous to the condensation of tripeptides with tetraethylpyrophosphite where only low molecular weight polyamides were obtained under various conditions.^{12–14}

The optical rotation of polymers prepared from the optically active *trans*-1,2- or *trans*-1,3-cyclohexanedicarboxylic acids was 20–50% lower than the rotation of the corresponding polymers prepared either by the polycondensation of diamines with dicarbonyl chlorides¹¹ or with reactive diesters.¹⁵ The difference in the rotation could be due to the lower molecular weight of the polymers obtained by the phosphite amide procedure; however, the difference is caused by racemization because it is known that oligopeptides of L-proline (tetramer or pentamer) account for 80% of the observed optical rotation of poly-L-proline.^{16–18}

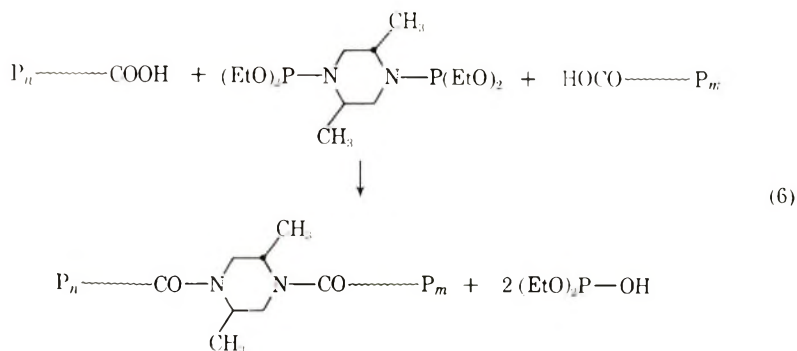
The reaction of optically active diacid VI and phosphite amide V was studied (1:2 mixture). After refluxing the mixture in toluene for 3 hr, the diamide product was isolated and purified. An optical rotatory dispersion spectrum of the product exhibited 90% of the observed rotational strength when compared to an authentic sample prepared by another route.¹¹ Part of the difference could be explained in terms of accuracy within the limits of experimental error of the measurement. Also a trace amount of phosphite by-product could not be completely eliminated from the sample. This may also account for the difference. Nevertheless, the extent of racemization was not as high as in the polymer preparation.

Because of the two conflicting results between polymer and model preparations, the high racemization during the polymerization may be due to the presence of pyridine for long periods of time. The basic pyridine could complex with the acidic α -hydrogen of the dicarboxylic acids which would result in racemization in polymer preparation.

The mixed anhydride reaction is known to cause racemization in the preparation of polypeptides.^{3a} The fact that the carboxyl component and not the amino component is racemized in the coupling of amino acids can be accepted also as an indication for the participation of the activated carboxyl group in the phosphite amide procedure.¹⁹ Therefore, the condensation of phosphite amides with carboxylic acids cannot be considered as a reaction of the activated amine group.

Postcondensation of Interfacial Polymers

It was found that polymers prepared by interfacial polycondensation of *trans*-1,2-cyclohexanedicarbonyl chloride with *trans*-2,5-dimethylpiperazine contain predominantly carboxylic end groups and only a minor fraction of amine end groups. The molecular weight of these polyamides could be increased in two ways: first, by converting the carboxylic end groups into activated derivatives such as active esters, which can then be coupled with an equivalent of the diamine; second by coupling the carboxylic end groups with a suitable active derivative of the diamine, e.g., a phosphite amide derivative. The first method has certain disadvantages. When dicyclohexylcarbodiimide is used as condensing agent,²⁰ side reactions such as the formation of anhydrides and acyl urea produced parallel to the formation of the active esters. Consequently, the coupling of the carboxylic end groups with 1,4-bis(diethoxyphosphido)-*trans*-2,5-dimethylpiperazine was investigated as a method to increase the molecular weight of polyamides [reaction (6)].



The second-order rate constant of the coupling reaction was estimated to be 6×10^{-4} l./mole-sec by determining the decrease of the carboxyl group content during the postcondensation. A similar value (5×10^{-4} l./mole-sec) was found for the optically active polyamide system at 85°C . The rate was found to be too low to be useful in the preparation of high molecular

weight polyamides from *trans*-1,2-cyclohexanedicarboxylic acid and phosphite amide derivatives of *trans*-2,5-dimethylpiperazine because of the high temperature and long reaction time necessary to attain a reasonable extent of reaction. Nevertheless, this method might be useful for increasing the molecular weight of polyamides which contain mostly carboxylic end groups. In addition, by this procedure it would be possible to obtain high molecular weight polymers from rather low molecular weight polyamides of high optical purity which can be obtained by simpler methods.^{11,15}

EXPERIMENTAL

General

During the synthesis, all operations were performed in dry solvents under a nitrogen atmosphere previously dried by using molecular sieve 4A. The purification of the starting materials and the manipulation of the phosphite amides were carried out under a dry nitrogen atmosphere. Triethylamine, pyridine, and toluene were dried over molecular sieve 4A and then with sodium ketyl.²¹ Dimethylformamide was dried over molecular sieve 4A. The solvents were finally distilled in a dry nitrogen atmosphere into storage flasks that were equipped with a three-way stopcock which allowed the withdrawal of small amounts of solvents in a stream of dry nitrogen. The products (Table 1) obtained from the piperidinophosphite (V) reactions were isolated using wet solvents at atmospheric conditions to insure complete hydrolysis of the mixed anhydride. The molecular weight of polymers was determined with a Hitachi-Perkin-Elmer Model 115 apparatus in chloroform at 40°C.

Materials

o-Phenylenechlorophosphite²² was redistilled before use (bp 48.2–48.4°C/0.3 mm). Diethyl chlorophosphite was prepared by refluxing 0.2 mole of triethyl phosphite with 0.1 mole of phosphorus trichloride and distilling the product twice (bp 64°C/50 mm, 147–147.5°C/760 mm).²³ Piperazine and *trans*-2,5-dimethylpiperazine were dried by azeotropic distillation using toluene. After recrystallization from toluene, the materials were stored in sealed ampoules under dry nitrogen in amounts required for the reactions. The (–) and (±)*trans*-1,2-cyclohexanedicarboxylic acids were prepared according to published procedures.²⁴ (±)Bicyclo[2.2.2]octane-*trans*-2,3-dicarboxylic acid and (±)bicyclo-[2.2.2]oct-5-ene-*trans*-2,3-dicarboxylic acid were prepared as described.²⁵

1,4-Bis(diethoxyphosphido)piperazine (I). Diethyl chlorophosphite (5.63 g, 36.0 mmole) was added to a stirred solution consisting of piperazine (1.546 g, 17.9 mmole), triethylamine (3.70 g), and 150 ml of toluene maintained at 0°C. After reaction at 0°C for 2 hr and at room temperature for 1 hr, the triethylamine hydrochloride was filtered off and washed with two portions of toluene (50 ml). The filtrate was concentrated by evaporation

at 26°C/0.05 mm, leaving a viscous colorless liquid residue; yield 5.36 g (92%).

ANAL. Calcd for $C_{12}H_{20}N_2O_4P_2$: C, 45.63%; H, 8.93%; N, 8.87%; P, 22.64%. Found: C, 45.51%; H, 8.98%; N, 8.80%; P, 22.51%.

1,4-Bis(diethoxyphosphido)-*trans*-2,5-dimethylpiperazine (II). Diethyl chlorophosphite (2.86 g, 8.3 mmole) was added to a stirred solution of *trans*-2,5-dimethylpiperazine (0.945 g, 8.30 mmole) and triethylamine (1.66 g) in toluene (100 ml) at 0°C. After 1 hr, the triethylamine hydrochloride was removed by filtration. The filtrate was concentrated by evaporation at 25°C/0.05 mm to a viscous colorless liquid (2.53 g, 85%).

ANAL. Calcd for $C_{14}H_{22}N_2O_4P_2$: C, 42.40%; H, 9.49%; N, 8.24%; P, 21.04%. Found: C, 42.28%; H, 9.58%; N, 8.18%; P, 20.93%.

1,4-Bis(1,2-*o*-phenylenedioxyphosphido)piperazine (III). A solution of piperazine (1.67 g, 19.4 mmole) and triethylamine (4.11 g, 40.6 mmole) in toluene (96 ml) was cooled to 0°C and stirred while *o*-phenylene chlorophosphite (6.80 g, 39.0 mmole) was added. The reaction temperature was allowed to attain room temperature slowly. After an additional 2 hr, triethylamine hydrochloride was filtered off and washed, first with 90 ml and then with 15 ml of toluene. About 40 ml of toluene was removed by distillation from the mixture. After cooling to -70°C, crystalline phosphite amide III separated. The product was filtered at -60°, washed with toluene and dried at 26°C/0.1 mm. Obtained 5.22 g (74%), mp 149-150°C. Another 0.86 g (12%) of phosphite amide II was obtained from the mother liquid.

ANAL. Calcd for $C_{16}H_{18}N_2O_4P_2$: C, 53.05%; H, 4.45%; N, 7.73%; P, 17.11%. Found: C, 53.16%; H, 4.57%; N, 7.65%; P, 17.01%.

1,4-Bis(1,2-*o*-phenylenedioxyphosphido)-*trans*-2,5-dimethylpiperazine (IV). To a stirred solution of *trans*-2,5-dimethylpiperazine (1.835 g, 16.1 mmole) and triethylamine (3.28 g, 32.4 mmole) in ether (100 ml) cooled to 0°C was added *o*-phenylene chlorophosphite (5.77 g, 33.1 mmole) during a 3 min period. After stirring at room temperature for 1 hr, triethylamine hydrochloride was filtered and washed with ether; then most of the solvent was removed *in vacuo*. The resulting solution (about 10 ml of ether) was cooled to -70°C and the phosphite amide IV which crystallized was filtered and washed with ether. The yield was 5.60 g (89%); mp 132.5-133.5°C.

ANAL. Calcd for $C_{18}H_{20}N_2O_4P_2$: C, 55.39%; H, 5.16%; N, 7.18%. Found: C, 55.18%; H, 5.49%; N, 7.15%.

1-Diethoxyphosphidopiperidine (V). Freshly distilled piperidine (16.4 g, 0.19 mole) (distilled from BaO or CaH₂) dissolved in 250 ml of diethyl ether was added during a period of 30 min to an ice-cold, stirred solution consisting of freshly distilled diethyl chlorophosphite (30 g, 0.19 mole), anhydrous triethylamine (21.2 g, 0.21 mole), and 500 ml of diethyl ether. After stirring the reaction mixture for 1 hr at 0°C and 1 hr at room tem-

perature, the precipitated triethylamine hydrochloride was removed by filtration and washed with diethyl ether. The ether was removed by distillation leaving a viscous residue which was vacuum distilled. After a large fore run (bp 56–100°C/28 mm), 1-diethoxyphosphidopiperidine (V) was collected, bp 101°C/28 mm. Obtained was 23.6 g (60%), $n_D^{21} = 1.4614$.

ANAL. Calcd for $C_9H_{20}NO_2P$: C, 52.67%; H, 9.82%; N, 6.82%. Found: C, 52.73%; H, 9.76%; N, 6.48%.

Typical Reaction of 1-Diethoxyphosphidopiperidine (V) with Various Dicarboxylic Acids

Phosphite amide V was reacted with an appropriate amount of dicarboxylic acid dissolved in approximately 10 ml of solvent (or enough solvent to dissolve the acid). The reaction conditions and product distributions are listed in Table I. The general work-up consisted of diluting the reaction mixture with approximately 40 ml of wet diethyl ether. The precipitate that formed was isolated by filtration and air dried. It was identified as the monopiperidino salt of the diacid by comparison with an authentic sample prepared by a different procedure. In addition, some free acid (identified by mp) can be isolated. The filtrate was concentrated to dryness at 26°C *in vacuo*. The oily residue which slowly crystallized after months, consisted of a mixture of products, solvent, and phosphite by-products. Generally, the residue was dissolved in a small quantity of chloroform and placed on the top of 30–40 g of Florsil in a chromatography column; it was eluted first with petroleum ether (bp 30–60°C) and then by a cyclohexane–ether mixture (1:1). After removing the solvent by evaporation, the solid residue was recrystallized from a small quantity of ethyl acetate–petroleum ether mixture. The product was identified as the monoamide when one equivalent of phosphite amide V was reacted with one equivalent of dicarboxylic acid. In the reaction of two equivalents of phosphite amide V with one equivalent of diacid, the diamide was isolated. Both monoamide and diamide could be isolated when pyridine was used as solvent. The products were identified by comparison of the infrared and NMR spectra and melting points with those of authentic samples prepared by a different procedure.

Typical Reaction of Phosphite Amide with Benzoic or Cyclohexanecarboxylic Acid

Piperazine- or *trans*-2,5-dimethylpiperazinephosphidoamines (I–IV, 10–20 mmole) were reacted with exactly equimolar amounts of benzoic or cyclohexanecarboxylic acid dissolved in 10 ml of solvent. After diluting the reaction mixture with approximately 30 ml of chloroform, the solution was washed with saturated sodium bicarbonate and finally with water. After evaporating to dryness, the residue was dissolved in 5 ml of ethyl alcohol and poured into boiling water. The diacylated piperazine or *trans*-2,5-dimethylpiperazine derivative was isolated by cooling the reaction

mixture to room temperature. The product was collected by filtration and dried *in vacuo*. The reaction conditions and yields of the diamides are given in Table II. In some cases, a crystalline solid was deposited on the walls during the reaction. This solid was soluble in water.

Reaction of 1-Diethoxyphosphidopiperidine (V) with (\pm)-*trans*-1,2-Cyclohexanedicarboxylic Acid (VI) in DMF

Piperidinophosphite (V) (3.39 g, 16.5 mmole) dissolved in 10 ml of dry DMF was added over a period of 20 min to a stirred solution consisting of *trans*-1,2-cyclohexanedicarboxylic acid (2.94 g, 16.5 mmole) and 25 ml. of DMF at room temperature. Ten minutes after the initial addition a precipitate formed which redissolved within 10 min after the addition was completed. The reaction mixture was stirred an additional hour. After the usual work-up and purification, the monoamide product, *trans*-2-piperidino-carbonylcyclohexanedicarboxylic acid was isolated. Obtained was 3.3 g (85%) of product, mp 120–121°C; on additional recrystallization it had mp 121° (authentic sample mp 121–121.5°C).

The reaction was repeated with the piperidinophosphite (V) being added rapidly by syringe. The reaction mixture was filtered when the precipitate appeared. The precipitate was washed twice with 2-ml portions of DMF, several times with wet diethyl ether, and air-dried. The obtained product was identified as the monopiperidine salt of diacid VI, mp 152–153°C. After vacuum sublimation, a product with mp 153–154°C was obtained; an authentic sample had mp 153–154°C.

Preparation of Monopiperidine Salts of Various Dicarboxylic Acids

One equivalent of anhydrous piperidine was added to the dicarboxylic acid dissolved in a large quantity of a suitable solvent. The reaction mixture was diluted with diethyl ether. The precipitate was collected by filtration and air dried. The product was purified by adding to hot ethyl acetate. The precipitate was reisolated by filtration and air dried. The conditions, the compound, solvent, product, melting point, and analysis are listed as follows. (\pm)Bicyclo[2.2.2]octane-*trans*-2,3-dicarboxylic acid, toluene, *trans*-monopiperidine salt, mp 164–165°C.

ANAL. Calcd for $C_{13}H_{23}NO_4$: C, 63.58%; H, 8.89%; N, 4.94%. Found: C, 63.53%; H, 8.82%; N, 5.08%.

(\pm)Bicyclo[2.2.2]oct-5-ene-*trans*-2,3-dicarboxylic acid, toluene, *trans*-monopiperidine salt, mp 156–158°C.

ANAL. Calcd for $C_{13}H_{23}NO_4$: C, 64.04%; H, 8.24%; N, 4.98%. Found: C, 64.07%; H, 8.02%; N, 4.96%.

(\pm)-*trans*-1,2-cyclohexanedicarboxylic acid, DMF, *trans*-monopiperidine salt, mp 156–158°C.

ANAL. Calcd for $C_{13}H_{23}NO_4$: C, 60.68%; H, 9.01%; N, 5.44%. Found: C, 60.78%; H, 9.06%; N, 5.43%.

cis-1,2-cyclohexanedicarboxylic acid, DMF, *cis*-monopiperidine salt, mp 143–144.5°C.

ANAL. Calcd for $C_{13}H_{23}NO_4$: C, 60.68%; H, 9.01%; N, 5.44%. Found: C, 60.61%; H, 9.09%; N, 5.37%.

Reaction of (\pm)-*trans*-1,2-Cyclohexanedicarboxylic Acid (VI) with 1,4-Bis(1,2-*o*-phenylenedioxyphosphido)piperazine (III). (\pm)-*trans*-1,2-Cyclohexanedicarboxylic acid (0.6679 g, 3.88 mmole) in 5.2 ml of pyridine was added, over a period of 10 hr, to a stirred solution consisting of 1.329 g (3.66 mmole) of phosphite amide III and 5.2 ml of pyridine maintained at 60°. During the addition, a crystalline solid separated from the reaction mixture. After the addition of the diacid, the reaction mixture was stirred at 60°C for 20 hr, diluted with 25 ml of methylene chloride and the solid material was isolated by filtration (obtained 0.59 g). The infrared spectrum of this substance showed the presence of $-NH_2^{\oplus}\ominus OOC-$ (salt).

ANAL. Calcd for $C_{24}H_{28}N_2O_8P_2$: P, 11.59%. Found: P, 12.0%.

The filtrate was evaporated *in vacuo*, leaving a dry residue which was dissolved in 30 ml of chloroform. The solution was washed with 10% sodium carbonate, 10% sulfuric acid, and finally with water. The solution was evaporated to 5 ml and pipetted into 200 ml of ether which was stirred. The polymer was isolated by filtration and dried *in vacuo*. A yield of 0.38 g (47%) was obtained. The infrared spectrum showed absorption at 1635 cm^{-1} (amide).

Polycondensation of (\pm)-*trans*-1,2-Cyclohexanedicarboxylic Acid (VI) with 1,4-Bis(diethoxyphosphido)-*trans*-2,5-dimethylpiperazine (II). Diethyl chlorophosphite (1.6 ml) was added to a stirred solution consisting of *trans*-2,5-dimethylpiperazine (0.567 g, 4.96 mmole) and methylene chloride (15 ml) maintained between 5–10°. After 15 min, 1.61 ml of triethylamine was added. The mixture was stirred for an additional period of 45 min at room temperature. After the triethylamine hydrochloride was filtered off and washed with methylene chloride, the solvent and the excess diethyl chlorophosphite were removed by evaporation at 60–70°C/0.2 mm, leaving a residue which was then dissolved in 7.5 ml of diethyl phosphite. To this solution (\pm)-*trans*-1,2-cyclohexanedicarboxylic acid (0.8455 g, 4.91 mmole) was added. The reaction mixture was heated at 85° for a period of 80 min. After cooling, 30 ml of ether was added and the precipitate which was isolated was redissolved in 5 ml of DMF at 100°C. The filtered solution was pipetted into 200 ml of water, and the polymer was isolated by filtration. After washing with water and drying, polymer, 1.10 g (89%) was obtained; $[\eta]^{25}$ (methyl alcohol) 0.113 dl/g.

Polycondensation of (\pm)-*trans*-1,2-Cyclohexanedicarboxylic Acid (VI) with 1,4-Bis(diethoxyphosphido)-*trans*-2,5-dimethylpiperazine (II). A solution consisting of phosphite amide IV, (0.7957 g, 2.25 mmole) and (\pm)-*trans*-1,2-cyclohexanedicarboxylic acid (II) (0.3955 g, 2.29 mmole) in pyridine (4 ml) was heated at 100°C for a period of 82 hr. The pyridine

was removed by evaporation at 60–80°C/10 mm. The residue was dissolved in 5 ml of DMF and pipetted into 300 ml of water. The polymer was washed thoroughly with water and dried at 120°C/0.05 mm; yield 0.52 g (92%). The polymer was reprecipitated by pipetting a chloroform solution into ether; $[\eta]^{25}$ (methyl alcohol) 0.108 dl/g, $M_n = 5060$. The infrared spectrum shows bands at 1635 (amide), 1725 (carboxyl), and 3480 cm^{-1} (amine).

Polycondensation of (\pm)*trans*-1,2-Cyclohexanedicarboxylic Acid (VI) with 1,4-Bis(1,2-*o*-phenylenedioxyphosphido)piperazine (III). (\pm)*trans*-1,2-Cyclohexanedicarboxylic acid (0.401 g, 2.33 mmole) and phosphite amide III (0.843 g, 2.33 mmole) in 3 ml of DMF was heated at 80°C for 7 hrs. After most of the solvent has removed by evaporation at 80–90°C/0.05 mm, the residue was heated with 8 ml of aqueous methyl alcohol at 60°C for 1 hr. Evaporation of the alcohol and water from the mixture left a residue which was dissolved in methylene chloride. The solution was washed with water. The polymer was isolated by precipitation with ether; yield 0.36 g (60%), $[\eta]^{25}$ (methyl alcohol) 0.053 dl/g.

Polycondensation of ($-$)*trans*-1,2-Cyclohexanedicarboxylic Acid (VI) with 1,4-Bis(diethoxyphosphido)-*trans*-2,5-dimethylpiperazine (II). ($-$)*trans*-1,2-Cyclohexanedicarboxylic acid (0.5774 g, 3.36 mmole, $[\alpha]_D^{27} - 18.9$ [$c = 2$, CHCl_3]) and phosphite amide II (1.043 g, 2.94 mmole) in 9 ml of pyridine was heated at 60°C for 20 hr and then at 90°C for 90 min. The solvent was removed by evaporation at 80°C/0.1 mm, leaving a viscous residue. The polymer which was precipitated with water was washed and dried *in vacuo*. The yield was 0.27 g (42%), $[\alpha]_D^{27} + 76$. After reprecipitation from chloroform into ether, the product had $[\alpha]_D^{27} + 90$ ($c = 0.5$, chloroform), content of carboxylic endgroups 0.65 mmole/g.

Similarly, polycondensation of ($-$)*trans*-1,2-cyclohexanedicarboxylic acid (0.5188 g, 30.1 mmole) with phosphite amide II (1.071 g, 30.1 mmole) in diethyl phosphite (4 ml) at 85°C, for 110 min gave 0.262 g (35%) of polymer; $[\alpha]^{27} + 71$ ($c = 1.27$, chloroform), containing 0.76 mmole COOH/g endgroups.

Polycondensation of (+)*trans*-1,3-Cyclohexanedicarboxylic Acid with 1,4-Bis(diethoxyphosphido)-*trans*-2,5-dimethylpiperazine (II). (+)*trans*-1,3-Cyclohexanedicarboxylic acid (0.5055 g, 2.95 mmole) with $[\alpha]_D^{28} + 21.95$ ($c = 1.68$, acetone), mp 131–133°C, and phosphite amide II (0.9747 g, 2.75 mmole) in pyridine (3 ml) was heated at 85°C for 49 hr. The polymer was precipitated with boiling water and purified by reprecipitation (chloroform solution to ether). The yield was 0.545 g (79%); $[\alpha]_D^{25} - 10.5$ ($c = 2$, chloroform); carboxyl group content, 0.34 mmole/g.

Increase in Molecular Weight of Poly(1,4-[(\pm)*trans*-1,2-cyclohexanedicarbonyl]-*trans*-2,5-dimethylpiperazine) by using 1,4-Bis(diethoxyphosphido)-*trans*-2,5-dimethylpiperazine (II). Poly(1,4-[(\pm)*trans*-1,2-cyclohexanedicarbonyl]-*trans*-2,5-dimethylpiperazine) (0.97 g, containing 0.534 mmole COOH/g, and less than 0.02 mmole NH_2 /g, $M_n = 4,080$) was dissolved at 80°C in pyridine (8.8 ml). Then 99.0 mg (0.279 mmole) of phos-

phite amide II was added. Parts of the reaction mixture was heated at 80°C for 3, 22, 50, and 166 hr, respectively. After reducing the volume of each fraction to 1 ml by evaporation of the solvent at 80°C/0.1 mm, the polymer was precipitated by boiling water. The initial $[\eta]^{25}$ (methyl alcohol) of the polymer was 0.111 dl/g. After postcondensation for 22, 50, and 166 hr, the $[\eta]^{25}$ was 0.129, 0.160, and 0.178 dl/g, respectively. During the postcondensation, the content of carboxylic endgroups of the polymer decreased from 0.470 mmole/g to 0.367 mmole/g after 3 hr, to 0.155 mmole/g after 22 hr, and to 0.068 mmole/g after 50 hr (determined from infrared spectra of the polymers, and by conductometric titration of the initial polymer).

Similarly, 0.820 g of a polymer containing 0.10 mmole COOH/g and less than 0.02 mmole NH₂/g was treated with 13.9 mg (0.049 mmole) of phosphite amide II in 8 ml of pyridine at 80°C for 2 hr; the intrinsic viscosity of the polymer (0.348) increased to 0.405 dl/g.

Condensation of optically active poly(1,4-[(+)-*trans*-1,2-cyclohexanedicarbonyl]-*trans*-2,5-dimethylpiperazine), (0.144 g, containing 0.109 mmole COOH/g) with phosphite amide II (3.1 mg, 0.011 mmole) in pyridine (2 ml) at 85° for 105 hr increased the intrinsic viscosity from 0.248 to 0.273 dl/g. The content of carboxylic endgroups decreased from 0.109 to 0.043 mmole/g. The optical rotation of the initial polyamide was $[\alpha]_D^{25} - 114.6$. After postcondensation, the optical rotation was $[\alpha]_D^{22.2} - 115.5$ ($c = 1.0$, methyl alcohol).

The authors are indebted to Dr. Y. Nishimura and Dr. M. Mizutori for valuable samples of the dicarboxylic acids and polymers that were used in the initial phase of this work. One of us (Jan Šebenda) is grateful for support from the Institute of Science and Technology, Ann Arbor, Michigan (March 1967 to March 1968). RAV gratefully acknowledges the support from the Monsanto Summer Fellowship (1967) and the Sherwin-Williams Company Summer Fellowship (1968).

A portion of this work will appear in the Ph.D. Dissertation of R. A. Veneski, The University of Michigan.

References

1. C. G. Overberger, G. Montaudo, Y. Nishimura, J. Šebenda, and R. A. Veneski, *J. Polym. Sci. B*, **7**, 219 (1969).
2. C. G. Overberger, G. Montaudo, M. Mizutori, J. Šebenda, and R. A. Veneski, *J. Polym. Sci. B*, **7**, 225 (1969).
3. Review. E. Schröder, and K. Lübke in *The Peptides*, Academic Press, New York, Vol. 1, 1965, (a) p. 78; (b) p. 128.
4. G. W. Anderson, J. Blodinger, R. W. Young, and A. D. Welcher, *J. Amer. Chem. Soc.*, **74**, 5304 (1952).
5. G. W. Anderson and R. W. Young, *J. Amer. Chem. Soc.*, **74**, 5307 (1952).
6. G. W. Anderson, J. Blodinger, and A. D. Welcher, *J. Amer. Chem. Soc.*, **74**, 5309 (1952).
7. R. W. Young, K. H. Wood, R. J. Joyce, and G. W. Anderson, *J. Amer. Chem. Soc.*, **78**, 2126 (1956).
8. S. Goldschmidt and F. Obermeier, *Ann.*, **588**, 24 (1954).
9. G. Schramm and H. Wisemann, *Chem. Ber.*, **91**, 1073 (1958).

10. R. Roeske, F. H. C. Stewart, R. J. Stedman, and V. du Vigneaud, *J. Amer. Chem. Soc.*, **78**, 5883 (1956).
11. C. G. Overberger, Y. Nishimura, J. Šebenda, and R. A. Veneski, to be published.
12. H. Kitaoka, S. Sakakibara, and H. Tani, *Bull. Chem. Soc. Japan*, **31**, 802 (1958).
13. S. G. Waley, *J. Chem. Soc.*, **1955**, 517.
14. M. L. Huggins, K. Ohtsuka, and S. Morimoto, in *Macromolecular Chemistry, Tokyo-Kyoto, 1967* (*J. Polym. Sci. C*, **23**), I. Sakurada and S. Okamura, Eds., Interscience, New York, 1968, p. 343.
15. C. G. Overberger and J. Šebenda, *J. Polym. Sci. A-1*, **7**, 2875 (1969).
16. E. S. Pysh, *J. Mol. Biol.*, **23**, 587 (1967).
17. A. J. Hopfinger and A. G. Walton, *J. Macromol. Sci. Phys.*, **133**, 171 (1969).
18. H. Okabayashi, T. Isemura, and S. Sakakibara, *Biopolymers*, **6**, 323 (1968).
19. M. Bodansky, private communication.
20. H. G. Khorana, *Chem. Ind. (London)*, **1955**, 1087.
21. K. Ziegler, F. Grössmann, H. Kleiner, and O. Schäfer, *Ann.*, **473**, 20 (1929).
22. L. Anschutz, W. Broecker, R. Neher, and A. Ohnheiser, *Chem. Ber.*, **76**, 218 (1943).
23. H. G. Cook, J. D. Ilett, B. C. Saunders, G. J. Stacey, H. G. Watson, I. G. E. Wilding, and S. J. Woodcock, *J. Chem. Soc.*, **1949**, 2921.
24. D. E. Applequist and N. D. Werner, *J. Org. Chem.*, **28**, 48 (1963).
25. J. B. Clements, *J. Org. Chem.*, **26**, 2595 (1961).

Received May 21, 1970

Revised September 22, 1970

NMR Identification of C₁₁ to C₁₀ Branched Hydrocarbons Derived from the Decomposition of Polyisobutylene

R. W. WARREN, D. S. GATES,* and G. L. DRISCOLL,
Sun Oil Company, Marcus Hook, Pennsylvania 19061

Synopsis

The composition of nonvolatile fluids obtained from thermally cracking and hydrogenating polyisobutylene was determined by using a combination of gas chromatography and nuclear magnetic resonance spectroscopy (NMR). This work involved the separation and characterization of a homologous series, C₁₁-C₁₀, of sixteen branched hydrocarbon species consisting of repeating isobutylene structures. As a result of this investigation, useful correlations between NMR spectra and molecular structure for highly branched hydrocarbons were developed. The data demonstrate that these hydrocarbons are unique species characterized by "crowded" and sterically hindered geminal methyl and isolated methylene groups. NMR solvent shift studies in benzene solutions indicate that it is possible to differentiate between maximally crowded geminal methyl groups and between maximally crowded methylene groups in these structures. Results of the benzene-induced solvent effects are discussed with respect to the stereochemistry of these molecules and related to existing solvent shift data. These results suggest that these hydrocarbons are polar or nearly polar materials. Successive losses of isobutylene units from stabilized tertiary radicals can account for the formation of the major species identified in these fluids. Higher carbon numbered species have lower refractive indices and densities and higher molal volumes than predicted by calculations.

INTRODUCTION

Oligomers and high molecular weight polymers of isobutylene have been prepared commercially for a number of years.¹ We became interested in comparing the structures of isobutylene oligomers when it was found that fluids prepared by thermally cracking high molecular weight polyisobutylene had physical properties different from those of commercial isobutylene oligomers. More specifically, the fluids prepared by thermal cracking had much better viscosity-temperature properties which are very useful in certain fluid applications. The purpose of this paper is to describe the characterization of the relatively nonvolatile fluids prepared by thermally cracking and hydrogenating high molecular weight polyisobutylene.

This work involved the determination of the molecular structures of a homologous series, C₁₁-C₁₀, of sixteen branched hydrocarbon species containing repeating isobutylene units. In addition to providing the identifi-

* Present address: Delaware County Community College, Media, Pa., 19063.

cation of the C_{11} - C_{10} oligomer structures, the results of this work: (1) provide useful correlations between NMR spectra and molecular structure for highly branched hydrocarbons, (2) describe the use of benzene-induced solvent shifts in the NMR determination of their molecular structure, (3) correlate proton chemical shifts with molecular "crowding," (4) compare the calculated and experimental values of their refractive indices and densities (for two species only) at 25°C and relate differences between the calculated and observed values to molal volume, and (5) discuss in light of previous data² the mechanisms which appear to be involved in the formation of these nonvolatile products.

EXPERIMENTAL

Apparatus

Gas chromatographic separations were obtained by using F&M Models 720 and 5750 gas chromatographs and Model 775 Prepmaster. All of these instruments were equipped with dual columns and thermal conductivity detectors (WX filaments). The chromatographic columns used with the analytical instruments consisted of 6-ft and 24-ft \times $\frac{1}{4}$ -in. o.d. copper tubing packed with 5.0% SE-54 silicone rubber on 60-80 mesh Chromosorb G (acid washed and silane treated (AW-S), 8-ft \times $\frac{1}{4}$ -in. o.d. copper tubing packed with 5.0% GE-SE-30 silicone rubber on 60-80 mesh Chromosorb G (AW-S), and 6-ft \times $\frac{1}{4}$ -in. o.d. copper tubing containing 10.0% Apiezon L grease on 60-80 mesh Chromosorb P (AW-S). The 775 Prepmaster utilized an 80-in. \times $\frac{3}{4}$ -in. o.d. stainless steel column containing 20% UC W98 silicone rubber coated on 10-60 mesh untreated Chromosorb P. The 6-ft and 24-ft SE-54 columns were temperature-programmed from 90 to 300°C at a rate of 7.5-8°C/min and were also run isothermally at temperatures ranging from 210 to 280°C. Figure 1 shows the separation obtained for these species when temperature-programmed over the 6-ft SE-54 silicone rubber column. The 6-ft Apiezon L column was used in series with the 24-ft SE-54 silicone rubber column and operated isothermally at temperatures of 125 and 270°C. Helium was used as carrier gas at a rate of 75 ml/min. for all analytical columns. The injection ports of the 720 and 5750 instruments were maintained at a temperature of 320°C and the detectors at a temperature of 340°C. The 80-in. preparative column was operated at 250-300°C and at a helium carrier gas flow rate of 370 ml/min. The injection port temperature was 335°C and the detector temperature 305°C.

A Perkin-Elmer Model 226 capillary gas chromatograph equipped with a flame ionization detector was used for purity determination of collected fractions. The capillary columns used for this work consisted of a 150-ft \times 0.01-in. capillary column of Ucon 50-HB-5100 and 150-ft and 50-ft \times 0.01-in. capillary columns of Apiezon L grease. The Ucon column was operated isothermally at temperatures ranging from 75 to 150°C and at pressures of 20 to 30 psi. The 50-ft Apiezon L column was operated isother-

mally at 200–230°C and at pressures of 20–25 psi. The 150-ft Apiezon L column was operated at 250°C and 40 psi.

The NMR spectra were obtained on Varian Models A-60 and HA-100 spectrometers. One NMR spectrum was obtained by using the Varian Model HR-220. The 60-MHz spectra were recorded with the use of carbon tetrachloride and hexadeuteriobenzene solutions containing 0.1–0.3 mole/l. of sample and about 1% of tetramethylsilane, TMS. Resonance positions (in Hz and ppm) were measured relative to the internal reference, TMS, at ambient temperatures ($33^\circ \pm 1^\circ\text{C}$). The 60-MHz spectra were run at sweep widths of 250 and 500 Hz. The 100-MHz spectra of the C_6D_6 solutions were obtained by using frequency sweep with the control signal locked on TMS. These spectra were recorded by using a sweep offset of 72 Hz and a sweep width of 100 Hz. The single 220-MHz spectrum was obtained by using a sweep width of 250 Hz and an offset of 165 Hz. Integrated intensities of the resonance peaks were measured with the A-60, HA-100, and HR-220 electronic integrators. Mass spectra were obtained by using a Consolidated Electrodynamics Corporation Model 21-103C mass spectrometer equipped with a Microtek high temperature inlet and a Varian Vac-Ion pumping system. The spectra were run at ionizing voltages of 9 and 12 eV.

Refractive indices of collected fractions were obtained with a Bausch and Lomb Abbé refractometer at 25°C. Reference samples of heptamethylnonane and isooctane were used for calibration before each series of determinations. Molecular weights were obtained by using a Mechrolab Model 301 vapor-pressure osmometer. Benzene was used as the solvent for all compounds examined. Densities at 25°C were obtained for two collected fractions by using a microcapillary pycnometer calibrated with distilled water.

Procedure

Preparation of Isobutylene Fractions. The isobutylene fractions to be analyzed were prepared by thermally cracking commercial polyisobutylene having a number-average molecular weight of 23,000 in a stirred, round-bottomed flask at about 375°C/1 mm Hg. The product was taken overhead continuously with essentially no reflux or fractionation. The distillate products and traps were combined and distilled to 100°C at 0.3 mm Hg and the overhead fractions discarded. The remaining nonvolatile thermally cracked polyisobutylene, which represented about 35–40% of the total charge, was hydrogenated in a 1-liter stainless steel hydrogenation reactor at 2500 psi hydrogen and 274°C for 6 hr. The catalyst was 0.5% palladium on 4–8 mesh coconut charcoal. The product was then fractionally distilled under vacuum from 40 to 250°C (270–520°C/760 mm Hg). Distillate fractions covering the complete boiling range were then taken for analysis.

Isolation and Identification of Components. The major branched hydrocarbon species of the distillate fractions were separated and isolated into chromatographic fractions of reasonably high purity by temperature-

programmed and isothermal gas chromatography. In most cases, chromatographic fractions representative of a single molecular species of each carbon number were obtained by using the 6-ft and 24-ft SE-54 silicone rubber columns under isothermal conditions ranging from 210 to 280°C. In certain instances, fractions consisting of hydrocarbons having several different carbon numbers were prepared by using the 80-in. \times $\frac{3}{4}$ -in. preparative column. These concentrates were then rechromatographed over the $\frac{1}{4}$ -in. diameter analytical columns and pure chromatographic fractions of single carbon number species collected.

In the separation of the C_{11} and C_{12} hydrocarbon species, a 24-ft SE-54 silicon rubber column was used in series with a 6-ft Apiezon L column and was operated at 120°C. This same combination of columns was used for the separation of the C_{23} and C_{24} hydrocarbon species at 270°C. The purity of all chromatographic fractions was determined utilizing capillary gas chromatography. The 150-ft Ucon capillary column was used for the examination of the C_{11} - C_{21} hydrocarbon species. The purity of the high molecular weight, C_{27} - C_{40} , hydrocarbon species was determined with the 50-ft and 150-ft Apiezon L capillary columns. The carbon numbers of these branched hydrocarbon species were determined by using a combination of (1) relative gas chromatographic retention time data obtained using SE-54 and SE-30 silicone rubber columns, (2) the relative gas chromatographic retention time of a reference branched C_{16} hydrocarbon, (heptamethylnonane), (3) mass spectrometric data, (4) molecular weight data obtained using vapor pressure osmometry and (5) integrated NMR data. The identification of all collected branched hydrocarbons, C_{11} - C_{40} species, was accomplished by NMR spectroscopy by use of 60-MHz, 100-MHz, and 220-MHz spectra obtained in both CCl_4 and C_6D_6 solvents.

Determination of Calculated and Experimental Physical Property Data.

Refractive indices of pure collected fractions of each hydrocarbon species were obtained using a Bausch and Lomb refractometer at 25°C. Calculated refractive indices were then obtained for each carbon number species by using an isomeric variation method and compared with the experimental values. Calculated densities at 25°C were also obtained for each carbon number species using this same method. The calculated densities of the C_{35} and C_{36} hydrocarbons were compared with the experimental values. These were the only species which were collected in sufficient quantities to allow this determination.

RESULTS

The gas chromatogram of the hydrogenated, thermally cracked polyisobutylene before fractionation is shown in Figure 1 and illustrates the complexity of these nonvolatile fluids. The series of peaks observed in this chromatogram represent a homologous series of two different basic species of branched hydrocarbons. One species is symmetrical, has an odd number of carbon atoms, and is terminated with two isopropyl groups. The second

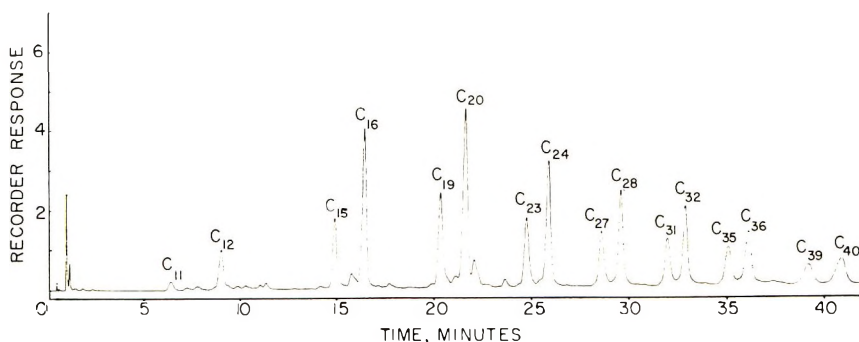


Fig. 1. Gas chromatogram of hydrogenated decomposition products of polyisobutylene.

species is nonsymmetrical, consists of an even number of carbon atoms, and is terminated with an isopropyl group and a tertiary butyl group. The incremental increase of carbon number for each series is due to an additional isobutylene unit in the hydrocarbon chain. It should be noted that no significant amounts of the odd-numbered carbon species which are terminated with two tertiary butyl groups were found to be present in these nonvolatile fractions. The carbon number of each collected component is indicated in the gas chromatogram shown in Figure 1. The presence of much lower concentrations of the C_{11} and C_{12} species relative to the concentrations of higher carbon numbered species is probably due to the loss of a portion of these hydrocarbons to the overhead fractions that were discarded in the first distillation. Purity and molecular weight data obtained for each collected

TABLE I
Purity and Molecular Weight Data for Collected Fractions

| Carbon No. | Purity, % ^a | Molecular weight | | Relative error, % |
|------------|------------------------|------------------|-----------------------|-------------------|
| | | Calculated | Observed ^b | |
| 11 | 99+ | 156.3 | 161 | +3.0 |
| 12 | 97.5 | 170.3 | 177 | +3.9 |
| 15 | 99+ | 212.4 | 214 | +0.7 |
| 16 | 99+ | 226.4 | 219 | -2.8 |
| 19 | 99+ | 268.5 | 271 | +0.9 |
| 20 | 99.0 | 282.5 | 275 | -2.7 |
| 23 | 96.7 | 324.6 | 322 | -0.8 |
| 24 | 96.9 | 338.6 | 344 | +1.4 |
| 27 | 99+ | 380.7 | 377 | -1.0 |
| 28 | 99+ | 394.7 | 397 | +0.6 |
| 31 | 98.8 | 436.8 | 426 | -2.5 |
| 32 | 98.7 | 450.8 | 444 | -1.5 |
| 35 | 97.3 | 492.9 | 490 | -0.6 |
| 36 | 99+ | 507.0 | 513 | +1.2 |
| 39 | 99+ | 549.0 | 544 | -0.9 |
| 40 | 99+ | 563.1 | 570 | +1.2 |

^a Capillary gas chromatography.

^b Vapor pressure osmometry.

hydrocarbon species, C_{11} – C_{40} , are given in Table I. The purity of these fractions varied from 96.7 to 99+ % and the calculated molecular weight of each carbon number species was in good agreement with the experimental molecular weight obtained using vapor pressure osmometry.

The identification of these branched hydrocarbons as determined by NMR spectroscopy is indicated by the structural assignments I–XVI. In these formulas maximally crowded geminal dimethyl groups are enclosed in brackets. The observed resonance positions in CCl_4 and assignments for the methylene and methyl protons of this series of hydrocarbons are summarized in Tables II and III. Methyl and methylene protons of the same

TABLE II
Summary of Methylene Resonance Positions in CCl_4

| CH_2 type | Molecular structure ^a | Designation | Resonance position, ppm | Multiplet ^b |
|-------------------|---|----------------|-------------------------|------------------------|
| Uncrowded | $\begin{array}{c} CH_3 \\ \\ -CH_2-C-H \\ \\ CH_3 \end{array}$ | a | 1.13, 1.21 | d |
| Slightly crowded | $\begin{array}{c} CH_3 \quad CH_3 \\ \quad \\ -C-CH_2-C- \\ \quad \\ CH_3 \quad CH_3 \end{array}$ | b ^c | 1.25 | s |
| Crowded | $\begin{array}{c} CH_3 \quad \left[\begin{array}{c} CH_3 \\ \\ -C- \\ \\ CH_3 \end{array} \right] \\ \quad \\ -C-CH_2- \\ \quad \\ CH_3 \quad \left[\begin{array}{c} CH_3 \\ \\ -C- \\ \\ CH_3 \end{array} \right] \end{array}$ | e,d | 1.33 | s |
| Maximally crowded | $\left[\begin{array}{c} CH_3 \\ \\ -C- \\ \\ CH_3 \end{array} \right] CH_2 \left[\begin{array}{c} CH_3 \\ \\ -C- \\ \\ CH_3 \end{array} \right]$ | e,f,g | 1.42 | s |

^a $\left[\begin{array}{c} CH \\ | \\ -C- \\ | \\ CH_3 \end{array} \right]$ = maximally crowded geminal methyl group.

^b d = doublet; s = singlet.

^c For C_{12} and C_{15} species only.

type and having the same degree of steric hinderance and crowding were found to have essentially the same chemical shifts in CCl_4 for each individual hydrocarbon species regardless of carbon number. Differentiation and assignment of a number of the maximally crowded methylene and maximally crowded geminal dimethyl groups in these compounds was possible from 100-MHz spectra obtained using C_6D_6 solvent. The observed proton resonance positions for these groups in C_6D_6 and their assignments in the C_{19} – C_{40} hydrocarbon species are summarized in Table IV. The 100-MHz spectra of the C_{20} , C_{24} , C_{28} , C_{35} , and C_{36} hydrocarbon species are given in Figures 2 through 6, respectively. One 220-MHz scan of the C_{10} hydrocar-

TABLE III
 Summary of Methyl Resonance Positions in CCl_4

| CH_3 type | Molecular structure | Designation | Resonance position, ppm | Multiplet ^a |
|---------------------------|---|----------------|-------------------------|------------------------|
| Isopropyl | $\begin{array}{c} \text{CH}_3 \\ \\ \text{H}-\text{C} \\ \\ \text{CH}_3 \end{array}$ | h | 0.88, 0.98 | d |
| Slightly crowded geminal | $\begin{array}{c} \text{CH}_3 \\ \\ \text{C} \\ \\ \text{CH}_3 \end{array}$ | i ^b | 0.87 | s |
| Crowded geminal | $\begin{array}{c} \text{CH}_3 \\ \\ \text{CH}_3 \\ \\ \text{C} \\ \\ \text{CH}_3 \end{array}$ | j | 0.98-1.0 | s |
| Maximally crowded geminal | $\left[\begin{array}{c} \text{CH}_3 \\ \\ \text{C} \\ \\ \text{CH}_3 \end{array} \right]$ | k,l,m,n | 1.08-1.10 | s |
| <i>tert</i> -Butyl | $\begin{array}{c} \text{CH}_3 \\ \\ \text{H}_3\text{C}-\text{C} \\ \\ \text{CH}_3 \end{array}$ | o | 0.98-1.0 | s |

^a d = doublet; s = singlet.

^b For C_{11} species only; uncrowded geminal methyls occur at 48.5-50 Hz (0.81-0.83 ppm).³

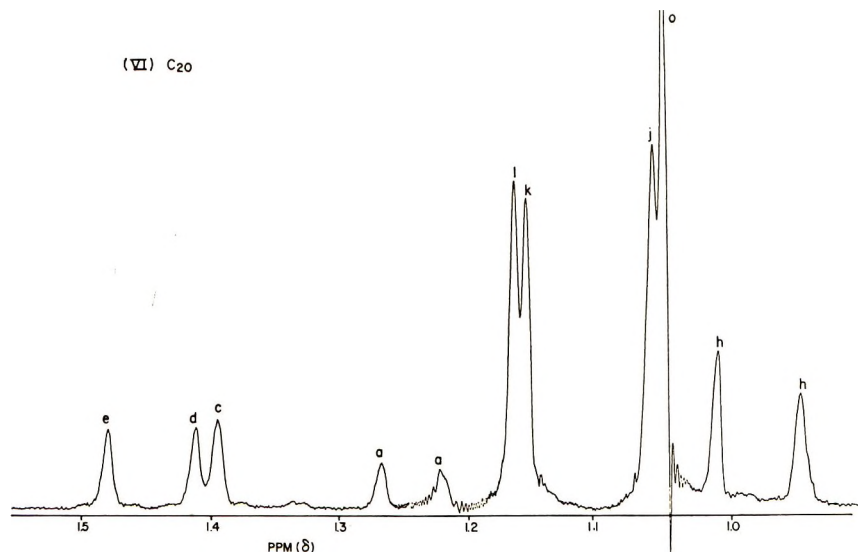


Fig. 2. NMR spectrum of C_{20} (VI) in C_6D_6 solution at 100 MHz.

TABLE IV
Summary of Resonance Positions for Crowded Methylene
and Geminal Methyl Groups in C_6D_6

| Compound | Resonance positions, ppm ^a | | | | | | | | | |
|-----------------|---------------------------------------|------|------|-------------------------|------|----------------------------------|------|------|-------------------|---|
| | Maximally crowded CH_2 | | | Crowded terminal CH_2 | | Maximally crowded geminal CH_3 | | | | |
| | e | f | g | e | d | k | l | m | n | |
| C_{19}^b (V) | — | — | — | — | 1.39 | — | 1.14 | — | — | — |
| C_{20} (VI) | 1.48 | — | — | 1.39 | 1.41 | 1.15 | 1.16 | — | — | — |
| C_{23} (VII) | — | 1.52 | — | — | 1.43 | — | 1.18 | — | — | — |
| C_{24} (VIII) | 1.52 | 1.53 | — | 1.41 | 1.43 | 1.17 | 1.18 | 1.20 | — | — |
| C_{27} (IX) | — | 1.52 | — | — | 1.43 | — | 1.18 | 1.20 | — | — |
| C_{28} (X) | 1.52 | 1.54 | 1.55 | 1.41 | 1.44 | 1.17 | 1.19 | 1.20 | 1.21 | — |
| C_{31} (XI) | — | 1.54 | 1.56 | — | 1.44 | — | 1.20 | — | 1.22 | — |
| C_{32} (XII) | 1.53 | 1.54 | 1.56 | 1.42 | 1.44 | 1.17 | 1.20 | 1.21 | 1.23 | — |
| C_{35} (XIII) | — | 1.55 | 1.57 | — | 1.45 | — | 1.20 | — | 1.23 | — |
| C_{36} (XIV) | 1.53 | 1.55 | 1.57 | 1.42 | 1.45 | 1.18 | 1.20 | 1.22 | 1.23 ^c | — |
| C_{39} (XV) | — | 1.56 | 1.58 | — | 1.45 | — | 1.21 | — | 1.24 ^c | — |
| C_{40} (XVI) | 1.54 | 1.56 | 1.58 | 1.42 | 1.45 | 1.18 | 1.21 | 1.22 | 1.24 ^c | — |

and 1.57(g')^d

^a Measured from 100-MHz spectra with TMS as internal standard.

^b Run at 60-MHz only.

^c Broad signal.

^d Resolved in 220-MHz scan only.

Δ values [$\Delta(\text{ppm}) = \delta CCl_4 - \delta C_6D_6$] for terminally and centrally located protons. Table V summarizes these results by showing the solvent shift data obtained from the 60-MHz spectra of the C_{11} - C_{10} hydrocarbon species in these two solvents.

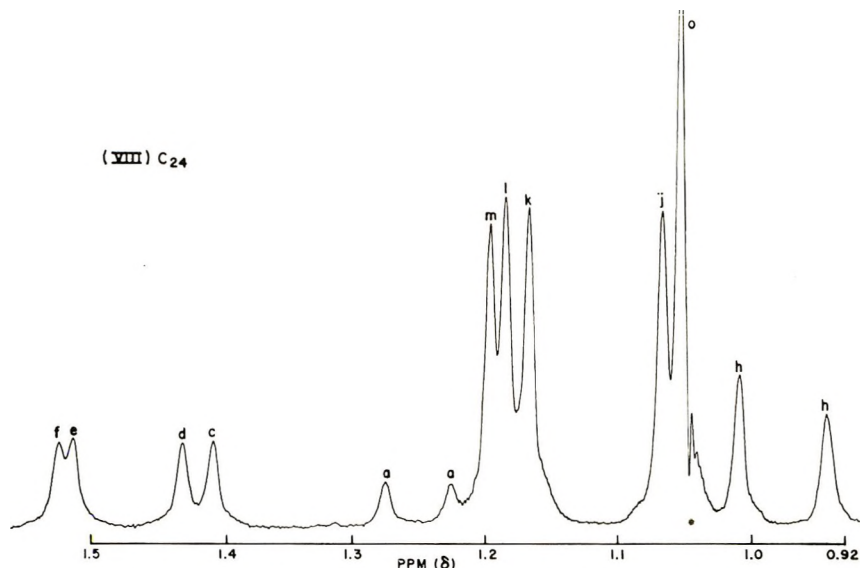


Fig. 3. NMR spectrum of C_{24} (VIII) in C_6D_6 solution at 100 MHz.

TABLE V
Solvent Shifts: $\Delta = \delta(\text{CCl}_4) - \delta(\text{C}_6\text{D}_6)$

| Carbon No. | Δ , ppm ^a | | | |
|-------------------|-----------------------------------|---|------------------------------------|-----------------------------------|
| | Maximally crowded CH ₂ | Maximally crowded geminal CH ₃ | (CH ₃) ₂ CH | (CH ₃) ₃ C |
| 11 | — | — | 0 | — |
| 12 | — | — | 0 | 0 |
| 16 ^b | — | -0.02 | -0.02 | -0.02 |
| 19 | — | -0.04 | -0.02 | — |
| 20 | -0.06 | -0.06 | -0.03 | -0.04 |
| 23 | -0.10 | -0.08 | -0.04 | — |
| 24 | -0.10 | -0.10 | -0.04 | -0.05 |
| 27 | -0.11 | -0.10 | -0.04 | — |
| 28 | -0.13 | -0.11 | -0.04 | -0.05 |
| 31 | -0.14 | -0.12 | -0.04 | — |
| 32 | -0.14 | -0.13 | -0.04 | -0.05 |
| 35 | -0.15 | -0.13 | -0.04 | — |
| 36 | -0.15 | -0.13 | -0.04 | -0.06 |
| 39 | -0.16 | -0.14 to -0.15 ^c | -0.04 | — |
| 40 | -0.16 | -0.14 to -0.15 ^c | -0.04 | -0.06 |
| 1800 ^d | -0.18 | -0.18 | — | — |

^a 0.1-0.3M solutions.

^b No appreciable solvent shift observed.

^c Broad peak.

^d Polyisobutylene; carbon no. based on number-average molecular weight.

In an attempt to show the effects of various aromatic solvents on these hydrocarbons, the chemical shifts of the maximally crowded methylene protons were determined for a mixture of C₃₁-C₃₆ species in a variety of substituted benzenes and in pyridine. The data suggested that the aromatic-

(X) C₂₈

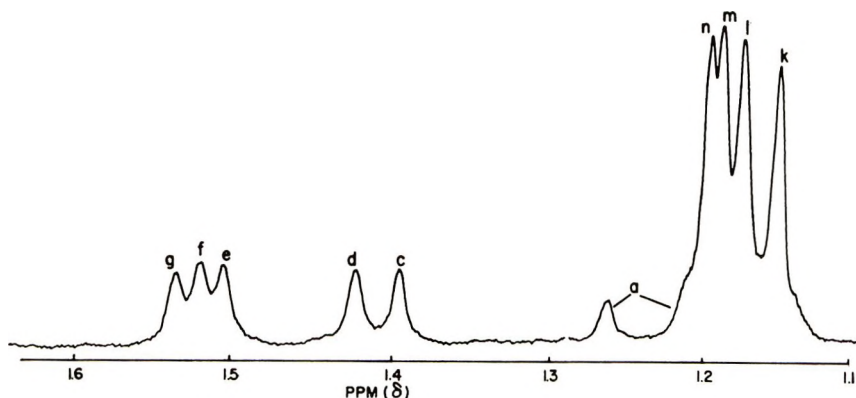


Fig. 4. NMR spectrum of C₂₈ (X) in C₆D₆ solution at 100 MHz.

TABLE VI
Physical Property Data

| Carbon No. | Refractive index RI | | Δ RI (Calc.-obs.) | Calculated ^b density (25°), g/cc |
|------------|-----------------------------------|--------------------|-----------------------------|---|
| | Calculated ^a (25°C) | Observed (25°C) | | |
| 11 | 1.4143 | 1.4165 | -0.0022 | 0.7375 |
| 12 | 1.4254 | 1.4257 | -0.0003 | 0.7561 |
| 15 | 1.4380 | 1.4380 | — | 0.7816 |
| 16 | 1.4460 | 1.4441 | +0.0019 | 0.7942 |
| 19 | 1.4533 | 1.4530 | +0.0003 | 0.8092 |
| 20 | 1.4592 | 1.4564 | +0.0028 | 0.8185 |
| 23 | 1.4636 | 1.4615 | +0.0021 | 0.8282 |
| 24 | 1.4684 | 1.4648 | +0.0036 | 0.8355 |
| 27 | 1.4713 | 1.4679 | +0.0034 | 0.8419 |
| 28 | 1.4753 | 1.4704 | +0.0049 | 0.8479 |
| 31 | 1.4772 | 1.4725 | +0.0047 | 0.8525 |
| 32 | 1.4805 | 1.4750 | +0.0055 | 0.8575 |
| 35 | 1.4818 | 1.4768 | +0.0050 | 0.8607 ^c |
| 36 | 1.4849 | 1.4780 | +0.0069 | 0.8651 ^d |
| 39 | 1.4856 | 1.4798 | +0.0058 | 0.8674 |
| 40 | 1.4881 | 1.4815 | +0.0066 | 0.8712 |

^a See Greenshields and Rossini.⁴

^b From calculated value of molal volume at 25°C.

^c Observed value = 0.8584 g/cc.

^d Observed value = 0.8631 g/cc.

induced solvent shifts for these hydrocarbon species are influenced by the diamagnetic anisotropy of the aromatic solvent used.

Table VI gives the refractive indices determined at 25°C for the C₁₁-C₄₀ hydrocarbon species. These values are compared with the calculated

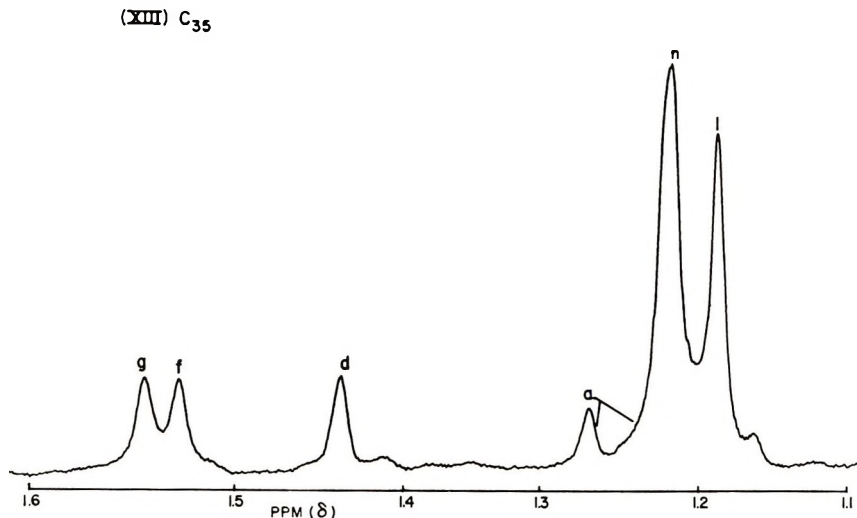


Fig. 5. NMR spectrum of C₃₅ (XIII) in C₆D₆ solution at 100 MHz.

values obtained for these compounds using the isomeric variation method of Greenshields and Rossini.⁴ The difference between the calculated and experimental refractive indices was found to increase with increasing carbon number. This table also includes density values which were obtained from

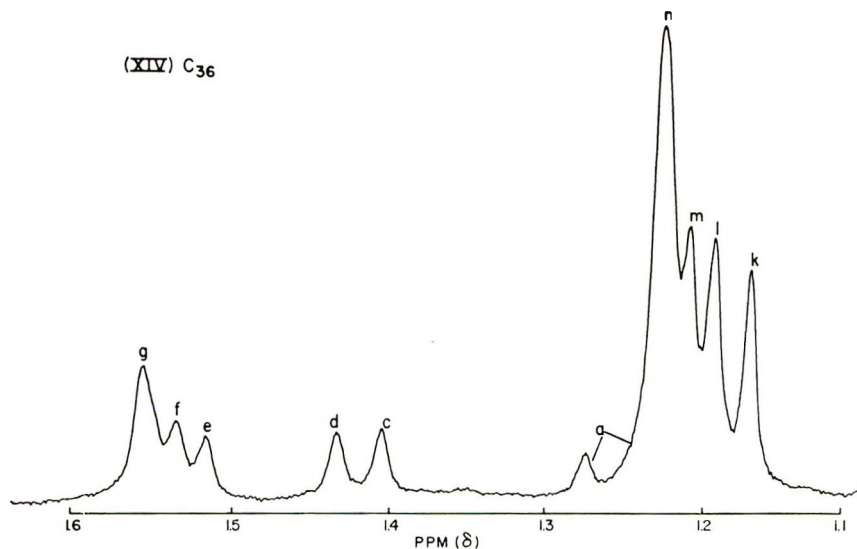


Fig. 6. NMR spectrum of C₃₆ (XIV) in C₆D₆ solution at 100 MHz.

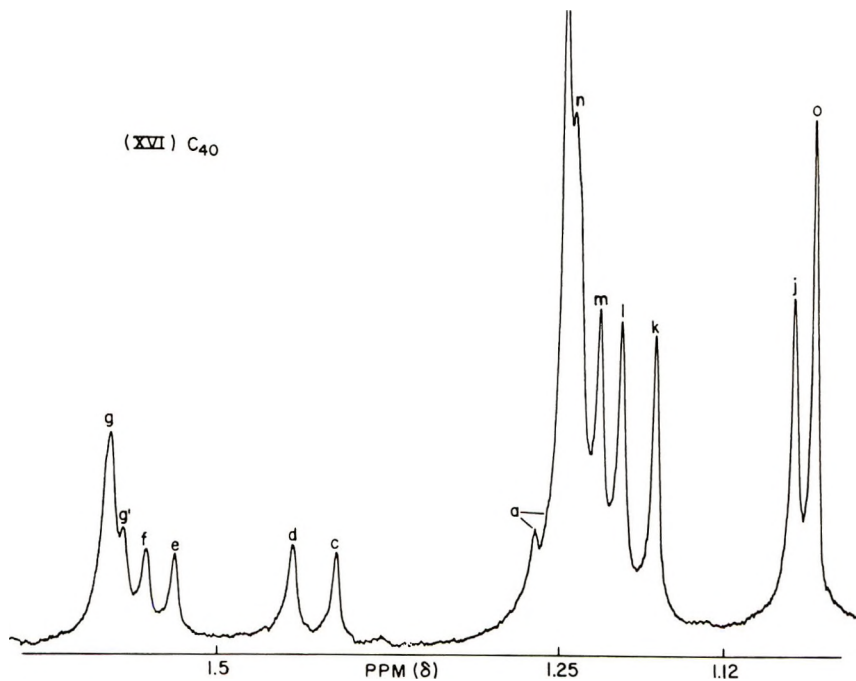


Fig. 7. NMR spectrum of C₄₀ (XVI) in C₆D₆ solution at 220 MHz.

the calculated molal volumes⁴ (25°C) of these hydrocarbon species and compares the calculated and experimental density values for two hydrocarbons, the C₃₅ and C₃₆ species. Positive deviations between calculated and observed density values were found for these two hydrocarbon species.

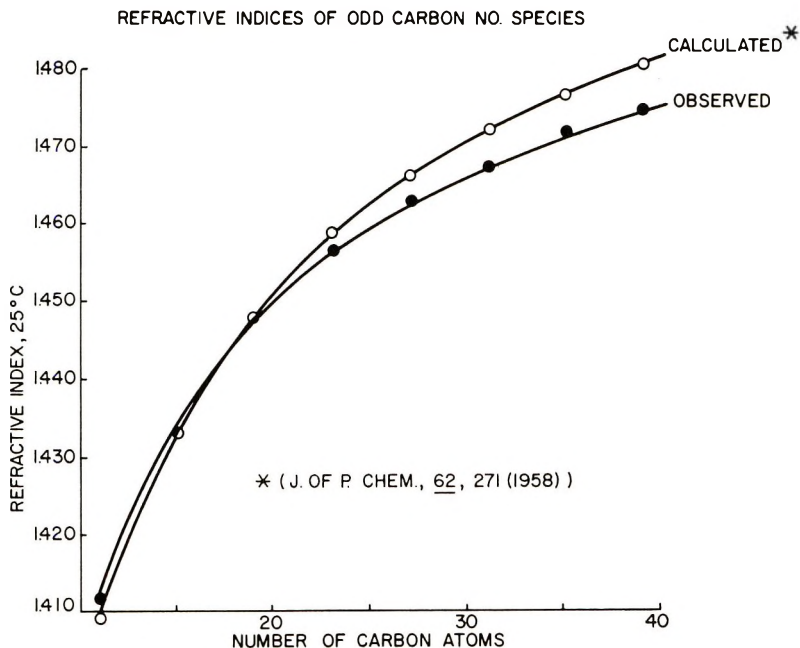


Fig. 8. Calculated and observed RI vs. carbon number.

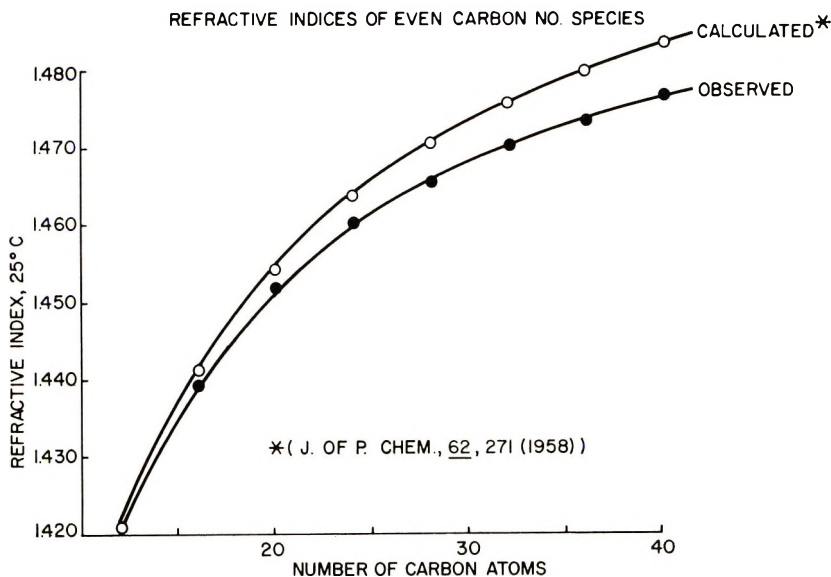


Fig. 9. Calculated and observed RI vs. carbon number.

Separate plots of the calculated and observed refractive indices versus the number of carbon atoms are given for both the odd-numbered carbon species and the even-numbered carbon species in Figures 8 and 9, respectively.

DISCUSSION

Nuclear Magnetic Resonance Spectra

The branched hydrocarbon species identified in this investigation are characterized by sterically hindered methylene and geminal methyl groups. The degree of steric hindrance can be considered in terms of the relative degree of "crowding" experienced by the individual methylene and methyl protons. In the crowding of methylene and geminal methyl protons there are two extremes: (1) uncrowded protons of methylenes and of isolated, internal geminal methyls in a branched chain³ and (2) maximally crowded protons of methylenes and geminal methyls in a polyisobutylene chain.^{3,5} Methylene and geminal methyl groups having proton crowding of types (1) and (2) occur in these hydrocarbon species with the exception of uncrowded geminal methyl groups. In addition, methylene and geminal methyl groups having intermediate degrees of proton crowding occur and are listed in Tables II and III. This crowding effect, although somewhat less pronounced in the lower carbon number species, becomes significantly greater with an increase in the carbon chain. As shown by Edwards and Chamberlain,⁵ and also indicated by Fisher-Hirschfelder-Taylor and Dreiding models of these structures, the introduction of a methylene between two internal geminal methyl groups or between an internal geminal methyl and a *tert*-butyl group (α to each group) causes significant bending of the hydrocarbon chain. This bending results in much greater crowding and steric hindrance of the various protons which in turn restricts free rotation of the individual methylene and geminal methyl groups. Resulting changes in anisotropy cause a downfield chemical shift of their proton resonance signals. This shift can be attributed to van der Waals repulsions of hydrogen nuclei⁶ and is influenced by the relative degree of crowding experienced by the individual methylene and methyl protons.

Edwards and Chamberlain⁵ and Bartz and Chamberlain³ noted that the lower limit of this downfield shift in branched paraffins (CCl_4 solutions) is 66 Hz (1.10 ppm) for internal geminal methyls and 85 Hz (1.42 ppm) for isolated methylenes. This occurs in the polymer, polyisobutylene, where the repeating isobutylene unit provides maximum crowding of both the geminal methyl and the isolated methylene groups. In this investigation, we have found that the lower carbon number, C_{11} , C_{12} , and C_{15} , branched hydrocarbon species have no maximally crowded geminal methyl groups. The single geminal methyl in the C_{11} species (I) has some degree of crowding and as defined in Table III is slightly crowded. This group gives a resonance singlet peak at 0.87 ppm. The resonance is shifted slightly downfield from the resonance singlet of a "normal" uncrowded geminal methyl at 0.81–0.83 ppm.³ The two methylene groups, (a), in this compound give the

predicted doublet resonance signal which corresponds to uncrowded methylenes of a branched chain.³ The C₁₂ and C₁₅ species (II and III, respectively) have geminal methyl groups which are more sterically hindered than the geminal methyl of the C₁₁ species. These methyls, (j), are crowded methyl groups and give a resonance singlet which is shifted to lower field and appears at 0.98 to 1.0 ppm. The C₁₂ species has a crowded *tert*-butyl group as do all of the even-numbered carbon species in this series of compounds. The crowded *tert*-butyl and crowded internal geminal methyls in these molecules cause a downfield shift of the resonance signal of the single methylene, (b), between them (α to each group). Methylene groups having this environment are slightly crowded and are found in only the C₁₂ and C₁₅ hydrocarbon species. Their characteristic resonance which appears at 75 Hz (1.25 ppm) is not observed in the NMR spectra of any of the other branched hydrocarbon species.

The C₁₆ hydrocarbon species (IV) is characterized by having both crowded and maximally crowded geminal methyl groups. This is the first molecular species in this series of compounds which has maximum crowding of a geminal methyl group. A geminal methyl group has maximum crowding when it is (1) adjacent (α) to two isolated methylene groups, and (2) β to two quaternary carbon atoms. This crowding is comparable to the maximum crowding of geminal methyls of polyisobutylene. The resonance signal for the maximally crowded geminal methyl in IV, like the resonance signal for the maximally crowded geminal methyls of polyisobutylene, is shifted downfield and appears at 65–66 Hz (1.08–1.10 ppm). The two isolated (uncoupled) methylenes, (c) and (d), in this molecule (referred to as the terminal isolated methylenes in the longer carbon chain species) are both adjacent to a maximally crowded geminal methyl group and are, therefore, more sterically hindered and crowded than the isolated methylenes, (b), of the C₁₂ and C₁₅ species. This increased methyl crowding causes a 5 Hz downfield shift of the methylene resonance to 80 Hz (1.33 ppm), where one single resonance peak is observed for both isolated terminal methylene groups. These methylene groups are crowded methylenes and are found in all of the higher carbon numbered species (C₁₆ and above). This is a new correlation for methylene protons which was not included in the methylene chemical shift data presented for a large number of hydrocarbons by Bartz and Chamberlain.³ Although the single resonance at 1.33 ppm (CCl₄ solution) confirms that these methylenes have essentially the same degree of crowding, the structure of the C₁₆ molecule IV indicates that these two methylene groups have slightly different molecular environments and should, therefore, be magnetically nonequivalent and give two separate proton resonance signals in NMR. The subsequent use of C₆D₆ as the NMR solvent resulted in a slight broadening of this methylene resonance peak suggesting magnetic nonequivalence of these two methylene groups. Subsequent NMR examinations of the higher, even-numbered carbon species (those terminated with both a *tert*-butyl and isopropyl group) in C₆D₆ solvent revealed in every case two distinct, separate signals for the terminal

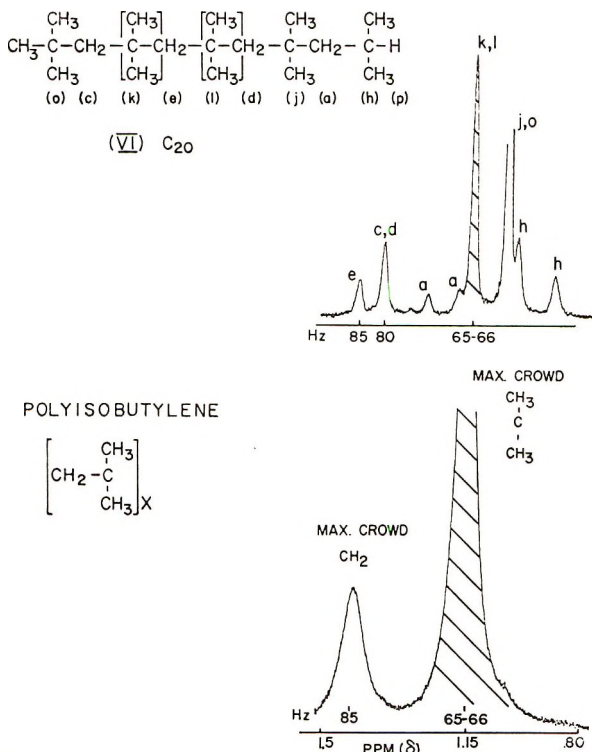
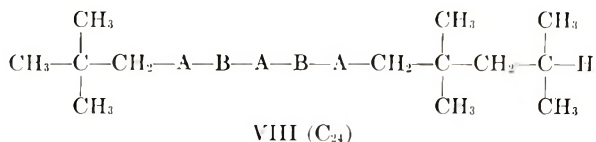
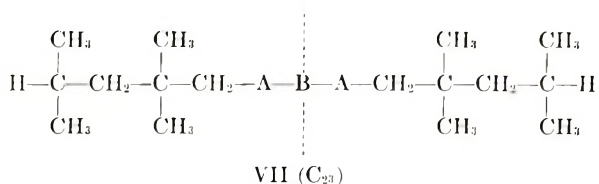


Fig. 10. NMR spectra of C₂₀ (VI) and polyisobutylene in CCl₄ solution at 60 MHz.

isolated methylene groups, (c) and (d), thus confirming their magnetic non-equivalence.

The C₁₉ hydrocarbon species is the only other compound in this series which has a single maximally crowded geminal methyl group. This molecular species, (V), which is symmetrical about the maximally crowded geminal methyl group, has two isolated methylenes, (d), having exactly the same molecular environment. These groups are, therefore, magnetically equivalent. The NMR spectrum of the C₁₉ species in both CCl₄ and C₆D₆ solvents shows, as expected, a single proton resonance peak for these crowded methylenes. All of the odd-numbered carbon species in this series are characterized by this molecular symmetry and have terminal, isolated, crowded methylene groups which are identical. The unsymmetrical C₂₀ hydrocarbon species (VI) is the first species of this hydrocarbon series which has a maximally crowded methylene group. An isolated methylene group has maximum crowding when it is adjacent to, or between, two maximally crowded geminal methyl groups such as in polyisobutylene. Figure 10 compares the NMR spectrum of the C₂₀ species with the NMR spectrum of polyisobutylene. The nonequivalence of the terminal isolated methylene groups, (c) and (d), in this compound as in the C₁₆ species was confirmed using C₆D₆ as the NMR solvent.

All of the subsequent higher carbon numbered hydrocarbons [C_{23} (VII) to C_{40} (XVI)] have an increasing number of maximally crowded geminal methyl and maximally crowded methylene groups, and consist of two basic species: (1) an odd-numbered carbon species terminated with two isopropyl groups and symmetrical about either a maximally crowded geminal methyl group or a maximally crowded methylene group and (2) an even-numbered carbon species terminated with both an isopropyl and *tert*-butyl group and without a center of symmetry. The C_{23} and C_{24} species are illustrated (VII and VIII) where A refers to maximally crowded geminal methyl groups and B corresponds to maximally crowded methylene groups.



Integrated intensities of the observed resonances for each carbon number species were consistent for the theoretical number of maximally crowded methylenes and maximally crowded geminal methyls predicted for each assigned structure. The number of maximally crowded geminal methyl and

TABLE VII
Summary of Maximally Crowded Groups in C_{16} to C_{40} Species

| Carbon No. | No. of $(\text{CH}_3)_2\text{CH}$ | No. of $(\text{CH}_3)_3\text{C}$ | Center of symmetry ^a | No. maximally crowded geminal CH_3 's | No. maximally crowded CH_2 's |
|------------|-----------------------------------|----------------------------------|---------------------------------|--|--|
| 16 | 1 | 1 | none | 1 | 0 |
| 19 | 2 | 0 | gem. CH_3 | 1 | 0 |
| 20 | 1 | 1 | none | 2 | 1 |
| 23 | 2 | 0 | CH_2 | 2 | 1 |
| 24 | 1 | 1 | none | 3 | 2 |
| 27 | 2 | 0 | gem. CH_3 | 3 | 2 |
| 28 | 1 | 1 | none | 4 | 3 |
| 31 | 2 | 0 | CH_2 | 4 | 3 |
| 32 | 1 | 1 | none | 5 | 4 |
| 35 | 2 | 0 | gem. CH_3 | 5 | 4 |
| 36 | 1 | 1 | none | 6 | 5 |
| 39 | 2 | 0 | CH_2 | 6 | 5 |
| 40 | 1 | 1 | none | 7 | 6 |

^a Symmetrical about maximally crowded geminal CH_3 or maximally crowded CH_2 .

maximally crowded methylene groups for the C_{16} to C_{10} species are summarized in Table VII. The number of maximally crowded methylene groups is always one less than the number of maximally crowded geminal methyl groups.

Typical 60-MHz NMR spectra of a symmetrical and unsymmetrical branched hydrocarbon species [C_{23} (VII) and C_{21} (VIII)] in CCl_4 solvent are

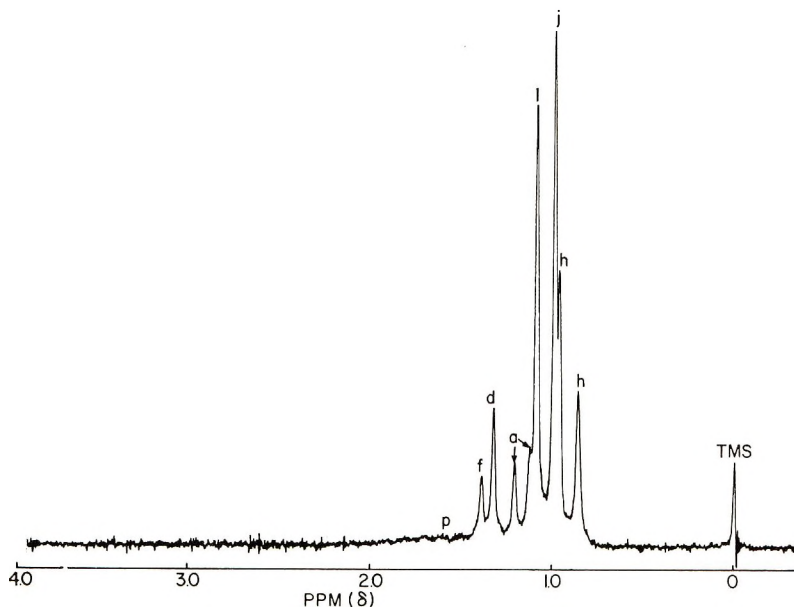


Fig. 11. NMR spectrum of C_{23} (VII) in CCl_4 solution at 60 MHz.

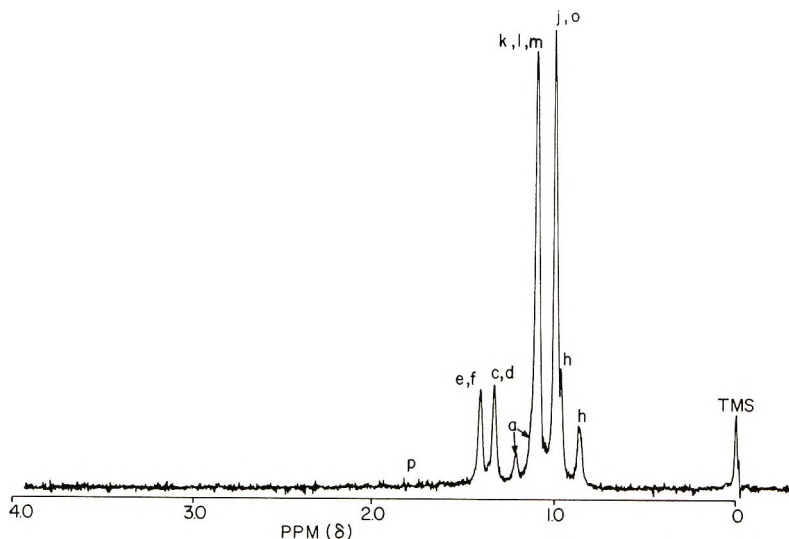


Fig. 12. NMR spectrum of C_{24} (VIII) in CCl_4 solution at 60 MHz.

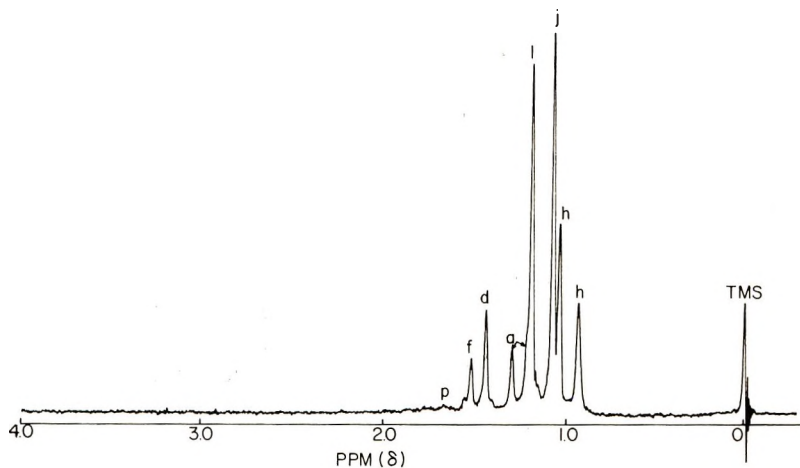


Fig. 13. NMR spectrum of C_{23} (VII) in C_6D_6 solution at 60 MHz.

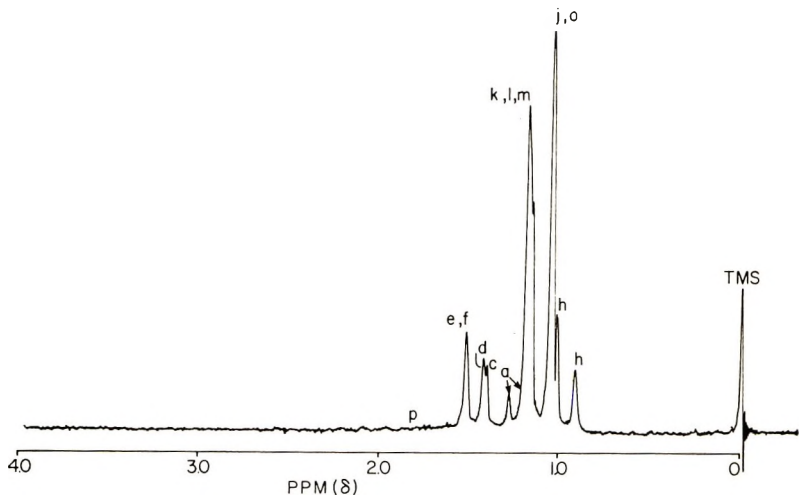
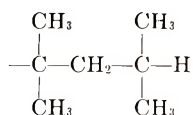


Fig. 14. NMR spectrum of C_{24} (VIII) in C_6D_6 solution at 60 MHz.

shown respectively in Figures 11 and 12 with their proton assignments. It should be noted that the resonance positions of the same proton types are essentially the same in CCl_4 regardless of the species carbon number (see Tables II and III). The NMR spectra of these same carbon number species in C_6D_6 solvent are given respectively in Figures 13 and 14. The C_6D_6 spectrum of the symmetrical C_{23} hydrocarbon shows a proton resonance singlet for the two identical terminal isolated methylenes, (d), at 86 Hz (1.43 ppm) and a single proton peak for the two equivalent maximally crowded geminal methyl groups, (l), at 70 Hz (1.18 ppm). In the C_6D_6 spectrum of the C_{21} species, the nonequivalent terminal methylenes, (c) and (d), are split into an expected doublet peak at 84–85 Hz (1.41–1.43 ppm). In addition,

the maximally crowded geminal methyl groups, (k), (l), and (m), now appear as a distorted singlet, a single peak having two unresolved shoulder peaks. This strongly suggested that these three maximally crowded geminal methyl groups have different molecular environments, in this molecule, i.e., different degrees of crowding. Although the proton resonance signal of the two maximally crowded methylenes, (e) and (f), appear as a singlet in this spectrum (run at a sweep width of 500 Hz), a perceptible amount of broadening was observed for this peak when the spectrum was run at a sweep width of 250 Hz. This peak broadening indicated that these methylene groups were also nonequivalent. NMR spectra of the C_{27} – C_{40} hydrocarbon species run at 60-MHz and in C_6D_6 solvent provided additional data which suggested the possibility of differentiating between maximally crowded geminal methyl groups and between maximally crowded methylene groups by means of benzene-induced solvent shifts. The data implied that maximally crowded geminal methyl and maximally crowded methylene groups which have varying degrees of crowding are not identical and have different chemical shifts in an anisotropic solvent such as C_6D_6 . The 100-MHz spectra of the C_{20} , C_{24} , C_{28} , C_{35} , and C_{36} hydrocarbon species in Figures 2–6, confirm the magnetic nonequivalence of (1) the crowded terminal isolated methylene groups (c) and (d) in the nonsymmetrical species and (2) the maximally crowded geminal methyl and maximally crowded methylene groups which have different degrees of crowding in both the nonsymmetrical and symmetrical species. As indicated previously, a summary of these proton resonance positions in C_6D_6 for the C_{19} – C_{40} hydrocarbon species is given in Table IV.

In the nonsymmetrical, even-numbered carbon species, relatively less proton crowding occurs in the carbon chain on the *tert*-butyl end of the molecule than on the end terminated with the isopropyl group; i.e., the dimethylpentyl group:



provides more molecular crowding than the *tert*-butyl group. Evidence for this are the facts that (1) the proton resonance signal of the terminal crowded methylene group (c) is upfield from the proton signal of the crowded methylene group (d) (compare the NMR spectra of the C_{35} and C_{36} species in Figs. 5 and 6, respectively), (2) the proton resonance signal of the maximally crowded geminal methyl group (k) is upfield from the proton signal of the maximally crowded geminal methyl group, (l) (see Fig. 2), (3) the proton resonance signal of the maximally crowded methylene group (e) is upfield from the resonance signal of the maximally crowded methylene group (f) (see Figs. 3 and 4), and (4) the resonance signal of the crowded *tert*-butyl group (o) appears at slightly higher field than the corresponding signal of the crowded internal geminal methyl group, (j) (see Figs. 2 and 3).

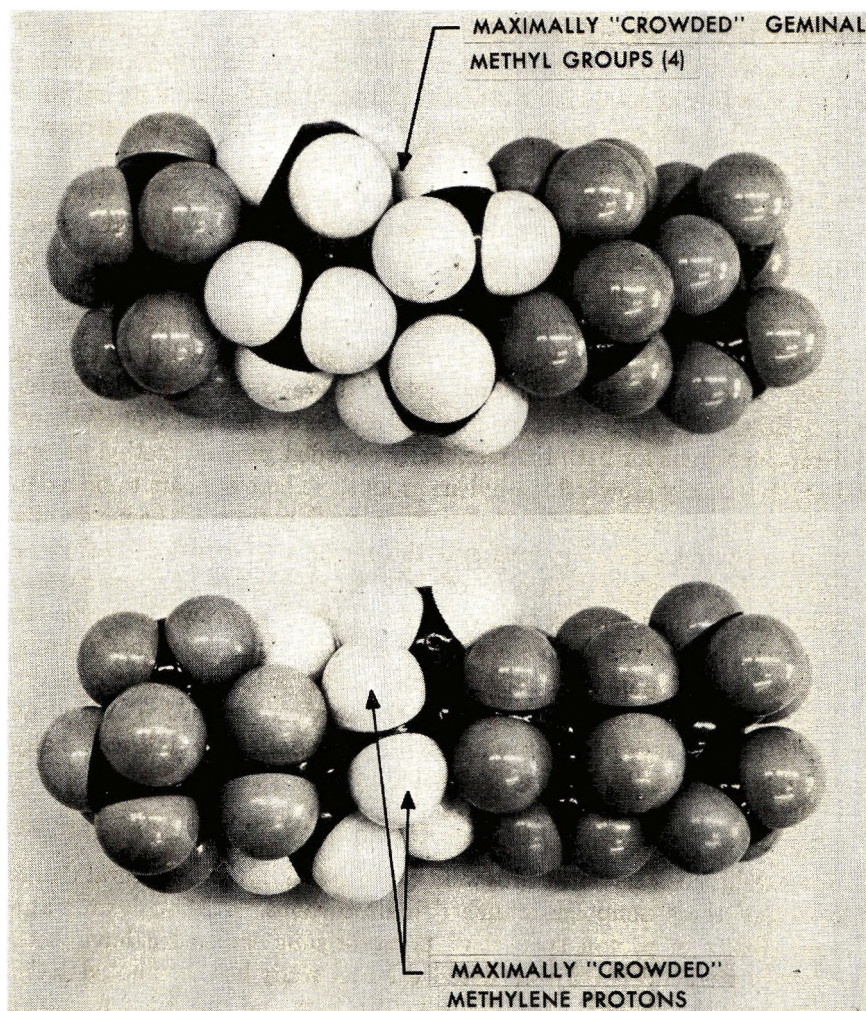


Fig. 15. Fisher-Hirschfelder-Taylor model of C_{20} (VI).

It should be noted that, although these last two groups are not of the same type, their relative field position appears to be related to the degree of molecular crowding for the individual methyl protons. Fisher-Hirschfelder-Taylor models of these hydrocarbon species also suggest that the side of the molecule having the *tert*-butyl group is the least crowded. Figure 15 shows one such model of the C_{20} species which indicates that these compounds are very rigid, sausage-shaped molecules having their geminal methyls oriented on one side of the chain and their methylene groups on the other. The C_{20} model gives additional evidence for extreme crowding of the geminal methyl and methylene groups in these structures. This crowding severely hinders rotation of all of the groups involved with the exception of the terminal isopropyl and tertiary butyl groups which also are hindered, but to a lesser degree. The difficulty encountered in the construction of

these models is also suggestive of significant molecular strain. Examination of the structures of the higher carbon numbered species clearly shows an increased crowding effect due to the additional number of maximally crowded geminal methyl and maximally crowded methylene groups in the center of the hydrocarbon chain. The increased crowding experienced by these groups causes a further downfield shift of their resonance peaks with the most crowded groups occurring at the lowest field positions of their respective geminal methyl and methylene categories. The 100-MHz spectrum of the C_{36} species which is shown in Figure 6 illustrates this by showing four separate proton signals for the maximally crowded geminal methyl groups and three separate proton signals for the maximally crowded methylene groups. In each category, the most crowded group occurs at the lowest field position. The 220-MHz spectrum of the C_{10} species in Figure 7 shows four proton signals for both the maximally crowded geminal methyl groups and the maximally crowded methylene groups. There appears to be a distinct similarity between the proton resonance peak pattern of the maximally crowded geminal methyl groups and the maximally crowded methylene groups in this spectrum. In each of these NMR regions of these spectra (Figs. 6 and 7), the proton resonance peaks of the most crowded groups are not completely resolved from one another and appear as broadened signals. Increased resolution of the 220-MHz scan results in the appearance of the proton signal which has been assigned to the maximally crowded methylene group (g') and shows partial resolution of the signal due to the maximally crowded geminal methyl groups designated by (n).

Solvent Effects

Benzene-induced solvent shifts were quite useful in the structural determination of these nonpolar branched hydrocarbons. Although aromatic solvent effects in proton spectra of polar organic molecules have been extensively studied,⁷⁻¹⁰ only one detailed NMR study has been noted in the literature which involved aromatic solvent effects and saturated nonpolar hydrocarbons.¹¹ In view of this fact, and since it has been reported that aromatic solvents tend to produce high-field dilution shifts for aliphatic solutes¹² and that benzene has little effect on the position of the angular methyl resonances of nonpolar saturated hydrocarbons such as steroids,¹³ we feel that the solvent effects that have been observed for these hydrocarbon species are particularly interesting. Some of the solvent effects described here are unique in that the solvent change from CCl_4 to C_6D_6 gives widely differing negative Δ values [$\Delta = \delta(CCl_4) - \delta(C_6D_6)$] for terminally and centrally located protons and gives rise to magnetic nonequivalence of isolated methylene and geminal methyl protons which have different degrees of molecular crowding. These values extend over the range -0.02 to -0.15 ppm. The solvent shift data which have been determined for these hydrocarbons are given in Table V and refer to hexadeuteriobenzene rather than benzene solutions. However, since there appears to be no significant isotope effect in aromatic induced solvent shifts,¹⁴ the following

observations which have been derived from these data, will be considered valid for benzene solutions: (1) the solvent shifts (Δ) for all of the protons of the C_{16} to C_{40} species are negative; (2) the magnitude of the solvent-induced shifts increases with carbon number and molecular size; (3) the positions of the proton resonances of the C_{11} , C_{12} , and C_{15} species are barely influenced on changing from CCl_4 to C_6D_6 solvent; and (4) for any given carbon number species (C_{20} and above), the centrally located protons of maximally crowded methylene and geminal methyl groups experience greater solvent shifts than protons of terminal isopropyl and *tert*-butyl groups.

Correlation of the magnitude and sign of Δ values with the molecular size of these hydrocarbons [points (1) and (2) above] is in agreement with previous solvent shift data reported for methyl resonances of saturated cycloparaffins by Winkler and Philipsborn.¹¹ In their work, Δ values toward lower field for alkyl-substituted cycloparaffins were plotted as a function of the length of the carbon chain along the main axis and an approximate linear relationship was found. In our work the carbon chain lengths of the C_{20} – C_{40} species which were approximated by using Dreiding models, taking into account van der Waals radii of hydrogen atoms, were plotted against the Δ values of geminal methyl protons having maximum crowding. The resulting graph proved to be an extension of the graph developed by Winkler and Philipsborn and showed a good linear dependence of solvent shift with molecular size or volume.

The above graphical correlation suggests that the larger molecular species (C_{20} and above) can accommodate on their surfaces a larger number of clustering or solvating benzene molecules. A cumulative solute-solvent interaction would then lead to larger benzene-induced solvent shifts. We can account for the observation in point (3) above by the greater flexibility of the C_{11} , C_{12} , and C_{15} species which would probably lead to a random orientation of these molecules with respect to the benzene solvent. Point (4) can be rationalized in terms of rotational averaging of the terminal isopropyl and *tert*-butyl methyl groups with respect to the solvating benzene molecules. This minimizes solvent effects and results in solvent shifts of comparatively lower magnitude for the terminal methyl protons. On the other hand, the protons of the maximally crowded methylene and geminal methyl groups of the more rigid molecules which experience little rotation and have essentially fixed positions in space, i.e., have stereospecificity with respect to the entire solute molecule, show a constantly increasing induced solvent shift of significant magnitude toward a downfield direction which is over and above that observed for the terminal methyl protons of the same molecule.

The data presented above suggest that there is some preferred mutual orientation of the solvent and solute molecules with the solvent molecule(s) being packed or oriented in a more or less orderly pattern about the solute molecule. In a random approach of benzene solvent molecules, we expect a shift to high field.¹⁵ A possible explanation of this preferred orientation

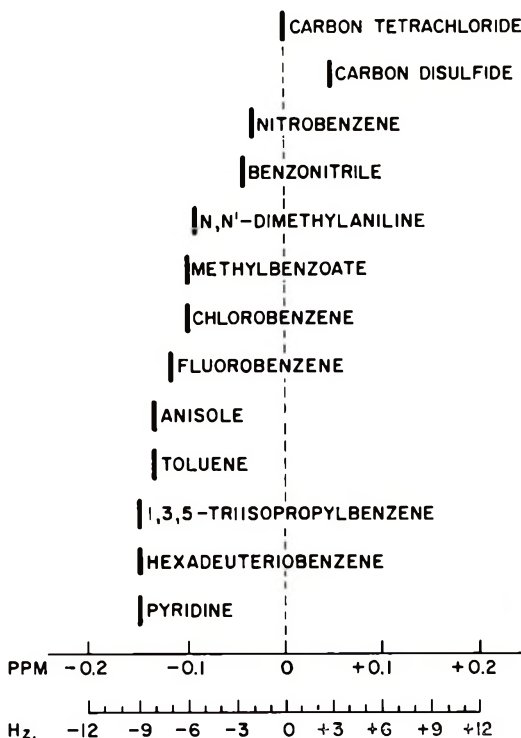


Fig. 16. Maximally crowded methylene proton resonance shifts for C_{31} - C_{36} species.

effect will be presented later. Proton shifts to lower field indicate that the most probable mode of solvation would be the one where the molecular plane of the benzene ring is perpendicular to or steeply inclined with respect to the axis or plane of the hydrocarbon solute such that the solute protons are in the plane (deshielding zone) of the aromatic ring. The fact that there is no net shielding effect seems to preclude the possibility of solute protons being either predominantly above or below the plane of the aromatic ring of neighboring solvent molecules.

The use of other aromatic solvents has produced additional evidence which indicates that the aromatic-induced solvent shifts observed for the protons of these hydrocarbon species are influenced by the magnetic anisotropy of the solvent molecules. Figure 16 shows the chemical shifts observed for the protons of methylene groups having maximum crowding for a mixture of C_{31} - C_{36} species when run in various aromatic solvents (0.15M solutions). The results show that in general the trend of the chemical shifts [$\Delta = \delta(CCl_4) - \delta(\text{solvent})$] appears to follow the electron-donating or withdrawing properties of the substituents on the benzene ring. The solute protons show a greater downfield shift in aromatic solvents substituted with electron-donating groups than in aromatic solvents substituted with electron-withdrawing groups. It is interesting to note that the rod-shaped solvent molecule, CS_2 , which has its largest diamagnetic susceptibility along

the axis of the rod, was the only solvent investigated that produced a net shielding effect on these hydrocarbon protons.

From the various solvent shift data obtained (Fig. 16), it is obvious that there is no correlation between the magnitude of the induced chemical shifts and the dielectric constant of the various solvents employed.¹⁶ In mixed solvent systems it was determined that the chemical shift differences were dependent on the mole fraction of C_6D_6 in CCl_4 . This behavior was also noted for other solvents shown in Figure 16. The concentration of the hydrocarbon solute was not found to be of great importance. At lower concentrations of solute (0.03–0.1*M*) in both CCl_4 and C_6D_6 solvents, the positions of the methylene and methyl proton resonance remained essentially constant.

For polar solutes, benzene-induced solvent shifts have been widely interpreted in terms of local dipole-induced dipole interactions resulting in a preferred mutual orientation of solute and solvent molecules, with shifts then arising due to the anisotropy of benzene.^{7–10} Wilson et al.,⁹ in a generalization of anisotropy shifts in benzene, have indicated that protons lying in regions of high electron density will be deshielded while those in regions of low electron density will be shielded.

A possible interpretation of stereospecific solvation by benzene of these species is one which is based on the unique nature of these hydrocarbon molecules. These hydrocarbon species, as previously described are characterized by extremely crowded geminal methyl and methylene groups. It is expected that the van der Waals repulsions occurring in the maximally crowded groups result in the creation of dipoles such that the "end-on" approach of benzene is the preferred one. It is postulated, therefore, that these hydrocarbons behave much the same way as polar molecules by having protons which are located in regions of high electron density deshielded in benzene. This can be accounted for by the end-on approach of benzene molecules to these high electron density regions (as opposed to a random approach). This is analogous to the end-on approach of benzene molecules to electron-rich areas of dipoles which has previously been described for polar compounds.⁹

In summary, the nature of the solvation by benzene of these hydrocarbon species has been considered. Whether the origin of these solvent-induced shifts can be more adequately described in terms of some other form(s) of interaction must await a more detailed study of this system.

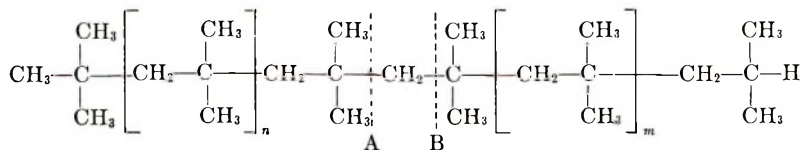
Physical Property Data

During the course of this investigation, a sufficient quantity of purified material (0.025–0.040 cc) was collected for these hydrocarbon species to allow the determination of their refractive indices at 25°C. Information concerning the physical properties of these materials seemed to be of significant value because these hydrocarbons are unique and interesting molecules which are characterized by a high degree of branching and molecular crowding, and in addition have not been previously reported in the litera-

ture. It was also recognized that this homologous series of hydrocarbons would be excellent reference compounds for evaluating empirical equations that have been used to calculate the isomeric variation in the values of physical properties of paraffin hydrocarbons. These equations involved only structural parameters. A comparison of the calculated refractive indices obtained from the calculated values of molal refraction and molal volume by using the method of Greenshields and Rossini⁴ with the experimental refractive indices obtained for these hydrocarbon species indicated certain trends in the deviations between the calculated and observed values. The tabulated data in Table VI and the curves given in Figures 8 and 9 show that the difference between the calculated and observed refractive indices become progressively larger, i.e., shows greater positive deviations, as the species carbon number is increased. Lower values for the observed refractive indices suggest that the higher carbon numbered species, beginning with C_{20} , have increasingly higher molecular volumes than predicted by computation. Since higher molecular volumes would mean lower densities by the relationship $D = M/V$, it follows that the experimental densities for these species should be somewhat lower than the calculated values. Experimental evidence for this is given in Table VI which shows positive deviations of 0.002 g/cc between the calculated and observed densities for two of these hydrocarbons, the C_{35} and C_{36} species. The experimental molal volumes were determined for these two species using the observed density values and were found to be 1.3 and 1.5 cc/mole higher than the calculated molal volumes. These deviations are in excess of the average deviation in molal volume (± 0.62 cc/mole) which was reported for a series of C_{12} - C_{20} hydrocarbons by Greenshields and Rossini.

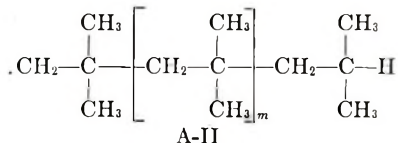
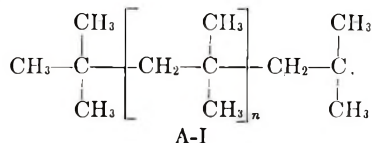
Mechanisms

The formation of the volatile thermal decomposition products of polyisobutylene was examined on the basis of a free-radical mechanism by Tsuchiya and Sumi.² In explaining the formation of these products their postulation of random initiation and radical processes seemed quite reasonable. Our data largely complement those of Tsuchiya and Sumi and generally reinforce their conclusions. While they concentrated on the very volatile products, with no positive identifications of products higher than C_{12} , we were concerned with the intermediate molecular weight species, C_{11} - C_{40} . In examining the formation of these relatively nonvolatile products on the same basis, we need only one additional consideration. Each random chain scission results not only in two types of radicals, but each radical type has two different types of chain ends. (Note that since we hydrogenated our products before analysis, we can draw no conclusions about the termination steps.) There are two possibilities of cleavage modes: A and B:

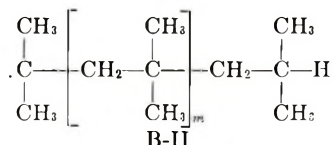
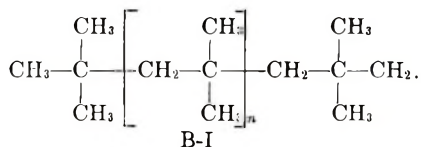


These lead to four types of products:

Type A Cleavage:



Type B Cleavage:



The major products, i.e., the even- and odd-numbered carbon species of this series, are derived respectively from radicals A-I and B-II which are both tertiary radicals. Primary radical A-II could lead to the same products as A-I, so no conclusions can be drawn about its fate. However, products derived from primary radical B-I which would consist of those species terminated with two *tert*-butyl groups are present in only trace amounts. The very minor component peak having a retention time of about 11.5 minutes in the gas chromatogram shown in Figure 1 was isolated and identified as the C₁₃ species of this series, 2,2,4,4,6,6-hexamethylheptane. We conclude, therefore, as did Tsuchiya and Sumi, that the primary radicals undergo different processes than do the tertiary radicals. The primary radicals are probably the source of most of the isobutylene produced in this cracking process. The data of Tsuchiya and Sumi suggest that ultimately these primary radicals eliminate odd-numbered carbon radical species which eventually are analyzed as the volatile products methane, neopentane (C₅), and 2,2,4,4-tetramethylpentane (C₉). In contrast to the very low concentrations of the C₁₃ and above species of this series which are found in the non-volatile fractions, these lower members are major components of the very volatile fractions identified by Tsuchiya and Sumi.

CONCLUSIONS

NMR data combined with benzene-induced solvent shifts have been extremely useful in elucidating the structural composition of the nonvolatile

fluids prepared by thermally cracking polyisobutylene. These fluids, which are adequately described as a mixture of odd- and even-numbered carbon species characterized by repeating isobutylene structures, might well have been expected from the probable mechanism of the reaction. Both type species in this series can arise from successive losses of isobutylene units from the stabilized tertiary radical resulting from the initiating chain cleavage. The proven structure of these oligomer fractions and a knowledge of the NMR correlation data obtained in their characterization will be helpful in determining the composition of the commercially available polyisobutylene fluids. We have found that the oligomers in these fluids do not have the regular repeating structure of the fluids prepared by thermal cracking. A more detailed study of the nature of the commercial fluids is currently in progress and should explain the differences between the physical properties of the two fluids.

We thank the Sun Oil Co. for permission to publish this paper. The authors also acknowledge Messrs. R. E. Bingham and H. C. Williamson for their technical assistance in this work, and thank Dr. L. A. Wilson, Varian Associates, for obtaining the 100- and 200-MHz NMR spectra. The authors are particularly grateful to Dr. W. C. Neikam for helpful discussions and recommendations concerning the solvent effect studies and to Dr. E. J. Rosenbaum who was always available for consultation and contributed important suggestions in the preparation of this paper. Our thanks are also due to Mr. R. W. King, who urged the extension of this work to obtain physical property data and drew our attention to the works of J. B. Greenshields and F. D. Rossini. We are also indebted to Mr. R. J. Bolinski, who kindly undertook the preparative-scale gas-chromatography separations and Mr. G. Myers Jr., who was responsible for the molecular weight determinations.

References

1. R. H. Dyer, paper presented at a Special Session of Insulations Subcommittee (No. 5), Symposium on Polybutene Oils, IEEE Insulated Conductors Committee Meeting, Boston, Mass., November 17, 1964.
2. Y. Tsuchiya and K. Sumi, *J. Polym. Sci. A-1*, **7**, 813 (1969).
3. K. W. Bartz and N. F. Chamberlain, *Anal. Chem.*, **36**, 2151 (1964).
4. J. B. Greenshields and F. D. Rossini, *J. Phys. Chem.*, **62**, 271 (1958).
5. W. R. Edwards and N. F. Chamberlain, *J. Polym. Sci. A*, **1**, 2299 (1963).
6. S. Gordon and B. P. Dailey, *J. Chem. Phys.*, **34**, 1084 (1961).
7. J. Ronayne and D. H. Williams, *Chem. Commun.*, **1966**, No. 20, 712.
8. J. Ronayne and D. H. Williams, *J. Chem. Soc. B*, **1967**, 540.
9. R. G. Wilson, D. E. A. Rivett, and D. H. Williams, *Chem. Ind. (London)*, **1969**, No. 25, 109.
10. T. Ledaal, *Tetrahedron Letters*, **1968**, No. 14, 1683.
11. T. Winkler and W. von Philipsborn, *Helv. Chim. Acta*, **51**, 183 (1968).
12. A. A. Bothner-By and R. E. Glick, *J. Chem. Phys.*, **26**, 1651 (1957).
13. N. S. Bhacca and D. H. Williams, *Tetrahedron Letters*, **1964**, No. 42, 3127.
14. J. Ronayne and D. H. Williams, *J. Chem. Soc. B*, **1967**, 805.
15. J. A. Pople, W. G. Schneider, and H. J. Bernstein, *High Resolution Nuclear Magnetic Resonance* McGraw-Hill, New York, 1959, p. 425.
16. G. M. Whitesides, J. J. Grocki, D. Holtz, H. Steinberg, and J. D. Roberts, *J. Amer. Chem. Soc.*, **87**, 1058 (1965).

Received July 2, 1970

Revised September 25, 1970

Propagation Rate Constant in Cationic Polymerization of Cyclic Dienes. I. Polymerization of Cyclopentadiene with Titanium Tetrachloride-Trichloroacetic Acid

S. KOHJIYA,* Y. IMANISHI, and T. HIGASHIMURA,
Department of Polymer Chemistry, Kyoto University, Kyoto, Japan

Synopsis

Cationic polymerization of cyclopentadiene induced by titanium tetrachloride-trichloroacetic acid was investigated in a toluene solution at -69 to -77°C . All manipulations were handled under vacuum conditions. Time-conversion curves were determined accurately by following the exothermicity of the fast reaction in an adiabatic system. The polymerization kinetics were developed on the basis of a fast initiation reaction and a nonstationary-state concentration (diminishing concentration) of active species, and the propagation rate constant k_2 was determined by substituting either an initial rate of polymerization or a final conversion for the kinetic equations. k_2 for the present system was determined to be 350 l./mole-sec, which is larger than those so far reported for some vinyl monomers in cationic polymerization. The present method can be commonly applied to reactive monomers for the determination of k_2 . The nature of termination reaction is discussed in connection with the determination of k_2 .

INTRODUCTION

For the mechanistic clarification of chemical reactions kinetics is a very useful method; this applies also to the polymerization reactions. In free-radical polymerizations not only the overall kinetics but also the rate constant of elementary reactions have been studied in detail, and the mechanisms of elementary reactions have been discussed further. In the case of anionic polymerization, kinetic studies of living polymer systems have made much contribution to an elucidation of the polymerization mechanism. On the other hand, such general kinetic patterns have not been established in cationic polymerizations, one reason clearly being the paucity of data about rate constants of elementary reactions. However much attention has recently been focused on the measurement of rate constants and some useful conclusions have been obtained.¹ Cationic polymerizations with iodine by Kanoh et al.,² and the polymerization of styrene with sulfuric acid^{3,4} and with perchloric acid⁵ by Pepper et al. are typical examples. In some

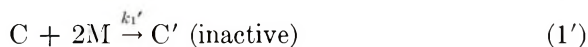
* Present address: Kyoto Institute of Technology, Department of Chemistry, Matsugasaki, Kyoto, Japan.

cases, however, the detailed study presented rather complicated problems.⁶ At any rate, only a few rate constants have been obtained under special conditions. In the case of cationic polymerization catalyzed by Friedel-Crafts halide only a few rate constants have been reported.⁷⁻¹⁰

The present investigation was started to establish a general method for obtaining the propagation rate constant kinetically under widely different conditions. For this purpose the cyclic dienes were found most suitable for investigation. We have been studying cationic polymerization of cyclic dienes.¹¹⁻¹⁶ In copolymerization studies¹²⁻¹⁵ and overall kinetics of polymerizations,¹²⁻¹⁴ cyclic dienes were found to be very reactive in cationic polymerization and to show complicated but interesting kinetic features. Here we chose the system cyclopentadiene (CPD)-titanium tetrachloride (TiCl₄)-trichloroacetic acid (TCA)-toluene because this system showed a very large rate of polymerization and, in particular, nonstationary-state kinetics; hence the propagation rate constant might be determined.¹²⁻¹⁴ To determine the propagation rate constant, the polymerization rate was followed accurately under rigorous conditions by a vacuum technique, and kinetic studies were made.

THEORETICAL

Previously we reported that the kinetic feature of the system CPD-TiCl₄-TCA-toluene by the usual technique¹² (not high vacuum) was explained by nonstationary-state kinetics analogous to that for the polymerization of styrene reported by Pepper et al.^{3,4} In the vacuum system similar elementary reactions may be assumed, that is,



Here eq. (1) is an initiation reaction, eq. (1') represents a kind of catalyst-consuming reaction in which biscyclopentadienyl titanium dichloride is formed from TiCl₄ and CPD.¹² Equation (2) represents a propagation reaction, eqs. (3) and (4) are spontaneous and monomer transfer reactions, respectively; eq. (5) shows unimolecular termination. Since CPD is very nucleophilic and TiCl₄ electrophilic,¹³ they react very rapidly so that the initiation reaction is very fast; that is, $k_1, k_1' \gg k_2, k_3, k_4, k_5$ is reasonably assumed.^{2-5,12} Reactions (1) and (1') are competing and one obtains

$$[P_0^*] = \frac{k_1}{k_1 + k_1' [M_0]} [C_0] \quad (6)$$

where $[C_0]$, $[P_0^*]$, and $[M_0]$ represent the initial concentrations of catalyst, active species, and monomer, respectively. From eqs. (5) and (6)

$$[P_t^*] = [P_0^*]e^{-k_1 t} = \frac{k_1}{k_1 + k_1'[M_0]} [C_0]e^{-k_1 t} \quad (7)$$

where $[P_t^*]$ represents the concentration of active species at time t . Therefore

$$-\frac{d[M]}{dt} = k_2[P_t^*][M_t] = \frac{k_1 k_2}{k_1 + k_1'[M_0]} [C_0][M_t]e^{-k_1 t} \quad (8)$$

For the initial rate of polymerization, we have

$$R_{p_0} = (-d[M]/dt)_{t=0} = \frac{k_1 k_2}{k_1 + k_1'[M_0]} [C_0][M_0] \quad (9)$$

$$[M_0]/R_{p_0} = (1/k_2[C_0]) + (k_1'/k_1 k_2[C_0])[M_0] \quad (10)$$

According to this equation the values k_2 and k_1'/k_1 can be obtained if R_{p_0} is measured at various $[C_0]$ and $[M_0]$. This is one of the two methods to determine the k_2 . As a second approach, integrating eq. (8) yields

$$\begin{aligned} \ln \frac{[M_0]}{[M_t]} &= \frac{k_2}{k_5} \frac{k_1}{k_1 + k_1'[M_0]} [C_0](1 - e^{-k_1 t}) \\ &= \ln([M_0]/[M_\infty])(1 - e^{-k_1 t}) \end{aligned} \quad (11)$$

Here $[M_\infty]$ is a monomer concentration at an infinite time, when the final conversion Y is attained. Equation (11) describes the time course of polymerization and gives the termination rate constant (k_5) by the curve-fitting method.

The final conversion Y can be expressed as

$$\begin{aligned} Y &= 1 - [M_\infty]/[M_0] \\ &= 1 - \exp\left\{-\frac{k_2}{k_5} \frac{k_1}{k_1 + k_1'[M_0]} [C_0]\right\} \end{aligned} \quad (12)$$

This equation is transformed to

$$\ln(1 - Y) = -\frac{k_2}{k_5} \frac{k_1}{k_1 + k_1'[M_0]} [C_0] \quad (13)$$

$$\frac{1}{\ln(1 - Y)} = -\frac{k_5}{k_2 [C_0]} - \frac{k_5 k_1' [M_0]}{k_2 k_1 [C_0]} \quad (14)$$

From this equation, rate constant ratios k_5/k_2 and k_1'/k_1 can be calculated. Reactions (3) and (4) were not taken into account above, because k_3 and k_4 are considered to be sufficiently smaller than k_2 when a polymer is produced. Moreover, even if k_3 and k_4 are taken into account, the discussion is not altered on a qualitative level. At present we cannot evaluate these values quantitatively.

Based on these theoretical considerations the following studies were made.

EXPERIMENTAL

Apparatus

As widely known, ionic polymerization is influenced strongly by a trace of water or other impurities. So, a handling under vacuum conditions is needed for quantitative study. In addition, the polymerization rate of cyclopentadiene is very large.¹²⁻¹⁴ Therefore we chose an adiabatic condition and followed mechanically the temperature rise accompanying the polymerization.

An outline of the apparatus is shown in Figure 1. These lines are principally the same as those developed by Plesch et al.¹⁶ with some modifications. A denotes the solvent purification lines, B is the reaction vessel and C denotes the monomer purification lines. The vacuum lines for catalyst are not shown in the figure but the catalyst vials were prepared also under vacuum.

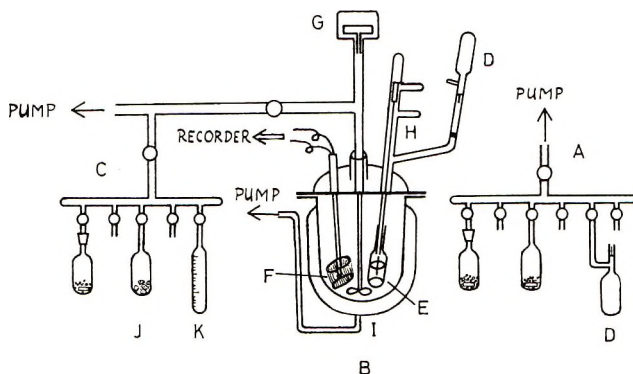


Fig. 1. Apparatus for polymerization (vacuum lines).

The equipment for recording the polymerization rate is as follows: platinum wire resistance, Wheatstone bridge, direct current amplifier, oscillograph (photocorder). The platinum wire is submerged in the polymerization mixture. The change of resistance accompanying the temperature rise of the reaction solution is amplified and put into the direct-writing oscillograph (Photocorder 2901, Yokogawa Electric Works). The polymerization rate was so large (half life = ca. 5-10 sec) that the platinum-resistance thermometer enclosed in a thin glass sheath, which is commercially available, was not sufficient to follow the fast reaction. This sort of thermometer always involves a time lag which cannot be ignored. Also the oscillograph must be used as a recorder instead of the self-balancing Wheatstone bridge to avoid a time lag.⁹

Reagents

Toluene. Toluene was used as a solvent throughout this experiment. Toluene was purified as reported previously.¹²⁻¹⁴ It was further purified on a vacuum line with the use of calcium hydride as a drying reagent (in some cases sodium-potassium alloy was used) and finally distilled into a solvent ampoule D fitted with a break-seal.

Cyclopentadiene (CPD). CPD was obtained as reported previously.¹²⁻¹⁴ It was collected in a flask connected to line C containing calcium hydride. After the similar treatment as toluene, it was distilled onto baked barium oxide (ampoule J) and stored at low temperatures.

Catalyst. Catalyst ampoules were prepared as Plesch did for perchloric acid.¹⁷ Titanium tetrachloride (TiCl_4) was distilled twice under reduced pressure and sealed into ampoules with a break-seal. The dilution of catalyst solution was performed on vacuum line and the dilute solution was divided into small glass vials (ca. 2 ml). Trichloroacetic acid (TCA) subjected to vacuum for about 10 hr, sublimed, and dissolved in toluene. The solution was distributed in vials. Choosing vials so that the molar ratio of TiCl_4 and TCA is nearly unity, the vials for TiCl_4 -TCA solution were prepared in a similar manner. One of the TiCl_4 vials was crushed in cold water and the quantity of TiCl_4 was determined by volumetric analysis.¹⁸ TCA was analyzed similarly, and for a TiCl_4 -TCA vial only the TiCl_4 content was determined.

Polymerizations

The toluene ampoule D was connected to the reaction vessel as shown in Figure 1 and a catalyst vial was placed on the holder E. After evacuating the reaction vessel for about 6 hr, the break-seal of D was broken and toluene was introduced into the reaction vessel. The required amount of CPD was distilled into the graduated ampoule K from ampoule J and further distilled into the reaction vessel. On cooling the reaction vessel with liquid nitrogen to ca. -75°C , the jacket of reaction vessel I was subjected to vacuum and adiabatic conditions established. The polymerization was started by crushing the catalyst ampoule by handling the breaking device H by a magnet under vigorous stirring. When the influence of stirring was investigated, a synchronous motor and an appropriate gear head were used for rotating G. By changing gear head, one could obtain various rotating speeds. The progress of the polymerization was recorded by the oscillograph. After a given time interval, a small amount of methyl alcohol was distilled into the reaction vessel and the reaction was terminated. The contents of the reaction vessel were transferred to a large quantity of methyl alcohol containing antioxidant (4,4'-thiobis-6-*tert*-butyl-3-methylphenol). The recovered polymer was washed with methyl alcohol and dried under reduced pressure. The intrinsic viscosity was measured at 30°C in toluene.

RESULTS

 R_{p0} , Y , and Effect of Stirring

In Figure 2 the conversion-time curves for various initial catalyst concentrations $[C_0]$ are shown. The initial rate of polymerization R_{p0} is very large and when $[C_0]$ is 2.20 mmole/l., the polymerization goes to completion within ca. 10 sec. However, the rate decreases rapidly towards the end, and if $[C_0]$ is below a critical value the polymerization stops before all monomers are consumed. This saturation phenomenon was found previously.¹²⁻¹⁴ In the vacuum system, however, the catalyst concentration required to obtain the same conversion under comparable conditions was only one fourth as much as that with the usual technique. The saturation phenomenon and the presence of the final conversion (Y) clearly indicate the

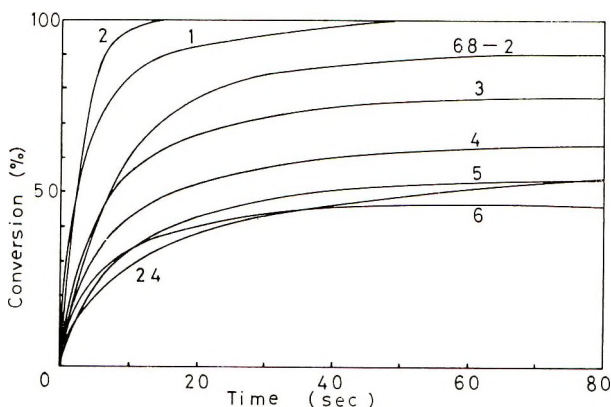


Fig. 2. Conversion-time curves for the polymerization of CPD with $T.Cl_4$ -TCA in toluene at $-75^\circ C$ and $[M_0] = 0.45$ mole/l., and various $[C_0]$; (2) 2.20 mmole/l.; (1) 1.53 mmole/l.; (68-2) 1.17 mmole/l.; (3) 0.940 mmole/l.; (4) 0.624 mmole/l.; (5) 0.469 mmole/l.; (24) 0.455 mmole/l.; (6) 0.362 mmole/l.

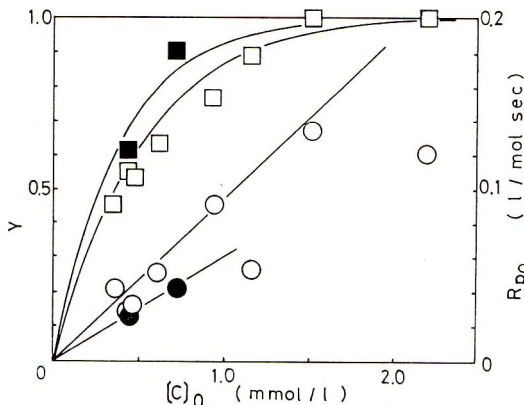


Fig. 3. Relationship between $[C_0]$ and $(\square, \blacksquare) Y$ or $(\circ, \bullet) R_{p0}$: $(\circ, \square) [M_0] = 0.455$ mole/l.; $(\bullet, \blacksquare) [M_0] = 0.185$ mole/l.

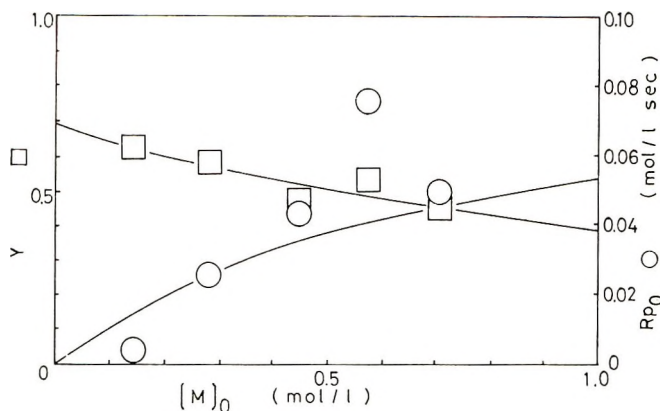


Fig. 4. Relationship between $[M_0]$ and (\square) Y or (\circ) R_{p_0} at $[C_0] = 0.36$ mmole/l.

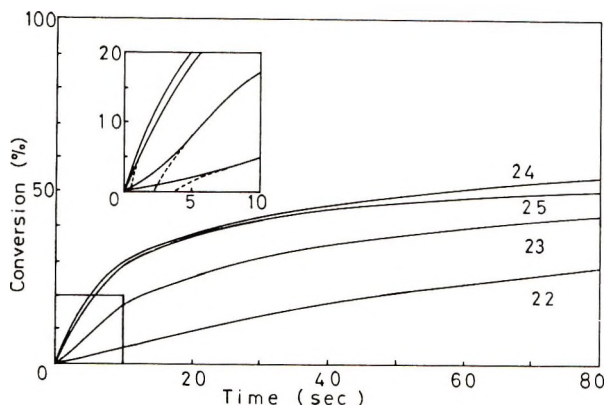


Fig. 5. Influence of stirring speed on polymerization at $[M_0] = 0.45$ mole/l.; $[C_0] = 0.44$ mmole/l.: (22) 100 rpm; (23) 144 rpm; (25) 240 rpm; (24) 360 rpm.

nonstationary-state concentration of active species coupled with an extremely fast initiation reaction.

Figure 3 shows the relationship between $[C_0]$ and Y or R_{p_0} . Both Y and R_{p_0} increase monotonously as $[C_0]$ increases.

At constant $[C_0]$ the initial monomer concentration $[M_0]$ was also changed. In this case the conversion-time curve shown in Figure 2 was also obtained. The influence of $[M_0]$ on Y and R_{p_0} is shown in Figure 4. As was found previously,¹¹ Y decreased as $[M_0]$ increased but R_{p_0} increased with increasing $[M_0]$.

As the polymerization rate is very large in the present system, the stirring of the polymerization mixture is expected to affect the polymerization in some way. In fact the agitation of the system influenced the conversion, as shown in Figure 5. As the rotating speed increased, the rate and the final conversion Y increased. In addition, at a slow stirring speed (below 300 rpm) an induction period of the polymerization exists. The induction pe-

TABLE I
 Polymerization Data of CPD with $TiCl_4$ -TCA in Toluene

| No. | Temp, °C | $[M]_0$, mole/l. | $[C]_0$, mmole/l. | RS, rpm ^a | t_n , sec ^b | R_{p0} , mole/l.-sec | Y | k_p , l./mole-sec | k_{tr} , sec ⁻¹ |
|------|-------------|----------------------|-----------------------|-------------------------|-----------------------------|---------------------------|-------|------------------------|---------------------------------|
| 68-2 | -73 | 0.458 | 1.17 | — | 0 | 0.0539 | 0.902 | 165 | — |
| 1 | -69 | 0.454 | 1.53 | — | 0 | 0.135 | 1.00 | 320 | — |
| 2 | -75 | 0.455 | 2.20 | — | 0.1 | 0.121 | 1.00 | 200 | — |
| 3 | -75 | 0.455 | 0.940 | — | 0 | 0.0937 | 0.769 | 360 | 0.140 |
| 4 | -75 | 0.455 | 0.624 | — | 0 | 0.0515 | 0.633 | 300 | 0.114 |
| 5 | -77 | 0.455 | 0.469 | — | 0 | 0.0327 | 0.538 | 250 | 0.093 |
| 6 | -77 | 0.455 | 0.362 | — | 0 | 0.0440 | 0.462 | 440 | 0.156 |
| 7 | -76 | 0.186 | 0.723 | — | 0 | 0.0449 | 0.912 | 420 | 0.099 |
| 8 | -76 | 0.297 | 0.646 | — | 0.3 | 0.0380 | 0.812 | 280 | 0.076 |
| 9 | -76 | 0.590 | 0.600 | — | 0 | 0.0867 | 0.840 | 450 | 0.082 |
| 12 | -71 | 0.883 | 0.827 | — | 1.0 | 0.122 | 0.899 | 375 | 0.060 |
| 13 | -73 | 0.286 | 0.380 | — | 0 | 0.0252 | 0.585 | 325 | 0.107 |
| 15 | -77 | 0.575 | 0.365 | — | 0 | 0.0783 | 0.533 | 675 | — |
| 16 | -76 | 0.715 | 0.379 | — | 0 | 0.0536 | 0.446 | 400 | 0.128 |
| 17 | -77 | 0.140 | 0.355 | — | 0 | 0.00344 | 0.616 | 83 | — |
| 19 | -77 | 0.185 | 0.446 | — | 0 | 0.0284 | 0.614 | 430 | 0.160 |
| 22 | -75 | 0.457 | 0.440 | 100 | 3.4 | — | 0.330 | — | — |
| 23 | -75 | 0.454 | 0.438 | 144 | 2.4 | — | 0.448 | — | — |
| 24 | -75 | 0.455 | 0.445 | 360 | 0 | 0.0307 | 0.582 | 250 | 0.082 |
| 25 | -76 | 0.458 | 0.451 | 240 | 0.3 | — | 0.502 | — | — |

^a Rotating speed of agitation. For No. 68-2-19, RS was around 400 rpm.

^b Induction period.

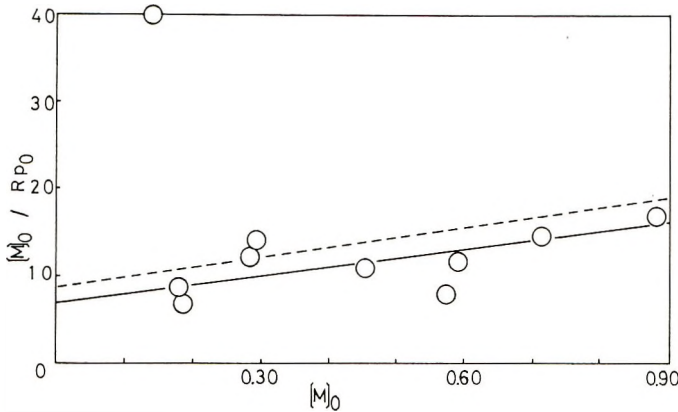


Fig. 6. $[M]_0/R_{p0}$ vs. $[M]_0$ plots according to eq. (10): (—), $k_2 = 410$ l./mole-sec $k_1'/k_1 = 1.43$ l./mole; (- -) $k_2 = 350$ l./mole-sec, $k_1'/k_1 = 1.41$ l./mole.

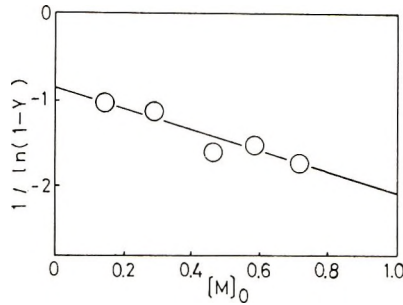


Fig. 7. Plot of $1/\ln(1 - Y)$ vs. $[M]_0$: (—) $k_3/k_2 = 3.0 \times 10^{-4}$ mole/l., $k_1'/k_1 = 1.41$ l./mole.

riod is supposedly the time required for the catalyst solution to diffuse in the polymerization mixture. However, above 300 rpm the induction period disappeared and the curves at 360 rpm and 240 rpm are in close coincidence. Therefore, if agitation speed exceeds 300 rpm, the influence of stirring on polymerization rate is insignificant. The present experiments were all conducted under these conditions.

The temperature rise in these experiments was not so large ($\Delta T = \text{ca. } 10^\circ\text{C}$ at $[M]_0 = 0.454$, 100% conversion). The influence of temperature rise at least on the initial rate can be ignored and the effect on the final conversion might be of minor importance.

All the polymerization data are collected in Table I.

Determination of Rate Constants

By using the kinetics developed in the theoretical section, the experimental results can be analyzed, and the propagation rate constant (k_2) as well as the unimolecular termination rate constant (k_3) can be derived.

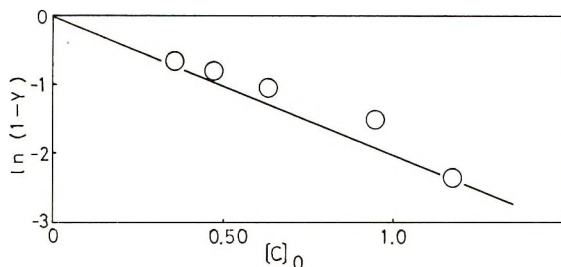


Fig. 8. Plot of $\ln(1 - Y)$ vs. $[C_0]$: (—) calculated from $k_5/k_2 = 3.0 \times 10^{-4}$ mole/l., $k_1'/k_1 = 1.41$ l./mole.

Determination of k_2 . There are two methods for calculating k_2 , i.e., from R_{p_0} only and from both R_{p_0} and Y .

First, according to eq. (10) we obtain k_2 and k_1'/k_1 from the linearity of the $[M_0]/R_{p_0}$ versus $[M_0]$ plot. In Figure 6 the plot of $[M_0]/R_{p_0}$ versus $[M_0]$ is shown.

The R_{p_0} values observed at various $[M_0]$ and $[C_0]$ were converted into the values at $[C_0] = 0.35$ mmole/l. according to eq. (9) and plotted in Figure 6. The reproducibility of R_{p_0} is not very good, and the experimental values in Figure 6 are somewhat scattered, but a straight line can be drawn. From the intersection and the tangent of the line, the following values were obtained.

$$k_2 = 410 \text{ l./mole-sec} \quad (15)$$

$$k_1'/k_1 = 1.43 \text{ l./mole} \quad (16)$$

Secondly, according to eq. (14), the linearity of the $1/\ln(1 - Y)$ versus $[M_0]$ plot gives k_5/k_2 and k_1'/k_1 . Plot of $1/\ln(1 - Y)$ versus $[M_0]$ is shown in Figure 7.

The solid line gives

$$k_5/k_2 = 3.0 \times 10^{-4} \text{ mole/l.} \quad (17)$$

$$k_1'/k_1 = 1.41 \text{ l./mole} \quad (18)$$

In Figure 8 the plot according to eq. (13) is shown. The solid line in the figure is the theoretical one calculated by using the values of eqs. (17) and (18). The rate constant ratio k_1'/k_1 was given by the usual technique as 1.47 l./mole.¹¹ The k_1'/k_1 values so far obtained are all in close agreement. So, the value 1.4 was chosen for k_1'/k_1 and then from eq. (9) the propagation rate constant k_2 at various $[M_0]$ and $[C_0]$ was calculated. The rate constants obtained in this way are collected in Table I. An algebraic mean of k_2 values for seventeen experiments gave $k_2 = 340$ l./mole-sec and standard deviation (SD) = 132. The values lying outside the SD (expt. 68-2, 2, 15, 17) were omitted and the rest averaged to give

$$k_2 = 350 \pm 71 \text{ l./mole-sec} \quad (19)$$

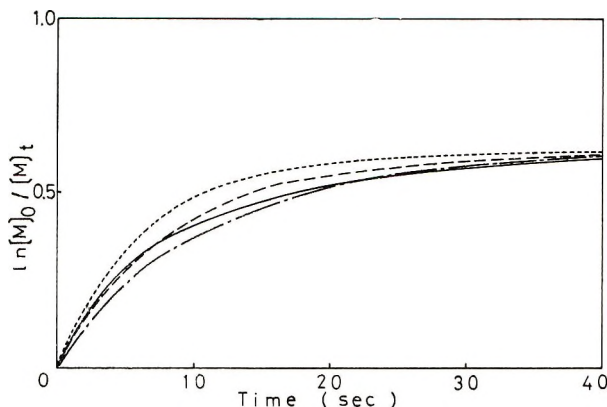


Fig. 9. Polymerization-time according to eq. (11): (—) observed; (· · ·), $k_5 = 0.156$, $k_2 = 440$; (- - -) $k_5 = 0.120$, $k_2 = 340$; (- - -) $k_5 = 0.090$, $k_2 = 250$.

The k_2 value determined from Figure 6, eq. (15), is within the range of experimental error. Thus the propagation rate constants from two different plots coincide reasonably. In Figures 3, 4, and 6 the theoretical curves calculated by using these rate constants are shown. The agreement between the observed and the calculated points is not completely satisfactory on a quantitative level, but the agreement is good enough for the semi-quantitative discussion.

Determination of k_5 . By use of k_2 values in Table I, the termination rate constant k_5 can be calculated according to eq. (12). The k_5 thus obtained are also tabulated in Table I and gave a mean value

$$k_5 = 0.11 \pm 0.06 \text{ sec}^{-1} \quad (20)$$

Now the time course of the polymerization was followed by using eq. (11), and the k_5 value was estimated by the curve-fitting method. As for the polymerization 6, the experimental result (the solid line) and the theoretical lines (the dotted lines) were plotted in Figure 9. In this case the theoretical curve which agrees with the experimental value at the final conversion should be

$$\ln([M_0]/[M_t]) = 0.62(1 - e^{-k_5 t}) \quad (21)$$

The dotted lines 1, 2, and 3 correspond to $k_5 = 0.16$, 0.12, and 0.09, respectively. The larger the k_5 value, the better the coincidence at the initial stage and the worse at the intermediate stage; if k_5 is small, the converse is true. From Figure 9 the best fit of k_5 was 0.12, so it is safe to say that k_5 of 0.11 sec^{-1} which came from other kinetics can also account for the time course of the polymerization. But the agreement of the theoretical with the experimental data was not sufficiently good even when the best value of k_5 was used. On the other hand, by using eq. (21), k_5 can be calculated from the experimental curve of Figure 9. The k_5 values thus calculated as a function of time t are shown in Table II. These pseudo first-order rate

TABLE II
 Change of k_5 with Time

| Time, sec | k_5 , sec ⁻¹ |
|-----------|---------------------------|
| 1 | 0.175 |
| 2 | 0.150 |
| 3 | 0.140 |
| 5 | 0.131 |
| 6 | 0.121 |
| 8 | 0.114 |
| 10 | 0.106 |
| 15 | 0.103 |
| 20 | 0.093 ₅ |
| 25 | 0.086 ₄ |
| 30 | 0.085 ₆ |

constants k_5 were within the limit of the value (20) but decreased monotonously with time and could not be regarded as a constant.

The nature of the termination rate constant k_5 is not clear at the present (see, however, the Discussion). But since the k_2 values were obtained without the k_5 values, the validity of the k_2 values is not influenced by the ambiguity of the k_5 value.

DISCUSSION

In the preceding section some rate constants and their ratio were determined.

$$k_1'/k_1 = 1.4 \text{ l./mole}$$

$$k_2 = 350 \pm 100 \text{ l./mole-sec}$$

$$k_5 = 0.11 \pm 0.06 \text{ sec}^{-1}$$

For the propagation rate constant in cationic polymerization of vinyl monomers the present data are compared with some literature values in Table III. Except for the radiation-induced polymerization in which free ions are involved, the k_p value of CPD is comparatively large, and it is exceeded only by the k_2 for the IB-AlBr₃-TiCl₄-*n*-heptane system investigated by Chemelir and Marek.⁹ Thus the high polymerizability of CPD in cationic polymerization is interpreted at least partly in terms of the large k_2 value. However the value 350 l./mole-sec is much smaller than k_2 for the radiation-induced polymerization of CPD. So it is probable that the TiCl₄-TCA-induced polymerization proceeds by an ion-pair mechanism as has been supposed from the structure of polycyclopentadiene.^{11,19} Furthermore according to the study of the polymer structure by Aso et al.,¹⁹ the k_2 value obtained here is composite, i.e., k_2 of 1,2-addition (ca. 55%) and 1,4-addition. Since the effect of polymerization conditions on the propagation mode is not significant,¹⁹ the validity of k_2 values is not affected by the type of propagation reaction.

TABLE III
 Propagation Rate Constant (k_2) in Cationic Polymerization of Vinyl Monomers

| Monomer | Catalyst | Solvent | Temp, °C | k_2 l./mole-sec | Reference |
|-------------------------|---|---|-------------|-----------------------|-----------|
| Styrene | H ₂ SO ₄ | (CH ₂ Cl) ₂ | 25 | 7.6 | 3, 4 |
| " | HClO ₄ | " | 30 | 17.0 | 5 |
| " | SnCl ₄ | " | " | 0.42 | 7 |
| " | I ₂ | " | " | 0.0037 | 2 |
| " | BF ₃ ·O(C ₂ H ₅) ₂ | " | " | 1.0-2.5 | 20 |
| " | " | C ₆ H ₆ | " | 0.15-0.20 | 20 |
| " | ReCl ₅ | " | 20 | 1.59 | 10 |
| " | " | C ₆ H ₆ -(CH ₂ Cl) ₂ (1:1) | " | 3.73 | 10 |
| Isobutyl vinyl ether | I ₂ | CCl ₄ | 30 | 0.083 | 2 |
| " | BF ₃ ·O(C ₂ H ₅) ₂ | <i>n</i> -C ₆ H ₁₄ - C ₆ H ₅ CH ₃ | -40 | 7.7 | 8 |
| Isobutene | AlBr ₃ -TiCl ₄ | <i>n</i> -C ₇ H ₁₆ | -14 | 6.3 × 10 ³ | 9 |
| α-Methyl- styrene | γ-radiation | Bulk | 30 | 3 × 10 ⁶ | 21 |
| Cyclopenta- diene | " | " | -78 | 5.8 × 10 ⁸ | 22 |
| " | TiCl ₄ -TCA | C ₆ H ₅ CH ₃ | -75 | 350 | This work |

The termination rate constant, 0.11 sec⁻¹, is very large compared to that of styrene-H₂SO₄-(CH₂Cl)₂ (0.0067 sec⁻¹), but the ratio k_5/k_2 is ca. 10⁻³ in either case. In the cationic polymerization the termination reaction cannot be ignored, whereas the mechanism of the termination reaction has not been made clear. In the kinetic treatment of the present system the unimolecular termination reaction was temporarily assumed, but as in Table II, the termination reaction does not seem to be completely unimolecular. As an alternative possibility for the termination reaction, the termination by monomer [eq. (22)] can be put forward in analogy with the reaction (1), which competes with the initiation reaction and can be regarded as a kind of termination reaction.



If the reaction (22) alone represents the termination reaction, we obtain

$$-d[M]/dt = (k_2[P_0^*] - k_5[M_0])[M_t] + k_5[M_t]^2 \quad (23)$$

$$Y = \frac{k_2}{k_5} \left(\frac{k_1}{k_1 + k_1'[M_0]} \right) \frac{[C_0]}{[M_0]} \quad (24)$$

However the plots according to eqs. (23) or (24) do not agree with the experimental findings, so the reaction (22) as a sole termination reaction cannot explain the reaction kinetics. Again alternatively, the termination by residual water in the system would be more feasible, that is



Since some water (of the order of several millimoles per liter) is usually present, which is much higher than P_r^* , the polymerization kinetics seems to be explained by assuming a first-order termination reaction, although the termination reaction is actually second-order as shown by eq. (25).¹² In the present case it was difficult to measure the residual water concentration, so a quantitative test of eq. (25) was not done. However, in analogy with Chemelir and Marek,⁹ who investigated the isobutene polymerization by a similar technique, 10^{-3} – 10^{-1} mmole/l. is suggested for the residual water concentration; this is comparable to the concentration of active species or the initiator concentration. In any event we cannot treat the termination reaction fully quantitatively at present and therefore cannot draw any definite conclusions about the reaction mechanism. All the reactions mentioned above may be involved in the termination reaction in this system, and only apparent unimolecular termination constant ($k_{5,\text{app}}$) could have been obtained:

$$k_{5,\text{app}} = k_5 + k_5'[\text{M}] + k_5''[\text{H}_2\text{O}]$$

so it is possible that the diminution of k_5 value with time as shown in Table II is due to the consumption of the monomer and the residual water resulting from the reactions (24) and (25).

The present method for obtaining the propagation rate constant has been developed on the basis of the kinetics involving the fast initiation reaction. Since the polymerization of cyclic dienes is, so far as has been investigated, accompanied by a fast initiation reaction under a variety of conditions, the present method promises the determination of the propagation rate constant under various sets of combinations of cyclic diene–catalyst–solvent–temperature. The experimental method established in this investigation may be applied to other polymerization systems which show a nonstationary-state character resulting from a very fast initiation reaction. The propagation rate constants in cationic polymerization will be determined in a variety of systems according to the present method.

The authors wish to express their gratitude to Prof. S. Okamura for continuous guidance and advice. Thanks are also due to Prof. S. Yamashita for encouragement and discussions.

References

1. T. Higashimura, in *Structure and Mechanism in Vinyl Polymerization*, T. Tsuruta and K. F. O'Driscoll, Eds., Dekker, New York, 1969, p. 313.
2. S. Okamura, N. Kanoh, and T. Higashimura, *Makromol. Chem.*, **47**, 19 (1961), and succeeding papers.
3. R. E. Burton and D. C. Pepper, *Proc. Roy. Soc. (London)*, **A263**, 58 (1961).
4. M. J. Hayes and D. C. Pepper, *Proc. Roy. Soc. (London)*, **A263**, 63 (1961).
5. D. C. Pepper and P. J. Reilly, *Proc. Roy. Soc. (London)*, **A291**, 41 (1966).
6. L. E. Darcy, W. P. Millrine, and D. C. Pepper, *Chem. Commun.*, **1968**, 1441.
7. N. Kanoh, T. Higashimura, and S. Okamura, *Kobunshi Kagaku*, **19**, 181 (1962).
8. G. J. Blake and D. D. Eley, *J. Chem. Soc.* **1965**, 7412.
9. M. Chemelir and M. Marek, in *Macromolecular Chemistry, Brussels-Louvain 1966*, (*J. Polym. Sci. C*, **22**), G. Smets, Ed., Interscience, New York, 1968, p. 177.

10. M. Kamachi and H. Miyama, *J. Polym. Sci. A-1*, **6**, 1537 (1968).
11. Z. Momiyama, Y. Imanishi, and T. Higashimura, *Kobunshi Kagaku*, **23**, 56 (1966).
12. Y. Imanishi, S. Kohjiya, Z. Momiyama, and T. Higashimura, *Kobunshi Kagaku*, **23**, 119 (1966).
13. Y. Imanishi, S. Kohjiya, and S. Okamura, *J. Macromol. Sci.-Chem.*, **A2**, 471 (1968).
14. S. Kohjiya, Y. Imanishi, and S. Okamura, *J. Polym. Sci. A-1*, **6**, 809 (1968).
15. Y. Imanishi, K. Hara, S. Kohjiya, and S. Okamura, *J. Macromol. Sci.-Chem.*, **A2**, 1423 (1968).
16. R. H. Biddulph and P. H. Plesch, *Chem. Ind. (London)*, **1959**, 1482.
17. A. Gandini and P. H. Plesch, *J. Chem. Soc.*, **1965**, 6019.
18. F. P. Treadwell and W. T. Hall, *Analytical Chemistry*, Vol. II, Wiley, New York, 1966, p. 573.
19. C. Aso, T. Kunitake, and Y. Ishimoto, *J. Polym. Sci. A-1*, **6**, 1163 (1968).
20. T. Higashimura et al., unpublished results.
21. E. Hubmann, R. B. Taylor, and F. Williams, *Trans. Faraday Soc.*, **62**, 88 (1966).
22. M. A. Bonin, W. R. Busler, and F. Williams, *J. Amer. Chem. Soc.*, **87**, 199 (1965).

Received June 23, 1970

Revised September 15, 1970

Polyaromatic Pyrazines: Synthesis and Thermogravimetric Analysis

JERRY HIGGINS, JOE F. JONES, and ALLAN THORNBURGH,
*Department of Chemistry, Illinois State University,
Normal, Illinois 61761*

Synopsis

The syntheses of five polyaromatic pyrazine polymers are described. These polymers were synthesized by the condensation of bis- α -haloaromatic ketones with ammonia in *N,N*-dimethylacetamide (DMAc) solvent in the presence of air or peroxides. The condensation of bis-*p*-(α -bromoacetyl)benzene (IIIa), bis-*p,p'*-(α -chloroacetyl)biphenyl (IIIb) bis-*p,p'*-(α -chloroacetyl)diphenyl ether (IIIc), bis-*p,p'*-(α -chloroacetyl)diphenylmethane (IIId), and α,α' -dibenzoyl- α,α' -dibromo-*p*-xylene (V) under these reaction conditions gave poly[2,5-(1,4-phenylene)pyrazine] (IVa), poly[2,5-(4,4'-biphenylene)pyrazine] (IVb), poly[2,5-(4,4'-oxydiphenylene)pyrazine] (IVc), poly[2,5-(4,4'-methylenediphenylene)pyrazine] (IVd), and poly[2,5-(1,4-phenylene)-3,6-diphenylpyrazine] (VI), respectively. Thermogravimetric analysis (TGA) of these polymers showed them to be thermally stable up to the temperature range of 450–550°C in air for short periods of time. The inherent viscosities of these polymers ranged from 0.18 to 1.30.

INTRODUCTION

Previously, we reported the preparation of 2,5-diphenylpyrazine (II) and three new polyaromatic pyrazine polymers (IVa, IVb, IVc) by the condensation of α -bromoacetophenone and bis- α -haloaromatic ketones with ammonia in *N,N*-dimethylacetamide (DMAc) solvent.¹ In addition, we described a new method in which some of these completely insoluble polymers could be dissolved by heating them in acid solutions containing a small amount of hydrogen peroxide.

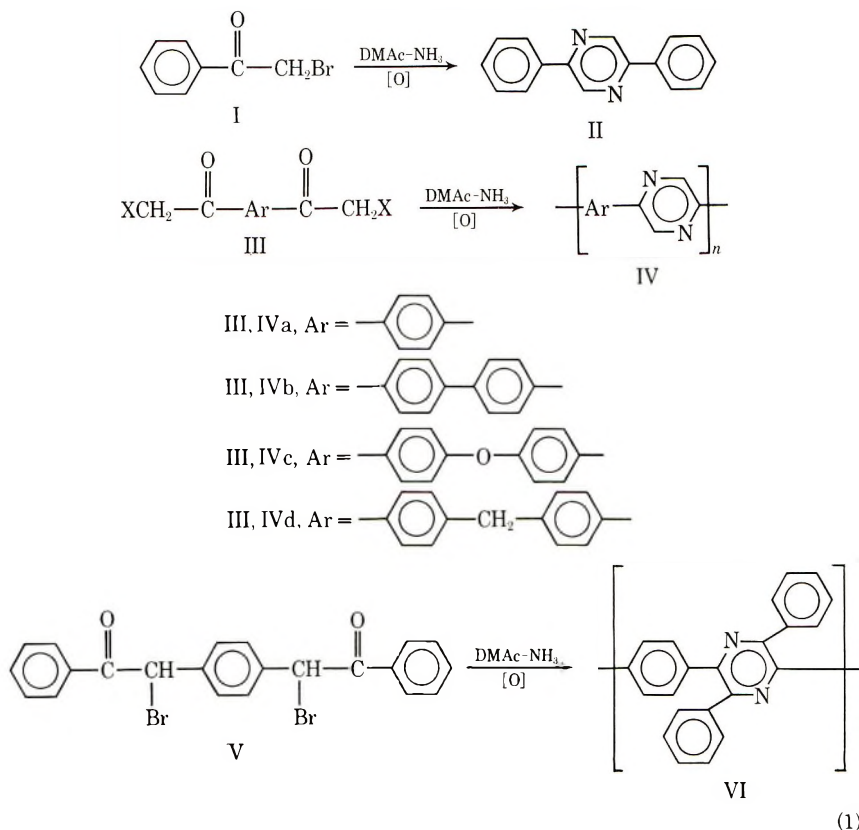
We would now like to report the detailed syntheses of two new polymers (IVd and VI) and of the three previously reported polymers. Also included in this paper are the thermogravimetric analysis data for all of the above polymers.

RESULTS AND DISCUSSION

Monomer IIIa was prepared by the bromination of *p*-diacetylbenzene² and purified by recrystallization from chloroform. Monomers IIIb, IIIc, and IIId were prepared by the Friedel-Crafts acetylation reaction with α -chloroacetyl chloride.³ Monomers IIIb and IIIc were purified by recrystallization from *N,N*-dimethylformamide and chloroform, respectively.

The purification of monomer III_d presented some problems and could be carried out only by repeated recrystallization from carbon tetrachloride in overall yields of about 10%. Monomer V was conveniently prepared by the bromination of α, α' -dibenzoyl-*p*-xylene⁴ in acetic acid and purified by recrystallization from carbon tetrachloride and benzene.

In order to determine the utility of the pyrazine forming reaction using α -haloaromatic ketones and ammonia, the study of the formation of the model compound, 2,5-diphenylpyrazine (II), was undertaken. The reaction of α -bromoacetophenone and ammonia was carried out in refluxing DMAc in the presence of air or peroxides. When air was used as the aromatizing oxidant, the reaction solution had to be refluxed for two days in order to aromatize the dihydropyrazine ring, and the yields of product ranged from 30 to 50% after recrystallization from methanol. Since the dihydropyrazine compound forms an orange-red solution, the change of this color to a light yellow solution is indicative of complete aromatization. The use of peroxide as the aromatizing oxidant proved to be far superior to the above method. When the peroxide was used, the reactants were refluxed for 1-2 hr in DMAc and then 30% hydrogen peroxide was added to the refluxing solution. Heating was continued until the orange-red solution turned to light yellow color. This method gave essentially quantita-



tive yields of 2,5-diphenylpyrazine. The latter technique did not produce any detectable N \rightarrow O groups as determined by infrared techniques and by the mixed melting point with an authentic sample of 2,5-diphenylpyrazine.⁵

Polymerizations were carried out in dimethylacetamide-ammonia solutions by stirring the monomers for 1 hr at room temperature, 1 hr at 60–70°, and then refluxing for 6–36 hr. The syntheses and structures of these polymers are shown in the scheme (1). Polymers IVa and IVb were insoluble in all common polymer solvents and precipitated from the DMAc solutions during the polymerization reactions.

Polymers IVc and IVd were soluble in formic acid but only partially soluble in DMAc and sulfuric acid. The phenyl-substituted polymer (VI) was very soluble in formic, phosphoric, and sulfuric acids. Polymer VI was also very soluble in DMAc, DMF, and dimethyl sulfoxide (DMSO). This result is in agreement with the increased solubilities of the phenyl-substituted polyquinoxalines reported by Wrasidlo and Augl.⁴ Since polymers IVa and IVb were completely insoluble in all common polymer solvents, a new technique was developed in which these heteropolymers could be dissolved for solution studies. It was found that these insoluble polymers were quite soluble in formic, phosphoric, and sulfuric acids when 0.25 ml of 30% H₂O₂ was added to 15 ml of the hot solvent-polymer mixtures. The polymers were also partially soluble in DMAc and DMF when

TABLE I
Polymer Properties

| Polymer | Solvent | Solubility | | Inherent viscosity ^b |
|---------|--------------------------------|---------------|---|---------------------------------|
| | | Solvent alone | With H ₂ O ₂ ^a | |
| IVa | HCO ₂ H | Insol. | Sol. | 0.40 ^a |
| | H ₂ SO ₄ | Insol. | Sol. | 1.30 ^a |
| | H ₃ PO ₄ | Insol. | Sol. | |
| | DMAc | Insol. | Part. sol. | |
| IVb | HCO ₂ H | Insol. | Sol. | 0.43 ^a |
| | H ₂ SO ₄ | Insol. | Sol. | 0.35 ^a |
| | H ₃ PO ₄ | Insol. | Sol. | |
| | DMAc | Insol. | Part. sol. | |
| IVc | HCO ₂ H | Sol. | Sol. | 0.40, 0.54 ^a |
| | H ₂ SO ₄ | Part. sol. | Sol. | 0.12 ^a |
| | H ₃ PO ₄ | Part. sol. | Sol. | |
| | DMAc | Part. sol. | Part. sol. | |
| IVd | HCO ₂ H | Sol. | Sol. | 0.37 |
| | H ₂ SO ₄ | Part. sol. | Sol. | |
| | H ₃ PO ₄ | Part. sol. | Sol. | |
| | DMAc | Part. sol. | Part. sol. | |
| VI | HCO ₂ H | Sol. | | 0.18 |
| | H ₂ SO ₄ | Sol. | | |
| | H ₃ PO ₄ | Sol. | | |
| | DMAc | Sol. | | |

^a 0.25 ml of H₂O₂/15 ml of solvent.

^b 0.25 g of polymer/100 ml of solvent.

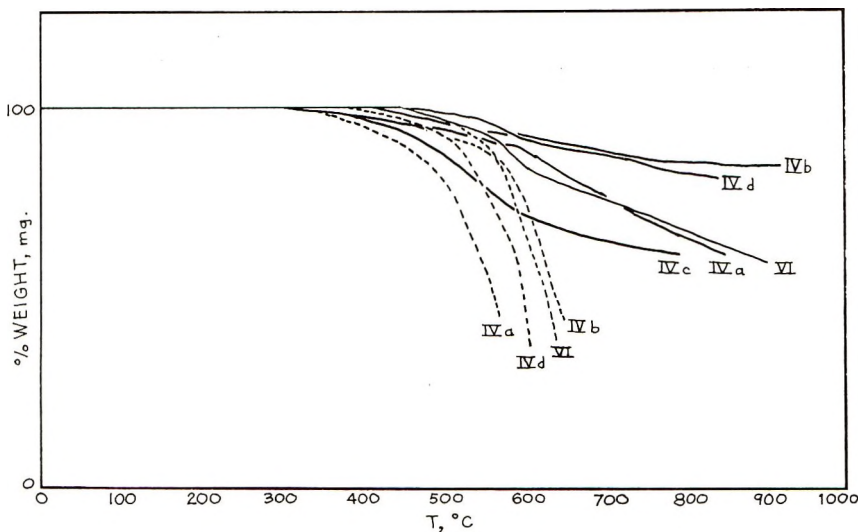


Fig. 1. Thermogravimetric analyses of polymers IVa-IVd and VI: (—) in nitrogen; (---) in air.

heated in the presence of peroxides. The increase in solubility is probably due to the introduction of the polar N-oxide group along the polymer chain.

Infrared spectra for these modified polymers showed a strong absorption band in the $1220\text{--}1270\text{ cm}^{-1}$ region and the oxidized model compound (II) gave a strong band at 1250 cm^{-1} ($\text{N} \rightarrow \text{O}$).⁶ These absorption bands were absent in the model compound and polymers IVa and IVb before the oxidation reactions were carried out. Although the polymers are apparently modified by the formation of the polar N-oxide groups, this technique should be very valuable, not only for the modification of the many already existing heteropolymers, but also for studying the solution properties of the insoluble ones.

Although the polymers were exposed to the same oxidation procedures as those for the model compound (II), there still remained a small absorption band at 1650 cm^{-1} in the infrared spectrum for each of the polymers. These absorption bands are probably due to a small amount of nonaromatized imine linkages, polymer endgroups, or both. The solubilities, thermal stabilities, and physical properties in general of the polypyrazine polymers appear to be quite similar to Stille's⁷ polyquinoxalines and Marvel's⁸ polybenzimidazoles. However, two attractive features of the polypyrazines are the accessibility of the monomers and no need of monomer stoichiometry in the polymer syntheses.

The thermal stabilities (Fig. 1) of all the polymers are very good in air and nitrogen, as evidenced by thermal gravimetric analysis. It is interesting to note that none of the polymers melted below 500°C except polymer VI. Polymer VI had a softening point around $270\text{--}300^\circ\text{C}$ yet was quite soluble in all common polymer solvents and exhibited thermal sta-

bility up to 550°C in an air atmosphere. Of the five polymers in this series, it appears from the evaluation of the physical properties and solubilities (Table I) that polymers IVc and VI would be more amenable to fabrication. As with the polyquinoxalines,^{4,7} the introduction of a heteroatom or the phenyl substitution in the polymer chain gives more desirable properties without the loss of thermal stability.

EXPERIMENTAL

Instruments

Nuclear magnetic resonance (NMR) spectra were obtained with a Hitachi Perkin-Elmer R20 instrument. Infrared spectra were taken on Beckman IR-8 and Perkin-Elmer Model 700 instruments. Melting points of all compounds are uncorrected.

Monomer Preparations

Preparation of Bis-*p*-(α -bromoacetyl)benzene (IIIa). To 15 g (0.092 mole) of *p*-diacetylbenzene in 200 ml of acetic acid was added dropwise 34 g (0.19 mole) of bromine. After the bromine addition was complete, the reaction mixture was stirred for 2 hr and the product filtered. The crude product was then dried *in vacuo* and recrystallized from chloroform to a constant melting point of 172–173°C (lit.² mp, 173°C). The yield of product was 39 g (64%).

Preparation of Bis-*p,p'*-(α -chloroacetyl)biphenyl (IIIb). To 31 g (0.20 mole) of biphenyl in 500 ml of carbon disulfide were added 80 g (0.60 mole) of aluminum chloride and 68 g (0.60 mole) of α -chloroacetyl chloride. The reaction mixture was refluxed for 12 hr, cooled to room temperature, and the carbon disulfide decanted from the thick oil. After hydrolysis in 10% hydrochloric acid, the crude product was filtered, dried *in vacuo*, and recrystallized from *N,N*-dimethylformamide (DMF) to a constant melting point of 224–225°C (lit.³ mp, 224°C). The yield of product was 30.6 g (50%).

Preparation of Bis-*p,p'*-(α -chloroacetyl)diphenyl Ether (IIIc). To 34 g (0.20 mole) of diphenyl ether in 500 ml of carbon disulfide were added 80 g (0.60 mole) of aluminum chloride and 68 g (0.60 mole) of α -chloroacetyl chloride. The reaction mixture was refluxed for 2 hr, cooled to room temperature, and the carbon disulfide decanted from the thick oil. After hydrolysis in 10% hydrochloric acid, the crude product was filtered, dried *in vacuo*, and recrystallized from chloroform to a constant melting point of 111–113°C (lit.³ mp, 111°C). The yield of product was 31 g (38%).

Preparation of Bis-*p,p'*-(α -chloroacetyl)diphenylmethane (III d). To 34 g (0.20 mole) of diphenylmethane in 500 ml of carbon disulfide were added 80 g (0.60 mole) of aluminum chloride and 68 g (0.60 mole) of α -chloroacetyl chloride. The reaction mixture was refluxed for 3 hr, cooled to room temperature, and the carbon disulfide decanted from the thick oil.

After hydrolysis in 10% hydrochloric acid, the crude product was filtered and dried *in vacuo*. The crude product was purified by repeated recrystallizations from carbon tetrachloride to a constant melting point of 124–125°C (lit.³ mp, 124–125°C). The yield of purified product was about 6 g (10%).

Preparation of α,α' -Dibenzoyl- α,α' -dibromo-*p*-xylene (V). To 150 ml of acetic acid were added dropwise 11.6 g (0.037 mole) of α,α' -dibenzoyl-*p*-xylene⁴ and 12.5 g (0.078 mole) of bromine. After spontaneous refluxing had ceased, the product precipitated from solution. The product was filtered and washed several times with water. The yield of crude product was 15 g (86%). The crude product was recrystallized from carbon tetrachloride and benzene to a constant melting point of 179–180°C. The yield of monomer grade product was 11 g (62%).

Anal. Calcd for $C_{22}H_{16}Br_2O_2$: C, 55.94%; H, 3.42%; Br, 33.85%. Found: C, 55.83%; H, 3.21%; Br, 34.00%.

Model Compound

Preparation of 2,5-Diphenylpyrazine (II). To 100 ml of *N,N*-dimethylacetamide (DMAc) saturated with ammonia was added 2 g of α -bromoacetophenone. The reaction was stirred at room temperature for 1 hr, heated at 50–60°C for 1 hr, and finally refluxed for 48 hr in the presence of air. The solution was poured into 400 ml of cold water and filtered. Recrystallization from methanol gave a product melting at 193–195°C (30–50%).

Alternate Procedure for II. The same procedure as above was followed except after 1–2 hr of refluxing 2 ml of 30% H_2O_2 was added to the refluxing solution and the solution maintained at reflux temperature until the orange-red color disappeared. The solution was then poured into 300 ml of water and filtered to give a quantitative yield of cream-colored product melting at 193–195°C (lit.⁵ mp, 195.5°C).

Preparation of Polymers

The procedure for the preparation of poly[2,5-(4,4'-oxydiphenylene)-pyrazine] is typical for all the polymerization reactions.

Preparation of Poly[2,5-(4,4'-oxydiphenylene)pyrazine] (IVc). To 150 ml of purified *N,N*-dimethylacetamide (DMAc), saturated with ammonia, was added 2 g of bis-*p,p'*-(α -chloroacetyl)diphenyl ether (IIIc). The reaction was stirred at room temperature for 1 hr, heated at 50–60° for 1 hr, and then refluxed for 20 hr in the presence of air. After refluxing for 2–4 hr the polymer began to precipitate from the hot DMAc. After the heating period was complete, the reaction mixture was cooled, poured into 500 ml water, and filtered. The polymer was dried *in vacuo* at 200°C for 18 hr to give a quantitative yield of product. The inherent viscosity in formic acid was 0.40.¹

Poly[2,5-(1,4-phenylene)pyrazine] (IVa). This polymer proved to be completely insoluble in all common polymer solvents tried. In order to obtain the viscosity of the polymer solution, the polymer sample was dissolved in 15 ml of 97% formic acid containing 0.25 ml of 30% H_2O_2 with heating until all the polymer had dissolved. In this solution the inherent viscosity was 0.40. The same procedure with concentrated sulfuric acid gave an inherent viscosity of 1.30.¹

Poly[2,5-(4,4'-biphenylene)pyrazine] (IVb). This polymer proved to be completely insoluble in all common polymer solvents tried. In order to obtain the viscosity, the same procedure as that for polymer IVa was used to dissolve this polymer in formic acid. The inherent viscosity was 0.43 in the $\text{HCO}_2\text{H}-\text{H}_2\text{O}_2$ solution and 0.35 in the $\text{H}_2\text{SO}_4-\text{H}_2\text{O}_2$ solution, respectively.¹

Poly[2,5-(4,4'-methylenediphenylene)pyrazine] (IVd). The inherent viscosity of this polymer was 0.37 in formic acid.

ANAL. Calcd for $(\text{C}_{17}\text{H}_{12}\text{N}_2)_n$: C, 83.61%; H, 4.92%; N, 11.48%. Found: C, 81.19%; H, 4.92%; N, 10.66%.

Poly[2,5-(1,4-phenylene)-3,6-diphenylpyrazine] (VI). This polymer was soluble in all common polymer solvents and had a softening point of 270°C. The inherent viscosity in formic acid was 0.18.

ANAL. Calcd for $(\text{C}_{22}\text{H}_{14}\text{N}_2)_n$: C, 84.97%; H, 5.27%; N, 9.75%. Found: C, 83.63%; H, 4.89%; N, 7.58%.

The authors are grateful to Drs. J. K. Stille, G. A. Loughran, and R. H. Barker for thermogravimetric analyses of the polymers. J. H. is especially thankful to Drs. C. S. Marvel, J. K. Stille, and R. B. Seymour for their helpful discussions during the course of this work. This work was supported in part by Illinois State University.

References

1. J. Higgins, J. F. Jones, and A. Thornburgh, *Macromolecules*, **2**, 558 (1969).
2. P. Ruggli and E. Gassenmeier, *Helv. Chim. Acta*, **22**, 503 (1939).
3. E. Gryszkiewicz-Trachimowski, O. Gryszkiewicz-Trachimowski, and R. S. Levy, *Bull. Soc. Chim. France*, **1958**, 1156.
4. W. Wrasidlo and J. M. Augl, *J. Polym. Sci. B*, **7**, 281 (1969).
5. G. Nomine, L. Penasse, and V. Deloroff, *Amer. Pharm. Fr.*, **16**, 436 (1958).
6. L. J. Bellamy, *The Infra-red Spectra of Complex Molecules*, 2nd ed., Clay London, 1958, pp. 267-271.
7. J. K. Stille and F. E. Arnold, *J. Polym. Sci. A*, **4**, 551 (1966) and references cited therein.
8. H. Vogel and C. S. Marvel, *J. Polym. Sci.*, **50**, 511 (1961).

Received October 6, 1970

Dependence of Reactivity of Propagation Centers of Oxide Catalysts for Ethylene Polymerization on Catalyst Composition and Activation Conditions*

YU. I. ERMAKOV, V. A. ZAKHAROV, and E. G. KUSHNAREVA,
*Institute of Catalysis, Siberian Branch of the
Academy of Sciences of the USSR, Novosibirsk, USSR*

Synopsis

The propagation rate constant K_p was used as a measure of reactivity of propagation centers in ethylene polymerization with oxide catalysts. This constant was determined by a radiotracer quenching technique for oxide catalysts of different compositions and activation conditions. For catalysts based on various transition metal oxides, an increase of K_p was observed in the series $W < Mo < Cr$ and $V < Cr$. In the case of chromium oxide catalyst it was shown that K_p value does not depend on the content of the transition metal in a catalyst. A change of propagation center reactivity was found when oxides of different composition (SiO_2 , Al_2O_3 , ZrO_2 , TiO_2) were used as supports. An increase of the vacuum activation temperature of a catalyst results in increasing K_p . Pretreatment of catalyst with different reducing agents (SO_2 , CO_2 , NH_3 , HCN) results in the change of K_p value in comparison with the catalyst activated by the vacuum treatment only. The data obtained on the variation of the reactivity of the propagation centers permit one to draw a conclusion about the composition of surface compounds as active centers of the oxide polymerization catalysts.

INTRODUCTION

To prove a relation between catalyst composition and reactivity of propagation centers is an important problem in investigating the mechanism of the catalytic polymerization. Firstly, it is necessary to develop methods of predicting catalytic activity in polymerization, and secondly it gives a valuable information about the composition of propagation centers. It is usually difficult to interpret unambiguously the dependence of polymerization rate on the catalyst composition, because when the catalyst composition and preparation conditions are varied, this can change both the number of active centers and the rates of separate elementary stages of a process. The dependence of molecular weight on the catalyst composition can be used to reach some conclusions as to the process mechanism. However, in general, molecular weight is a function of the number of propagation centers, rate constants of many elementary stages, and concentration of transfer agents in a polymerization system. This is why the interpreta-

* Presented to the Symposium on Macromolecular Chemistry, Budapest, August 1969.

tion of the molecular weight dependence on catalyst properties can not always be unambiguous.

It is reasonable to compare polymerization catalysts on the basis of the kinetic characteristics of separate elementary stages. In particular, the propagation rate constant K_p that characterizes reactivity of a single active center in a chain propagation reaction can serve as a measure of the propagation center reactivity. For catalysts of different composition and preparation conditions a change of the propagation rate constant is strict evidence of the change in the structure of the active center.

In the present paper the propagation rate constants for oxide catalysts of different composition and prepared under various activation conditions were determined. Data obtained were used to draw a conclusion as to the composition of the propagation center and the mechanism of the initiation and propagation steps of the polymerization process.

EXPERIMENTAL

Catalysts

The compositions of oxide catalysts used in this work are given in Table I.

The preparation technique and the conditions of the vacuum treatment of chromium catalysts were described earlier.¹

TABLE I
Compositions of Oxide Catalysts

| Catalyst number | Transition metal oxide | Support | Specific surface area, m ² /g | Transition metal content, wt-% |
|-----------------|-------------------------------|--|--|--------------------------------|
| I | CrO ₃ | Silica-alumina (3% Al ₂ O ₃) | 300 | 2.5 |
| II | CrO ₃ | Silica | 400 | 0.5-5 |
| III | CrO ₃ | Alumina | 170 | 1.4 |
| IV | WO ₃ | Alumina | 170 | 3.5 |
| V | MO ₃ | Alumina | 170 | 3.5 |
| VI | V ₂ O ₅ | Silica-alumina (3% Al ₂ O ₃) | 300 | 3.5 |

Oxide catalysts containing W, Mo, and V were prepared by impregnation of the support with solutions of ammonium molybdate, ammonium vanadate, and heteropolyacid of the composition H₇P(W₂O₇)₆. Drying, calcination, and vacuum activation were the same as in the case of chromium oxide catalysts.¹ After the vacuum activation, molybdenum and tungsten oxide catalysts were reduced with hydrogen at 400°C and 500°C, and the vanadium oxide catalyst was reduced with carbon monoxide at 300°C. In some cases chromium oxide catalysts were also treated with different reducing agents after vacuum activation. This treatment was carried out

under static conditions at 300°C and under an initial pressure of 100–600 torr for 2 hr. The catalysts were then subjected to vacuum for 2 hr, usually at the temperature of the preceding reduction.

To obtain a radioactive carbon monoxide, $^{14}\text{CO}_2$ was reduced with charcoal at 1000°C. The specific radioactivity of carbon monoxide thus obtained was measured after transformation into BaCO_3 with a Geiger-Müller top-counter.

Polymerization Procedure and Determination of the Number of the Propagation Centers

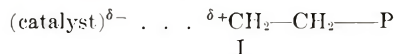
Ethylene was polymerized at 75°C and 15 kg/cm² in a solvent (benzine) in a stainless steel autoclave with stirring. The apparatus used, the polymerization technique, and the reagent characteristics were described in the preceding report.¹ The number of propagation centers was determined by a quenching technique with radioactive methanol $^{14}\text{CH}_3\text{OH}$. From the obtained number n of propagation centers (in moles/g), the polymerization rate V (in moles/g-hr) at the moment of inhibitor injection, and concentration of ethylene C_m (in moles/l.), the propagation rate constant K_p (in l./mole-hr) was calculated according to eq. (1):

$$V = K_p n C_m \quad (1)$$

RESULTS AND DISCUSSION

Study of Supported Catalysts Containing Different Transition Metal Oxides

For all the studied oxide catalysts, when polymerization was stopped by methanol $^{14}\text{CH}_3\text{OH}$ it was found that the polymers purified from a catalyst residue were radioactive (Table II). Therefore in polymerization by means of oxide catalysts containing different transition metals the active bond has the same type of polarization:



where P is a polymer chain.

This type of polarization in the case of chromium oxide catalyst was earlier explained by us on the assumption that a propagation chain is connected with a catalyst through an oxygen atom. We believe that there may be other explanations of such an active bond polarization, but in this paper the explanation of experimental data will be done on the basis of the supposition formulated in the preceding paper.¹ However, conclusions concerning the active center environment made from data on the change of active center reactivity probably will be the same as if the active bond were one of the possible types of bond between transition metal and carbon.

As will be shown below, the reduction of a transition metal in an oxide catalyst is a necessary stage of the propagation centre formation. In the

TABLE II
 Polymer Radioactivity, the Number of Propagation Centers, and Propagation Rate Constants for Different Oxide Catalysts^a

| Catalyst | Additional treatment after vacuum activation | Polymerization rate at the moment of inhibitor injection, g C ₂ H ₄ /g catalyst-hr | Polymer radioactivity, counts/sec | $n \times 10^6$, mole/g catalyst | $K_p \times 10^{-1}$, l./mole-hr |
|----------|--|--|-----------------------------------|-----------------------------------|-----------------------------------|
| III | Reduced by H ₂ at 400°C | 1.22 | 496 | 0.12 | 0.37 |
| V | Reduced by H ₂ at 400°C | 0.25 | 1810 | 0.13 | 0.070 |
| | | 0.14 | 2810 | 0.14 | 0.036 |
| IV | Reduced by H ₂ at 500°C | 0.14 | 5080 | 0.20 | 0.022 |
| | | 0.10 | 3700 | 0.29 | 0.012 |
| I | Reduced by CO at 300°C | 76 | 403 | 0.51 | 5.0 |
| | | 100 | 537 | 0.90 | 4.0 |
| VI | Reduced by CO at 300°C | 0.21 | 4680 | 0.17 | 0.043 |
| | | 0.15 | 1270 | 0.041 | 0.13 |

^a Polymerization at 75°C; ethylene pressure 15 kg/cm².

case of the chromium oxide catalyst this stage can proceed during the interaction with the reaction medium. When dealing with catalysts based on molybdenum, tungsten, and vanadium oxides a preliminary reduction is necessary to obtain an active catalyst. This is due to the greater stability of the highest oxidation degree of these metals in their oxides and surface compounds as compared with chromium compounds. Table II gives the number of propagation centers and propagation rate constants for different catalysts. It should be noted that the kinetic properties of propagation centers depend on the nature of the support and on the reducing agent used for activation (see below). Therefore when studying the role of a transition metal the support and the activation conditions of the catalysts compared must be the same.

These data show that the nature of a transition metal in an oxide catalyst influences the value of K_p . The propagation rate constants decrease in the series of Cr > Mo > W and Cr > V. For catalysts reduced by H₂ in the case of Cr, Mo, and W the number of propagation centers is in the same order. However it should be noted that the reduction of the chromium oxide catalyst by H₂ results in an abrupt decrease in the concentration of propagation centers. It can be supposed that in the case of the tungsten and molybdenum oxide catalysts the treatment with H₂ also gives a low yield of active centers during its formation from the active component of the catalyst. But without any reduction these catalysts are not active at all.

In the vanadium oxide catalyst the number of propagation centers is low in comparison with the chromium oxide catalyst activated by the similar method.

Effect of Chromium Concentration on the Number of Propagation Centers and Propagation Rate Constant

For the catalyst on silica with different chromium content the values of n and K_p were determined. At chromium concentrations varying from 0.5 to 5% K_p was practically constant (Table III), so the dependence of the

TABLE III
 n and K_p for Catalyst II at Various Chromium Contents^a

| Run | Weight of catalyst, g | Cr content, wt-% | Polymerization rate at the injection of inhibitor, g C ₂ H ₄ /g catalyst-hr | $n \times 10^6$, mole/g | $K_p \times 10^{-6}$, l/mole-hr |
|-------|-----------------------|------------------|---|--------------------------|----------------------------------|
| 6-VI | 0.20 | 0.5 | 16.0 | 0.24 | 2.37 |
| 7-VI | 0.09 | 1.0 | 50.0 | 0.68 | 2.66 |
| 19-VI | 0.10 | 2.5 | 145.0 | 2.05 | 2.48 |
| 8-VI | 0.10 | 5.0 | 130.0 | 1.62 | 2.90 |

^a Polymerization at 75°C ethylene pressure 15 kg/cm².

polymerization rate on the chromium concentration was determined by the change of the number of propagation centers (Fig. 1). The steady-state polymerization rate per gram of catalyst was maximum, when chromium content was 2.5–5 wt-%. The highest steady-state concentration of active centers and the maximum polymerization rate per gram of chromium was observed for catalysts with 1–2.5 wt-% of Cr.

Increasing the number of propagation centers with the increase of the chromium content in the catalyst may be due to gradual involvement of the centers of the support surface in reduction with CrO₃, resulting in an active catalyst component. The possible reason for the decrease of the propagation center concentration may be the covering effect by aggregates of Cr₂O₃ which are formed in the reduction of Cr⁺⁶ during interaction of the catalyst with the reaction medium.

The dependence of K_p of the chromium content in the catalyst may serve as an evidence that the propagation centers in the chromium oxide catalyst are practically homogeneous. The structure of propagation centers does not change with variation of chromium concentration in the investigated range.

Effect of Support on Propagation Rate Constant

The nature of the support influences the number of propagation centers and the propagation rate constant for chromium oxide catalysts. In the preceding report¹ this influence was explained by the structure of the active

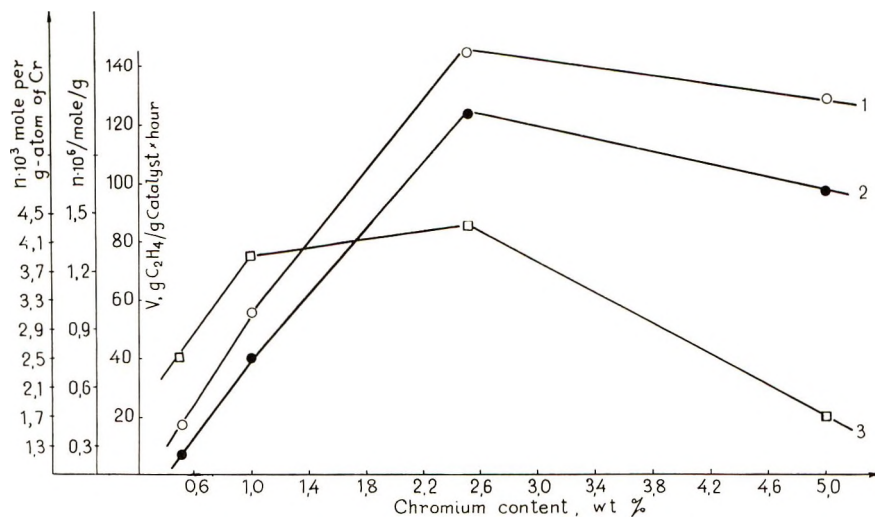
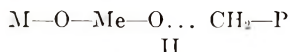


Fig. 1. Dependence of (1) the steady-state polymerization rate, (2) the steady-state concentration of propagation centers (in mole/g catalyst), and (3) steady-state concentration of propagation centers (in mole/g-atom Cr) on the chromium content in catalyst II. Polymerization at 75°C; ethylene pressure 15 kg/cm².

center in which a chromium atom is connected to the cation of the support through an oxygen atom:



where Me denotes transition metal and M is the cation of the support.

Effect of Activation Temperature on Reactivity of the Propagation Center

Catalyst I was activated under the usual conditions (at 400°C) and at a higher temperature (at 710°C). After the high-temperature activation a part of the catalyst was kept under water vapor at the room temperature and then was activated at 430°C. In Figure 2 the experimental kinetic curves for ethylene polymerization with catalysts activated in different ways are presented.

Increasing the activation temperature to 710°C appreciably raises the catalyst activity. After contact of the catalyst with water vapor and subsequent activation at a lower temperature the polymerization rate decreases. The data on the number of active centers and the propagation rate constants for these catalysts are given in Table IV. The porous structure of catalyst I was not changed when the activation temperature increased from 400°C to 710°C. The data obtained show it is the increase of the propagation rate constant that causes the increase in the catalyst activity at a higher activation temperature. So the structure of a propagation center depends on the temperature of vacuum treatment.

TABLE IV
 n and K_p for Chromium Oxide Catalysts Activated at Different Temperatures^a

| Catalyst treatment | Polymerization time, min | Polymerization rate at injection of inhibitor, g C ₂ H ₄ /g catalyst-hr | $n \times 10^6$, mole/g | $K_p \times 10^{-6}$, l./mole-hr |
|--|--------------------------|---|--------------------------|-----------------------------------|
| Activation at 400°C under vacuum | 37 | 33.5 | 1.27 | 0.94 |
| Activation at 710°C under vacuum | 25 | 90 | 1.30 | 2.45 |
| Treatment by water vapor after activation at 710°C, then activation at 430°C | 71 | 44 | 2.06 | 0.76 |

^a Catalyst I; polymerization at 75°C; ethylene pressure 1.5 kg/cm².

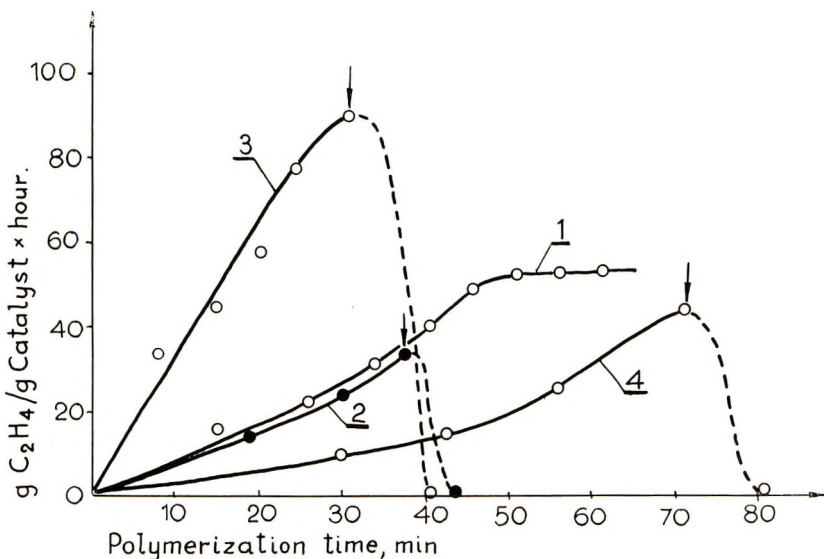


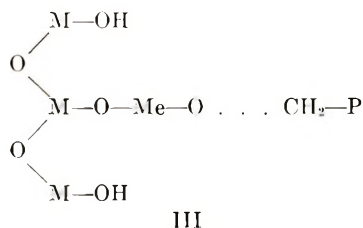
Fig. 2. Kinetic curves for ethylene polymerization with catalyst I activated at different temperatures: (1, 2) 400°C; (3) 710°C; (4) catalyst activated at 710° and then treated with water vapor and evacuated at 430°C.

The molecular weight of the polymer obtained with the catalyst activated at 710°C was lower than that obtained when the catalyst activation temperature was 400°C. Under middle pressure the molecular weight of polyethylene obtained with the chromium oxide catalyst is proportional to the ratio of K_m/K_p , where K_m is the rate constant of chain transfer with monomer. Thus, increasing the catalyst activation temperature results predominantly in an increase in K_m in comparison with K_p .

Clark² has proposed that the effect of the activation temperature on

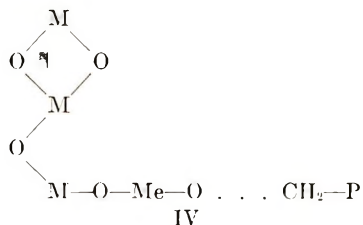
molecular weight of polymer may be due to removal of surface hydroxyls. However Clark explained the molecular weight decrease by diminution of the absorbed monomer concentration. This conclusion does not agree with our data on increasing the polymerization rate and the propagation rate constant when the activation temperature increases from 400 to 710°C.

When the catalyst activated at 710°C is treated with water vapor, surface hydroxyls appear again, and the propagation rate constant decreases and becomes practically equal to K_p for the catalyst activated at 430°C. The overall catalyst activity and the molecular weight also change to values which are typical of the catalyst activated at 400°C. Taking into account the influence of surface hydroxyls on the active center reactivity, the composition of the propagation center on the surface of a supported oxide catalyst may be represented by the structure III,



where M denotes the element the oxide of which was used as a support.

After high-temperature treatment it is possible to obtain a structure of type IV:



Effect of Reduction of Catalyst by Carbon Monoxide

The treatment of chromium oxide catalysts with carbon monoxide at 200°C results in their deep reduction and an increase in the catalytic activity in ethylene polymerization.

The average oxidation number was determined in reduced catalysts by iodometric analysis.³ The method used permits determination of more than 3×10^{-6} g-atom of chromium of oxidation number more than 3 per gram of a catalyst. It is important to carry out this analysis under nitrogen, since oxidation proceeds rapidly when the catalysts reduced with CO come in contact with air at room temperature.

The analysis showed the absence of chromium at oxidation number more than 3 in catalysts reduced with CO at 200°C. These catalysts had no signal from Cr^{+5} in the ESR spectrum (measured at $\sim 20^\circ\text{C}$).

The effect of CO treatment depends on the temperature of this treatment. In Figure 3 the experimental kinetic curves for the polymerization with catalysts treated with CO at different temperatures are given. After the reduction the catalysts were evacuated under 10^{-3} torr at the same temperature. The catalysts reduced at 200 and 300°C were the most active. The catalyst activity decreased when the reduction temperature increased further up to 400°C. The catalysts treated with CO at 100°C were not reduced and their activity was practically the same as that of the catalysts activated under vacuum.

The results of the determination of the concentration of active centers and the propagation rate constants for reduced catalysts on different supports are given in Table V. In all the cases the treatment of catalysts with carbon monoxide results in an increase in the propagation rate constant. As the number of active centers depends on the catalyst composition, the method of its preparation, and polymerization conditions, it can either increase or decrease after treatment with CO.

The reduction of catalyst I with ^{14}C O was also performed at 300°C. The polymer, purified from catalyst by the procedure described in the preceding paper,¹ had no radioactivity. This result indicates that carbon monoxide is not involved in the formation of a catalyst-carbon active bond.

When catalyst which had been reduced with ^{14}C O was not removed from the polymer, the polymer films had radioactivity. Hence this radioactivity was due to the ^{14}C O bonded to the catalyst. This radioactivity corresponded to the content of 6.5×10^{-6} mole of ^{14}C /g catalyst after polymerization.

The catalyst reduced with ^{14}C O was reoxidized and then activated in *vacuo*. After such a treatment the catalyst activity decreased and became

TABLE V
Effect of Reduction with CO for Different Catalysts^a

| Catalyst | Polymerization rate at injection of inhibitor, g | | |
|----------------|--|-----------------------------|--------------------------------------|
| | $\text{C}_2\text{H}_4/\text{g}$ catalyst-hr | $n \times 10^6$, mole/g | $K_p \times 10^{-6}$, l./mole-hr |
| I, unreduced | 49 | 1.35 | 1.30 |
| | 65 | 1.86 | 1.25 |
| I, reduced | 206 | 1.36 | 5.4 |
| | 370 | 2.30 | 5.8 |
| II, unreduced | 90 | 1.20 | 2.70 |
| | 95 | 1.37 | 2.48 |
| II, reduced | 260 | 1.86 | 5.00 |
| | 450 | 3.05 | 5.25 |
| III, unreduced | 10.0 | 1.90 | 0.19 |
| | 15.0 | 3.40 | 0.16 |
| III, reduced | 27.0 | 1.76 | 0.54 |
| | 31.5 | 2.05 | 0.55 |

^a Reduction at 300°C; polymerization at 75°C; ethylene pressure 15 kg/cm².

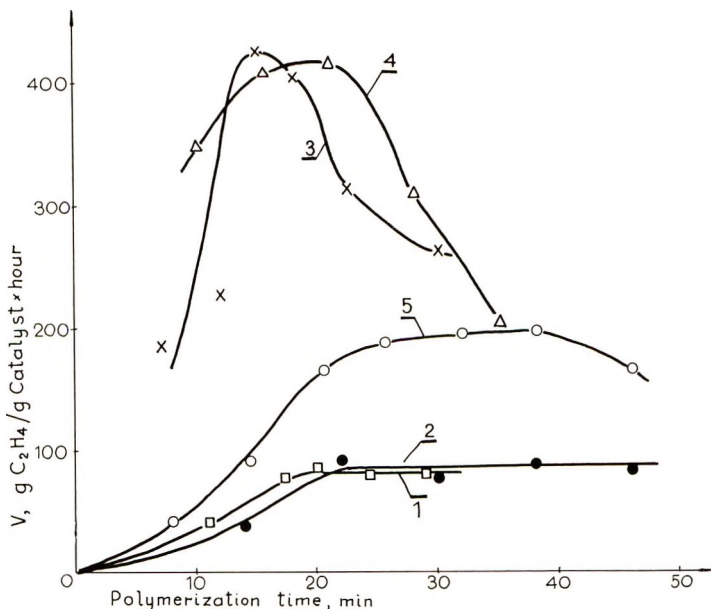


Fig. 3. Kinetic curves for polymerization with catalyst II: (1) vacuum activation only; (2) treatment with CO at 100°C; (3) treatment with CO at 200°C; (4) treatment with CO at 300°C; (5) treatment with CO at 400°C. Polymerization at 75°C; ethylene pressure 15 kg/cm².

equal to the activity of the catalyst prepared with by the usual vacuum activation. The polymer films containing this reoxidized catalyst had no radioactivity. Hence, removal of carbon monoxide takes place when the catalyst reduced with CO is oxidized and activated under vacuum. Table VI gives values of K_p for the catalyst after different treatments. Reoxidation of the catalyst results in decreasing K_p to the value typical of unreduced catalyst.

The results obtained permit some conclusions on the mechanism of formation of the propagation centers.

The formation of propagation centers (or initiation process) in the polymerization with oxidate catalysts may be presented by the scheme:



In this scheme n is a propagation center, that is, the surface compound with an active bond between catalyst and polymer; A is an active component, that is, the initial surface compound, from which as a result of a set of consecutive reactions a propagation center arises. We regard the catalyst state after vacuum activation as an initial one. The results of the preliminary treatment of catalyst with carbon monoxide show that one of the steps of the initiation process is the reduction of the active component. Catalysts reduced with CO at a temperature of 200°C do not contain

TABLE VI
 Effect of Reoxidation^a

| Catalyst treatment | Polymer- ization time, min | Polymeriza- tion rate at injection of inhibitor, g C ₂ H ₄ /g catalyst-hr | $n \times 10^6$, mole/g | $K_p \times 10^{-6}$, l./mole-hr |
|---|-------------------------------------|--|-----------------------------|--------------------------------------|
| Vacuum activation | 37 | 33.5 | 1.27 | 0.94 |
| Vacuum activation + reduction with CO | 15 | 100.0 | 0.90 | 4.00 |
| Oxidation of reduced catalyst + vacuum activation | 35 | 33.0 | 0.98 | 1.21 |

^a Polymerization at 75°C, ethylene pressure 15 kg/cm².

chromium with the oxidation number more than 3, but these catalysts have the same number of propagation centers as the catalyst after vacuum treatment only. Hence, one can conclude that a propagation center is a surface compound of chromium having an oxidation number not more than 3.

The formation of Cr⁺² compounds during a high-temperature reduction is also possible,⁴ but we consider that the experimental data obtained to date are insufficient for an unambiguous choice between Cr⁺³ and Cr⁺² in the propagation centers.

From our point of view the surface compounds of transition metals with the highest oxidation number serve as the active component in oxide catalysts.

The reduction is a necessary condition for formation of the propagation centers. In the case of chromium oxide catalysts activated under vacuum the reduction occurs during their interaction with the reaction medium during the initial period of polymerization. In the case of catalysts, based on W⁺⁶, Mo⁺⁶, and V⁺⁵ compounds, however, the reduction by ethylene does not proceed under mild polymerization conditions, so in this case a preliminary high-temperature reduction or the use of reducing agents (promoters) in polymerization is necessary.

The preliminary reduction by carbon monoxide results in the change of active center reactivity. We assume the change of reactivity to be due to the formation of the surface compounds of chromium where CO serves as a ligand. The data obtained when carbon monoxide labeled with ¹⁴C was used for the catalyst reduction confirm such a mechanism. After the high-temperature vacuum treatment of a catalyst reduced with ¹⁴CO a small quantity ($\sim 6.5 \times 10^{-6}$ mole/g) of strongly bonded ¹⁴CO remained on the catalyst surface. Reoxidation of reduced catalysts resulted in the elimination of radioactivity in the catalyst and decreasing reactivity of a propagation center to the value typical of the initial unreduced catalyst.

The treatment of chromium oxide catalyst by different reducing agents (SO₂, NH₃, HCN) can also change the propagation rate constant. We

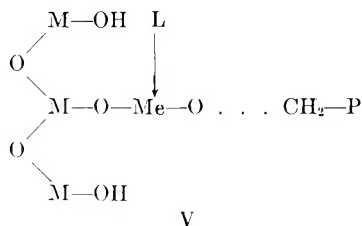
give here the results of the determination of K_p for catalyst I treated after the vacuum activation with different compounds (Table VII).

TABLE VII
Dependence of K_p on Reducing Agent^a

| Reducing agent | $K_p \times 10^{-6}$, l./mole-hr |
|-----------------|--------------------------------------|
| SO ₂ | 0.75 |
| CO | 5.0 |
| NH ₃ | 9.0 |
| HCN | 10.5 |

^a Catalyst I, polymerization at 75°C.

As in the case of catalysts reduced with CO this change of reactivity of the active center may be due to the formation of the surface chromium complexes containing reducing agents or products of its partial oxidation as ligands. The composition of the active centers of oxide catalysts may be represented by the structure V,



where L is a ligand.

CONCLUSION

The results of the influence of the catalyst composition and activation conditions on the reactivity of the propagation centers confirm the concept that propagation centers in the polymerization oxide catalysts are surface complexes in which a transition metal has one of the low oxidation numbers (see structure V). Changing the nature of the support cation M, transition metal Me, ligand L, and removing surface hydroxyls affects the reactivity of the propagation center. The structure V shows only the closest environment of the transition metal and does not show the real spatial structure of the propagation centers. In fact, all the elements composing structure V are in the sixfold or fourfold coordinations more or less distorted. However, there are as yet no exact direct data about the real spatial structure of the propagation centers in oxide catalysts up to now.

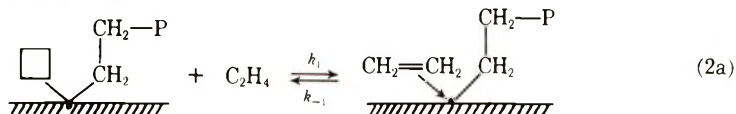
On the basis of the results obtained it is possible to suppose the following general scheme of formation of the propagation centers and the growth of the polymer chain in the ethylene polymerization with oxide catalysts.

(1) The formation of an active component of a catalyst proceeds during

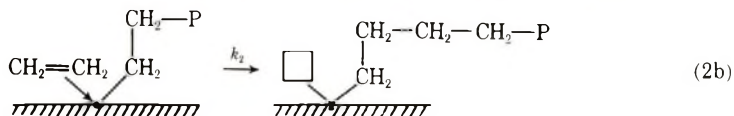
the interaction of transition metal oxide with a support. The structure of compounds thus obtained depends on the catalyst composition and its preparation conditions. In the case of chromium oxide catalysts the active component seems to be a surface chromate-type compound^{5,6} in which the chromium oxidation number is 6.

(2) When a catalyst is treated with reducing agents or interacts with the reaction medium the active component is reduced, forming a surface coordination compound with a free vacancy. Then this compound during the interaction with monomer forms the propagation center (surface compound with a carbon-catalyst active bond).

(3) The reaction of chain growth consists of two stages: (a) π -complex formation [eq. (2a)],



(where the point symbolizes an active center on the catalyst surface) and (b) insertion of the coordinated monomer into the active bond [eq. (2b)],



k_1 , k_{-1} , and k_2 are rate constants.

The mechanism of the propagation, including the monomer coordination and insertion stages, was examined by Cossee⁷ and Natta⁸ et al. for the polymerization with Ziegler-Natta catalysts.

The meaning of the value of K_p calculated by eq. (1) depends on the relative rates of the elementary stages of the propagation process. If the first stage (π -complex formation) is a reversible reaction, one can obtain for the value of K_p the general equation (3):

$$K_p = k_1 k_2 / (k_2 + k_{-1} + k_1 C_m) \quad (3)$$

We will consider three cases.

Case 1. For $k_2 \gg k_{-1} + k_1 C_m$, $K_p = k_1$, and the eq. (1) is transformed into

$$V = k_1 n C_m \quad (4)$$

Case 2. For $k_{-1} \gg k_2 + k_1 C_m$, then $K_p = K_a k_2$, where $K_a = k_1 / k_{-1}$ and K_a is an equilibrium constant for the π -complex formation. In this case:

$$V = K_a k_2 n C_m \quad (5)$$

Case 3. For $k_1 C_m \gg k_2 + k_{-1}$, then $K_p = k_2 / C_m$; in this case:

$$V = k_2 n \quad (6)$$

Equation (6) for case 3 does not correspond to the first-order propagation reaction with respect to the monomer concentration.¹⁰ Thus, assuming a two-stage mechanism of the chain growth with chromium oxide

catalyst, the propagation rate constant is either the rate constant of π -complex formation (case 1) or the product of the equilibrium constant of the first stage and the rate constant of the insertion act (case 2). The results obtained up to now are insufficient to permit one to distinguish between these two possibilities.

Regarding the data on the influence of the active center composition on reactivity, it is possible to conclude that K_p increases when one can expect an increase of the strength of the dative bond between olefin and a transition metal. On changing the transition metal from W to Mo and then to Cr, for example, it is reasonable to expect a decrease of the oxidation number of the transition metal in the propagation center and hence an increase of the π -complex stability.

An increase in electronegativity of the support cation may lead to a decrease in the positive charge on the chromium atom of the propagation center. The removal of hydroxyls of the catalyst surface appears to cause the same effect. Decreasing the positive charge on the transition metal also may increase the stability of π -complex.

It is known⁹ that the stability of π -complexes of transition metals with such ligands as CO, phosphines, etc. is much higher than that of complexes containing olefins as ligands only. It is likely that the introduction of CO or NH_3 , into the surface complexes of chromium-oxide catalyst brings about the same effect.

We think that the change of K_p measured in our experiments is due to the change of the stability of the π -complex. If $K_p = k_1$ (case 1) the increase of the strength of the bond between ethylene and the transition metal may decrease the activation energy of the first stage. If $K_p = K_a k_2$ (case 2), the propagation rate constant increases as a result of the rise of the stability constant K_a .

References

1. Yu. I. Ermakov and V. A. Zakharov, report presented at the 6th International Congress on Catalysis, Moscow; Preprint 16.
2. A. Clark, *Ind. Eng. Chem.*, **59**, No. 7, 29 (1967).
3. A. Matsumoto, H. Tanaka, and N. Goto, *Bull. Chem. Soc., Japan*, **38**, 45 (1968).
4. L. L. Van Reijen, W. M. H. Sachtler, P. Cossee, and D. M. Brower, in *Proceedings of the 3rd International Congress on Catalysis, Amsterdam 1964*, Amsterdam, 1965, p. 829.
5. T. Hill and J. Habeshaw, in *Proceedings of the 3rd International Congress on Catalysis, Amsterdam 1964*, Amsterdam, 1965, p. 975.
6. L. G. Karakchiev, Yu. I. Ermakov, and G. P. Kolovertnov, *Kinetika Kataliz*, **8**, 168 (1967).
7. P. Cossee, P. Ross, and I. H. Schachtschneider, report presented at the 6th International Congress on Catalysis, Moscow, 1968; Preprint 14.
8. G. Natta, A. Zambelli, I. Pasquon, and G. M. Ghiongo, *Chim. Ind. (Milan)*, **48**, 1296 (1966).
9. M. A. Bennet, *Chem. Rev.*, **62**, 611 (1962).
10. V. A. Zakharov and Yu. I. Ermakov, Report presented at International Symposium on Macromolecular Chemistry, Budapest, August 1969.

Received October 2, 1969

Revised December 30, 1970

Reactivity of Ethylene in the Radically Initiated Copolymerization of Ethylene with Vinylacetate*

M. RÄTZSCH, W. SCHNEIDER, and D. MUSCHE

Synopsis

The study of the literature shows that in the copolymerization of ethylene and vinylacetate there is an evident dependence on the relative reactivity of ethylene. For this change of the r -value of ethylene there are two explanations: real change of reactivity of the ethylene, or effects of heterogeneity. The experiments were carried out under pressures from 100 to 300 ats and at temperatures from 60 to 200°C, as well as under 1200-2400 ats and at 160-240°C. We find that the change of the r -value of the ethylene is caused by heterogeneity effects and the r -values obtained must be considered as apparent r -values.

INTRODUCTION

In the last years the importance of ethylene copolymers has considerably increased. The properties of these copolymers, which range from elastic via viscous to plastic products, vary in dependence of the volume on the VAc (vinylacetate) content. The fields of application are continuously expanding.

The study of the literature (Table I) shows that the composition of the copolymers of ethylene vinylacetate does not only depend on the relation of the starting monomer, but seems obviously to be dependent on the reaction conditions (pressure and temperature).

As can be seen from Table I, the r -value of the ethylene increases with increasing pressure and temperature, whereas the r -value of the vinylacetate (with exception of the paper by Erussalimsky³) remains constant.

Since below a pressure of 300 ats and above a pressure of 1200 ats the system ethylene vinylacetate has not yet been investigated, it is interesting to study the dependence of the composition of the copolymers on the reaction conditions in these pressure ranges.

With regard to the dependence of the copolymer composition on the reaction conditions, there are two explanations:

- (1) Either there is a real change of reactivity of the ethylene in dependence on pressure and temperature; or
- (2) The originating copolymers separate from the at first homogenous phase of the starting monomers (Fig. 1) and form with a part of the vinylacetate a solution in which the monomer vinylacetate becomes enriched, so

* This paper was presented at the IUPAC Meeting in Budapest.

TABLE I
Copolymerization Parameters of the System Ethylene-Vinylacetate

| r_{Eth} | r_{VAc} | $T, ^\circ\text{C}$ | p, atm | Solvent | Ref. |
|------------------|------------------|---------------------|-----------------|---------|------|
| 0.77 ± 0.04 | 1.02 ± 0.02 | 70 | 400 | Benzol | (1) |
| 0.97 ± 0.03 | 1.02 ± 0.02 | 130 | 400 | Benzol | (1) |
| 1.07 ± 0.06 | 1.08 ± 0.19 | 90 | 1050 | — | (2) |
| 1.0 ± 0.4 | 1.3 ± 0.4 | 90 | 1000 | — | (3) |
| 1.01 | 1.0 | 150 | 850 | — | (4) |
| 0.16 | 1.14 | 60 | 100 | — | (5) |
| 0.70 | 3.70 | 60 | 1200 | — | (5) |

that the subsequently resulting copolymerisates have a higher content on vinylacetate. The ethylene concentration in this liquid phase naturally depends on pressure and temperature, so that the dependence of the reactivity of the ethylene on pressure and temperature is thus altogether simulated.

Since in benzene as a solvent the heterogeneity effects mentioned under (2) must be excluded as the cause for the dependence of the copolymer composition on the reaction conditions, the copolymerization of ethylene and vinylacetate was also investigated in solution.

EXPERIMENTAL

The experiments below a pressure of 300 ats were carried out in a stainless steel agitating autoclave with a capacity of 2 liters. We worked with AIBN at 60, 80, and 85°C, with di-tert-butylperoxide at 166°C and with cumenhydroperoxide at 200°C.

The experiments at pressures above 1200 ats were carried out in a continuously operating system and at a temperature range from 180 to 240°C. The plant consisted of a tubular reactor having a volume of 9.8 liters. The compression was carried out in three stages. The vinylacetate was injected into the second stage. The initiators, being dissolved in paraffin oil, were injected directly into the reactor. Di-lauroylperoxide was used at 160–180°C, tert-butylperbenzoate at 220–240°C, mixtures of the two peroxides at 180–220°C as well as oxygen at temperatures above 220°C.

The ethylene used had a purity of 99.97% by volume, and the vinylacetate a purity of 99.97% by weight.

The yield of the polymerization tests was always below 10%. The vinylacetate content of the copolymers was determined by saponification (0.5 *n* ethanolic KOH in xylene), elementary analysis and IR-spectroscopy.

The phase diagram for the system ethylene vinylacetate was found in a 200 ml steel autoclave with circulating pump by means of sample taking.

RESULTS

Figure 2 shows the dependence of the composition of the copolymers on the composition of the starting mixture at 80°C and under pressures of 100,

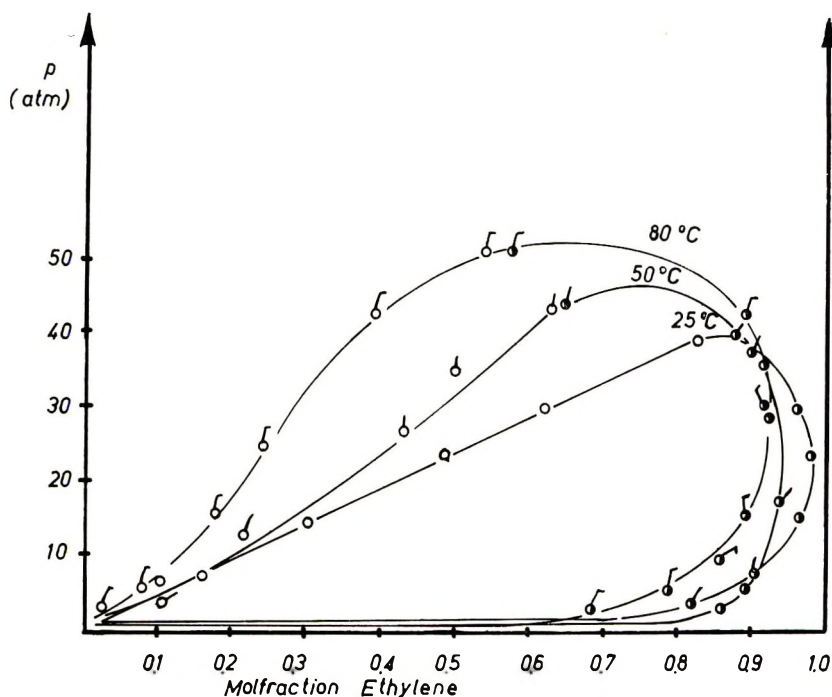


Fig. 1. Liquid-vapor equilibrium, ethylene-vinylacetate. (○) liquid phase; (●) vapor phase.

150, and 250 ats. Some values were obtained at 85°C, but the temperature difference of 5°C between the used values has in this connection only a very small influence, so that it is not to be seen in the diagram. A pressure dependence of the composition of the copolymers can be clearly seen from Fig. 2. On the one hand—independent on the pressure—the curves with VAc contents exceeding 55 mole-% in the starting mixture show that the copolymers obtained have the same composition as the starting mixture; on the other hand, the curves with a VAc content less than 55 mole-% in the starting mixture show a pressure dependence. The latter curves become flatter with increasing pressure, i.e., they tend to ideal copolymerization.

Almost only ideal copolymerization was observed with a VAc content between 10 to 30% by weight in the reaction mixture and within a pressure range above 1200 to 2400 ats, and at 180 to 240°C.

The fact that only at high VAc contents in the reaction mixture no pressure dependence of the copolymer composition could be observed, indicates that the dependence of the copolymer composition on pressure at a low vinylacetate content in the starting mixture can be traced back to the heterogeneity effects, and not to a real change of reactivity.

Figure 3 shows the dependence of the course of the copolymerization curves on temperature at a pressure of 100 ats. The same heterogeneity effects can be observed in this case. The copolymerization curves approximate to the ideal curve at increasing temperature and at the same

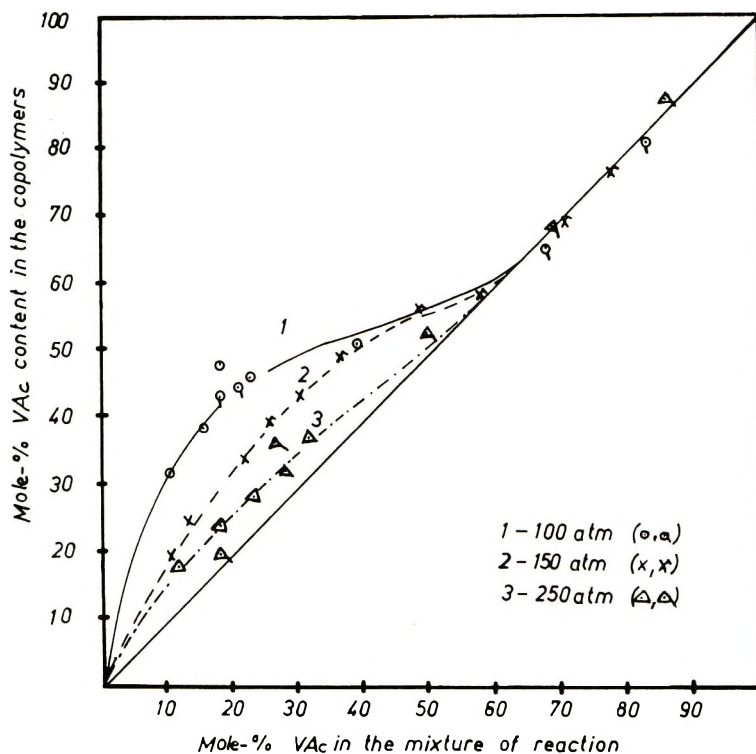


Fig. 2. Copolymerization in the bulk at 80 and 85°C of ethylene and vinylacetate.

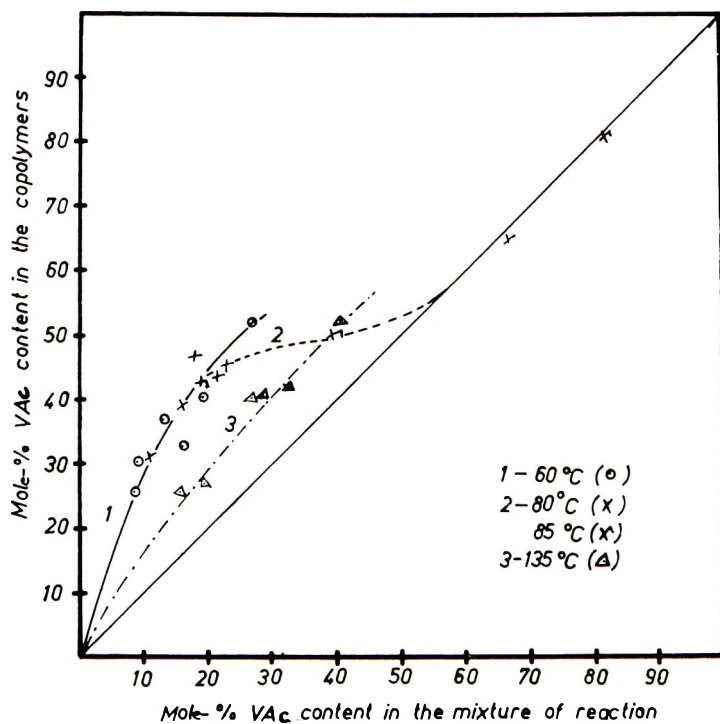


Fig. 3. Copolymerization in the bulk at 100 atm of ethylene and vinylacetate.

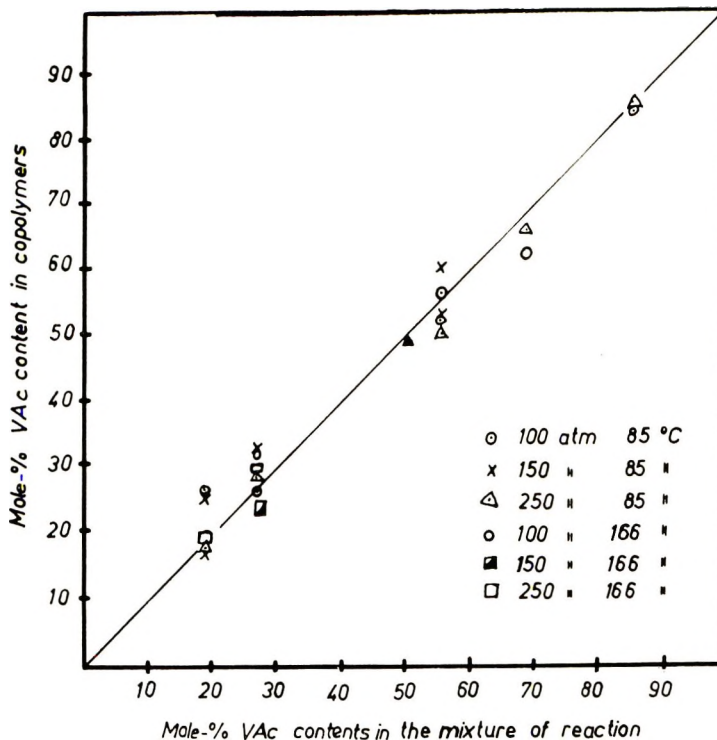


Fig. 4. Copolymerization of ethylene and vinylacetate at 85 and 166°C in benzol.

pressure; whereby also in this case the copolymer composition is independent on the temperature at a VAc content above 55 mole-% in the starting mixture.

A completely different dependence of the copolymer composition on the relation of the monomers in the starting mixture under various pressures and at temperatures of 85°C and 166°C is indicated in the copolymerization in benzene as a solvent. The copolymerization diagram is shown in Fig. 4. In the whole range of the composition, no pressure dependence of the copolymer composition was observed at pressures of 100, 150, and 250 ats, and temperatures of 85°C and 166°C, when the copolymerization was carried out in benzene. This result supports the assumption that the pressure dependence of the copolymer composition is in fact a case of heterogeneity effects.

A temperature-dependent change of the copolymer composition at a copolymerization in benzene below a pressure of 300 ats was not observed and is thus in contradiction to the results of Terterjan, who found an increase of the r -value of the ethylene under a pressure of 400 ats, and at a temperature change from 70 to 130°C (Table II).

By evaluating the experimental results according to Fineman and Ross⁷ and Mayo and Lewis,⁸ the values in Table II were obtained. The values obtained in this way must be considered as apparent r -values (r'), as they were obtained under test conditions which, owing to the appearance of the homogeneity effects, do not satisfy the copolymerization. As indicated in

TABLE II
Copolymerization Parameters of the System Ethylene-Vinylacetate

| r'_{Eth} | r'_{VAc} | $T, ^\circ\text{C}$ | p, atm |
|-------------------|-------------------|---------------------|-----------------|
| 0.16 | 1.12 | 60 | 100 |
| 0.18 | 1.05 | 80 | 100 |
| 0.49 | 1.02 | 135 | 100 |
| 0.45 | 1.0 | 60 | 150 |
| 0.47 | 1.0 | 80 | 150 |
| 0.52 | 1.02 | 60 | 250 |
| 0.67 | 0.95 | 80 | 250 |
| 0.73 | 1.0 | 135 | 250 |
| 0.85 | 1.02 | 166 | 245 |
| 0.83 ^a | 0.96 ^a | 166 | 245 |
| 0.89 | 1.0 | 200 | 250 |
| 0.84 ^a | 0.93 ^a | 200 | 250 |
| 1.2 | 1.1 | 160 | 1200 |
| 1.2 | 1.1 | 210 | 1200 |
| 1.2 | 1.1 | 220-240 | 2000 |
| 1.2 | 1.1 | 220-240 | 2400 |

^a By evaluating according to Mayo and Lewis.

Table II, the apparent r -value of the ethylene increases continuously with the pressure and the rising temperature and approaches to value 1, while the r' -value of the vinyl acetate remains almost unchanged. The same dependence is also indicated in the quoted literature values, whereby the r -value of the vinyl acetate with $r = 3.70$ at 60°C and a pressure of 1200 atms quoted by Erussalimsky, is inexplicably high and should be checked once more.

References

1. R. A. Terterjan, A. J. Dinzes, and M. W. Rüsakow, *Neftekhimiya V*, **3**, 340 (1965).
2. N. L. Zutty and R. D. Burkhart, *Polymerization and Polycondensation Processes*, Amer. Chem. Soc., Washington, 1962, p. 57; *J. Polym. Sci. A*, **1**, 1137 (1963).
3. US Patent 3,168,456 (1965).
4. F. E. Brown and G. E. Ham, *J. Polym. Sci. A*, **2**, 3623 (1964).
5. B. Erussalimsky, N. Tumarkin, F. Duntoff, and S. Lyubetzky, *Makromol. Chem.*, **104**, 288 (1967).
6. M. Rätzsch and M. Triller, unpublished paper.
7. M. Fineman and S. D. Ross, *J. Polym. Sci.*, **5**, 259 (1950).
8. F. R. Mayo and F. M. Lewis, *J. Amer. Chem. Soc.*, **66**, 1594 (1944).

Received January 23, 1970

Revised August 18, 1970

Structure of Chlorinated Poly(vinyl Chloride).

I. Determination of the Mechanism of Chlorination from Infrared and NMR Spectra

M. KOLÍNSKÝ, D. DOSKOČILOVÁ, B. SCHEIDER, and J. ŠTOKR, *Institute of Macromolecular Chemistry, Czechoslovak Academy of Sciences, Prague*, E. DRAHORÁDOVÁ, *Institute of Physical Chemistry, Czechoslovak Academy of Sciences, Prague*, and V. KUŠKA, *Institute of Petrochemistry, Nováky, Czechoslovakia*

Synopsis

Infrared and NMR spectra of chlorinated poly(vinyl chloride) (CPVC) and of chlorinated α -deuterated poly(vinyl chloride) (α -*d*-CPVC) have been measured. It was found that the CDCl_2 unit of α -*d*-PVC does not undergo chlorination. By assuming an analogous mechanism of chlorination in normal PVC, the populations of all the three possible types of two-carbon sequences ($-\text{CH}_2-\text{CHCl}-$, $-\text{CHCl}-\text{CHCl}-$, $-\text{CHCl}-\text{CCl}_2-$) in CPVC could be determined. The mechanism of chlorination of PVC is discussed from the viewpoint of the previous findings on the conformational structure of this polymer. Differences in structure between suspension- and solution-chlorinated PVC have been established.

Chlorinated poly(vinyl chloride) (CPVC) prepared by conventional chlorination procedures contains a maximum of about 72.5% Cl. This chlorine content corresponds to the addition of one Cl atom per monomer unit of PVC. The structure of CPVC has been studied by infrared and NMR spectra by many authors.¹⁻⁹ In these papers the authors tried to decide, whether chlorination takes place on CH_2 or CHCl groups and to determine the distribution of Cl atoms in the chain. A consistent introduction of the assumption that only one additional Cl atom can enter one monomeric unit leads to the expectation of only three types of two-carbon units in CPVC, namely, $-\text{CH}_2-\text{CHCl}-$, $-\text{CHCl}-\text{CHCl}-$, and $-\text{CH}_2-\text{CCl}_2-$; attempts have been made to identify these three types of units in CPVC by spectroscopic methods.^{2,9} For the determination of two-carbon or three-carbon sequences by infrared spectra, scissoring vibrations of CH_2 groups have been analyzed,² and the intensity ratio of CH_2 (sciss) at 1428 cm^{-1} to the CHCl (def) at 1195 cm^{-1} has also been used.⁴ NMR studies of the structure of CPVC have been based on the determination of the intensity ratio of the CH_2 and CHCl bands,^{7,8,10} and the assumption that not more than one Cl atom can enter one monomeric unit was likewise applied in their evaluation.⁷

None of these papers has succeeded in determining unequivocally if the above-mentioned assumption (one Cl per monomer unit) was valid, and if chlorination took place in the CH_2 or CHCl group. Therefore we attempted to solve these questions by the analysis of infrared and NMR spectra of α -*d*-CPVC.

EXPERIMENTAL

Commercial suspension poly(vinyl chloride) (PVC) of *K* value 71 was dissolved in tetrahydrofuran and precipitated by methanol. The Cl content was 56.8%. Poly(vinylidene chloride)¹¹ was obtained by polymerization in inert medium at 50°C to ca. 5% conversion from refined and freshly redistilled vinylidene chloride. It was initiated by 2×10^{-3} mole/l. of azobisisobutyrate methyl ester. The Cl content was 72.68%. The sample of vinyl chloride–vinylidene chloride copolymer was commercial Saran B (15% VC + 85% VDC) precipitated from trichlorobenzene with methanol. The Cl content was 64.76%.

Powdered PVC was chlorinated with gaseous chlorine by two methods:¹² (a) in water–chloroform suspension (1:7) under stirring at 50°C (samples 1–9, containing 0–71.7% Cl, Table I); (b) in carbon tetrachloride solution (samples A–F, containing 0–69.6% Cl, Table I). Various commercial samples of CPVC included in Table I were precipitated from tetrahydrofuran solution by methanol.

Deuterated vinyl chloride was prepared by the method of Francis et al.¹³ 1,1-Dichloro-2-bromoethane-*d*-1 was obtained by addition of DBr to vinylidene chloride at –75°C under ultraviolet irradiation. This was dehalogenated by Zn in ethanol, yielding crude α -*d*-vinyl chloride. After rectification the pure product had a bp –13.1°C at atmospheric pressure. The Purity was followed chromatographically.

α -*d*-PVC was prepared by two methods. Suspension-polymerized α -*d*-PVC was prepared by polymerization of α -*d*-vinyl chloride in aqueous medium (ratio 1:2), with an addition of methocel and with dilauroyl peroxide as initiator at 50°C; conversion was 80%. Block-polymerized α -*d*-PVC was initiated by 5×10^{-3} mole/l. of azobisisobutyrate methyl ester and polymerized at 50°C with stirring; conversion was 55%. The Cl content was 54.6% Cl; deuteration in the α -position was 96% (by NMR). This polymer was used in most experiments, but no appreciable difference between the results obtained with block- and suspension-polymerized α -*d*-PVC was observed.

α -Deuterated chlorinated poly(vinyl chloride) (α -*d*-CPVC) was prepared by chlorination in water–chloroform suspension,¹² as described above for PVC. Parallel chlorination series were run in H_2O and D_2O suspension in order to check for possible deuterium–hydrogen exchange during chlorination. As no appreciable difference between the two series was observed, such exchange is assumed to be absent.

Chlorine was determined by the standard method of Schöniger¹⁴ as

modified by Petránek and Ryba.¹⁵ All reagents and solvents used were purified and redistilled.

For the determination of deuterium in α -*d*-PVC and α -*d*-CPVC, the polymer was subjected to combustion in a stream of oxygen, and the ratio D_2O/H_2O in the combustion products was determined by mass spectrometry.¹⁶

For measurement of NMR spectra, 15% (w/v) solutions of the samples in $SOCl_2$ were prepared, with hexamethyldisiloxane as internal standard. The $SOCl_2$ was purified chemically and freshly distilled onto the degassed sample in the measuring cell which was then sealed under nitrogen. The sealed cell was then heated to 100°C for several hours under slow rotation, until complete homogenization. NMR spectra were measured at 100°C on the JEOL-3-60 spectrometer operating at 60 Mcps.

Infrared spectra of CPVC were measured on the Zeiss UR-10 spectrometer by the KBr pellet technique using the same weight concentration of polymer (15 mg per pellet) in all samples. The spectra of the original samples exhibited a high background which could be removed by reprecipitation of the samples from a cyclohexanone solution with methanol. The chlorine content was not affected by this reprecipitation, and in all quantitative infrared studies, these reprecipitated samples were used.

RESULTS

Deuterium Content of α -*d*-CPVC

Infrared spectra of α -*d*-PVC chlorinated to a various degree were measured and two typical spectra are shown in Figure 1. It was observed that the intensity of the C-D stretching band at 2200 cm^{-1} does not decrease upon chlorination. This was surprising, because even if chlorine did not enter the $CDCl$ group, the intensity of the C-D stretching band would be expected to decrease somewhat in samples of equal weight concentration. Our observation could only be explained by the assumption that the absorbance differs in samples of different chlorine content. For this reason, infrared spectroscopy appeared unsuitable for the determination of deuterium, and the deuterium content of α -*d*-PVC and various samples of α -*d*-CPVC was therefore determined by mass spectrometry. By this method, in all samples of α -*d*-CPVC (58.3–67.8% Cl), the deuterium content was constant and equal to that of α -*d*-PVC within experimental error ($\pm 2\%$).

Determination of the Content of CH_2 , $CHCl$, and CCl_2 Groups from the Ratio CH_2/CH

NMR Spectra. As in NMR spectra of PVC, in CPVC the regions of CH_2 and CH bands are also clearly separated (Fig. 2). The bands at higher τ values (8.88–6.53) correspond to methylene group protons, bands

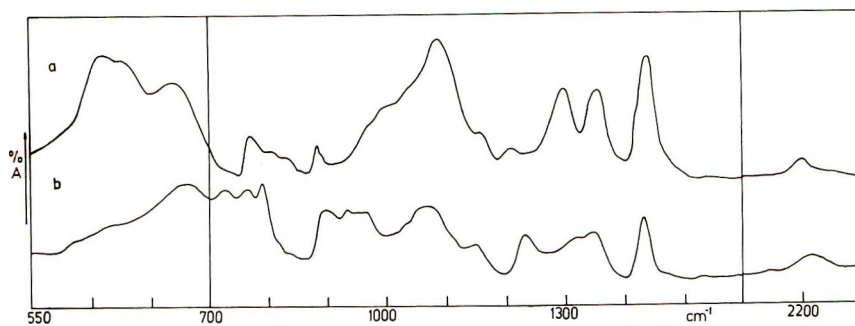


Fig. 1. Infrared spectra of α -deuterated poly(vinyl chloride): (a) α -d-PVC; (b) α -d-CPVC ($j = 0.71$).

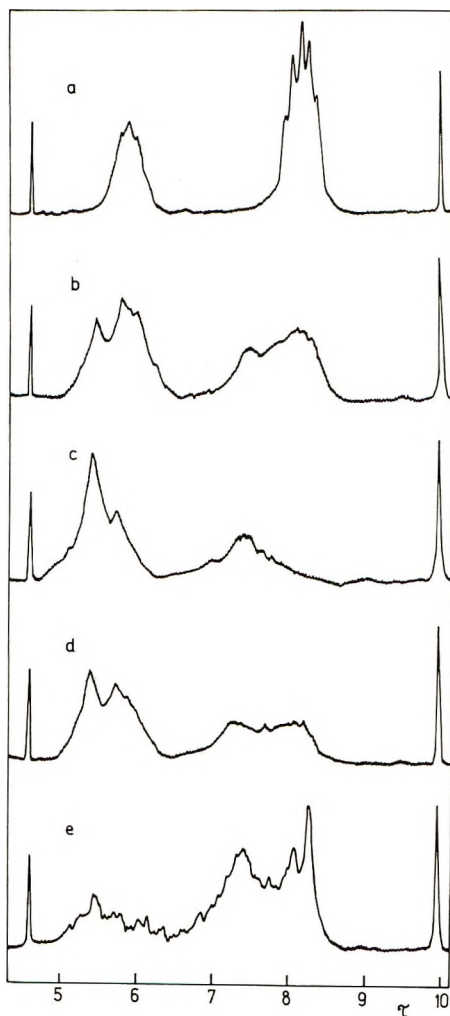


Fig. 2. NMR spectra of chlorinated poly(vinyl chloride): (a) PVC; (b) CPVC-6 ($j = 0.72$); (c) CPVC-D ($j = 0.70$); (d) CPVC-8 ($j = 0.91$); (e) α -d-CPVC ($j = 0.71$).

at lower τ values (6.53–4.80) correspond to CHCl groups. For the determination of the ratio CH₂/CHCl, the integrated areas of both these band groups have been determined. The upper integration limits of both these band groups coincide with the upper limits of the corresponding bands in PVC. With increasing degree of chlorination, both the CH₂ and CHCl bands broaden and shift to lower τ values. By measurement of the spectra of poly(vinylidene chloride) and of the vinyl chloride–vinylidene chloride copolymer in SOCl₂ solution, the CH₂ band of the —CCl₂—CH₂—CCl₂— group was found to lie at 6.52 τ , i.e., somewhat lower than would correspond to the above indicated lower limit of the CH₂ band group. From the fact that the spectra of all our samples of CPVC exhibit a minimum around 6.5 τ it can be concluded that the content of polyvinylidene type units in our samples is negligible, and that the upper limit of the CHCl band region in PVC can be simultaneously considered as the lower limit of the CH₂ band group in CPVC.

From the ratio of the CH₂ and CHCl band areas ($2R$) and from the analytical chlorine content, the populations of all the three one-carbon groups, CH₂ (x), CHCl (y) and CCl₂ (z) can be determined by means of eqs. (1)–(7)

$$R = [x]/[y] \quad (1)$$

$$j = (a_{\text{CPVC}} - a_{\text{PVC}})/73.2 - a_{\text{PVC}} \quad (2)$$

$$[y_0] + [d] = 0.5 \quad (3)$$

$$[x] + [y] + [z] = 1 - [d] \quad (4)$$

$$[x] = R(3 - j - 2[d])/2(2R + 1) \quad (5)$$

$$[y] = (3 - j - 2[d])/2(2R + 1) \quad (6)$$

$$[z] = 1 - [d] - [x] - [y] \quad (7)$$

where a is the weight content of Cl in the respective polymer, j is the molar content of additional Cl (referred to one monomeric unit) which entered the chain upon chlorination, $[y_0]$ is the molar content of CHCl groups in unchlorinated PVC and $[d]$ is the molar content of CCl groups in α -d-PVC. The obtained values of $[x]$, $[y]$, and $[z]$ for suspension- and solution-chlorinated PVC are shown in Table I and for suspension-chlorinated α -d-PVC in Table II. All these results are summarized in Figure 3.

Infrared Spectra. As in the work of Fredericsson and Crowo,⁴ the ratio R of CH₂ and CH groups was obtained from the bands at 1430 (CH₂ sciss.) and 1200 cm⁻¹ (CHCl def.) (Fig. 4). Maximum absorbances were used, and the ratio of extinction coefficients was determined from NMR spectra. The determination of R by NMR and infrared spectra is compared in Figure 5. The results agree well for both the suspension- and solution-chlorinated PVC.

TABLE I
Structure of Various Samples of Chlorinated Poly(vinyl Chloride)^a

| Sample | j | R | x | y | z | xy | yy | yz |
|----------------------|------|------|------|------|------|------|---------|------|
| PVC | 0.00 | 1.00 | 0.50 | 0.50 | 0.00 | 1.00 | 0.00 | 0.00 |
| CPVC-1 | 0.11 | 0.98 | 0.48 | 0.51 | 0.03 | 0.96 | (-0.02) | 0.06 |
| CPVC-2 | 0.23 | 0.86 | 0.44 | 0.51 | 0.05 | 0.88 | 0.02 | 0.10 |
| CPVC-3 | 0.41 | 0.72 | 0.38 | 0.53 | 0.09 | 0.76 | 0.06 | 0.18 |
| CPVC-4 | 0.57 | 0.62 | 0.34 | 0.54 | 0.12 | 0.68 | 0.08 | 0.24 |
| CPVC-5 | 0.65 | 0.57 | 0.31 | 0.55 | 0.14 | 0.62 | 0.10 | 0.28 |
| CPVC-6 | 0.72 | 0.49 | 0.28 | 0.58 | 0.14 | 0.56 | 0.16 | 0.28 |
| CPVC-7 | 0.84 | 0.44 | 0.25 | 0.58 | 0.17 | 0.50 | 0.16 | 0.34 |
| CPVC-8 | 0.91 | 0.38 | 0.23 | 0.59 | 0.18 | 0.46 | 0.18 | 0.36 |
| CPVC-A | 0.46 | 0.54 | 0.33 | 0.62 | 0.05 | 0.66 | 0.24 | 0.10 |
| CPVC-B | 0.58 | 0.33 | 0.24 | 0.73 | 0.03 | 0.48 | 0.46 | 0.06 |
| CPVC-C | 0.64 | 0.37 | 0.25 | 0.68 | 0.07 | 0.50 | 0.36 | 0.14 |
| CPVC-D | 0.70 | 0.29 | 0.21 | 0.73 | 0.06 | 0.42 | 0.46 | 0.12 |
| CPVC-E | 0.79 | 0.25 | 0.18 | 0.74 | 0.08 | 0.36 | 0.48 | 0.16 |
| CPVC-F | 0.79 | 0.25 | 0.18 | 0.74 | 0.08 | 0.36 | 0.48 | 0.16 |
| Rhenoflex (FRG) | 0.25 | 0.75 | 0.41 | 0.55 | 0.04 | 0.82 | 0.10 | 0.08 |
| Trovidur HT (FRG) | 0.50 | 0.58 | 0.34 | 0.58 | 0.08 | 0.68 | 0.16 | 0.16 |
| PC-Smola (USSR) | 0.29 | 0.72 | 0.40 | 0.56 | 0.04 | 0.80 | 0.12 | 0.08 |
| PC-Pulver (GDR) | 0.29 | 0.76 | 0.41 | 0.54 | 0.05 | 0.82 | 0.08 | 0.10 |

^a Samples CPVC 1-8 chlorinated in suspension, samples CPVC A-F chlorinated in solution.

TABLE II
Structure of Various Samples of Chlorinated α -*d*-Poly(vinyl Chloride)

| j | R | x | y^a | z | xy^b | yy^b | yz^b |
|------|------|------|-------|------|--------|--------|--------|
| 0.20 | 4.04 | 0.41 | 0.10 | 0.01 | 0.82 | 0.16 | 0.02 |
| 0.32 | 2.90 | 0.37 | 0.13 | 0.02 | 0.74 | 0.22 | 0.04 |
| 0.38 | 2.70 | 0.35 | 0.13 | 0.04 | 0.70 | 0.22 | 0.08 |
| 0.44 | 2.28 | 0.33 | 0.14 | 0.05 | 0.66 | 0.24 | 0.10 |
| 0.50 | 2.11 | 0.31 | 0.15 | 0.06 | 0.62 | 0.26 | 0.12 |
| 0.51 | 1.72 | 0.30 | 0.17 | 0.05 | 0.60 | 0.30 | 0.10 |
| 0.53 | 1.62 | 0.28 | 0.17 | 0.07 | 0.56 | 0.30 | 0.14 |
| 0.60 | 1.44 | 0.27 | 0.19 | 0.06 | 0.54 | 0.34 | 0.12 |
| 0.65 | 1.17 | 0.24 | 0.21 | 0.07 | 0.48 | 0.38 | 0.14 |
| 0.71 | 1.06 | 0.23 | 0.22 | 0.07 | 0.46 | 0.40 | 0.14 |

^a y = content of CHCl groups only.

^b y = sum of CHCl + CDCl groups, with content of CDCl constant and equal to 0.48 in the whole series.

DISCUSSION

The content of the one-carbon units CH₂, CHCl, and CCl₂ in normal CPVC ($[d] = 0$) can be obtained from the analytical Cl content and ex-

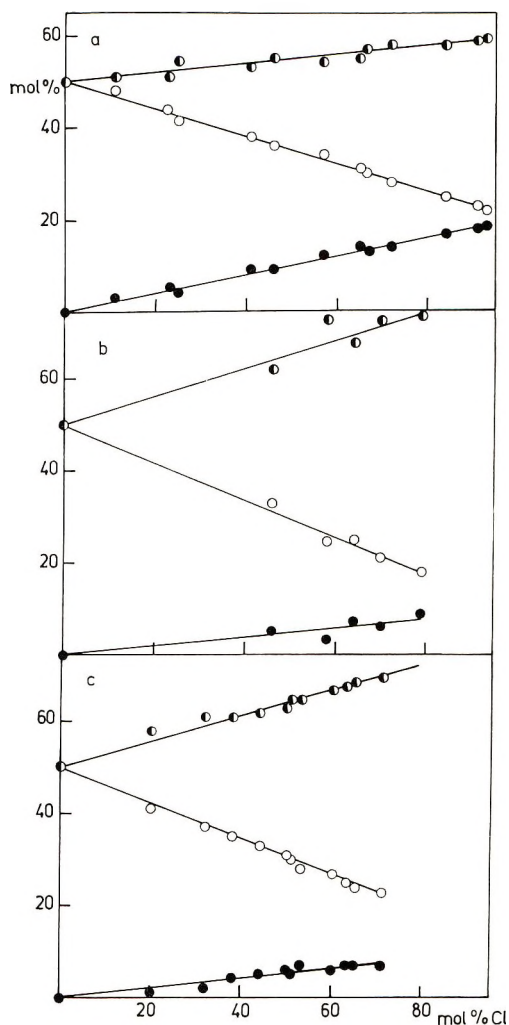


Fig. 3. Content of (○) CH_2 , (◐) CHCl , and (●) CCl_2 groups in chlorinated poly(vinyl chloride): (a) suspension-chlorinated CPVC; (b) solution-chlorinated CPVC; (c) suspension-chlorinated α -d-CPVC. Here y is defined as the sum of $\text{CHCl} + \text{CDCl}$ groups, with the content of CDCl groups being constant and equal to 0.48 in the whole series. Both block polymerized and suspension polymerized samples are included.

perimental NMR or infrared CH_2/CH values, without any additional data or assumptions about the chlorination mechanism, and may be used for the basic characterization of the various chlorinated samples. From Table I it is seen that the structure of suspension- and solution-chlorinated CPVC of equal chlorine content differs considerably. Suspension-chlorinated CPVC contains more CCl_2 groups than the solution-chlorinated samples. The differences in the range of C-Cl stretching frequencies in infrared spectra of suspension- and solution-chlorinated PVC with comparable chlorine content also confirm a difference in distribution of Cl atoms in

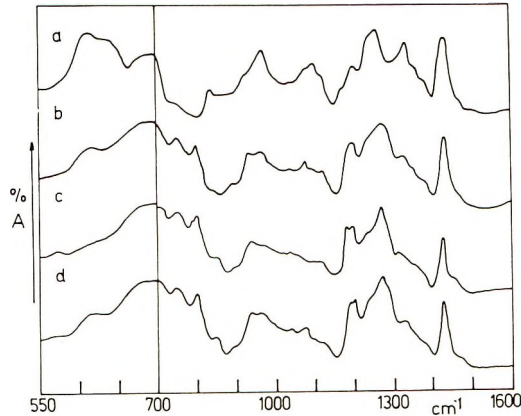


Fig. 4. Infrared spectra of chlorinated poly(vinyl chloride): (a) PVC; (b) CPVC-6 ($j = 0.72$); (c) CPVC-D ($j = 0.70$); (d) CPVC-8 ($j = 0.91$).

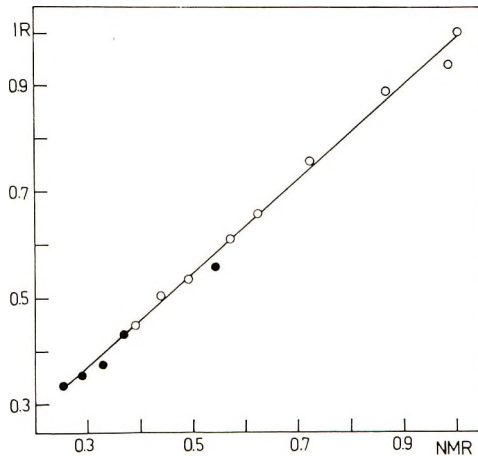


Fig. 5. Comparison of values of R (CH_2/CH) as determined by NMR and infrared spectra: (○) suspension-chlorinated; (●) solution-chlorinated.

both cases. Surprisingly enough, the structure of our α -*d*-CPVC, which was chlorinated in suspension, resembles more closely that of solution-chlorinated CPVC (Table II). We assume that this might be caused by differences in polymer structure prior to chlorination.

Determination of the relative amounts of CH_2 , CHCl , and CCl_2 groups makes possible the differentiation of various types of CPVC, but does not yield any information about the mechanism of chlorination. All previous considerations of the mechanism of chlorination were based on the well established experimental finding that CPVC with more than 72.5% Cl cannot be prepared. This was usually explained by one of two assumptions: either that one C atom can carry only one Cl atom, or that one monomeric unit can add only one Cl atom.

Because of the experimentally determined presence of the CCl_2 group, the first assumption cannot be valid. Our present experimental finding that the deuterium content of α -*d*-PVC does not change upon chlorination

indicates that chlorine cannot enter the CDCl group and therefore probably also not the CHCl group of original PVC. Together with the proved existence of CCl_2 groups in CPVC, this rules out the second assumption, and permits the appearance of the $-\text{CHCl}-\text{CCl}_2-$ group, with two additional chlorine atoms in one monomeric unit. Independent evidence for the appearance of this group has also been obtained by pyrolysis and gas chromatography.¹⁷ Constancy of deuterium content upon chlorination also rules out the presence of the polyvinylidene type unit, $-\text{CH}_2-\text{CCl}_2-$, which is moreover excluded by NMR evidence. Only the following three types of two-carbon sequences can therefore appear in CPVC: $-\text{CH}_2-\text{CHCl}-$, $-\text{CHCl}-\text{CHCl}-$, and $-\text{CHCl}-\text{CCl}_2-$.

From a purely chemical point of view, there seems to be no reason why the CHCl group could not be chlorinated.¹⁸ The impossibility of the chlorination of the CHCl group can only be given by steric reasons. In our studies of PVC model compounds¹⁹⁻²¹ it has been established that in the major conformers staggered bond angles are preserved, and forms carrying two large substituents ($\text{Cl}-$, $-\text{CH}_2-$) in γ position with parallel $\text{C}-\text{Cl}$ or $\text{C}-\text{C}$ bonds (Fig. 6) do not appear. Chlorination of the CHCl group would always lead to the formation of at least two $\text{C}-\text{Cl}$ or $\text{C}-\text{C}$ bonds in such a forbidden orientation. The experimental finding that chlorine does not enter the CHCl group of PVC is therefore in full agreement with the known conformational structure of PVC model compounds.

On the other hand, one Cl atom can enter the CH_2 group of both syndiotactic and isotactic PVC without any steric hindrance at all. Two atoms of Cl can enter CH_2 groups which are part of syndiotactic (ss) or heterotactic (si) triads. Of course, even in the chlorination of the CH_2 group, the above steric rule must be maintained. Because of this, if two atoms of Cl have entered one CH_2 group, the neighboring group cannot be chlorinated at all. If only one Cl atom has entered the CH_2 group, the neighboring group can be chlorinated, but only by one Cl atom.

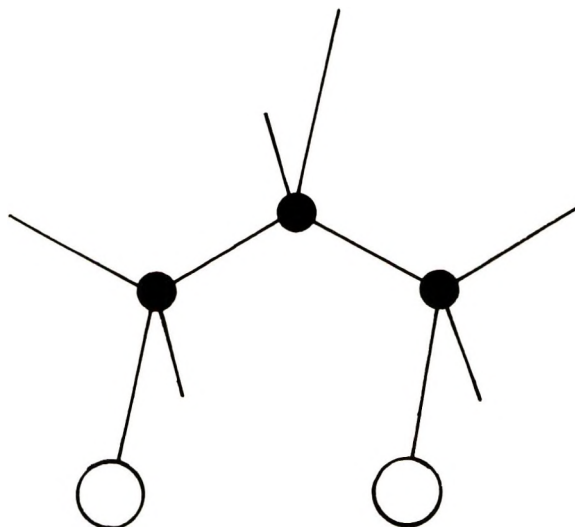


Fig. 6. Forbidden structure of a CPVC unit: (●) C atom; (○) Cl or C atom.

The proposed mechanism of chlorination of PVC can most simply be defined so that only two atoms of Cl can enter into two neighboring monomeric units of the original PVC (sequence $xyxy$), and always only into CH_2 groups. Of the various possible four-carbon sequences, only the types $yyxy$, $yyyy$ and $zyxy$ can therefore appear. In the chain, these can combine in different ways, but always observing the above steric rule. Based on this mechanism, from the experimentally determined values of x , y , and z , the populations of all permitted two-carbon sequences xy , yy , and yz can be calculated from the relations

$$[x] = 1/2 [xy] \quad (8)$$

$$[y] = 1/2 [xy] + [yy] + 1/2 [yz] \quad (9)$$

$$[z] = 1/2 [yz] \quad (10)$$

and are given in the last three columns of Table I for CPVC and of Table II for α -d-CPVC. From Table I, suspension-chlorinated CPVC is seen to contain more $-\text{CHCl}-\text{CHCl}_2-$ groups than the solution-chlorinated samples which must therefore contain longer sequences of $-\text{CHCl}-$ groups. Determination of longer than two-carbon sequences will be the subject of a subsequent communication.

References

1. H. Fuchs and D. Louis, *Makromol. Chem.*, **22**, 1 (1957).
2. H. Germar, *Makromol. Chem.*, **86**, 89 (1965).
3. Y. Fukawa, S. Takatono, M. Matsui, and H. Okado, *Kogyo Kagaku Zasshi*, **65**, 284 (1962).
4. O. Frederiksen and J. A. Crowe, *Makromol. Chem.*, **100**, 231 (1967).
5. H. Kaltwasser and W. Klose, *Plaste Kautschuk*, **13**, 515 (1966).
6. H. Kaltwasser and W. Klose, *Plaste Kautschuk*, **13**, 583 (1966).
7. J. Petersen and B. Rånby, *Makromol. Chem.*, **102**, 83 (1967).
8. S. Sobajima, N. Takagi, and H. Watase, *J. Polym. Sci. A-2*, **6** 223 (1968).
9. G. di Svegliado and F. Z. Grandi, *J. Appl. Polym. Sci.*, **13**, 1113 (1969).
10. P. Q. Tho and P. Berticat, *Europ. Polym. J.*, **4**, 265 (1968).
11. Z. Macháček, *Chem. Listy*, **49**, 1448 (1955).
12. V. Heidingsfeld, V. Kuška, and J. Zelinger, *Angew. Makromol. Chem.*, **3**, 141 (1968).
13. J. E. Francis and L. C. Leitch, *Can. J. Chem.*, **35**, 500 (1957).
14. W. Schöninger, *Microchim. Acta*, **1**, 123 (1955).
15. J. Petránek and O. Ryba, *Coll. Czech. Chem. Commun.*, **29**, 2847 (1964).
16. J. Petránek and M. Ryska, *Special Volume Tech. Univ. of Pardubice*, 1970.
17. S. Tsuge, T. Okumoto, and T. Takeuchi, *Macromolecules*, **2**, 277 (1969).
18. G. Natta and E. Mantica, *J. Amer. Chem. Soc.*, **74**, 3152 (1952).
19. D. Doskočilová, J. Štokr, B. Schneider, H. Pivcová, M. Kolínský, J. Petránek, and D. Lim, in *Macromolecular Chemistry, Prague 1965 (J. Polym. Sci. C, 16)*, D. Wichterle and B. Sedláček, Eds., Interscience, New York, 1967, p. 215.
20. B. Schneider, J. Štokr, D. Doskočilová, S. Sýkora, J. Jakesš, and M. Kolínský, in *Macromolecular Chemistry, Brussels-Louvain 1967 (J. Polym. Sci. C, 22)* G. Smets, Ed., Interscience, New York, 1969, p. 1073.
21. J. Štokr, S. Dirlikov, B. Obereigner, and B. Schneider, *J. Mol. Structure*, in press.

Received August 10, 1970

Revised October 7, 1970

NOTES

Polycondensation of Resin-Acid Dimers with Diamines

It has been previously reported¹ that abietic acid (I) can be dimerized in good yields when acid-catalyzed dimerization is closely controlled. Of further interest is the purification and the use of these diabetic acids in preparing polyamides with multifunctional amines. Floyd² has reported the polycondensation of multifunctional amines with combinations of dimerized rosin and polymeric fatty acids. The resulting polyamides were tailored to be low \overline{DP} polyamides suitable as epoxy curing agents.

Purification of Diabetic Acid

The crude diabetic acids from the dimerization reaction¹ have the following typical properties: dimeric species by GC, 81.0%; acid, as abietic acid, 83.3%; Fisher-Johns softening, 140–150°C; ring and ball softening, 154.5°C. The properties, while sufficient for certain commercial applications, are inadequate for polycondensation to high polymer. Insofar as is known, no report has been made of truly high-purity, monomer-free diabetic acids. The approximately 20% monomeric species as measured by gas chromatography must necessarily be eliminated if polymer of high \overline{DP} was to be obtained. A good method for purification of the crude diabetic acids was provided by heating *in vacuo* at 260°C three times for approximately 1 hr in a sublimator having a 2-cm distillation path. The volatile portions were rejected, and the nonvolatile residue was collected for use in the subsequent polycondensations. At a pressure of 0.05–0.2 torr, the purification is slow at 250°C, and at 270°C the formation of anhydride linkages became detectable in the infrared spectra. The distillation yielded a nonvolatile fraction of the following properties: dimeric species by GC, 98.3%; acid, as abietic acid, 90.6%; Fisher-Johns softening, 198–203°C; the infrared showed detectable anhydride moieties.

This purified material was then examined in more detail for its suitability for use in polycondensation processes. The following characterizations were obtained on the purified dicarboxylic products.

pK_a observed in 50:50 tetrahydrofuran–methanol was 9.20. By comparison pK_a 's of acetic acid and abietic acid under the same conditions were 7.85 and 8.91, respectively. Correction to a value in aqueous media (by using the known pK_a of acetic acid of 4.75) yields pK_a 's of 5.81 and 6.10 for abietic and resin-acid dimers, respectively. Only one inflection point was observed for the resin-acid dimers from pH's 4 to 11. Hence, all carboxyl groups of the resin-acid dimers must be equivalent.

The infrared spectra of typical, crude reaction products from a dimerization were compared to those of the resin-acid dimers. A typical reaction product before purification shows: moderate absorption at 5.63 μ (probably lactone), weak absorption at 5.77 μ (possibly anhydride), weak absorption at 6.69 μ (aromatic), strong absorption at 13.2 μ (possibly aromatic absorption by dehydroabietic acid). The assignments are generally in agreement with those of Hummel and Pohl.³ By contrast the purified dimer fraction exhibits only detectable anhydride absorption at the above wavelengths. Its infrared spectrum is typical of an aliphatic, carboxylic acid with hydroxyl absorption and hydrogen bonding from 2.6 to 4.2 μ , strong carboxyl absorption at 5.90 μ , and a shoulder at 6.2 μ (possibly conjugated diene absorption).

The ultraviolet spectrum has a maximum at 251 m μ with a molar extinction coefficient of 1.09×10^4 in methanol solvent. A molecular weight of 605 was used for calculation of the extinction coefficient. A small portion, approximately 10% of the dimer fraction

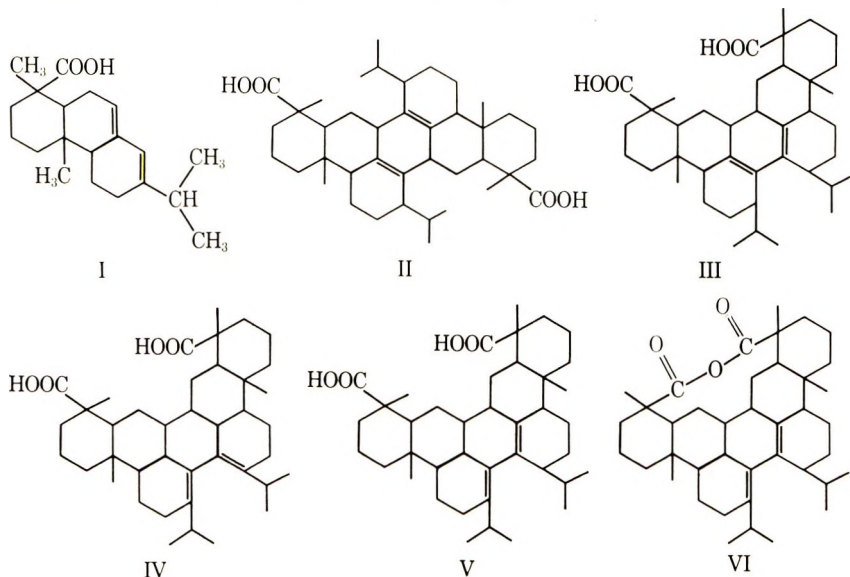
was found to be insoluble in methanol. The ultraviolet spectrum of this material was obtained in tetrahydrofuran solution, and the extinction coefficient and shape of the spectrum was the same, within experimental error, as that obtained with the methanol-soluble material.

The nuclear magnetic resonance spectrum of the dimer fraction suggested a mixture of compounds.

Thin layer chromatography revealed the dimer was composed of at least three structures which were not monomer.

The dimer region of the gas chromatograms¹ of crude diabetic acid products was analyzed by mass spectrometry after methylation by diazomethane. The dimer region has at least 12 components. Samples at three points in the dimer portion of the chromatogram revealed the expected value of 632 for the mass-to-charge ratio.

Thus, the resin-acid dimers appear to be a mixture of related compounds possessing conjugated diene structures. Bardyshev reports a similar conclusion and finds a molar extinction coefficient at 251 $m\mu$ equal to 19840.⁴ Brus and co-workers⁵ have postulated that abietic acid (I) dimerized to structure II. Morillon⁶ postulated either II or III. Bardyshev and Strizhakov⁴ concluded that diabetic acid is more probably IV or V, more likely V. It seems probable that the purified materials we have obtained by somewhat different means are actually a number of structural isomers. The anhydride absorption may be attributable to abietic anhydride or, alternatively, to the internal anhydride VI reported by Bardyshev and Strizhakov.⁴ It would be expected



that VI could continue the polycondensation with diamines easily, whereas abietic anhydride would act as an end-capper.

Polymerizations

The purified diabetic acids (DAB) were reacted with an approximately equimolar amount of hexamethylenediamine (assuming the molecular weight of DAB is 605, or twice that of abietic acid) in a sealed tube at 220°C for 2 hr, then 2 hr at 270°C while connected to a vacuum pump at 0.1 torr.

The polyamide product was characterized as follows.

The infrared spectrum was similar to that of nylon 66 and typical of an aliphatic amide. Free amine (but no carboxyl) groups were detectable.

A dilute alcoholic solution is basic, and on titration with HCl an equivalent weight

of 1050 was found. Titration with HCl and with NaOH in the presence of a large excess of formalin showed no inflection points in the curves. The assumption is thus made that the polymer chain has amino end groups and the equivalent weight thus corresponds to a molecular weight of 2100. The calculated molecular weight for a degree of polymerization of 6 is 2171.

The polyamide is soluble in CHCl_3 and THF and insoluble in acetone and benzene.

The softening temperature found was 210–230°C on the Fisher-Johns melting point apparatus.

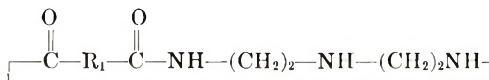
The dilute solution viscosity $(\eta_{sp}/c)_{1\%}$ was 0.076 dl/g (CHCl_3 , 25°C).

A total monomer charge of 3.307 g yielded 2.60 g of polymer.

In a separate polymerization DAB was reacted with 2 moles of diethylenetriamine (DET) per mole of diabetiac acid. It was hoped to prepare an amino-terminated polyamide of low molecular weight. This would be an analog of the commercially available Versamides in which the diabetiac acid is replaced by dimeric fatty acids. The condensation was conducted as before in a sealed vial at elevated temperatures followed by vacuum heating. The product obtained had the following characteristics:

Amine number by HCl titration, 82 mg KOH/g of polyamide; equivalent weight by end group titration, 688 g/eq; infrared spectrum, small free (secondary) amine, amide bands, no detectable zwitterion absorption; Fisher-Johns softening, 220–225°C; dilution solution viscosity $(\eta_{sp}/c)_{1\%}$, 0.050 dl/g (CHCl_3 , 25°C).

The desired amino-terminated polymer of composition $(\text{DET})_2\text{-(DAB)}_1$ was, therefore, not obtained. The yield was 79% based on this composition, or 96% based on $(\text{DET})_1\text{-(DAB)}_1$. The most likely structure is a 1:1 adduct, possibly a cyclic structure such as VII which would be consistent with the above data:



VII

where R_1 = hydrocarbon portion of DAB, calculated: 671 g/eq. Evidently the second amine molecule could not enter the polymerization since the first amine molecule had consumed both carboxyl groups.

The above polyamides were employed as curing agents for Dow Epoxy Resin 331 (diglycidyl ether of bisphenol A). After 7 hr at room temperature and 7 hr at 110°C, the resin was only partly cured. The resin swelled substantially in chloroform at this point and partially dissolved.

Discussion

The experimental conditions for polymerization are very similar to those used in nylon 66 formation.⁷ The latter leads to higher molecular weight polymers. The lower molecular weight polyamides derived here may be the result of the steric hindrance at the carboxyls in DAB, requiring more forcing conditions than with nylon 66. The lower yields indicate that some lower molecular weight species were probably lost during the vacuum heating. This is consistent with the idea that the polyamidization is slow at the hindered carboxyl.

Alternatively, the failure to form high polymer may be attributable to anhydride impurities which limited the polymer DP. A further possibility is that cyclic structures have formed. Certainly such large rings are not appealing as a likely event but the facile loss of the amine components and the small amine endgroup concentrations observed must be reconciled with sizable equivalent weights. The unexpectedly high molecular weights also might be partially due to imidazoline formation. The sluggish behavior as an epoxy curing agent also suggests a low free amino concentration. Since the polymer is of a low DP, a cyclic structure is indicated.

References

1. R. G. Sinclair, D. A. Berry, W. H. Schuller, and R. V. Lawrence, *Ind. Eng. Chem., Prod. Res. Dev.*, **9**, 60 (1970).
2. D. E. Floyd, U. S. Pat. 2,823,189 (1958).
3. D. O. Hummel and U. Pohl, *Farbe Lack*, **72**, 517 (1966); *Chem. Abstr.*, **65**, 10793 (1966).
4. I. I. Bardyshev and O. D. Strizhakov, *Dokl. Akad. Nauk SSSR*, **181**, 343 (1968).
5. G. Brus, L.-V. Thoi, and H. Francois, *Peintures, Pigments, Vernis*, **29**, 36 (1953).
6. Y. Morillon, *Double Liaison*, **106**, 91 (1964).
7. W. R. Sorenson and T. W. Campbell, *Preparative Methods of Polymer Chemistry*, 2nd ed., Wiley, New York, 1968, p. 72.

RICHARD G. SINCLAIR
DAVID A. BERRY

Battelle Memorial Institute
Columbus Laboratories
Columbus, Ohio 43201

WALTER H. SCHULLER
RAY V. LAWRENCE

Naval Stores Laboratory
Southern Utilization Research
and Development Division
Agricultural Research Service, USDA
Olstee, Florida 32072

Received April 24, 1970

Microbead Polymerization of Styrene-divinylbenzene with Sulfated Poly(vinyl Alcohol) Suspending Agent

In our previous studies,¹ carboxymethyl cellulose was employed as a suspending agent for styrene-divinylbenzene mixtures in water to obtain copolymer beads of 20–30 mesh size. It is of interest to have available beads of much smaller size for detailed studies of the sulfonation rates and the ion-exchange characteristics of the sulfonated polymers² and for use in various separation applications.

Recent experiments carried out by us have shown that poly(vinyl alcohol) with a low degree of sulfonation (1–2% of sulfate groups) yielded stable suspensions of fine droplets of styrene-divinylbenzene mixtures in water. Transparent and spherical polystyrene beads crosslinked with 2, 4, and 8 mole-% of commercial-, pure *m*-, and pure *p*-divinylbenzene with a narrow particle size distribution were obtained by using poly(vinyl sulfate) suspending agent. The yields of 125–250 μ sieve cut were 70–90% (Table I),

TABLE I
Experimental Data for Typical Runs of Styrene-DVB Bead Polymerization^a

| Crosslinking monomers (A) | Mole-% of A | Weight of A, g | Weight of styrene, g | Weight of beads, g | | |
|---------------------------|---------------|----------------|----------------------|--------------------|---------------|---------------|
| | | | | <125 μ | 125–250 μ | 250–500 μ |
| Commercial | 2 | 0.648 | 11.388 | 0.9 | 10.0 | — |
| DVB (c-DVB) ^b | 4 | 1.280 | 10.780 | 0.2 | 9.2 | 1.1 |
| | 8 | 2.543 | 9.603 | 1.5 | 10.0 | — |
| | <i>m</i> -DVB | 2 | 0.300 | 11.700 | 0.8 | 9.1 |
| <i>m</i> -DVB | 4 | 0.595 | 11.405 | 0.4 | 9.4 | 1.3 |
| | 8 | 1.176 | 10.823 | 2.2 | 9.2 | — |
| | <i>p</i> -DVB | 2 | 0.300 | 11.700 | 0.2 | 9.3 |
| <i>p</i> -DVB | 4 | 0.595 | 11.405 | 0.6 | 10.1 | — |
| | 8 | 1.176 | 10.823 | 1.3 | 9.6 | 1.0 |

^a Conditions: 0.75 g of poly(vinyl sulfate) dissolved in 200–250 ml of water was the suspending medium; benzoyl peroxide initiator, 2 wt-% based on monomers; reaction temperature 80°C.

^b Commercial DVB was found to contain 46.27% of DVB (31.25% of *m*-DVB and 15.02% of *p*-DVB, Dow Chemical).

while the use of carboxymethyl cellulose dispersion agent under similar conditions yielded 500–800 μ size beads in 40–50% yield. The difficulty encountered previously in the preparation of bead copolymers of the styrene–8 mole-% *m*-divinylbenzene system was eliminated by using poly(vinyl sulfate) suspending agent. Typical bead size distribution curves of 125–250 μ sieve cut are in Figure 1.

Preparation of Poly(vinyl Sulfate) Suspending Agent

Poly(vinyl alcohol) (DuPont, Grade 52-22), 20 g, was suspended uniformly in a sulfating mixture prepared from 15 ml of sulfuric acid (96% ACS grade) and 100 ml of pure ethyl alcohol at room temperature (20–25°C). The mixture was allowed to stand for 24 hr at room temperature. The paste was then diluted with 100–125 ml of water and poured slowly into 750 ml of methanol under fast stirring. The fine, granular precipitate was then collected on a filter and washed several times with methanol until the washings were acid free. The material was allowed to dry under vacuum at room temperature and powdered. The yield of poly(vinyl sulfate) was 17–18 g and was found to contain ~0.5 wt-% of sulfur by acid titration.

Styrene was purified by distillation under reduced nitrogen pressure, after removal of the inhibitor. *m*-Divinylbenzene and *p*-divinylbenzene of >99.8% purity were prepared by gas chromatography.³

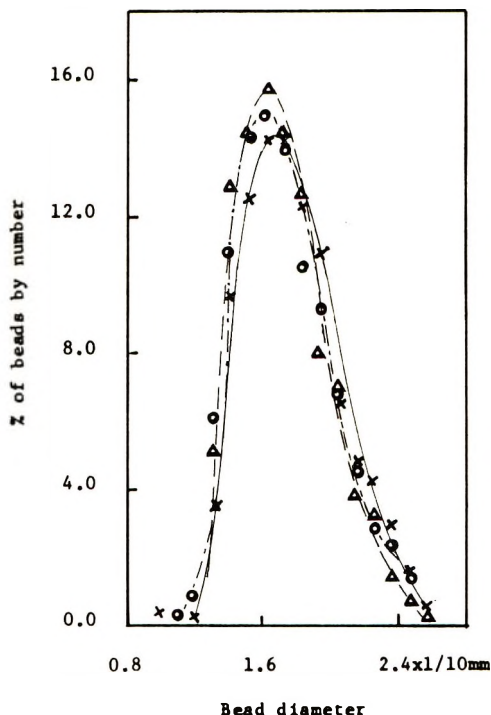


Fig. 1. Size distribution curve of crosslinked bead copolymers of styrene with 4 mole-% of (X) *c*-DVB, (Δ) *m*-DVB, and (O) *p*-DVB.

Polymerization Procedure

Styrene-divinylbenzene mixture (12 g) of appropriate composition, containing 2 wt-% of benzoyl peroxide, was added to a solution of 0.75 of poly(vinyl sulfate) in 200–250 ml of water at 80°C. The solution was kept stirred uniformly under an atmosphere of nitrogen. The speed of stirring was adjusted so that a stable vortex persisted in the swirling motion of the liquid and no air bubbles or foam developed. After 20 hr of polymerization, the copolymer beads were collected and separated into different size fractions by sieving through 500, 250, and 125 μ standard screens with stirring under a constant flow of tap water. The bead size distribution curves of 125–250 μ sieve cut were determined by diameter measurements of about 600 individual beads from each sieve size cut by using a microscope micrometer.

Acknowledgment

The authors acknowledge partial support of this research under Contract AT(30-1)-3644 between the Atomic Energy Commission and Hunter College of the City University of New York.

References

1. R. H. Wiley, J. K. Allen, S. P. Chang, K. Musselman, and T. K. Venkatachalam, *J. Phys. Chem.*, **68**, 1776 (1964).

2. D. H. Freeman and W. L. Zielinski, Jr., Ed., National Bureau of Standards Technical Note 509, Feb. 1970.
3. R. H. Wiley, G. DeVenuto, and T. K. Venkatachalam, *J. Gas. Chromatog.*, **5**, 590 (1967).

RICHARD H. WILEY
K. S. KIM
S. P. RAO

Department of Chemistry
Hunter College of the City University of New York
New York, New York 10021

Received June 30, 1970

**Photo-Graft Polymerization of Methyl Methacrylate
onto Styrene-Vinylbenzophenone Copolymer**

Some studies of polymerization or graft copolymerization initiated by the alkali metal complexes of aromatic ketone or of polyvinylbenzophenone have been extensively developed.¹⁻⁷ Benzophenone is known to be a sensitizer in photopolymerization. Photochemical reduction of benzophenone in the presence of methanol⁸ or isopropanol⁹ has also been investigated and thought to proceed through the $n \rightarrow \pi^*$ triplet state of benzophenone. The investigation of photolysis of polyvinylbenzophenone has been recently reported.¹⁰

An attempt is made in the present note to induce photo-graft polymerization of methyl methacrylate (MMA) onto styrene-vinylbenzophenone (St-VBzph) copolymer and to study the effects of temperature, solvent, and other additives like methanol on the graft copolymer yield.

St-VBzph copolymer was prepared by Friedel-Crafts reaction of polystyrene (obtained by the living polymerization method; $M_n = 25.8 \times 10^4$) with benzoyl chloride in the presence of aluminum chloride.⁴⁻⁶ The copolymer was purified by the reprecipitation in a dioxane-water system and then in a benzene-methanol system. The content of vinyl benzophenone unit was determined from the extent of benzoylation and the elemental analytical data to be approximately 4%. The stretching vibration of the carbonyl group in St-VBzph copolymer appears at 1655 cm^{-1} in the infrared spectrum (see Fig. 2). It is also observed that the absorption in the ultraviolet spectrum based on the $n \rightarrow \pi^*$ transition of the carbonyl group of St-VBzph copolymer is present at $344 \text{ m}\mu$.

St-VBzph copolymer, MMA, solvent, and additive were placed in a glass tube which

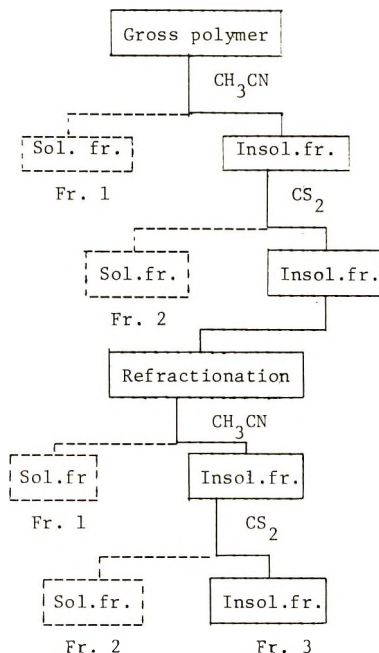


Fig. 1. Elution fractionation of photo-grafted product: (—) solid layer; (---) liquid layer; (Fr. 1) PMMA; (Fr. 2) St-VBzph copolymer; (Fr. 3) graft copolymer.

TABLE I
Photo-Graft Polymerization of Methyl Methacrylate onto Styrene-Vinylbenzophenone Copolymer^a

| Expt. | Reaction temp, °C | St-VBzph copolymer, g | Solvent (10 ml) ^b | Me-OH, ml | Time, hr | Gross polymer, g | Conversion of MMA, % | MMA homopolymer, g | St-VBzph copolymer, g | Grafting efficiency of stock polymer, % ^c | Grafting efficiency of MMA, % ^d | Graft polymer | | |
|-------|-------------------|-----------------------|------------------------------|-----------|----------|------------------|----------------------|--------------------|-----------------------|--|--|---------------|-----------------------|------------------------------------|
| | | | | | | | | | | | | Wt, g | Yield, % ^e | Composition, wt-% MMA ^f |
| 1 | 20-24 | 0.20 | B | 0 | 6 | 0.66 | 9.2 | 0.35 | 0.08 | 60.0 | 23.9 | 0.21 | 105 | 42.9 |
| 2 | " | 0.40 | B | 0 | " | 0.70 | 6.0 | 0.14 | 0.33 | 17.5 | 53.3 | 0.26 | 65 | 73.1 |
| 3 | " | " | B | 1 | " | 0.94 | 10.8 | 0.24 | 0.14 | 65.0 | 55.6 | 0.54 | 135 | 51.9 |
| 4 | " | " | B | 2 | " | 0.98 | 11.6 | 0.26 | 0.11 | 72.5 | 55.2 | " | " | 46.3 |
| 5 | 56-58 | 0.20 | B | 0 | 4 | 0.98 | 16.7 | 0.44 | Trace | ~100 | 43.6 | 0.53 | 265 | 62.3 |
| 6 | " | 0.22 | B | 4 | " | 1.68 | 31.2 | 0.55 | " | " | 62.3 | 0.84 | 382 | 73.8 |
| 7 | " | " | T | 0 | " | 2.20 | 42.3 | 0.82 | " | " | 58.6 | 0.95 | 432 | 76.8 |
| 8 | " | " | T | 2 | " | 2.16 | 41.5 | 1.15 | " | " | 40.7 | 0.96 | 436 | 77.1 |

^a Source, Toshiba SHL-100UV-2 mercury lamp; distance, 10 cm.

^b B, benzene; T, toluene.

^c (Weight of stock copolymer participated in grafting/weight of stock copolymer initially used) $\times 100$.

^d [Weight of grafted poly(methyl methacrylate)/total weight of poly(methyl methacrylate)] $\times 100$.

^e Based on the stock copolymer initially used.

^f Deduced from the weights of fractions.

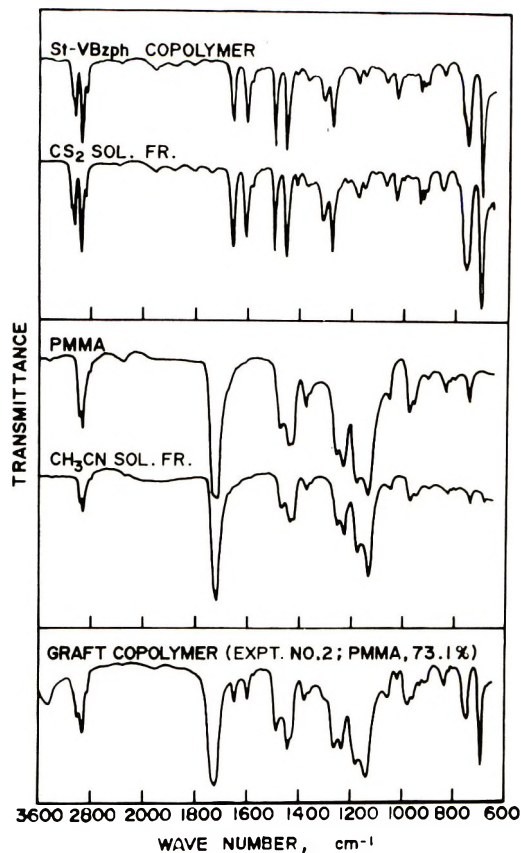


Fig. 2. Infrared spectra of styrene-vinyl benzophenone copolymer, poly(methyl methacrylate), and photo-graft polymerization products.

transmits light of wavelength longer than 300 $m\mu$. After repeating thawing and evacuation, the tube was sealed under vacuum and then irradiated at a distance of 10 cm from the source of a Toshiba SHL-100UV-2 mercury lamp.

Polymerization was terminated by pouring the slightly viscous solution into a larger amount of methanol. The gross polymer film cast from its benzene solution was repeatedly elution-fractionated by using acetonitrile and carbon disulfide as solvents into three fractions as shown in Figure 1.

Infrared spectra of fractions 1, 2, and 3 together with those of poly(methyl methacrylate) and St-VBzph copolymer are given in Figure 2. From these spectra fractions 1, 2, and 3 were found to be poly(methyl methacrylate), unreacted St-VBzph copolymer, and St-VBzph-MMA graft copolymer, respectively.

The results of the photo-graft polymerization of MMA onto St-VBzph copolymer are listed in Table I.

The grafting at lower temperatures (at 20–24°C) led to recovery of unreacted St-VBzph stock copolymer and a graft copolymer which was soluble in benzene. On the other hand the grafting at higher temperature (at 56–58°C) yielded almost no recovery of stock copolymer and formation of a graft copolymer which swelled in benzene.

The decrease of the absorption at 1655 cm^{-1} due to the carbonyl group is found to be much larger in the graft copolymer obtained at higher temperature than that at lower temperature. Both the St-VBzph copolymer and the graft copolymer obtained here

become insoluble on prolonged standing at room temperature. It can be seen from these facts that crosslinking, as well as grafting, through the carbonyl groups easily takes place by heat and/or ultraviolet irradiation.

It must be noted in Table I that the reaction was considerably enhanced when toluene was used instead of benzene or a small amount of methanol was added to the benzene solution, leading to high values of both the yield of graft copolymer and the grafting efficiency. It is considered that the formation of benzophenone ketyl radicals on St-VBzph stock copolymer may be facilitated by the action of methanol or toluene. It should be mentioned, in fact, that with the St-VBzph copolymer irradiated in methanol the absorption band at 1655 cm^{-1} characteristic of the carbonyl group disappeared, while a band due to OH group at 3500 cm^{-1} appeared. It is suggested that grafting of MMA onto St-VBzph copolymer may be induced by its ketyl radical. In view of the fact that the infrared spectrum of the graft copolymer shows the presence of residual benzophenone unit, however, a small fraction of the stock copolymer ketyl radical is thought to take part in the initiation.

References

1. S. Smith, *J. Polym. Sci.*, **38**, 259 (1959).
2. A. Zilkha, P. Neta, and M. Frankel, *J. Chem. Soc.*, **1960**, 3357.
3. S. Inoue, T. Tsuruta, and J. Furukawa, *Makromol. Chem.*, **36**, 77 (1959); *ibid.*, **42**, 12 (1960).
4. H. Takida and T. Moriyama, *Kobunshi Kagaku*, **22**, 724 (1965); *ibid.*, **24**, 57 (1967).
5. D. Braun and I. Löflund, *Makromol. Chem.*, **53**, 219 (1962).
6. G. Greber and G. Egle, *Makromol. Chem.*, **54**, 136 (1962).
7. K. Nobutoki and H. Sumitomo, *Bull. Chem. Soc. Japan*, **40**, 2725 (1967); *ibid.*, **42**, 1519 (1969).
8. H. Göth, P. Cerutti, and H. Schmid, *Helv. Chim. Acta*, **48**, 1393 (1965).
9. W. M. Moore and M. D. Ketchum, *J. Phys. Chem.*, **68**, 214 (1964).
10. C. David, W. Demarteau, and G. Geuskens, *Polymer*, **10**, 21 (1969).

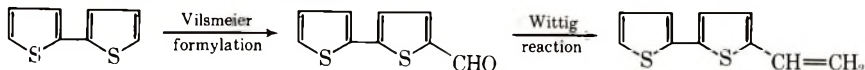
HIROSHI SUMITOMO
KOJI NOBUTOKI
KAZUMICHI SUSAKI

Faculty of Agriculture
Nagoya University
Chikusa, Nagoya, Japan

Received June 9, 1970

Synthesis and Polymerization of 5-Vinyl-2,2'-Bithiophene

Conjugated heterocycles are very reactive compounds which can be used to synthesize useful intermediates including polymers. Although the chemistry of bithiophenes has been investigated,¹⁻¹⁰ vinyl bithiophene monomers and polymers have not been reported. In our investigation of 2,2-bithiophene, 5-vinyl-2,2'-bithiophene monomer was successfully synthesized and polymerized.



2,2'-Bithiophene was mono- and diformylated with relative ease in the 5 and 5,5' positions both products having been isolated from the reaction between 2,2'-bithiophene, phosphorus oxychloride and dimethylformamide in toluene solvent at 100°C.^{11,12} The 5-formyl derivative was converted in good yield to 5-vinyl-2,2'-bithiophene via the Wittig reaction. The new 5-vinyl-2,2'-bithiophene derivative is a light yellow oil with a naphthalene-like odor boiling at 82–84°C and 0.02 mm pressure. The infrared spectrum has typical vinyl absorption bands at 1430, 1410, 985, and 905 cm⁻¹. The NMR spectrum in CHCl₃ shows a typical pattern for vinyl protons at 5.12, 5.50, and 6.75δ. The UV absorption spectrum in EtOH has three major absorption bands at 340mμ, and 198mμ characteristic of 5-substituted 2,2'-bithiophene derivatives.¹²

The 5-vinyl-2,2'-bithiophene monomer was polymerized thermally without catalyst and with free radical, cationic, anionic and Ziegler-Natta catalysts. Copolymers of 5-vinyl-2,2'-bithiophene with *N*-vinylindole and 4-vinyldibenzofuran were also prepared by free radical initiation. All the polymers were obtained as light yellow powders soluble in benzene, toluene, THF, DMF, and DMSO and insoluble in water, alcohols and the common hydrocarbons. Small quantities of insoluble polymer were also isolated from the cationic and Ziegler-Natta initiated polymerizations. Transparent films were cast from THF solutions of the polymers. Gel permeation chromatographic analysis indicated that the number average and weight average molecular weight of the homopolymers were greater than 20,000. The molecular weight of the copolymers were greater than 10,000. The elemental analyses of the homopolymers agreed with the theory. The elemental analysis of the copolymers which had been prepared from equimolar quantities of the monomers, indicated that 50/50 and 80/20 copolymers were formed with vinyldibenzofuran and vinylindole respectively. The composition of the copolymers were unchanged after extraction with boiling methanol for 72 hr. Also, the single glpc distribution peaks were unchanged and showed no bimodality by computer programmed analysis. The polymerization data are summarized in Table I.

EXPERIMENTAL

Melting points are uncorrected and were taken on a Hoover Unimelt apparatus. Polymer softening temperatures were recorded as the range in which the polymers turned to a clear melt. NMR spectra were taken with a Varian AR-100 spectrometer using tetramethylsilane as an internal standard. Infrared spectra were obtained with a Perkin-Elmer 521 grating spectrophotometer. The UV absorption spectra were measured in EtOH solution with a Cary 14 recording spectrophotometer. Glpc analyses were carried out in THF at ambient temperature with 10⁴, 10³, 250, and 60-Å polystyrene columns and with 1500, 1000, 500, and 200-Å Bioglass packed columns. *A_w* and *A_n* values corresponding to chain extended molecular sizes were determined by a computer programmed analysis of the chromatograms. Elemental analyses were determined by the Berkeley Analytical Laboratory of Berkeley, California.

Synthesis of 5-Vinyl-2,2'-bithiophene

5-Formyl-2,2'-bithiophene. The procedure of Curtis and Phillips¹² was repeated. POCl₃, 113.5 g (0.74 mole) was added in small portions to 2,2'-bithiophene (Eastman

TABLE I
 Polymerization and Copolymerization of 5-Vinyl-2,2'-bithiophene

| Monomer, g | Solvent | Temp, °C | Initiator, g | Time, h | Yield, % | Softening Range, °C | \bar{A}_w/\bar{A}_n |
|---|--------------------------|----------|--|---------|----------|--|-----------------------|
| 5-Vinyl-2,2'-bithiophene, 8.8 | None | 130-140 | Δ | 16 | 59 | 99-111 | 9.07 |
| 5-Vinyl-2,2'-bithiophene, 1.9 | Benzene | 80 | AIBN, 0.008 | 24 | 15.7 | 112-122 | 4.71 |
| 5-Vinyl-2,2'-bithiophene, 1.9 | CH_2Cl_2 | -78 | $\text{BF}_3 \cdot (\text{C}_2\text{H}_5)_2\text{O}$, 0.013 | 4.5 | 68 | 128-140 ^a 235-250 ^b | 5.33 |
| 5-Vinyl-2,2'-bithiophene, 5.0 | Benzene | 55 | Et_3AlCl , 0.78 $\alpha\text{-TiCl}_3$, 0.40 | 24 | 76 | 177-185 ^a 263-273 ^b | 5.40 |
| 5-Vinyl-2,2'-bithiophene, 5.0 | THF | -78 | <i>n</i> -BuLi, 0.214 | 24 | 52 | 158-170 | 1.85 |
| 5-Vinyl-2,2'-bithiophene, 5.0 | None ^c | 150 | Benzoylperoxide, 0.051 | 48 | 57.7 | 150-162 | 1.51 |
| 5-Vinyl-2,2'-bithiophene, 5.0 <i>N</i> -Vinylindole, 3.7 | None ^c | 150 | Benzoylperoxide | 48 | 30 | 135-143 | 1.81 |

^a Melting range of soluble fraction.

^b Melting range of insoluble fraction.

^c Polymerization carried out in a sealed tube at 10^{-6} mm vacuum.

Organic Chemicals) 80 g (0.48 mole) and 64 g (0.87 mole) DMF in 650 ml toluene. After the exothermic reaction had subsided, the mixture was heated on a steam bath for 2.5 hr, cooled, and a warm saturated solution of 600 ml of sodium acetate was added. The organic layer was separated and then evaporated to give a yellow residue which was recrystallized from benzene/pet ether (30–60°) (1/5) to give 1.5 g 5,5'-diformyl-2,2'-bithiophene as yellow plates, m.p. 217–8°C (lit.¹² 217–8°). The filtrate was evaporated and the residue obtained was recrystallized from benzene/pet ether (60–90°) (1/10) to give 39 g (0.21 mole) (42%) pure 5-formyl-2,2'-bithiophene, m.p. 58–9° (lit.¹² 58–9°). Calcd. for C₇H₆OS₂: C, 55.67; H, 3.09; S, 32.99. Found: C, 55.48; H, 3.09; S, 32.99.

5-Vinyl-2,2'-bithiophene. 5-Formyl-2,2'-bithiophene, 19.4 g (0.10 mole) was added to a small excess of methylenetriphenylphosphine (0.12 mole) (Wittig Reagent) prepared from triphenylmethylphosphonium bromide and *n*-butyllithium in 300 ml anhydrous ether in a dry nitrogen atmosphere. The mixture was stirred 3 h at 25°C and then refluxed 21 h under a nitrogen atmosphere. The mixture was cooled and then passed through a 300 × 50 mm chromatographic column containing Alcoa Chromatographic alumina Grade F-20 to separate the products. The crude vinyl compound, which was eluted first, was passed through a second chromatographic column to remove trace impurities using benzene as the eluent. The eluent was evaporated to give 17 g (88%) of an orange oil. The oil was purified further by distillation at 82–84°C and 0.02 mm vacuum to give 6.2 g of a light yellow oil and 10.8 g of polymer. Other preparations of the monomer avoided the distillation step and the monomer was obtained pure by passage through a third chromatographic column. The vinyl monomer was identified and characterized by IR, NMR, and UV spectroscopy. Extinction coefficients were calculated from the UV absorption spectrum: 340m μ (Σ_{\max} 18,200), 242m μ (Σ_{\max} 8160) and 198m μ (Σ_{\max} 15,456). Calcd. for C₁₀H₈S₂: C, 62.50; H, 4.17; S, 33.33. Found: C, 62.42; H, 4.24; S, 33.12.

Polymerization

Bulk polymerizations were carried out in heavy-walled Pyrex glass polymerization tubes. Monomer samples were degassed through three freeze-thaw cycles after addition of the initiator in the free radical polymerizations and the tubes were sealed at 10⁻⁵ to 10⁻⁶ mm pressure. Solution polymerizations were carried out in 100 and 200 ml three necked flasks equipped with stirrer, reflux condenser, thermometer and gas-inlet. Moisture was rigorously excluded by flaming the entire apparatus prior to introduction of solvent and monomer. Oxygen was excluded by maintaining a blanket of purified argon over the solution. The catalyst was then added to the stirred mixture. At the termination of the polymerization the entire reaction mixture was added to a large excess of methanol. The polymer was filtered, washed with methanol and purified by repeated precipitation from benzene or THF with methanol. After repeated washing with fresh methanol the polymer was vacuum dried at 40–50° for 24 to 48 hours.

Catalysts

Benzoyl peroxide, boron trifluoride etherate (Eastman), azobisisobutyronitrile (K & K Chemicals), titanium trichloride (Stauffer Chemical), and *n*-butyllithium, 1.6 M in hexane (Foote Mineral) were used as received. Aluminum alkyls (Texas Alkyls, Inc.) were used without purification as 25% solutions in benzene or toluene.

Solvents

Solvents used were of spectrograde purity. Benzene was dried over sodium wire; THF was dried over calcium hydride and distilled from potassium metal.

The analytical data are presented for those polymers prepared in Table I. Anal. Calcd. for $(\text{C}_{10}\text{H}_8\text{S}_2)_n$, poly-5-vinyl-2,2'-bithiophene: C, 62.50%; H, 4.17%; S, 33.33%. Found: C, 62.51%; H, 4.34%; S, 33.22%. Anal. Calcd. for $(\text{C}_{30}\text{H}_{41}\text{NS}_3)_n$, 80/20

poly-5-vinyl-2,2'-bithiophene-*N*-vinylindole: C, 66.78%; H, 4.60%; N, 1.96%; S, 26.66%. Found: C, 66.52%; H, 4.53%; N, 2.24%; S, 26.27%. Anal. Calcd. for $(C_{24}H_{18}OS_2)_n$, 50/50 poly-5-vinyl-2,2'-bithiophene-4-vinyldibenzofuran: C, 74.54%; H, 4.68%; S, 16.9%. Found: C, 73.95%; H, 4.74%; S, 16.01%.

The infrared spectra of the vinyl polymers (film) showed the disappearance of the vinyl bands at 985 and 905 cm^{-1} and the appearance of aliphatic C-H stretching bands at 2920 and 2825 cm^{-1} .

REFERENCES

1. H. Wynberg, A. Logothetis, and D. VerPloeg, *J. Am. Chem. Soc.*, **79**, 1972 (1957).
2. H. Wynberg and A. Bantjes, *J. Org. Chem.*, **24**, 1421 (1959).
3. H. Wynberg and A. Bantjes, *J. Am. Chem. Soc.*, **82**, 1447 (1960).
4. S. Gronowitz and H. Karlsson, *Arkiv Kemi*, **17**, 89 (1960).
5. J. Uhlenbroek and H. Bijloo, *Rec. Trav. Chim.*, **79**, 1181 (1960).
6. G. Phillips and R. Curtis, *J. Chromatog.*, **9**, 366 (1962).
7. K. Miller, *J. Engineering Data*, **8**, 605 (1963).
8. R. Atkinson, R. Curtis, and G. Phillips, *J. Chem. Soc.*, 7109 (1965).
9. S. Gronowitz and J. Skramsted, *Arkiv Kemi*, **28**, 115 (1967).
10. K. Schulte, G. Henke, G. Rucker, and S. Foerster, *Tetrahedron*, **24**, 1899 (1968).
11. E. Lescot, N. G. Buu-Hoi, and N. Xuong, *J. Chem. Soc.*, 3234 (1959).
12. R. Curtis and G. Phillips, *Tetrahedron*, **23**, 4419 (1967).

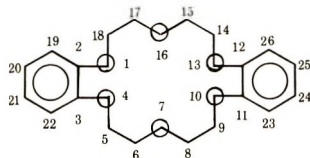
EDWARD GIPSTEIN
WILLIAM A. HEWETT
OMAR U. NEED

IBM Research Laboratory
San Jose, California

Received July 9, 1970

Novel Polyamides from Macrocyclic Ethers

Recent reports by C. J. Pedersen¹ described a family of macrocyclic ethers which complex the cations of alkali metals and alkaline earth metals. Among these compounds, 2,3,11,12-dibenzo-1,4,7,10,13,16-hexaoxacyclooctadeca-2,11-diene (I), hereafter referred to as dibenzo-18-crown-6, is particularly suited for the preparation of intermediates which can be used to incorporate the complexing properties into the backbone of a polymer.

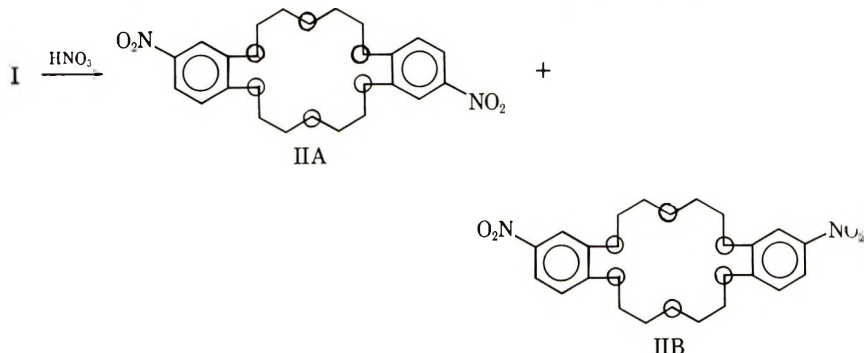


I

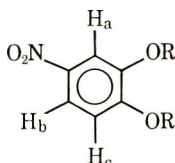
We have converted compound I to two isomeric diamines via the dinitro derivatives and have prepared polyamides by condensation of the diamines with aromatic diacid chlorides. These polymers complex some alkali metal cations but not alkaline earths.

DISCUSSION

Dibenzo-18-crown-6 (I) was prepared according to Pedersen¹ and nitrated with a mixture of nitric acid and acetic acid in a chloroform-acetic acid solution.



Product II is thereby obtained as a mixture of two geometric isomers, A and B, which are readily separated by fractional crystallization. We cannot be absolutely certain of their respective structures. One compound was much more insoluble than the other and melted considerably higher (245–251°C vs. 208–213°C). The former was assigned the *trans* structure by arguments of symmetry. As expected, the infrared spectra of IIA and IIB are very similar in the functional group region above 1100 cm^{-1} , but show differences in the "fingerprint region" below this frequency. Ultraviolet spectra of the two isomers are virtually identical. The nuclear magnetic resonance spectrum of IIB (NMR of IIA could not be obtained due to its insolubility) in DMAC at 140°C is somewhat surprising. The spectrum shows an unusual AB pattern of a small doublet at 2.05τ



and a large singlet at 2.20τ for H_b and H_c . The two peaks have practically merged at this temperature. H_a is a normal doublet (split only by H_b) centered at 2.79τ . The known model compound, 4-nitroveratrole (in DMAC at 140°C) shows an almost identical spectrum—a small doublet centered at 2.04τ , a large peak (with a shoulder) centered at 2.17τ , and a doublet for H_a centered at 2.76τ . Interestingly, the model gives a "normal" spectrum at room temperature, H_a coupling with H_b but not H_c . Here, H_b is a quartet centered at 2.27τ , H_a a doublet centered at 2.45τ , and H_c a doublet centered at 2.99τ . Thus, the 1,2,4-trisubstituted structure for the dinitration product of crown is confirmed.

The diamines were prepared by catalytic hydrogenation of II.

Polyamides were synthesized by solvent polymerization of the diamines with both *iso*- and terephthaloyl chloride in hexamethylphosphoramide (HMP) or dimethylacetamide (DMAC). The consistently best results were obtained with the *trans*-diamine and isophthaloyl chloride in HMP. This polyamide had an intrinsic viscosity of 0.9–1.1 (HMP at 30°C). It fused above 220°C , with decomposition.

Because the polyamide was insoluble in normally good polyamide solvents such as DMAC, it was necessary to cast from hexafluoroisopropanol (HFIP). Fairly tough film was obtained. Table I presents characteristic properties for such film.

TABLE I
Properties of Polyamide Films*
from *trans*-Diamine and Isophthaloyl Chloride

| | Tensile modulus (Kpsi) | Tenacity (Kpsi) | Elongation (%) | Dielectric constant (10^3 Hz) | Dissipation factor (10^3 Hz) | Resistivity (ohm-cm) |
|---------------------------------------|------------------------|-----------------|----------------|----------------------------------|---------------------------------|----------------------|
| As-cast | 286 | 9.9 | 12 | 3.86 | 0.013 | 2.3×10^{14} |
| Complexed with 52 mole % K^+ | 346 | 11.2 | 12 | 3.82 | 0.013 | 2.8×10^{14} |

* Film thickness 1–2 mils, all properties measured at 23°C .

Cationic complexing of the film was achieved in a heated 20% aqueous solution of the metal chloride. The ability of several cations to form complexes with polyamide film is shown in Table II. Like Pedersen, we found maximum complexing with K^+ . However, we observed much greater selectivity. While Pedersen found that dibenzo-18-crown-6 (I) itself forms strong complexes with Ca^{++} , Ba^{++} , and Cs^+ ions, we found that the polyamide film does not. Table II shows that the film complexes most of the alkali metal cations. Complexing increases with increasing size (i.e., $\text{Li}^+ < \text{Na}^+ < \text{K}^+$) as the ions fit more and more snugly into the central cavity and favorable charge interactions become greater. The Cs^+ cation is apparently too large and cannot form a stable complex.

TABLE II
Complexing Ability of Polyamide Film

| Cation | Ionic diameter | Mole %, complexed |
|------------------|----------------|-------------------|
| Li^+ | 1.20 | 24 |
| Na^+ | 1.90 | 54 |
| Ca^{++} | 1.98 | 0 |
| K^+ | 2.66 | 64 |
| Ba^{++} | 2.70 | 0 |
| Cs^+ | 3.34 | 0 |

Table I also shows that the complexed potassium ion has little effect on the mechanical and electrical properties of the film. The constancy of the electrical resistivity is particularly good evidence for the complexed nature of the ionic component.

EXPERIMENTAL

Preparation of Dinitro and Diaminodibenzo-18-Crown-6

Dibenzo-18-crown-6 (I) was obtained by the method of Pedersen.

Into a 3-liter flask equipped with a mechanical stirrer, water condenser, and dropping funnel was placed 50 g (0.130 mole) compound I and 1.0 l. chloroform. After dissolution of the polyether by stirring, 750 ml glacial acetic acid was added, followed by a nitrating solution of 35 ml (0.057 mole) concentrated nitric acid ($d = 1.42$) in 100 ml acetic acid. The latter was added dropwise over 30 minutes. The reaction was stirred without heating for an hour, during which it successively turned green, blue, and yellow. After refluxing on a heating mantle for 3 hours, the reaction was filtered, giving 25.0 g of tannish *trans*-dinitro derivative, m.p. 237–246°C. Recrystallization from dimethylformamide (DMF) gave 21.7 g of yellow crystals, m.p. 247–252°C. Yield of crude was 40.0%, pure—34.7%. On sitting, the mother liquor deposited 16.0 g of yellow crystalline *cis*-dinitro derivative, m.p. 206–232°C. Total recovery of dinitro derivative was 85%.

Trans Isomer. ANAL. Calcd. for $C_{20}H_{22}N_2O_6$: C, 53.28; H, 4.90; N, 6.27. Found: C, 53.75; H, 5.02; N, 6.05.

UV Spectrum (95% ethanol).

| λ_{\max} | log ϵ |
|------------------|----------------|
| 338 | 4.193 |
| 298 | 4.093 |

Cis Isomer. ANAL. Calcd. for $C_{20}H_{22}N_2O_6$: C, 53.28; H, 4.90; N, 6.27. Found: C, 53.29; H, 5.16, N, 6.32.

UV Spectrum (95% ethanol).

| λ_{\max} | log ϵ |
|------------------|----------------|
| 338 | 4.170 |
| 298 | 4.086 |

The diamino derivatives were prepared by the catalytic hydrogenation of the dinitro compounds. This was done in a Parr Series 3910 medium pressure hydrogenator. Into a 500 ml shaker bottle was placed 2.00 g (4.40 mmole) *trans*-dinitro derivative. This was suspended in 220 ml dimethylformamide (DMF), and two teaspoons of Grace No. 28 aqueous based Raney nickel catalyst were added. Hydrogenation was rapid, being essentially complete in 40 minutes. Total pressure drop was 47 lbs. Filtration gave a nearly colorless solution, which was evaporated to 1.44 g of solid, yield 83%. The *trans*-diamine was purified by sublimation at 220–240°C, 0.05 mm Hg. The product was a white solid, m.p. 199–203°C. *Cis*-diamine was sublimed at 210–220°C, 0.05 mm Hg to a white solid, m.p. 180–184°C.

Preparation of Polyamides

Into a 250 ml 3-necked flask equipped with a mechanical stirrer and a nitrogen inlet was placed 17.00 g (0.0436 mole) *trans*-diamino derivative. This was readily dissolved on addition of 125 ml HMP. Slow addition of 8.77 g (0.0432 mole) isophthaloyl chloride started polymerization, which was quite exothermic. The reaction was cooled to room temperature in a water bath, then continued overnight under nitrogen. Polymerization was accompanied by a darkening of the solution and a visible increase in viscosity. The reaction solution was poured into a blender containing water and crushed ice. Vigorous stirring produced a white, fibrous solid that was filtered, washed with water, and

dried at room temperature in a vacuum oven over phosphorus pentoxide. Recovery of polyamide was 97% based on amine. The intrinsic viscosity was 1.04 (HMP at 30°C).

Results obtained with other combinations of intermediates under similar condensation conditions are given in Table III.

TABLE III

| Diamino derivative | Acid chloride | Intrinsic Viscosity (HMP 30°C.) |
|---|--|------------------------------------|
| 1:1 mixture of <i>trans</i> and <i>cis</i> | Terephthaloyl | 0.71 |
| " | Isophthaloyl | 0.69 |
| " | 1:1 mixture of terephthaloyl and isophthaloyl | 0.72 |
| <i>cis</i> | Isophthaloyl | 1.01 |

The films were prepared by casting, on stainless steel plates from solutions containing approximately 10% polymer in hexafluoroisopropanol (HFIP). The solution was left to dry in the air for one minute, then placed in an oven at 50°C overnight, followed by a final drying at 120°C for another 16 hours. The film was then extracted in a steam-heated bath of de-ionized water for three days. This treatment assured a maximum of 0.5% residual solvent. Complexing of the film was achieved by heating in a 20% solution of the metal chloride in water. The amount of salt in the films was calculated from chloride determinations.

Reference

1. C. J. Pedersen, *J. Amer. Chem. Soc.*, **89**, 7017, (1967).

W. M. FEIGENBAUM
R. H. MICHEL*

Film Research Laboratory
Experimental Station
E. I. du Pont de Nemours and Co., Inc.
Wilmington, Delaware 19898

Received July 13, 1970

* Inquiries should be addressed to this author.

Grafting of Chlorinated Polyindene with Methyl Methacrylate*

Introduction

Grafting of polymers by radiation techniques is well known in the literature. Among the methods for direct photoinitiation to attach graft chains onto the polymeric backbone, the introduction of carbon-chlorine bonds as labile sites is reported.¹ Methyl methacrylate is one of the comonomers most employed for grafting according to this method.

One of the major difficulties in this class of polymers is the complete removal of the homopolymer eventually formed during the process. It is sometimes possible to use a convenient solvent system to overcome this problem, although a universal procedure for isolating sequence copolymers from their associated polymeric environment does not exist.²

This work deals with the grafting of chlorinated polyindene under photochemical conditions using methyl methacrylate as the comonomer.

Experimental

Chlorinated polyindene was prepared as reported in a previous paper.³ Methyl methacrylate (Rohm and Haas, bp 100°C/760 mm) was distilled over hydroquinone. Acetone (Merck, p.a.) was used as received. Freshly distilled water was used. Nitrogen (Oxigenio do Brasil) was employed to remove oxygen from the initial reaction system.

Grafting Technique. Chlorinated polyindene film (6 g), methyl methacrylate (20 g), acetone (150 ml), and water (26 ml) were irradiated in a quartz flask using as UV source a Hanovia, 200 watts, 654A36 mercury lamp, with a Vycor filter, for 18 hours, at room temperature (25–30°C), under magnetic stirring. The fragmented graft film was separated by filtration, dried and weighed. Yield: 9.2 g. The homopolymer was recovered by the addition of ethyl alcohol, filtered, dried and weighed as before. Yield: 3.6 g. The graft polymer was dissolved in benzene and precipitated in about 3 volumes of methanol. This treatment was repeated 3 times and the product was filtered, dried, and weighed as before. Yield: 8.5 g.

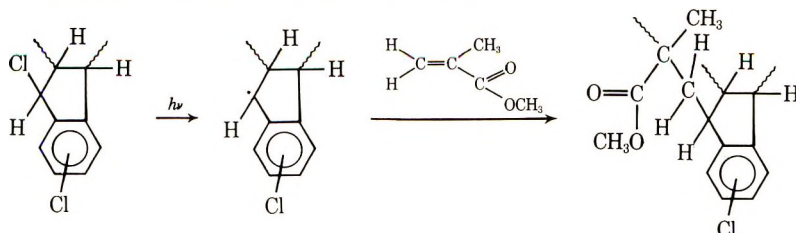
The whole polymer was extracted with acetone, as a whitish colloidal dispersion. The product was finally precipitated in methanol, filtered, dried and weighed. Yield: 8.3 g.

Blank reactions were run with non-chlorinated polyindene, as well as with methyl methacrylate without any indene polymer. The procedure was identical. No modification was observed with the non-chlorinated polyindene blank. Poly(methyl methacrylate) gave a yield of 5.0 g, and was completely soluble in the reaction medium.

All experimental data, including IR and combustion analysis, are summarized in Table I.

Results and Discussion

The UV irradiation of the chlorinated polyindene is considered to involve abstraction of a benzylic chlorine atom, according to the reaction:



(*) Presented in part before the Sociedade Brasileira para o Progresso da Ciência, Annual Meeting, Bahia, July, 1970.

TABLE I
Grafting of Chlorinated Polyindene with Methyl Methacrylate

| Experiment no. | Polymer | Molecular weight ^a | Elemental Analysis (%) | | | O ^d | I.R. absorption ^e (cm ⁻¹) | Solubility ^g |
|----------------|---------------------------|-------------------------------|------------------------|----------------|-----------------|----------------|--|---|
| | | | C ^b | H ^b | Cl ^c | | | |
| WO-2 | Graft copolymer | 9,600 | 62.8 | 6.3 | 13.3 | 17.6 | Present | Acetone (+) (colloidal dispersion) Benzene (+) C Cl ₄ (+) |
| WO-1 | Chlorinated polyindene | 5,100 | 63.7 | 4.2 | 29.8 | 2.3 | Absent | Acetone (-) Benzene (+) C Cl ₄ (+) |
| WO-3 | Poly(methyl methacrylate) | 13,400 | | | | | Present | Acetone (+) Benzene (+) C Cl ₄ (+) |
| WO-4 | Polyindene | 2,600 | 92.9 | 6.9 | | | Absent | Acetone (-) Benzene (+) C Cl ₄ (+) |

^a Isothermal distillation apparatus (benzene).

^b Perkin Elmer Elemental Analyzer, model 240.

^c Schöniger's procedure.

^d By difference.

^e Perkin Elmer I.R. Spectrophotometer, model 621 (K Br).

^f 1150-1180 cm⁻¹ (db) assigned to C—O—C vibration, 1240-1270 cm⁻¹ (db) assigned to C—O vibration, and 1730 cm⁻¹ assigned to C—O vibration.

^g 1% w/v.

The formation of a free radical in the benzylic position is expected, as discussed in a previous paper,³ since molecular models indicate that position is sterically favored for a subsequent attack.

In order to eliminate the contamination of the graft copolymer with methyl methacrylate homopolymer, during the reaction, several solvent systems were tried. We found acetone-water 6:1 v/v to be the most convenient. This solvent pair permits total solubility of the methyl methacrylate homopolymer, as proved by the blank experiment, while the indene-containing polymer remains insoluble. This technique permits the statement that no poly(methyl methacrylate) is present in the graft copolymer.

To be sure that no residual chlorinated polyindene was still present in the graft copolymer, several solvents were tested. We found dry acetone to be the best one, being a non-solvent for the initial polymer and a colloidal dispersion medium for the graft copolymer. The characteristic of some graft copolymers of forming colloidal dispersions in good solvents for one of the components is reported in the literature.⁴

The solubility of the physical mixture of the homopolymers in acetone was tested.

The complete dispersion of the graft product in acetone indicates a yield of 100%, regarding the initial chlorinated polyindene.

The IR spectrum of the graft copolymer presents peaks corresponding to chlorinated polyindene and to poly(methyl methacrylate),⁵ as shown in Table I.

Elemental analysis for chlorinated polyindene and for the graft copolymer suggested loss of about seven chlorine atoms on average.* Assuming that for each broken carbon-chlorine bond a branch of poly(methyl methacrylate) started, and since an increase of about 4500 in the molecular weight occurred, it might be concluded that each branch contains on average about seven units of methyl methacrylates.†

This research was supported by funds provided by Banco Nacional do Desenvolvimento Econômico (BNDE), Coordenação do Aperfeiçoamento do Pessoal de Nível Superior (CAPES) and Conselho Nacional de Pesquisas (CNPq).

References

1. H. A. J. Battaerd and G. W. Tregear, *Graft Copolymers*, Interscience Publishers, New York, 1967, p 28.
2. R. J. Ceresa, "Block and Graft Copolymers" in H. F. Mark, N. G. Gaylord, and M. Bikales, (Eds.), *Encyclopedia of Polymer Science and Technology*, Vol. 2, Interscience Publishers, New York, 1965, p 510.
3. E. B. Mano, W. D. Vilar, O. Coutto Filho, and A. S. Gomes, *Rev. Bras. Tecnologia* (Rio de Janeiro), in press.
4. Y. Gallot, E. Franta, P. Rempp, and H. Benoit, *J. Polym. Sci., C*, **4**, 473 (1963).
5. H. A. Willis, V. J. I. Vicky, and P. J. Hendra, *Polymer*, **10**, 737 (1969).

ELOISA B. MANO
ODYR DO COUTTO FILHO
WALTER D. VILAR
AULTON S. GOMES

Instituto de Química
da Universidade Federal
do Rio de Janeiro
Rio de Janeiro, Brazil

Received September 8, 1970

Revised September 21, 1970

* Loss of chlorine atoms = $(29.8 \times 5100 - 13.3 \times 9600) / 35.5 \times 100 = 6.85$ atoms/average chain.

† Methyl methacrylate units = $4500 / 7 \times 100 = 6.73$ units.

Copolymerization Studies on Alkenylcarboranes*

Vinyl-, isopropenyl-, and allylcarborane¹⁻³ do not polymerize well by free radical initiation. Under selected conditions, they were noted to polymerize when treated with ionic initiators such as aluminum chloride or phenyl lithium. Free radical initiated copolymerization of certain alkenylcarboranes with methyl acrylate² and butadiene⁴ have been successful; however, little is known concerning the nature of the copolymerization reactions. A study of the copolymerization behavior of vinylcarborane (VC) and isopropenylcarborane (IPC) with methyl methacrylate (MMA) and styrene was carried out to determine the copolymerization characteristics of monomeric carboranes with other typical vinyl compounds. In the copolymerization studies, emphasis was placed on the effects of small concentrations of VC or IPC on the rate of polymerization of MMA and styrene and on the intrinsic viscosity of the resulting copolymers.

Copolymerizations were carried out in toluene with 2,2'-azobisisobutyronitrile as the initiator. Polymerization rate measurements were followed by a dilatometric technique⁵ and solution viscosity measurements were made in toluene solution at 30°C using Cannon dilution viscometers. Copolymerizations were carried to 10-12% conversion and the copolymers isolated and purified by reprecipitation from toluene solution on the addition of methanol followed by drying under vacuum for a period of 24 hours.

Copolymerization reactions were carried out at three different concentrations of the carborane compounds with both MMA and styrene. Molar ratios of MMA or styrene to VC and IPC were varied from approximately 30:1 to 5:1. Results of the rate determinations are shown in Table I (VC) and Table II (IPC). R_{p0} refers to the rate of polymerization of MMA or styrene in the absence of comonomer, otherwise the same conditions applied as were employed in the copolymerization. In a like manner the $[\eta]_0$ values apply to the intrinsic viscosities of the homopolymers of MMA and styrene.

TABLE I
Copolymerization Data for Vinyl Carborane (VC) with MMA and Styrene

| No. | [VC] moles/l | [MMA] moles/l | [Sty- rene] moles/l | Molar Ratio MMA (S)/VC | R_p , % min | R_p/R_{p0} | $[\eta]$ | $[\eta]/[\eta]_0$ |
|-----|-----------------|------------------|---------------------------|---------------------------------|------------------|--------------|----------|-------------------|
| VC | | | | | | | | |
| 1 | | 5.0 | | | 0.21 | 1.0 | 0.49 | 1.0 |
| 2 | 0.15 | 4.46 | | 29.7 | 0.211 | 1.0 | 0.625 | 1.27 |
| 3 | 0.44 | 3.97 | | 9.02 | 0.207 | 1.0 | 0.43 | 0.87 |
| 4 | 0.77 | 3.52 | | 4.57 | 0.22 | 1.05 | 0.36 | 0.73 |
| 5 | | | 4.8 | | 0.063 | 1.0 | 0.35 | 1.0 |
| 6 | 0.15 | | 4.13 | 27.5 | 0.075 | 1.2 | 0.25 | 0.71 |
| 7 | 0.44 | | 3.70 | 8.4 | 0.044 | 0.7 | 0.20 | 0.57 |
| 8 | 0.77 | | 3.27 | 4.25 | 0.038 | 0.6 | 0.17 | 0.48 |

It may be noted that neither carborane derivative appeared to affect the polymerization rate of MMA at any of the three concentrations as evidenced by the constant R_p/R_{p0} ratio of near 1.0. The intrinsic viscosity of the copolymers showed a tendency to decrease slightly with increasing carborane concentration. At the lower concentrations the $[\eta]/[\eta]_0$ ratios were greater than 1.0 indicating a higher molecular weight material than for polymethyl methacrylate. The low boron content (Table III) of the MMA copolymers indicates that VC and IPC do not copolymerize with MMA to any significant extent. These results are in sharp contrast to the reported methyl acrylate-

* This work was performed under the sponsorship of the U. S. Army Missile Command, Redstone Arsenal, Alabama, under Contract DAAH01-69-C-0772.

TABLE II
Copolymerization Data for Isopropenyl Carborane (IPC)
with MMA and Styrene

| No. | [IPC] moles/l | [MMA] moles/l | [Sty- rene] moles/l | Molar Ratio MMA (S)/IPC | R_p , % min | R_p/R_{p0} | $[\eta]$ | $[\eta]/[\eta]_0$ |
|-----|------------------|------------------|---------------------------|----------------------------------|------------------|--------------|----------|-------------------|
| IPC | | | | | | | | |
| 1 | | 5.0 | | | 0.21 | 1.0 | 0.49 | 1.0 |
| 2 | 0.13 | 4.46 | | 34.3 | 0.23 | 1.1 | 0.610 | 1.24 |
| 3 | 0.41 | 3.97 | | 9.68 | 0.24 | 1.14 | 0.585 | 1.18 |
| 4 | 0.68 | 3.52 | | 5.18 | 0.22 | 1.05 | 0.455 | 0.93 |
| 5 | | | 4.8 | | 0.063 | 1.0 | 0.35 | 1.0 |
| 6 | 0.13 | | 4.13 | 31.8 | 0.093 | 1.5 | 0.284 | 0.81 |
| 7 | 0.41 | | 3.70 | 9.02 | 0.045 | 0.7 | 0.256 | 0.78 |
| 8 | 0.68 | | 3.27 | 4.8 | 0.039 | 0.6 | 0.198 | 0.56 |

TABLE III
Elemental Analysis Data for Copolymers

| No. | Calculated | | | Found | | |
|-------|------------|------|-------|-------|------|------|
| | % C | % H | % B | % C | % H | % B |
| VC-2 | 58.30 | 8.01 | 3.38 | 59.40 | 7.79 | 0.1 |
| VC-3 | 54.98 | 8.04 | 10.06 | 59.15 | 7.70 | 0.64 |
| VC-4 | 51.69 | 8.06 | 16.62 | 58.81 | 7.60 | 0.76 |
| IPC-2 | 58.56 | 8.04 | 3.09 | 59.33 | 7.85 | 0.25 |
| IPC-3 | 55.65 | 8.11 | 9.32 | 59.90 | 7.97 | 0.14 |
| IPC-4 | 52.84 | 8.18 | 15.34 | 59.45 | 7.99 | 0.30 |
| VC-6 | 88.75 | 7.72 | 3.50 | 90.9 | 7.50 | 1.50 |
| VC-7 | 81.86 | 7.78 | 10.33 | 88.8 | 7.92 | 3.20 |
| VC-8 | 75.11 | 7.84 | 17.03 | 87.9 | 7.70 | 4.20 |
| IPC-6 | 89.07 | 7.75 | 3.21 | 89.60 | 7.98 | 1.3 |
| IPC-7 | 82.65 | 7.86 | 9.56 | 88.66 | 7.81 | 3.0 |
| IPC-8 | 76.38 | 7.96 | 15.74 | 88.27 | 7.87 | 3.8 |

isopropenylcarborane copolymerization² which gave products containing up to 22% boron. In addition, the generally low boron content of the MMA copolymers shows that the copolymer composition is relatively independent of the ratio of comonomers in the charge, at least over the range studied.

Several obvious differences were noted in the styrene copolymerizations. First, the rate of polymerization was noted to decrease markedly with an increase in the carborane concentration. A similar tendency was observed in the intrinsic viscosity of the copolymers. In these instances, the $[\eta]/[\eta]_0$ ratio decreased to near 0.5 at the higher concentrations of the carborane derivatives. These results indicated that the carborane derivatives were influencing the polymerization, likely through their active participation in the reactions. This point was confirmed from the elemental analysis data. The boron content of the copolymers displayed a tendency to increase as the VC or IPC concentration increased. The percent of boron found ranged from 1.3% at the lowest concentration to approximately 4.0% at the highest. The values were slightly higher for the styrene-VC copolymers than for styrene-IPC. Although the carborane deriva-

tives did copolymerize with styrene, they entered into the copolymerization somewhat reluctantly as evidenced by the low boron content of the copolymers relative to that present in the comonomer charge.

The failure of alkenylcarboranes to polymerize has been attributed to the steric inhibition imposed by the bulky carborane nucleus. Hence, it was expected that the alkenylcarboranes would display a tendency to inhibit the rate of polymerization of vinyl monomers, and also, caused a pronounced lowering of the copolymers molecular weight. The expected behavior was observed in the styrene copolymerizations, where limited quantities of the carborane derivatives were introduced into the copolymers with noted lowering of both polymerization rate and the intrinsic viscosity of the copolymers. In contrast, the carborane derivatives did not copolymerize with MMA to any appreciable extent as evidenced by the constancy in rate and intrinsic viscosity, and low boron content of the copolymers. These results are indicative of the poor polymerizability of alkenylcarboranes in copolymerization reactions with other common vinyl monomers.

The difference between the styrene and MMA copolymerizations may be attributed to differences in polarity of the two monomers and their intermediate radicals relative to that of the alkenylcarboranes. Both styrene and MMA are highly reactive monomers which give chain-end radicals of low reactivity because of resonance stabilization effects. Through similar considerations, VC and IPC would likely show a high reactivity as a monomer and low reactivity as a radical (resonance stabilization) since the electron withdrawing character of the carborane nucleus is well known and has been compared with that of the cyano group.⁴ Since the polar nature of the intermediate radicals of MMA, VC, and IPC are similar in character, it is doubtful that they would prefer to interact with the VC or IPC monomers to any significant extent because of the overriding steric effects. In contrast, the intermediate radical from styrene, although of low reactivity, is apparently polarized in the opposite way to VC and IPC, and this difference in polarity serves as the driving force to partially overcome the steric effects and produce the limited extent of copolymerization observed. It is evident that these factors are only of secondary importance relative to the inhibition of copolymerization of the comonomer pairs by the steric hinderance associated with the carborane nucleus.

References

1. H. L. Goldstein and T. L. Heying, U. S. Patent 3,109,031 (October 29, 1963).
2. J. Green, N. Mayes, and M. S. Cohen, *J. Polymer Sci. A*, **3**, 3275 (1965).
3. T. L. Heying and E. W. Cox, U. S. Patent 3,137,734 (June 16, 1964).
4. J. L. Clark, J. T. Duke, T. B. Larchor, and W. K. Taft, U. S. Patent 3,093,687 (June 11, 1963).
5. M. G. Baldwin and S. F. Reed, Jr., *J. Polymer Sci. A*, **1**, 1919 (1963).
6. T. Onak, *Advances in Organometallic Chemistry*, Vol. 3, Academic Press, New York, N. Y., 1965, p. 337.

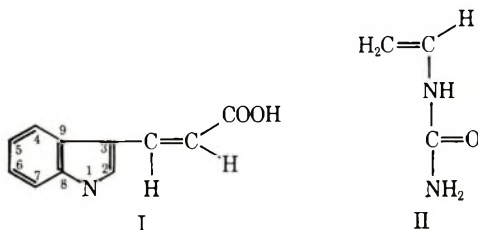
SAMUEL F. REED, JR

Rohm and Haas Company
Redstone Research Laboratories
Huntsville, Alabama 35807

Received August 31, 1970

Preparation of Indole-3-Acrylic Acid-Vinylurea Copolymer

Under conditions of free radical polymerization, indole-3-acrylic acid (IAcA) (I) and vinylurea (VU) (II) form a copolymer of sufficient MW to be impermeable to a viscose membrane. Neither monomer will homopolymerize to such an extent under the same



conditions.¹ The copolymer is a white microcrystalline solid with a solubility in water of 18.11 g/l at 25°C. The saturated aqueous solution has a pH of 3.5 and behaves as a buffer. The UV absorption maximum occurs at 258 nm, suggesting that the ring of copolymerized IAcA is more nearly like indoline than indole and that the 2,3 ring double bond has been involved in the polymerization. The carbon-hydrogen analysis (Table I) and the UV extinction coefficient ($E_{1\%} = 37 \pm 4$) are but little affected by varying the monomer ratios in the copolymerization. Prominent IR peaks are found at 1390, 1443, 1485, 1708, 1722 (sh.), and 2900–3400 cm^{-1} . None of these peaks can readily be ascribed to a vinyl group, and the compound does not react with KMnO_4 . The NMR spectrum exhibits two broad signals: one between 0.90 δ and 3.40 δ with a maximum at 1.98 δ , and one between 6.3 δ and 7.4 δ , maximum at 6.97 δ . The two peaks integrate at a ratio of 1:6.

TABLE I

Effect of Varying the Starting Ratios of Indole-3-acrylic Acid (IAcA) and Vinylurea (VU) on the Carbon-Hydrogen Content of the Copolymer

| Monomer Ratio IAcA:VU | | C% | H% |
|--------------------------|----------------------|-------|------|
| 1 | 1 | 65.8 | 5.4 |
| 9 | 1 | 66.3 | 5.0 |
| 1 | 9 | 65.4 | 5.6 |
| Calc. 2 | 1 (in the copolymer) | 65.22 | 5.22 |

The copolymer is quite toxic having an LD_{50} in mice of 34 mg/Kg.² When treated with aqueous solutions of ethanol, urea or guanidine hydrochloride at reflux temperatures, it undergoes a change which results in a marked increase in water solubility with a corresponding decrease in solubility in organic solvents. The appearance of an IR band at 1558 cm^{-1} in each of the treated products suggests that this is the result of internal amide formation. This is further supported by the fact that the treated copolymers are essentially neutral in aqueous solution.

Experimental

For the 1:1 ratio, VU (0.1 mole) was dissolved in 50 ml H_2O . IAcA (0.1 mole) was suspended in the same solution to which 2.5 M NaOH was added dropwise to effect solution. $\text{K}_2\text{S}_2\text{O}_8$ (50 mg) and NaHSO_3 (50 mg) were added. All procedures were carried out under an N_2 blanket. The mixture was sealed under N_2 and allowed to stand at 20–23° for ten days. Every second day, an additional 10 mg each of $\text{K}_2\text{S}_2\text{O}_8$ and NaHSO_3 were added. The solution was dialyzed for seven days against tap water

and for two days against distilled water, concentrated through the membrane, and freeze-dried. Yield: 62% of theoretical (assuming 2:1 IAcA:VU).

Instruments used in analysis of the products were the Beckman model DK-2 Spectrophotometer, Perkin-Elmer model 620 IR Spectrophotometer and Varian model HA-100 Spectrometer.

References

1. C. G. Overberger, G. Montando, and S. Ishida, *J. Polym. Sci. A-1*, **7**, 35 (1969).
2. Cancer Chemotherapy National Service Center, National Cancer Institute, NSC 127925.

R. OWEN ASPLUND

Department of Chemistry
University of Wyoming
Laramie, Wyoming 82070

Received June 1, 1970

Revised July 22, 1970

ERRATA

Polymers Containing Anthraquinone Units: Polyimidazoles and Polypyrrolones from 1,2,5,6-Tetraaminoanthraquinone

ROLFE PENSE and C. S. MARVEL

[article in *J. Polym. Sci. A-1*, **8**, 3189 (1970)]

The drawing for Figure 1 on p. 3190 should be interchanged with one which appears as Figure 1 on p. 3230 in the same issue.

The drawing for Figure 2 on p. 3195 should be interchanged with one which appears as Figure 2 on p. 3231.

Polymer Containing Anthraquinone and Quinoxaline Units: Polypyrrolones

PRABIR K. DUTT and C. S. MARVEL

[article in *J. Polym. Sci. A-1*, **8**, 3225 (1970)]

The drawing for Figure 1 on p. 3230 should be interchanged with one which appears as Figure 1 on p. 3190 in the same issue.

The drawing for Figure 2 on p. 3231 should be interchanged with one which appears as Figure 2 on p. 3195.

Contents (continued)

NOTES

| | |
|---|-----|
| RICHARD G. SINCLAIR, DAVID A. BERRY, WALTER H. SCHULLER, and RAY V. LAWRENCE: Polycondensation of Resin-Acid Dimers with Diamines | 801 |
| RICHARD H. WILEY, K. S. KIM, and S. P. RAO: Microbead Polymerization of Styrene-divinylbenzene with Sulfated Poly(vinyl Alcohol) Suspending Agent . . . | 805 |
| HIROSHI SUMITOMO, KOJI NOBUTOKI, and KAZUMICHI SUSAKI: Photo-Graft Polymerization of Methyl Methacrylate onto Styrene-Vinylbenzophenone Copolymer | 809 |
| EDWARD GIPSTEIN, WILLIAM A. HEWETT, and OMAR U. NEED: Synthesis and Polymerization of 5-Vinyl-2,2'-Bithiophene | 813 |
| W. M. FEIGENBAUM and R. H. MICHEL: Novel Polyamides from Macrocyclic Ethers | 817 |
| ELOISA B. MANO, ODYR DO COUTTO FILHO, WALTER D. VILAR, and AILTON S. GOMES: Grafting of Chlorinated Polyindene with Methyl Methacrylate | 821 |
| SAMUEL F. REED, JR.: Copolymerization Studies on Alkenylcarboranes | 825 |
| R. OWEN ASPLUND: Preparation of Indole-3-Acrylic Acid-Vinylurea Copolymer . . | 829 |
| ERRATA | 831 |

The *Journal of Polymer Science* publishes results of fundamental research in all areas of high polymer chemistry and physics. The *Journal* is selective in accepting contributions on the basis of merit and originality. It is not intended as a repository for unevaluated data. Preference is given to contributions that offer new or more comprehensive concepts, interpretations, experimental approaches, and results. Part A-1 *Polymer Chemistry* is devoted to studies in general polymer chemistry and physical organic chemistry. Contributions in physics and physical chemistry appear in Part A-2 *Polymer Physics*. Contributions may be submitted as full-length papers or as "Notes." Notes are ordinarily to be considered as complete publications of limited scope.

Three copies of every manuscript are required. They may be submitted directly to the editor: For Part A-1, to C. G. Overberger, Department of Chemistry, University of Michigan, Ann Arbor, Michigan 48104; and for Part A-2, to T. G. Fox, Mellon Institute, Pittsburgh, Pennsylvania 15213. Three copies of a short but comprehensive synopsis are required with every paper; no synopsis is needed for notes. Books for review may also be sent to the appropriate editor. Alternatively, manuscripts may be submitted through the Editorial Office, c/o H. Mark, Polytechnic Institute of Brooklyn, 333 Jay Street, Brooklyn, New York 11201. All other correspondence is to be addressed to Periodicals Division, Interscience Publishers, a Division of John Wiley & Sons, Inc., 605 Third Avenue, New York, New York 10016.

Detailed instructions in preparation of manuscripts are given frequently in Parts A-1 and A-2 and may also be obtained from the publisher.

Coming soon from Wiley-Interscience—

The Second Edition of the Most Comprehensive Book in the Field of Polymer Science

TEXTBOOK OF POLYMER SCIENCE

Second Edition

By FRED W. BILLMEYER, JR., *Rensselaer Polytechnic Institute*

In the last 50 years, the field of polymer science has developed into a discipline essential to most aspects of our modern technology. Because this development has been so rapid, it has been difficult for educational systems and texts to keep pace. *Textbook of Polymer Science* was originally published in 1962 to help fill this gap, and this new Second Edition continues to supply up-to-date information on the field.

To up-date the original treatment of the theory and practice of all major phases of polymer science, engineering, and technology, the author has made extensive revisions and additions throughout the entire work.

Part I:

An introduction to concepts and characteristics of macromolecules, Part I now includes material on solubility parameters, free-volume theories of polymer solution thermodynamics, gel-permeation chromatography, vapor-phase osometry, and scanning electron microscopy.

Part II:

The advances gained from new data on the crystalline nature of polymers are now treated in a thorough discussion of the structure and properties of bulk polymers.

Part III:

The format and content of Part III, concerned with polymerization kinetics, have been revised to include recent advances and new references, as well as further data and explanations of recently discovered processes.

Part IV:

The material on commercially important polymers has been rearranged, and now includes information on aromatic heterochain, heterocyclic, ladder, and inorganic polymers.

Part V:

The comprehensive discussion of polymer processing in Part V now includes many new references for plastics, fiber, and elastomer technology.

1971 In Press



WILEY-INTERSCIENCE

a division of JOHN WILEY & SONS, Inc.

605 Third Avenue, New York, New York 10016

In Canada: 22 Worcester Road, Rexdale, Ontario